p. 246

FINAL REPORT

EXHIBIT "A"

USE OF PHOTOSTRESS AND STRAIN GAGES TO ANALYZE BEHAVIOR OF WELDMENTS

Prepared by

Dr. S. C. Gambrell, Jr.
Department of Engineering Science and Mechanics
College of Engineering
The University of Alabama
Tuscaloosa, Alabama

Prepared for

NASA/MSFC
through the University of Alabama in Huntsville

Contract No. NAG8-293
SUB93-101

BER Report No. 591-97

Fall 1993

The University of Alabama
College of Engineering
Bureau of Engineering Research
Box 870201
Tuscaloosa, Alabama 35487-0201
Telephone: (205) 348-1591

FRONTISPIECE

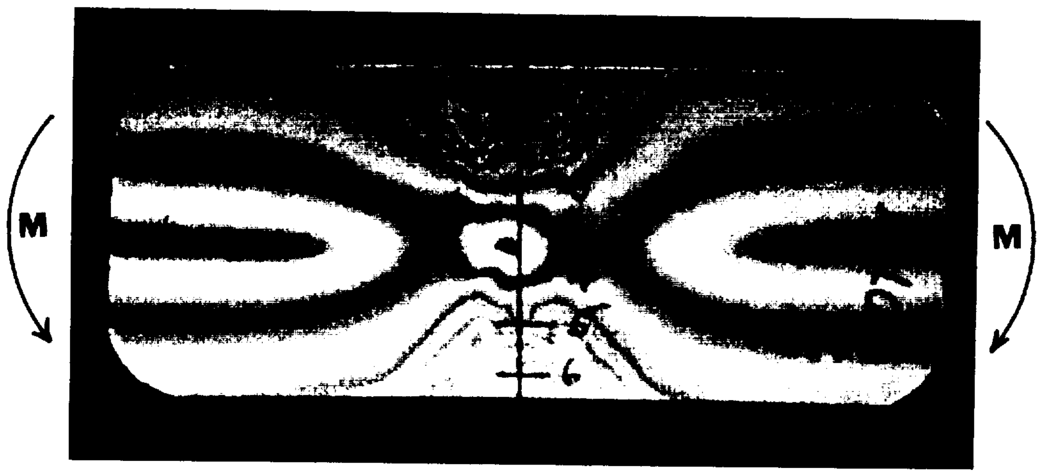

2219-T87 Parent Material

2319 Filler

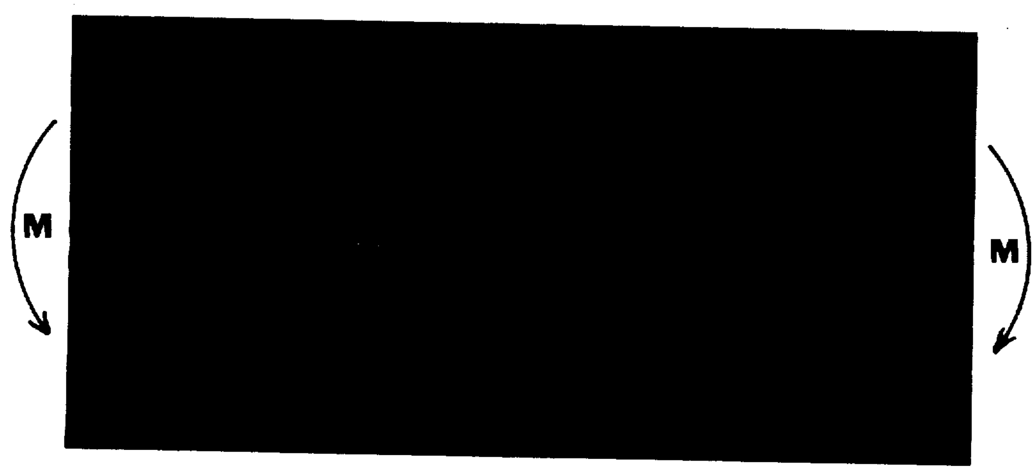

6061-T6 Aluminum

FINAL REPORT

EXHIBIT "A"

USE OF PHOTOSTRESS AND STRAIN GAGES TO ANALYZE BEHAVIOR OF WELDMENTS

Prepared by

Dr. S. C. Gambrell, Jr.
Department of Engineering Mechanics
College of Engineering
The University of Alabama
Tuscaloosa, Alabama

Prepared for

NASA/MSFC
through the University of Alabama in Huntsville

Contract No. NAG8-293
SUB93-101

BER Report No. 591-97

Fall 1993

TABLE OF CONTENTS

LIST OF PHOTOGRAPHS

LIST OF FIGURES

Figure #	Title	Page

Figure #	Title	Page

Figure #	Title	Page

Figure #	Title	Page

ABSTRACT

Tensile and pure bending tests were conducted on specimens having welded joints made from 2219-T87 aluminum alloy and 2319 filler. Data were collected using photoelastic coatings and strain gages. Stress-strain relationships and contraction ratios were determined at several points in a grid covering the weld material and heat affected zone. Material behavior was non-linear and non-uniform at all points in the grid and contraction ratios did not conform to those predicted by Chakrabarty's plasticity theory. Yielding in joints made using four new welding procedures was examined. None of the new procedures produced more uniform yielding in the joint.

I. PURPOSE AND TASK DESCRIPTION

The purpose of this research is to continue work begun in 1991 on characterization of mechanical behavior of 2219-T87 aluminum welded joints. Research since 1991 indicates that behavior of these welded joints is quite complex and highly variable with significant differences in behavior on a point by point basis. This project consisted of four primary tasks in which welded tensile and pure bending specimens were tested to determine general behavior of the joint. Both Photostress and strain gages were used to collect data. Color photographs of fringe patterns developed in the photoelastic coating bonded to welded joint specimens were taken and are quite descriptive in showing overall yielding characteristics of the joint. Primary tasks for the project are listed in the following paragraphs.

A. Task 1

NASA personnel will develop up to ten new procedures for laying the weld in material 1.375 inches thick. Specimens will be machined from heat treated panels and tested in tension. Photostress will be used to view the fringe pattern through the weld to determine the strain distribution produced in specimens made from panels prepared by each new procedure. The procedures producing the most uniform yielding in the welded joints will be identified. Weld beads will be ground off. Two specimens from each new procedure will be tested. Still photographs will be made of the fringe pattern in one specimen. For the second specimen, the fringe pattern will be videotaped throughout the loading cycle.

B. Task 2

After the welding procedures from Task 1 which produce the most uniform yielding of the joints have been identified, specimens from up to three of those procedures will be instrumented with linear 1/32 inch strain gages to determine the strain distribution in the weld material and in material within the heat affected zone. Three strain gages will be placed at intervals of 0.344 inches across the 1.375 inch dimension through the weld at the weld centerline and along a line located 1/2 inch below the centerline of the weld. Stress-strain curves will be prepared for each gage position along both lines. Thus, the variability of material behavior in the joint will be determined at six different locations within the joint. Results from these tests on specimens from the new welding procedures will be compared with results from similar tests conducted on specimens from the old welding procedure (contract NAG8-212, SUB92-195). Depending upon the amount of material available from each welded panel, up to three repetitions of each test will be conducted to provide an average value of the representative joint behavior. Weld beads will be ground off for these tests.

C. Task 3

Using pure bending specimens made from heat treated panels 1.375 inches thick welded in accordance with normal procedures, tests will be conducted having the weak side in tension and then the strong side in tension to determine behavior of the joint in pure bending. Photostress will be applied to the surface through the weld and one linear strain gage will be placed at the weld center on the outer surface of both the tension and compression sides of the joint. Weld beads will be ground off. The neutral axis of the non-uniform material will be located for both conditions and bending moment versus strain gage readings will be plotted. Also, bending moment versus shear strain (from Photostress) will be plotted at several positions along the centerline of the weld on either side of the neutral axis. Specimen dimensions will be 17" x 1.375" x 1.0" with the bending moment applied around an axis normal to the 1.375 inch dimension. To obtain average behavior, three specimens each will be tested for the weak side in tension and for the strong side in tension. One additional specimen for each orientation will be video-taped to observe the complete development of the fringe pattern.

D. Task 4

Using as welded specimens made from panels of 1/2 inch thick material, tensile tests will be conducted to determine the ratio of transverse to longitudinal strain as a function of applied stress for positions at the centerline of the weld, at halfway between the centerline of the weld and the fusion boundary, at the fusion boundary, and at 1/2 and 3/4 inches from the weld centerline. Two-element X gages, 1/32 inch long, will be used to measure strains at each location. To obtain the greatest accuracy, measured strains in both transverse and longitudinal directions will be corrected for effects of transverse sensitivity to obtain the true strains. Weld beads will be ground off. Specimens will have cross-sectional dimensions of 1/2" x 2". Three repetitions of the test will be conducted.

These tests will provide an indication of the true contraction ratio at the several locations in the welded joint.

E. Modifications to Tasks

1. For Task 1, NASA personnel developed four new welding procedures which were tested as specified. Only one of the new procedures was significantly different and was chosen for further testing.

2. For Task 2, the new welding procedure identified in Task 1 was tested extensively. Instead of using linear strain gages as specified, small two-element gages were used at each location to obtain both longitudinal and transverse strains. These two data components provided for determining stress-strain curves for each point as well as plastic stress versus contraction ratio curves.

Also, because of interesting information on contraction ratios recently obtained when testing 1/2 inch thick material, task two was further modified to include tests on 1.4" thick material welded using the normal procedure to determine contraction ratios at several locations in the welded joint. Tests conducted on these specimens welded using normal procedures were the same as those conducted on specimens welded using the new procedure selected from task one.

To better define the stress-strain and contraction ratio characteristics of the joints, ten locations in the joint were chosen for investigation rather than six as specified. The four added locations were on the OD and ID faces of the joint at the centerline of the weld and at a line one-half inch away from the weld centerline.

Because of the additional work required to perform tests for Task 2 as modified, only two repetitions of each test were conducted rather than three as specified.

3. For Task 4, thirteen locations were chosen for investigation rather than four as specified. The nine additional locations provided for a much more complete characterization of mechanical behavior of the joint. Only two repetitions, rather than three, of each test were conducted at the additional nine locations. Because the welded panels obtained from NASA were only 11.75 inches wide, rather than 17 inches wide as specified, specimens made from these panels were shorter than desired. Therefore, because of the influence of pins and fillets on the stress distribution, no data were taken at locations 3/4 inch away from the weld centerline.

F. Data Analysis

Each test was designed for three repetitions so that a least squares fit of the data scatter could be made. Except for special cases where variations were made in the three repetition sequence because of task modification, curves shown in graphs represent three tests. A software package installed on an IBM RS6000 work station which uses both a linear and nonlinear analysis for curve fitting was used to produce graphs from the complete data base obtained from the two or three specimens in a set. Results obtained from each of the four primary tasks will be presented in detail in the following sections of this report.

II. BACKGROUND

The basic foundation for this research project was developed during 1991 and 1992 when testing 2219-T87 aluminum welded specimens using Photostress became of interest to personnel in the Metallurgy Research Branch, Metallic Materials Division, Materials and Processes Laboratory of NASA at the Marshall Space Flight Center. Gambrell (1) and other personnel of the Metallurgy Research Branch initially tested approximately twenty tensile test specimens during the summer of 1991 to determine if Photostress was of value in characterizing mechanical behavior of welded joints. Success was obtained in several areas and, in perhaps the most important aspect of the work, a whole field understanding of the stress-strain behavior of the joint was obtained by observing the fringe pattern in the photoelastic coating covering the joint. Testing continued through 1992 during which time additional significant knowledge was gained about mechanical behavior of the joints.

Recent research using Photostress on as welded and heat treated specimens of 2219-T87 parent material and 2319 weld material indicated that behavior of welded joints can be highly irregular and non-uniform (2)(3)(4)(5). Specimens in an as welded condition having welds 1/8 and 1/2 inch thick exhibited a large strain gradient from the weld centerline outward for nearly one inch with the 1/2 inch material showing distinct zones of constant strain within the strain gradient. Material 1.40 inches thick in a heat treated condition exhibited a totally non-linear, non-uniform behavior through the weld thickness with one side of the weld being much weaker and more ductile than the other side. It is thought that this difference in behavior through the weld is, in part, caused by procedures used when laying the weld bead.

When testing specimens 1/2 inch thick by 2 inches wide it was observed that, at the weld centerline, the maximum normal strain seemed to have a value close to the maximum shearing strain giving rise to the possibility that constraint by the parent material on either side of the weld prevented the normal plastic deformation associated with a standard tensile test. Data taken at points in the heat affected zone away from the weld centerline seemed to indicate that this material was not constrained to the same extent as the weld material. This difference in behavior at the various points seemed to indicate that the contraction ratio as defined by Chakrabarty (6) may not be valid. Later work has shown that contraction ratios are different at different points, and, at each point, are a function of the applied stress.

Variability in behavior at different locations in welded joints tested in this previous work indicated that additional work is needed to more clearly define the general behavior of aluminum welded joints.

III. ORIENTATION FOR DATA COLLECTION, AND EQUIPMENT

Figure 1 shows the dogbone and pure bending test specimens used in tests. Panels of parent material were TIG welded by NASA personnel at the junction of the two halves of parent material

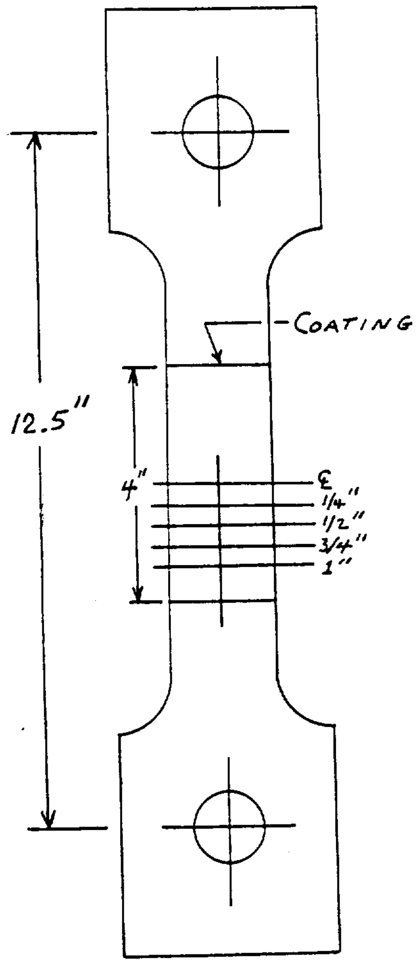

Tensile Specimen

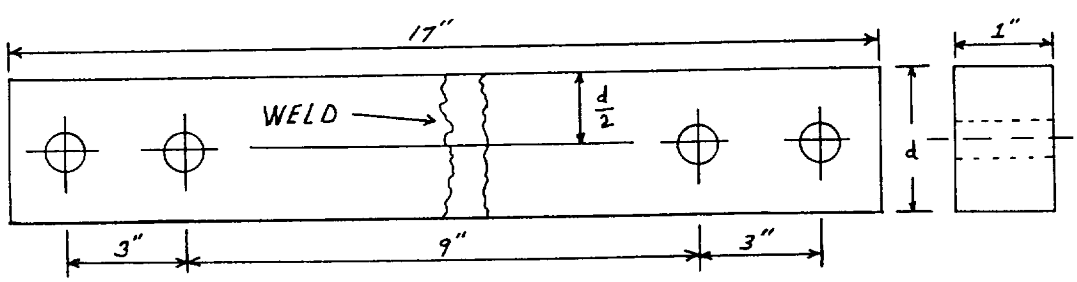

Bending Specimen

Figure 1. Typical Specimens

and were taken to the University of Alabama for machining in the College of Engineering machine shop. Dogbone specimens used in Task 4 had only 7.25 inches between hole centers due to smaller than requested panel widths received from NASA. Horizontal lines on dogbone specimens indicate locations along the vertical centerline where data were taken. Specimens for Tasks 1 and 2 had, in addition to the vertical centerline, another vertical grid line on either side of the centerline to facilitate data collection along horizontal lines through the thickness of the weld. These additional lines can be seen in photographs of the 1.4 inch thick specimens.

Tests for the four tasks in this project were conducted using a SATEC 55 kip universal testing machine as seen in Photo 1. Other items of equipment shown include a reflection polariscope with uniform field compensator, a telemicroscope, and a digital automatic recorder-printer for measuring maximum shearing strain. A model P-3500 static strain indicator was used for taking data from strain gages. A SB-10 switching and balancing unit was used for multiple gage installations.

Strain gages were bonded using M-Bond 200 adhesive and photoelastic coatings were bonded using PC-8 adhesive. All gages, photoelastic coatings, adhesives, and strain measuring equipment were obtained from Measurements Group, Inc., in Raleigh, NC. (7)(8)(9)(10)(11)(12)(13)(14)

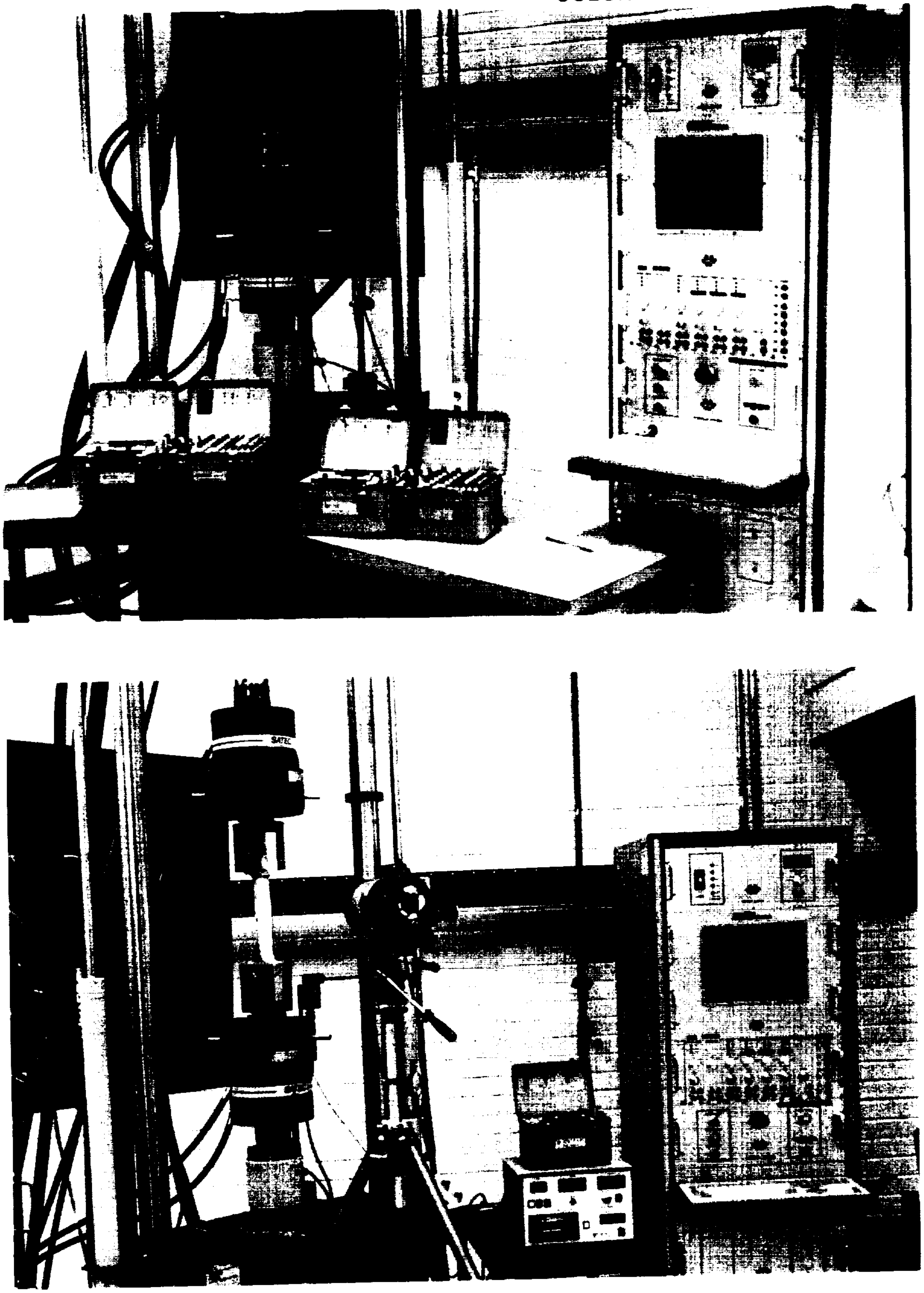

Photo 1. Test Machine and Equipment

IV. SPECIMEN BEHAVIOR, DATA CORRECTION, AND CONTRACTION RATIO

A. Bending

Although test panels were fabricated by NASA personnel in a manner as careful and uniform as possible, specimens made from these panels were not nearly identical. No specimen was completely straight and, for most specimens, parent material sections on either side of the weld did not lie in the same plane. Therefore, there was some bending present in tensile tests of all specimens and, because of progressive non-uniform yielding starting in the weld and moving outward toward the parent material, the magnitude of the bending strain changed as the stress increased. Photo 2 shows an example of the bend present in most specimens. In several graphs depicting stress-strain behavior of the specimens, the initial bending strain in the specimen may be clearly seen as an offset on the strain axis at zero stress. Therefore, one must not consider the stress-strain curves in this report as being obtained from ASTM type tensile tests for material properties. Rather, they represent the realistic, non-uniform behavior of an imperfect welded specimen subjected to load.

B. Discontinuous Yielding and Strain Hardening

All specimens 1/2" thick by 2" wide exhibited distinct discontinuous yielding characteristics. This behavior was observed when using strain gages as large increases in strain which occurred for small increases in load and when using photoelastic coatings as instantaneous jumps or changes in the fringe pattern while the load was increased. For the as welded

Photo 1.(continued) 4-Point Loading Bracket for Bending

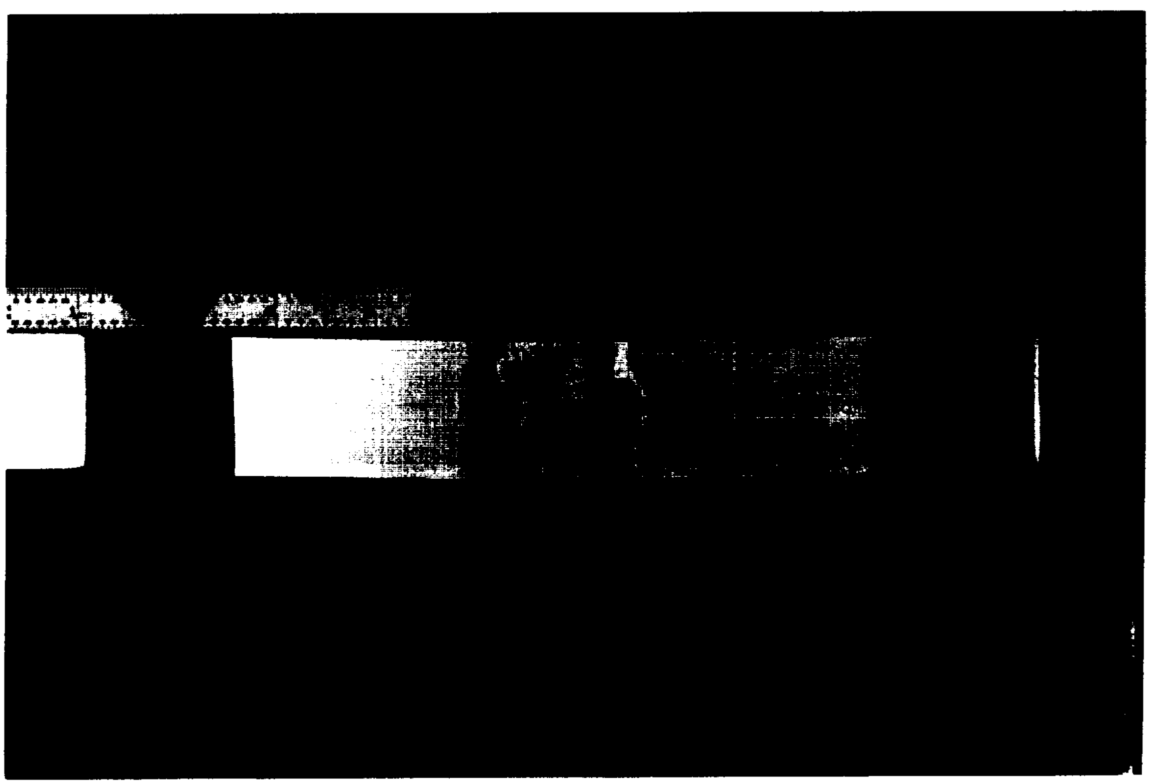

Photo 2. Typical Peaked Specimen

1/2" thick specimens, discontinuous yielding usually began between 20 and 25 ksi. Discontinuous yielding was most prominent at points up to 1/2" away from the weld centerline and less distinct at points 3/4" and 1" away.

In previous work (2) it was observed that the 1/2" thick as welded material was highly inelastic in the weld material in its virgin state but became an elastic material when loaded a second time. During this project, a similar test was conducted on the 1.4" thick material to determine its strain hardening characteristics. Figure 2 shows the highly inelastic first load and the elastic second load stress-strain curves for specimen N5-1 for the 1.4" thick heat treated material. See Figure 2-1 for locations of the points OD and C. While loading specimen N5-1 for the first time, the stress was taken to 44,120 psi. Note that, upon loading the specimen for the second time, the major departure from near linear behavior occurs between 41,000 and 45,000 psi. Therefore, near perfect strain hardening has been obtained during the second loading.

C. Corrections to Strain Measurements

1. Bridge non-linearity

Wheatstone bridges using strain gages in a quarter bridge circuit are non-linear in strain (15). Corrections were made to measured strains using the equations

$$\epsilon' = \hat{\epsilon} + n$$

where ϵ' is the corrected strain, $\hat{\epsilon}$ is the measured strain, and n is the correction factor given by

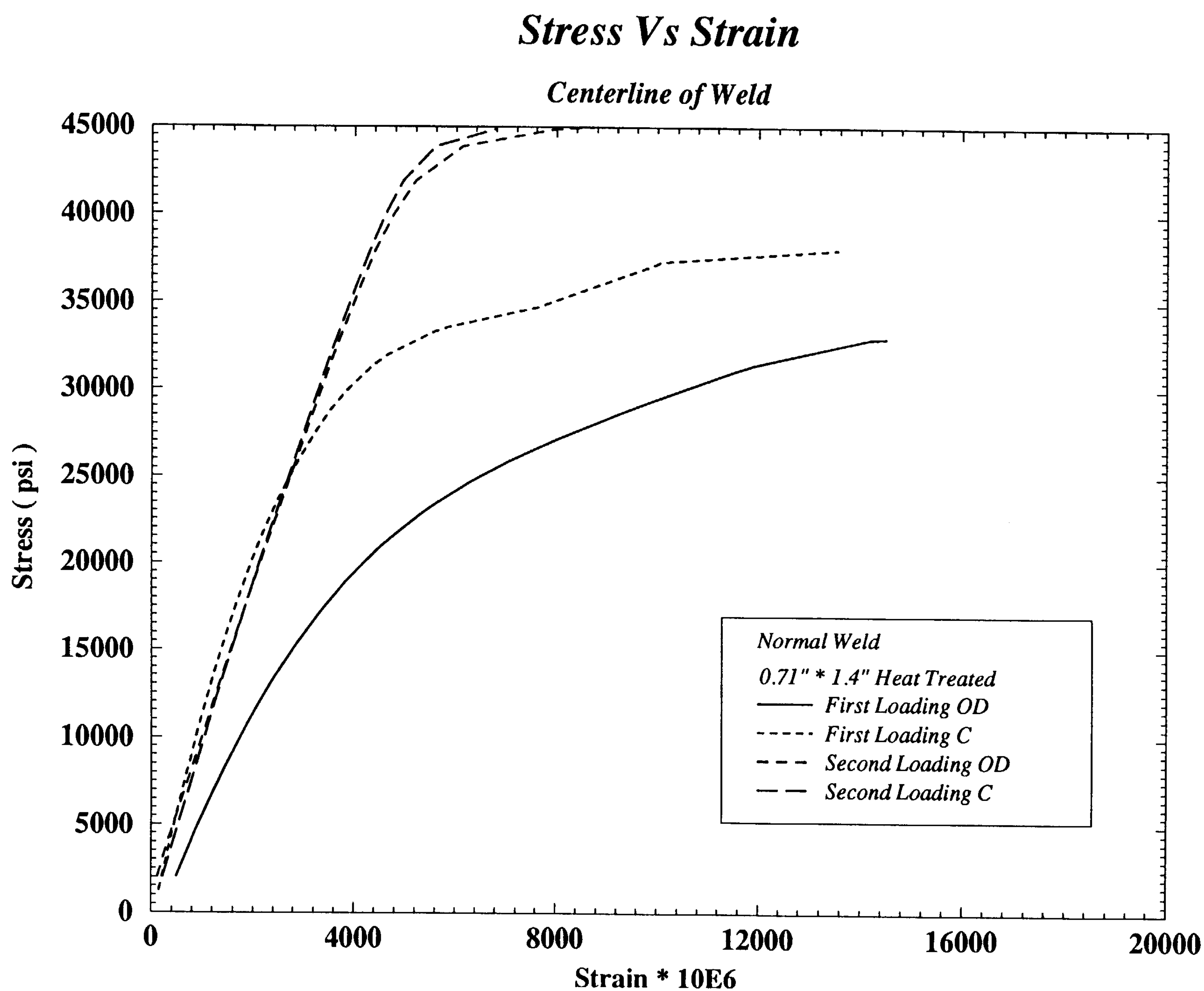

Figure 2. Strain Hardening, Centerline, OD and C Points

$$n = \frac{F(\hat{\epsilon})^2 x 10^{-6}}{2 - F\hat{\epsilon} x 10^{-6}}$$

where F is the manufacturer's gage factor. For values of strain above 0.0025, corrections can become significant and are needed for greater accuracy at strain values approaching 0.02 which were measured during this research project. All measured strains were corrected as indicated above.

2. Transverse sensitivity

To measure strains in an arbitrary biaxial strain field, strains in two perpendicular directions must be measured. In this project, strains were measured on uniaxial tensile and pure bending specimens in directions parallel and perpendicular to the direction of maximum principal stress. Because the onset of yielding occurred at low stress levels, Poisson's ratio for the weld and heat affected zone did not apply and the relationship between the maximum and minimum principal strains was basically unknown. (This relationship was obtained as a function of stress during conduct of this research project.) Therefore, to obtain greatest accuracy in measurement, values of strain were corrected for the effects of transverse sensitivity of the strain gages. Equations for the corrections (16) are

$$\epsilon_1 = \frac{\epsilon_1'(1 - \mu_0 K_{t1}) - K_{t1}\epsilon_2'(1 - \mu_0 K_{t2})}{(1 - K_{t1}K_{t2})}, \text{ and}$$

$$\epsilon_2 = \frac{\epsilon_2'(1 - \mu_0 K_{t2}) - K_{t2}\epsilon_2'(1 - \mu_0 K_{t1})}{(1 - K_{t1}K_{t2})}$$

where ϵ_1' and ϵ_2' are strains in the 1 and 2 directions which were corrected for bridge non-linearity, K_{t1} and K_{t2} are transverse sensitivity factors for gages oriented in the 1 and 2 directions, μ_0 = 0.285 and is Poisson's ratio for the standard strain gage calibration coupon, and ϵ_1 and ϵ_2 are the true strain values in the 1 and 2 directions. All measured strains were corrected as indicated above.

D. Contraction Ratios

Strain gages were used to measure strains on the surface of the specimen in directions parallel and perpendicular to the direction of maximum principal stress. Therefore, in-plane contraction ratios can be determined by forming the ratio of the perpendicular strain to the parallel strain (transverse strain/longitudinal strain). These contraction ratios (ϵ_2/ϵ_1) were obtained as a function of applied plastic stress and are presented in graphs later in this report.

In an attempt to better characterize the total deformation of the welded joints, out-of-plane contraction ratios were calculated assuming that deformation occurred at constant volume or that

$$\epsilon_1 + \epsilon_2 + \epsilon_3 = 0$$

where ϵ_3 is the out-of-plane strain or the strain perpendicular to the surface of the specimen. Values of ϵ_1 and ϵ_2 were obtained using two-element gages on the surface at each point of interest as described previously. Figures presented later in this report dealing with out-of-plane (ϵ_3/ϵ_1) contraction ratios were developed based upon the assumption of constant volume indicated above.

V. RESULTS FROM TASK 1

Four new welding procedures were developed at NASA for the 1.4" thick heat treated specimens in an effort to obtain a welded joint which would yield in a more uniform manner than the normal weld procedure previously tested (2). The four new procedures were identified as:

WG-OD = Wide Groove, Outside Diameter, WG-1, WG-2,

WG-ID = Wide Grove, Inside Diameter, WG-3, WG-4,

AS = Alternate Sides Each Pass, AS-7, AS-8, and

NTR = Not Tightly Restrained, NTR9, NTR10.

Fringe patterns photographed from photoelastic coatings applied to the welded joints are seen in Photos 1-1, 1-2, and 1-3 for the four new welding procedures. In all photos, the OD is to the left of the fringe pattern. Photo 1-1 shows yielding characteristics for the Wide Groove, OD and ID specimens. Yielding in joints made from these two procedures is quite similar to that in specimens made from normal welding procedures (Photo 1-4). Photo 1-2 shows yielding characteristics for the Alternate Sides Each Pass and the Not Tightly Restrained specimens. Yielding in joints made from the Alternate Sides Each Pass procedure is quite similar to that in specimens made from the normal welding procedure. However, yielding in joints made from the Not Tightly Restrained procedure initiates from the ID side of the weld rather than the OD side. Also, it was determined that, even for the same welding procedure, specimens made from two different panels using the NTR procedure can have quite different characteristics. Photo 1-3 shows yielding

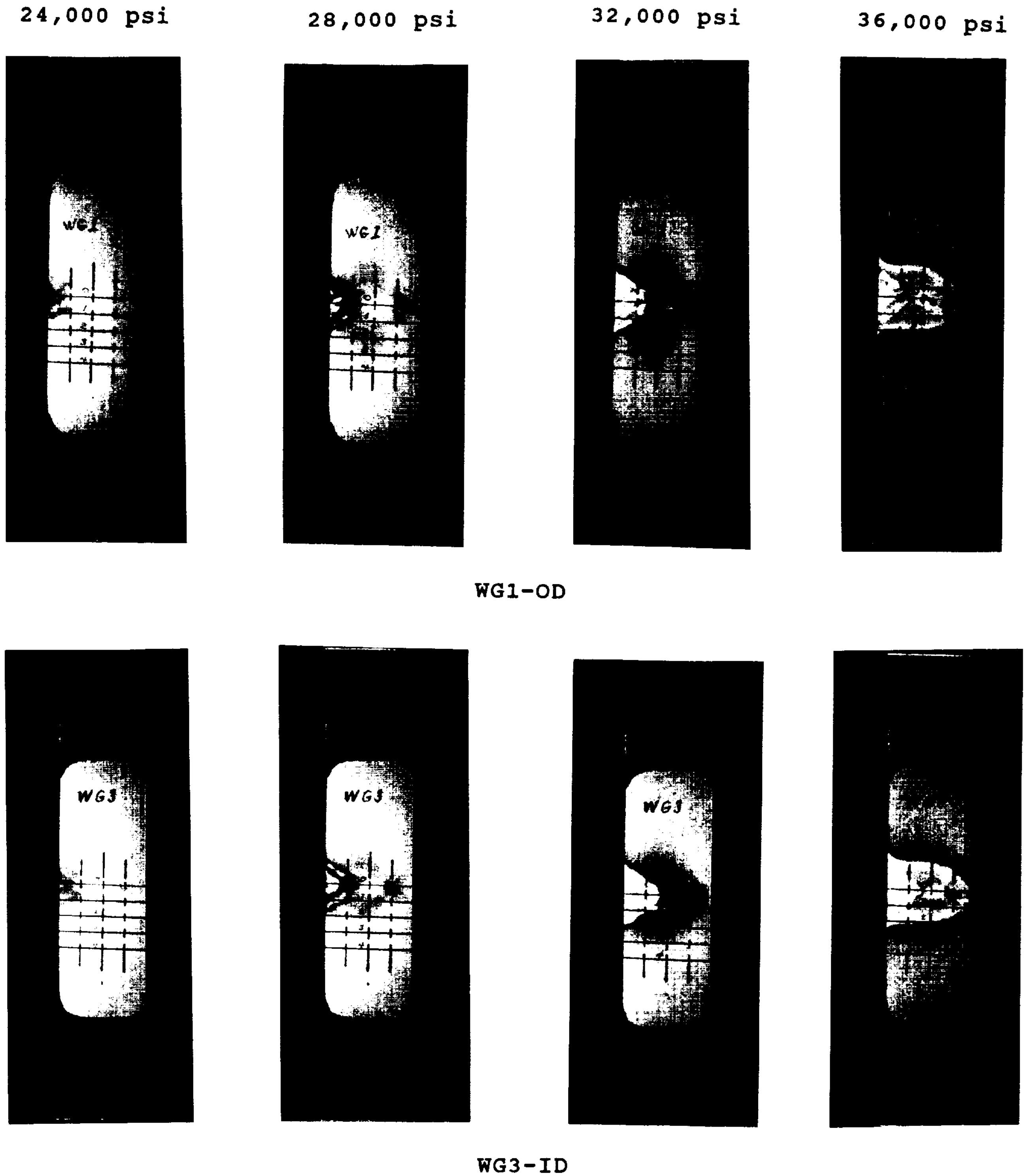

Photo 1-1. Yield Sequence, WG1-OD and WG3-ID

24,000 psi | 28,000 psi | 32,000 psi | 36,000 psi

AS-7

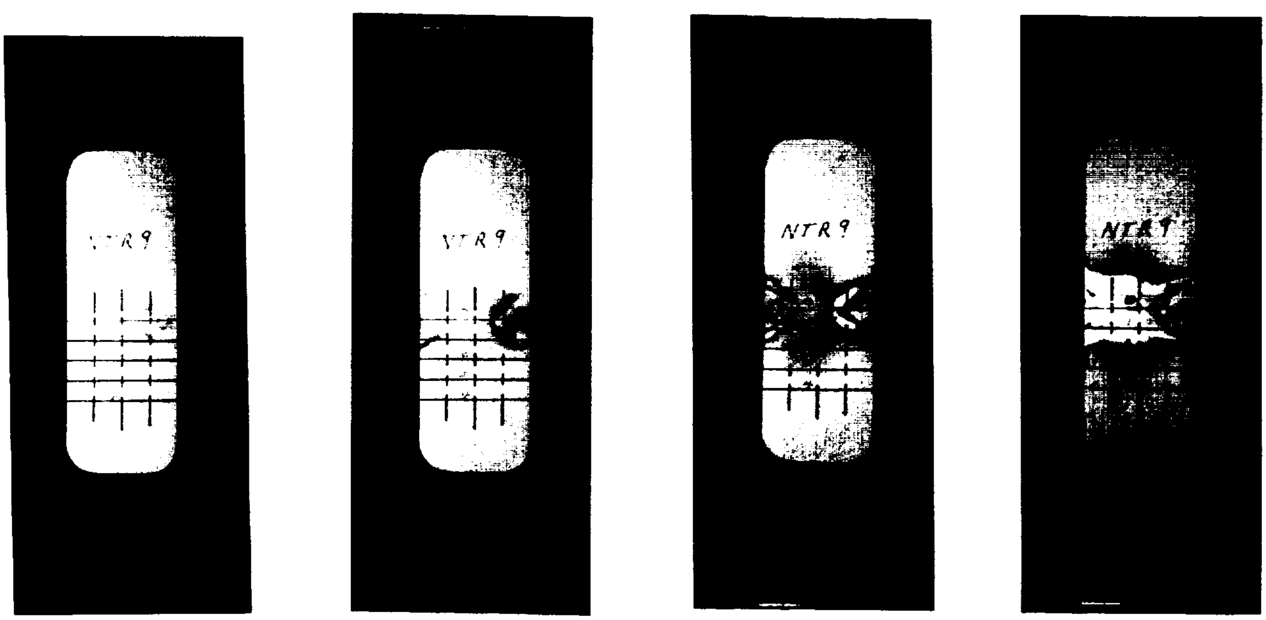

NTR-9

Photo 1-2. Yield Sequence, AS7 and NTR9

24,000 psi

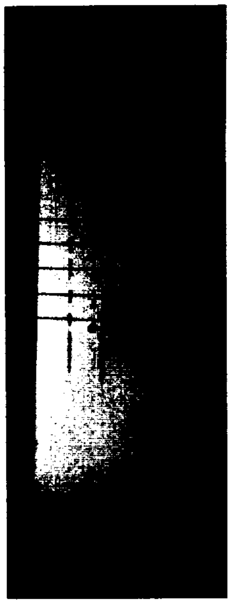

28,000 psi

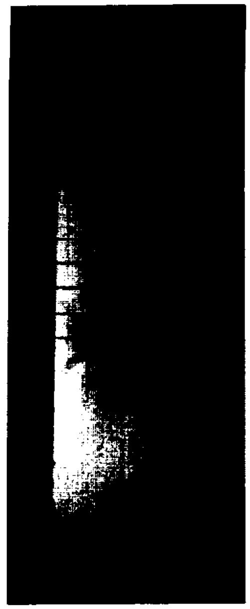

32,000 psi

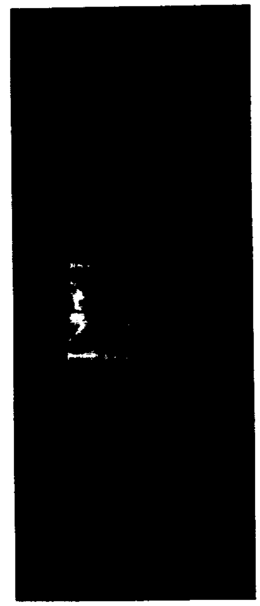

36,000 psi

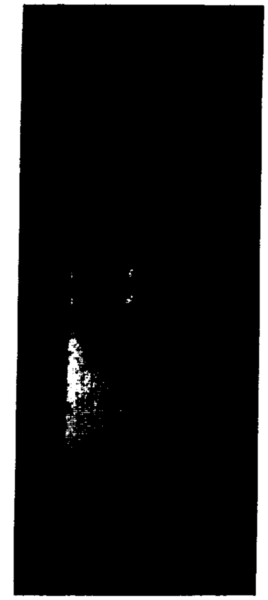

NTR-10

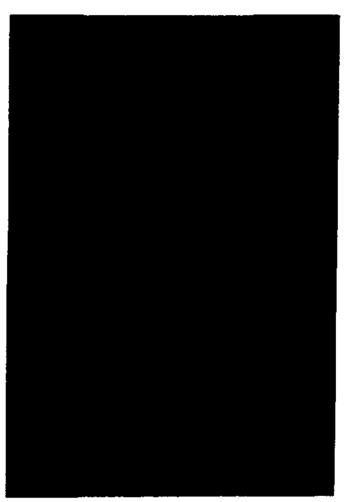

NTR-9

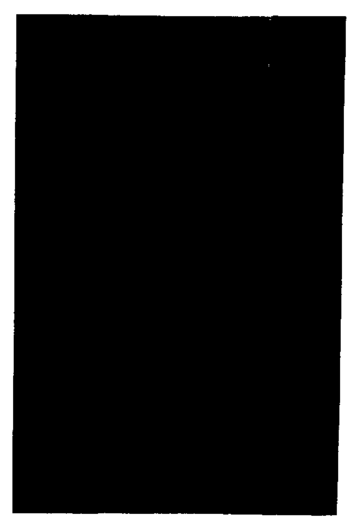

NTR-10

Photo 1-3. Yield Sequence, NTR10, and Weld Etchings

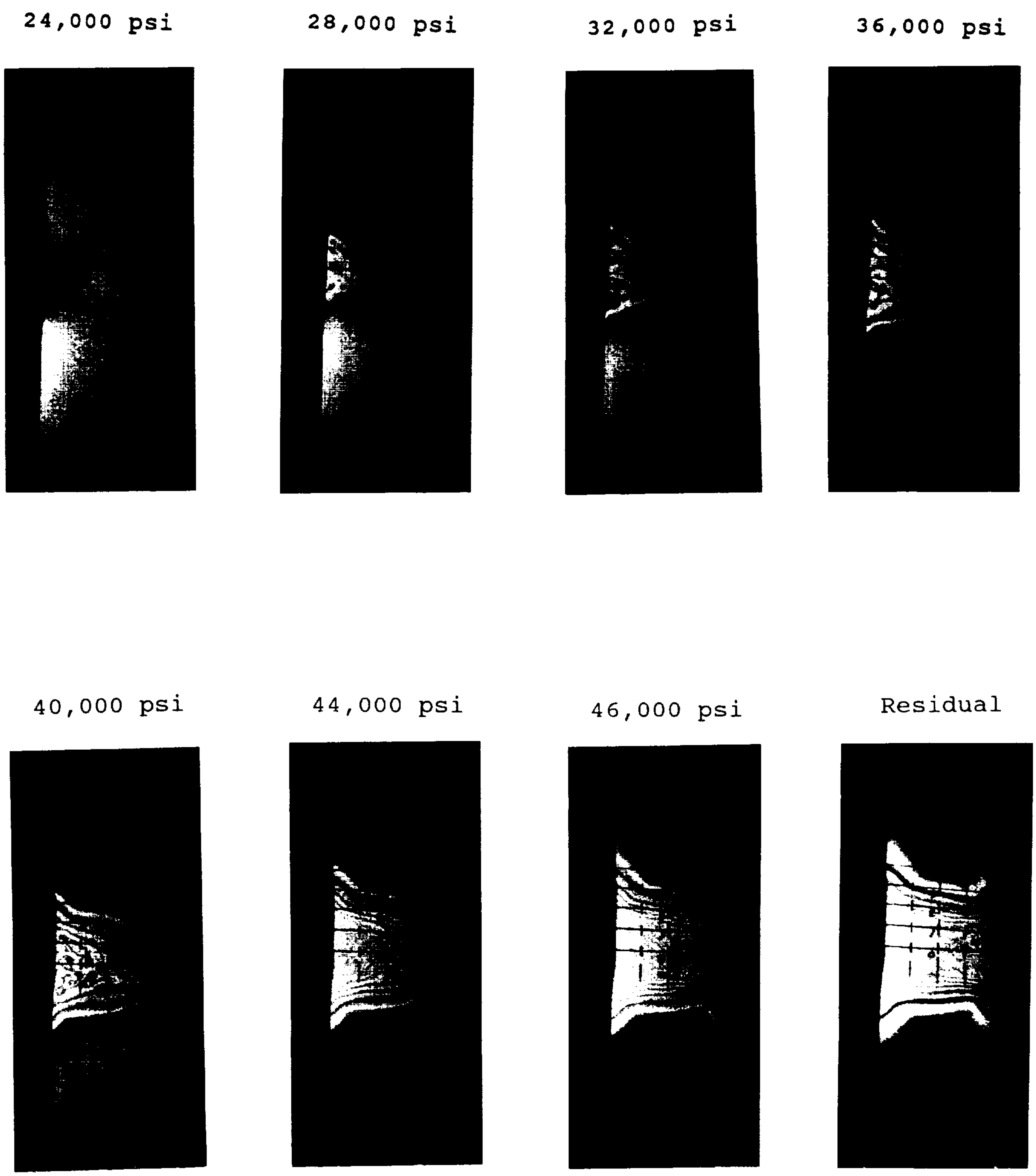

Photo 1-4. Yield Sequence, Normal Weld Procedure

characteristics in specimens made from the NTR-10 panel whereas Photo 1-2 shows yielding characteristics in specimens made from the NTR-9 panel. Note that, at common stress levels, the NTR fringe patterns are quite different in Photos 1-2 and 1-3. This difference is most likely related to the different welds produced by the NTR welding procedure as seen in etchings of the two welds in Photo 1-3. This indicates that, as the evidence clearly shows, two welds made by the same welding procedure may be quite different in shape, in mechanical properties, and in yielding characteristics.

For the photographs, specimens were loaded in increments of 2000 psi after which the load remained constant while photographs were taken. When making a videotape, specimens were loaded using a monotonic stress rate of 4,500 psi per minute. Specimens were stressed to 45,000 psi. Both the photographs and the videotape of yielding for each weld procedure were viewed by NASA personnel to determine which procedure, if any, resulted in more uniform yielding of the welded joint. Fringe patterns from the four new procedures were compared to fringe patterns from the normal welding procedure previously used in welding the joint. Videotapes of the yielding process in the normal weld procedure and in all four new weld procedures have been given to NASA.

VI. RESULTS FROM TASK 2

A. New NTR Procedure

After viewing the still photographs and videotape of tests conducted under Task 1, NASA personnel selected the NTR weld procedure for further analysis. In an effort to obtain data which would be reasonably consistent, specimens from panels made by the new NTR procedure were made from the NTR-10 panel. No data from the NTR-9 panel are included in results presented in the following. NTR welded joints behaved in a manner similar to joints made by the normal welding procedure except that yielding initiated from the ID side of the joint. Thus, in terms of strength and ductility, the ID side is weaker and more ductile than the OD side. Exactly the opposite is true when testing specimens made from the normal weld procedure. Figure 2-1 is a sketch of the grid pattern used for data collection when testing specimens made from 1.4 inch thick material. Proportional limits in the NTR specimens for the points identified in Figure 2-1 are given in the following:

Along the centerline................	OD = 12,000 psi
	LC = 10,000 psi
	C = 10,000 psi
	RC = 9,000 psi
	ID = 7,800 psi
Along the 1/2" line.................	OD = 13,300 psi
	LC = 12,600 psi
	C = 12,000 psi
	RC = 18,800 psi
	ID = 12,800 psi

Figures 2-2 and 2-3 show material behavior at the centerline of the weld and at a line 1/2 inch from the weld centerline. Note, in general, that the curves reflect increasing strength and less ductility as one moves from the ID side toward the OD side

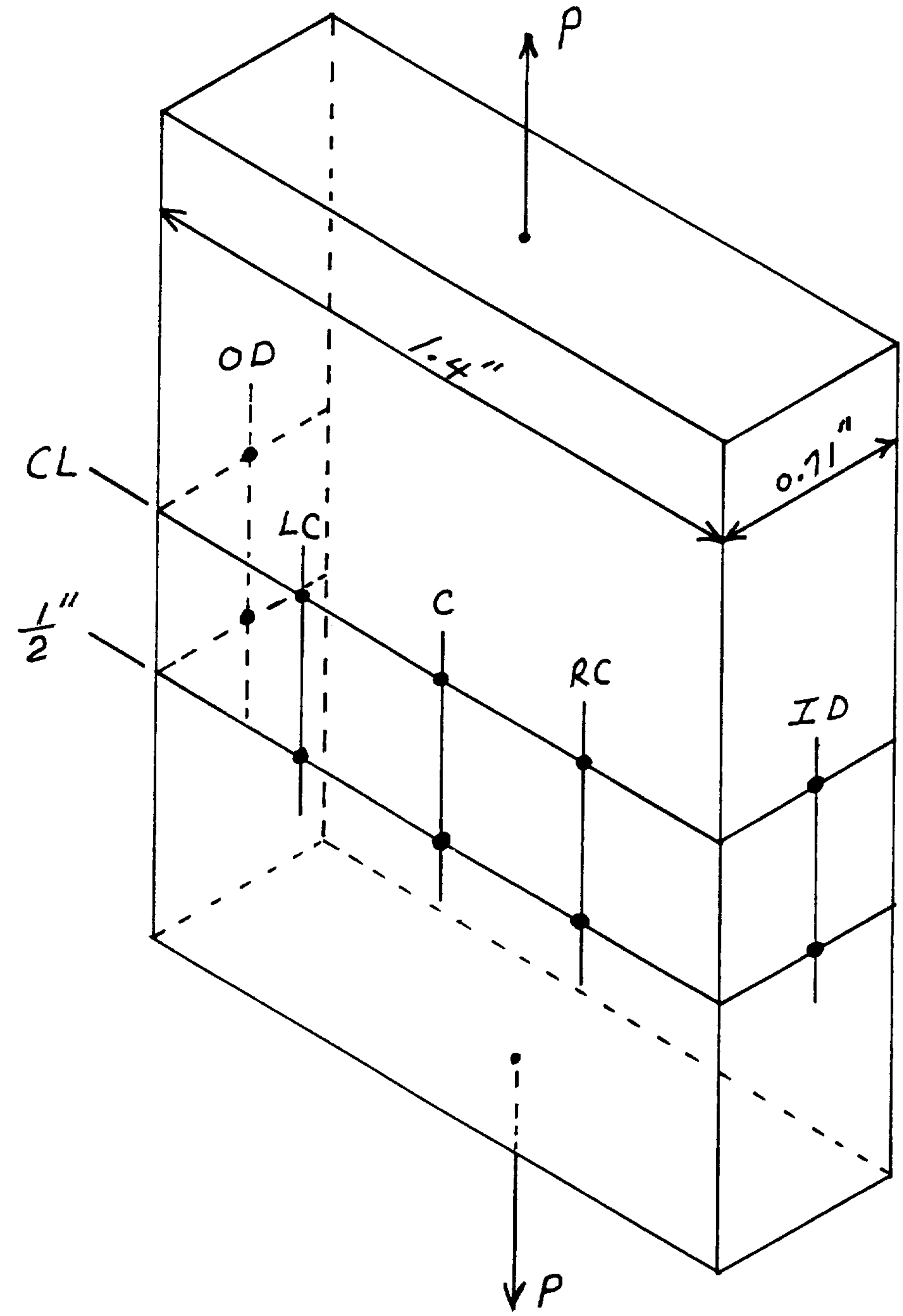

Figure 2-1. Grid Pattern, 0.71" x 1.4" Specimens

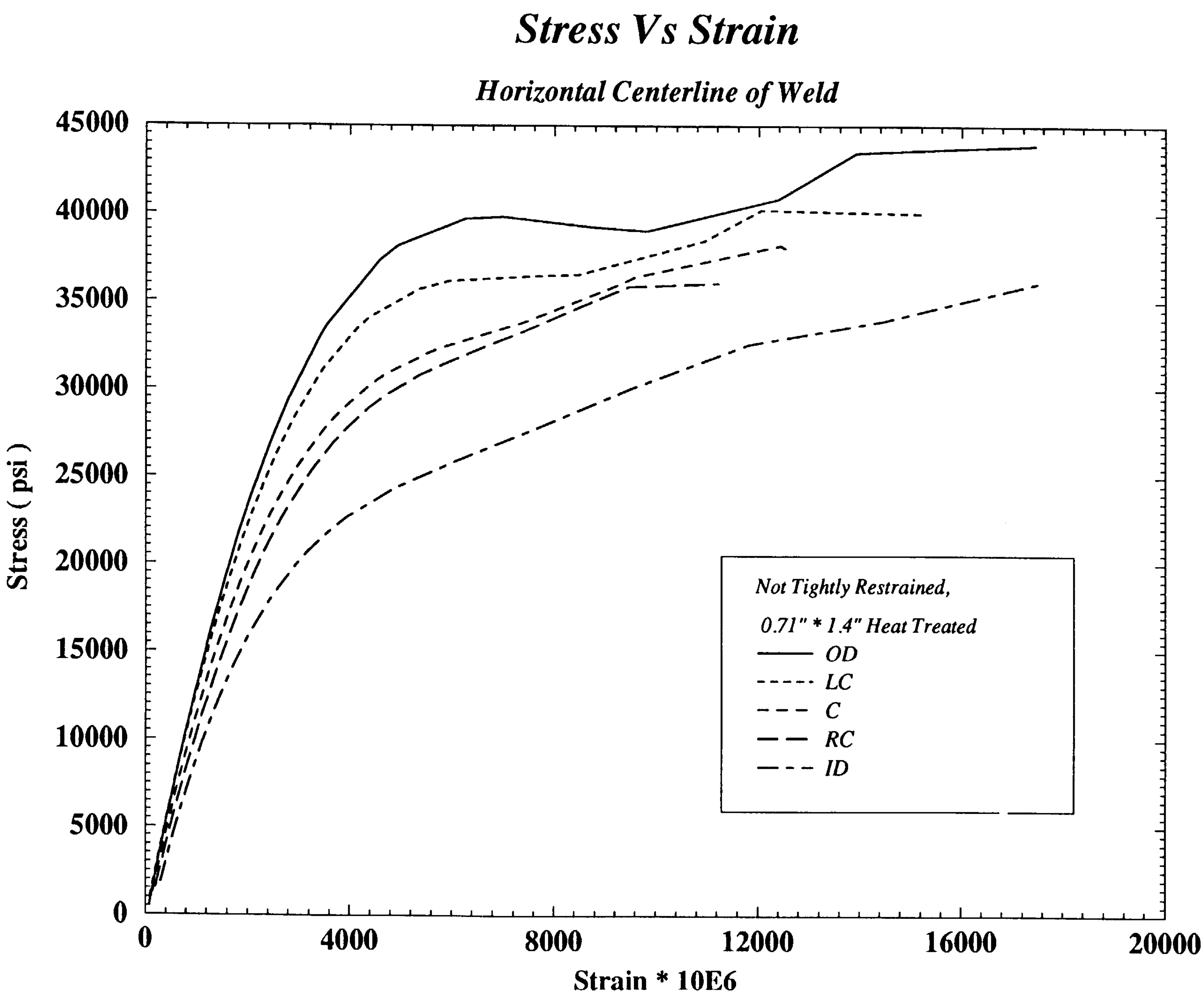

Figure 2-2. Material Behavior, Horizontal Centerline, NTR

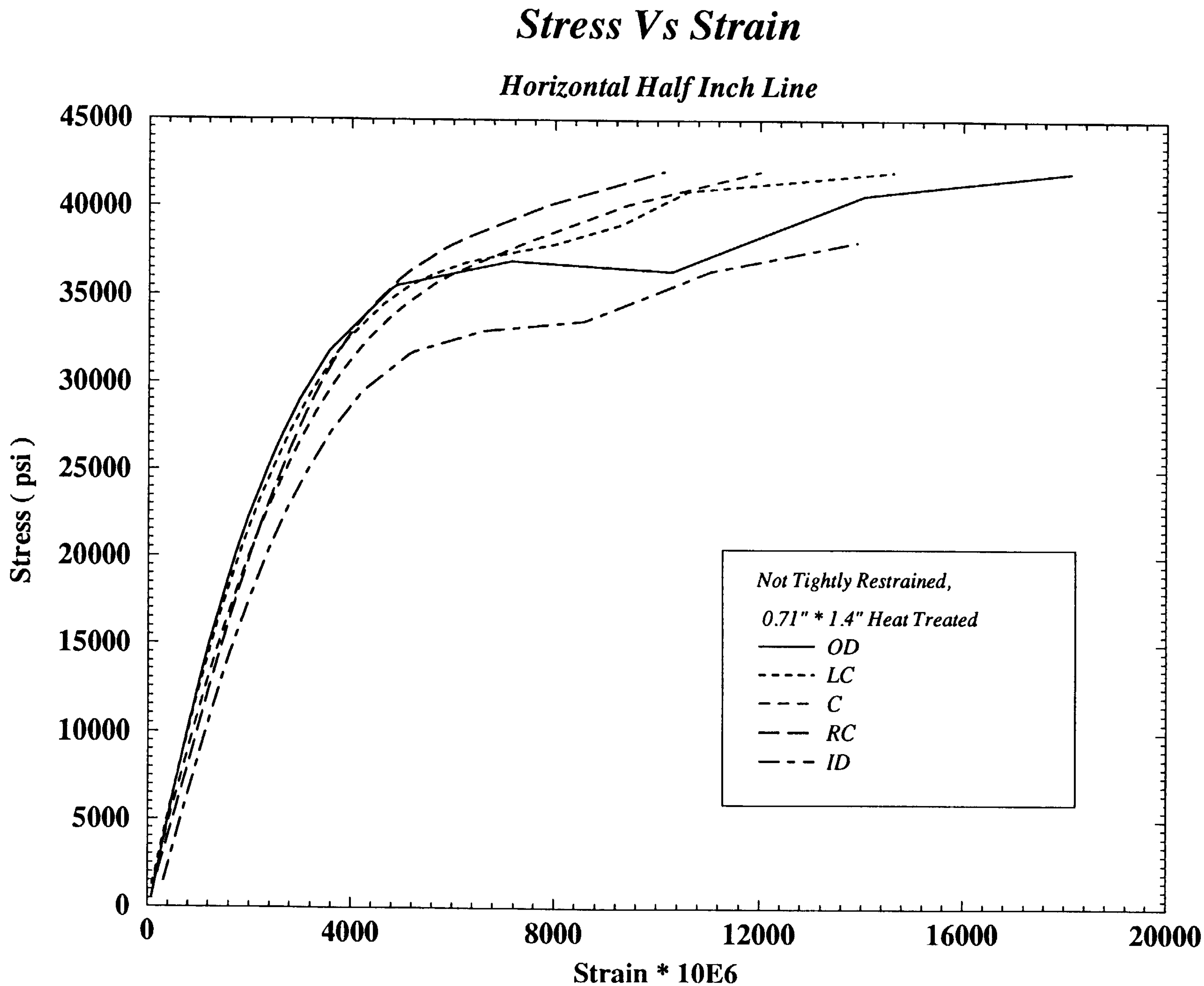

Figure 2-3. Material Behavior, Half Inch Line, NTR

of the specimen. Figures 2-4 through 2-8 indicate the relative strength and ductility at points along vertical lines passing through the weld centerline and the 1/2 inch line. It is interesting to note in Figure 2-4 that, along the vertical line OD, material on the half inch line is more ductile and less strong than material on the centerline of the weld. The reason for this apparent discrepancy can be explained by observing Photo 1-3 and noting that, as yielding progresses, there are higher fringe orders on the OD side near line 2 (the 1/2" line) than there are at line zero (the centerline of the weld). Thus it is clear from the photograph that, for the OD side, material at a point on the 1/2 inch line is more ductile than material on the centerline. These yielding characteristics are not seen in the fringe patterns on the ID side of the specimen, or at points LC, C, and RC.

Figures 2-9 and 2-10 show the in-plane contraction ratios for points on the horizontal centerline of the weld and the horizontal half inch line respectively. Note that, at points OD and RC in Figure 2-9, the contraction ratio approaches 0.5 rather closely as the plastic stress approaches 30,000 psi and that, at other points, the contraction ratio varies between 0.22 and 0.45. The contraction ratios in Figure 2-10 for the half inch line range generally between 0.15 and 0.38 and, up to a plastic stress of approximately 10,000 psi, are between 0.28 and 0.35.

Out-of-plane contraction ratios are shown in Figures 2-11 and 2-12 for the horizontal centerline of the weld and the half inch line respectively. Note that, in general, there is much

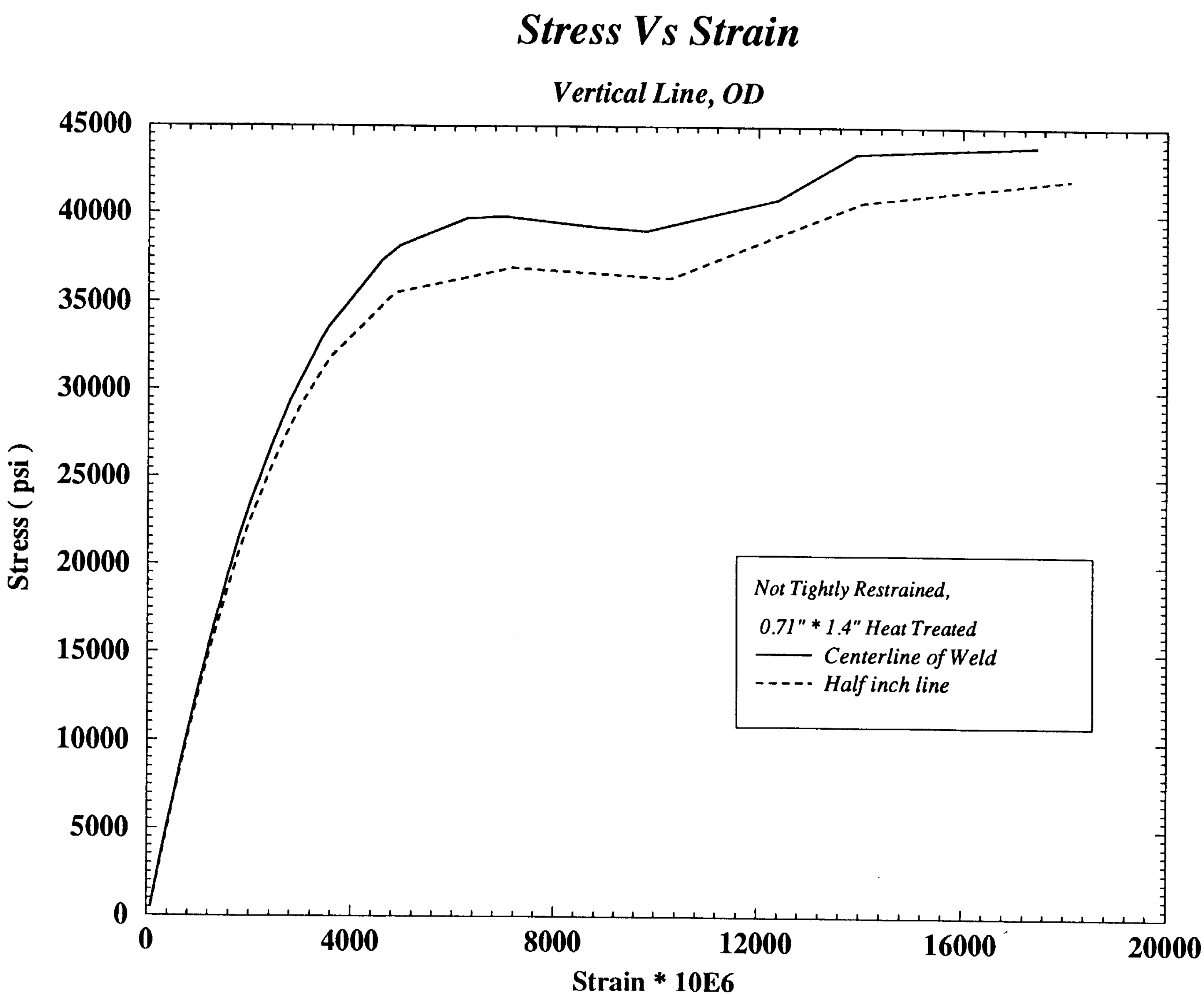

Figure 2-4. Material Behavior, Vertical OD Line, NTR

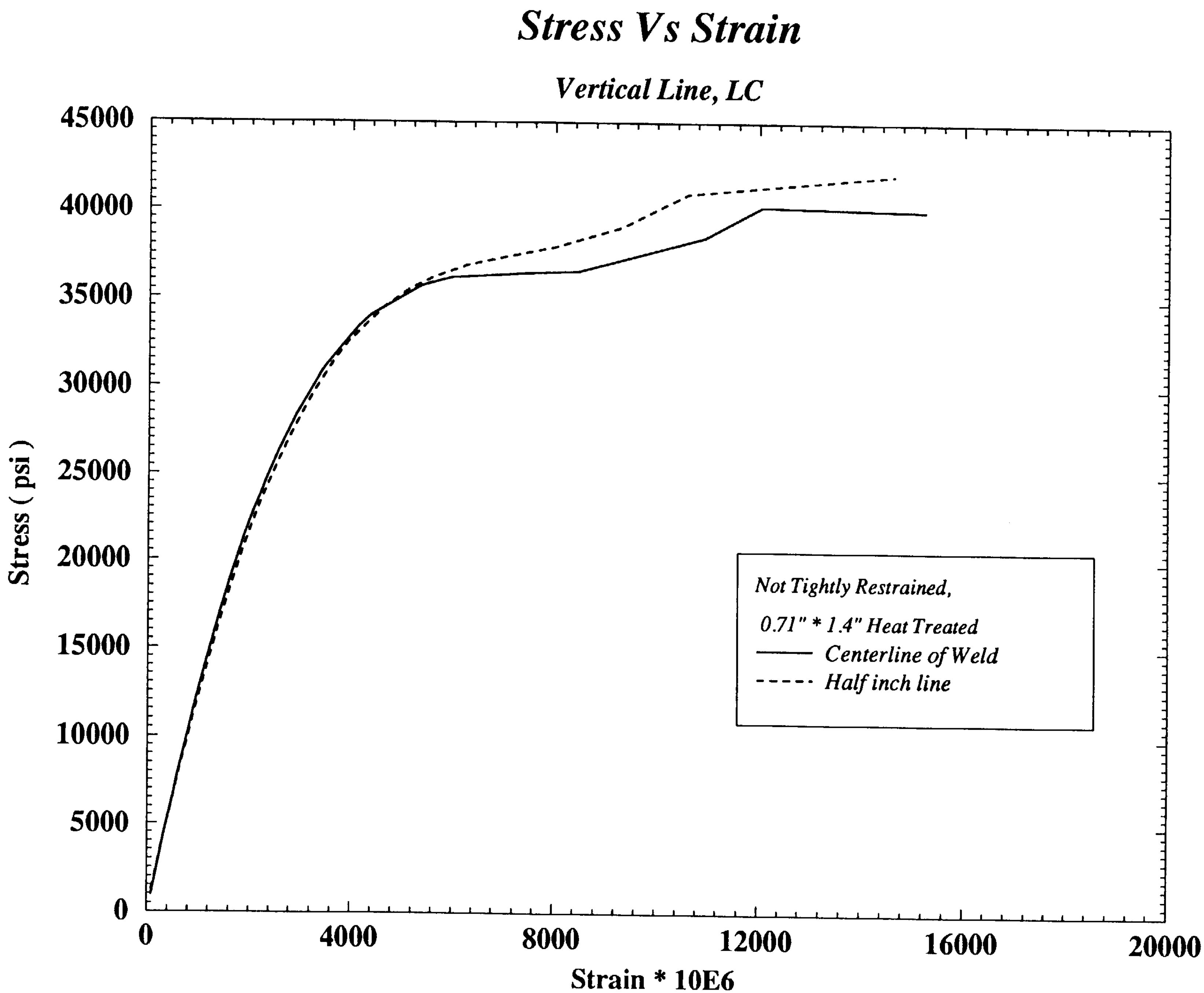

Figure 2-5. Material Behavior, Vertical LC Line, NTR

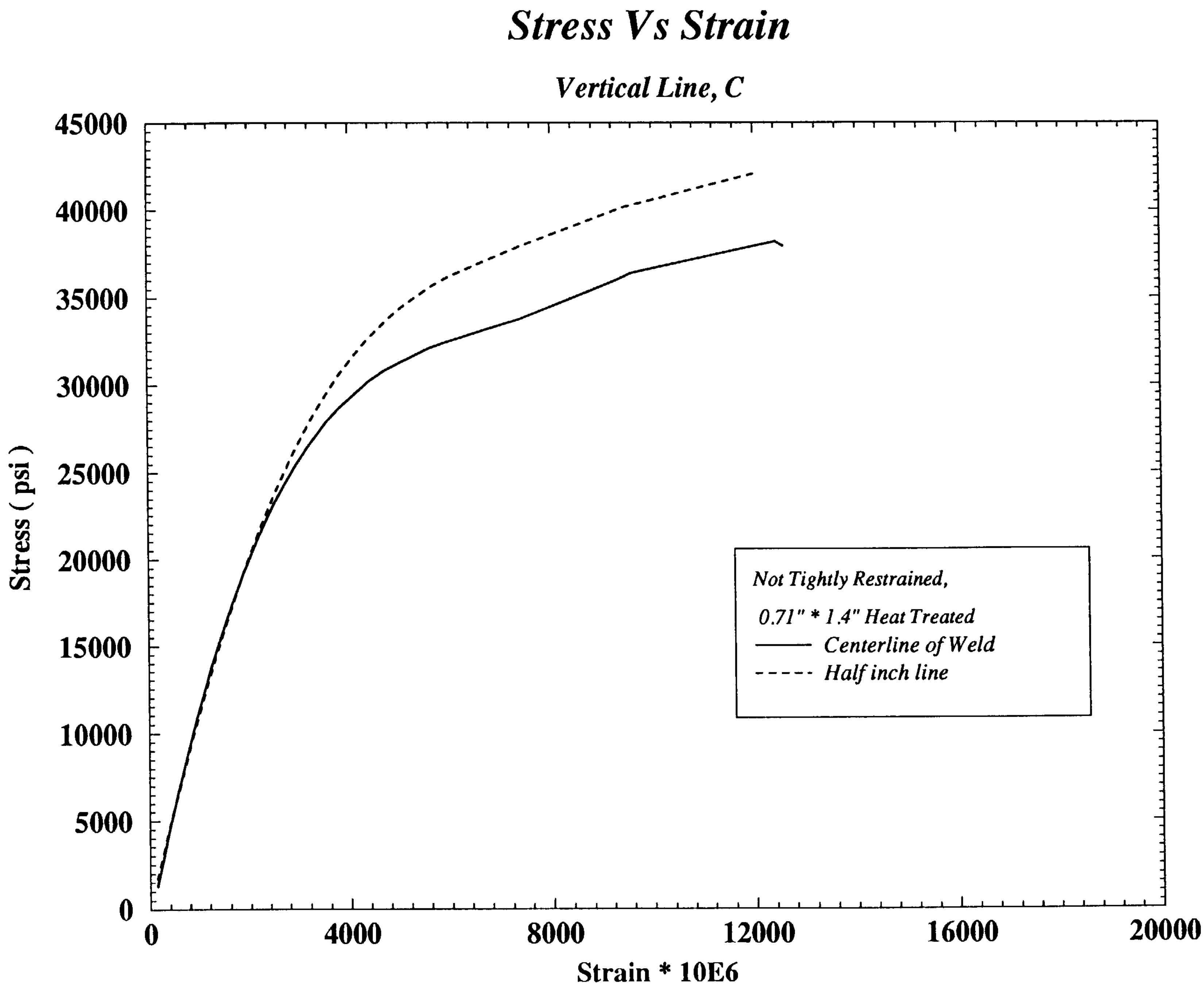

Figure 2-6. Material Behavior, Vertical C Line, NTR

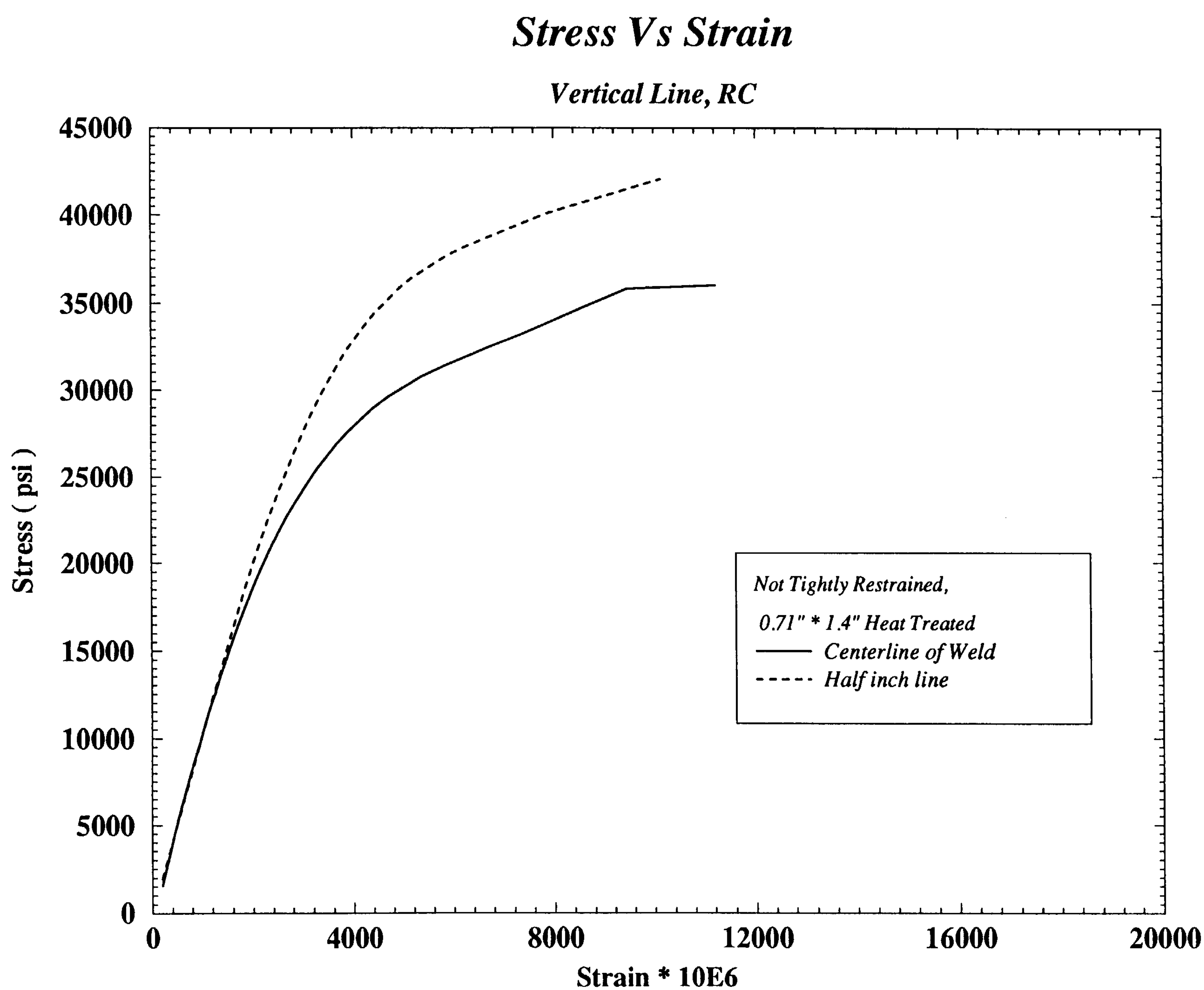

Figure 2-7. Material Behavior, Vertical LC Line, NTR

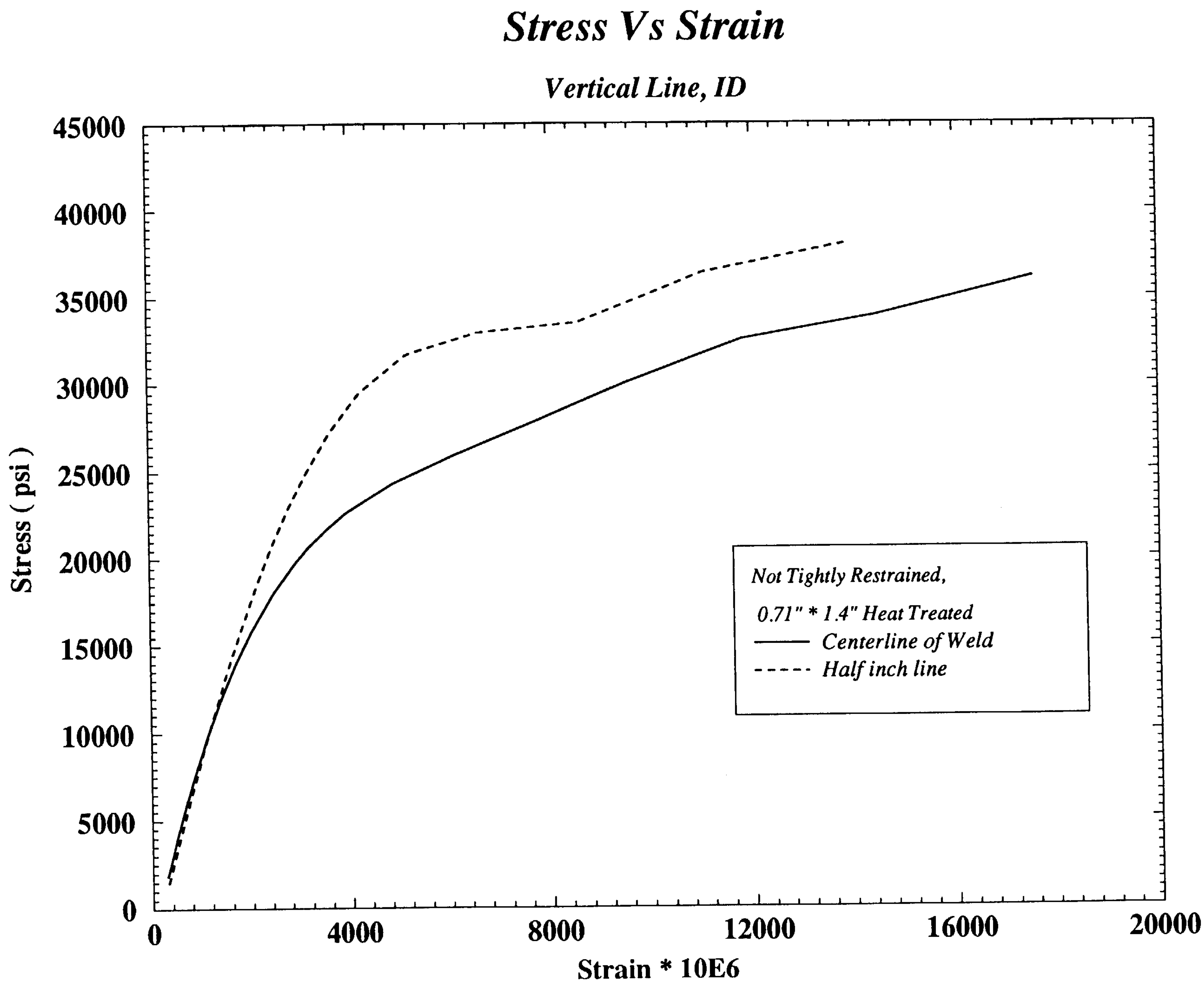

Figure 2-8. Material Behavior, Vertical ID Line, NTR

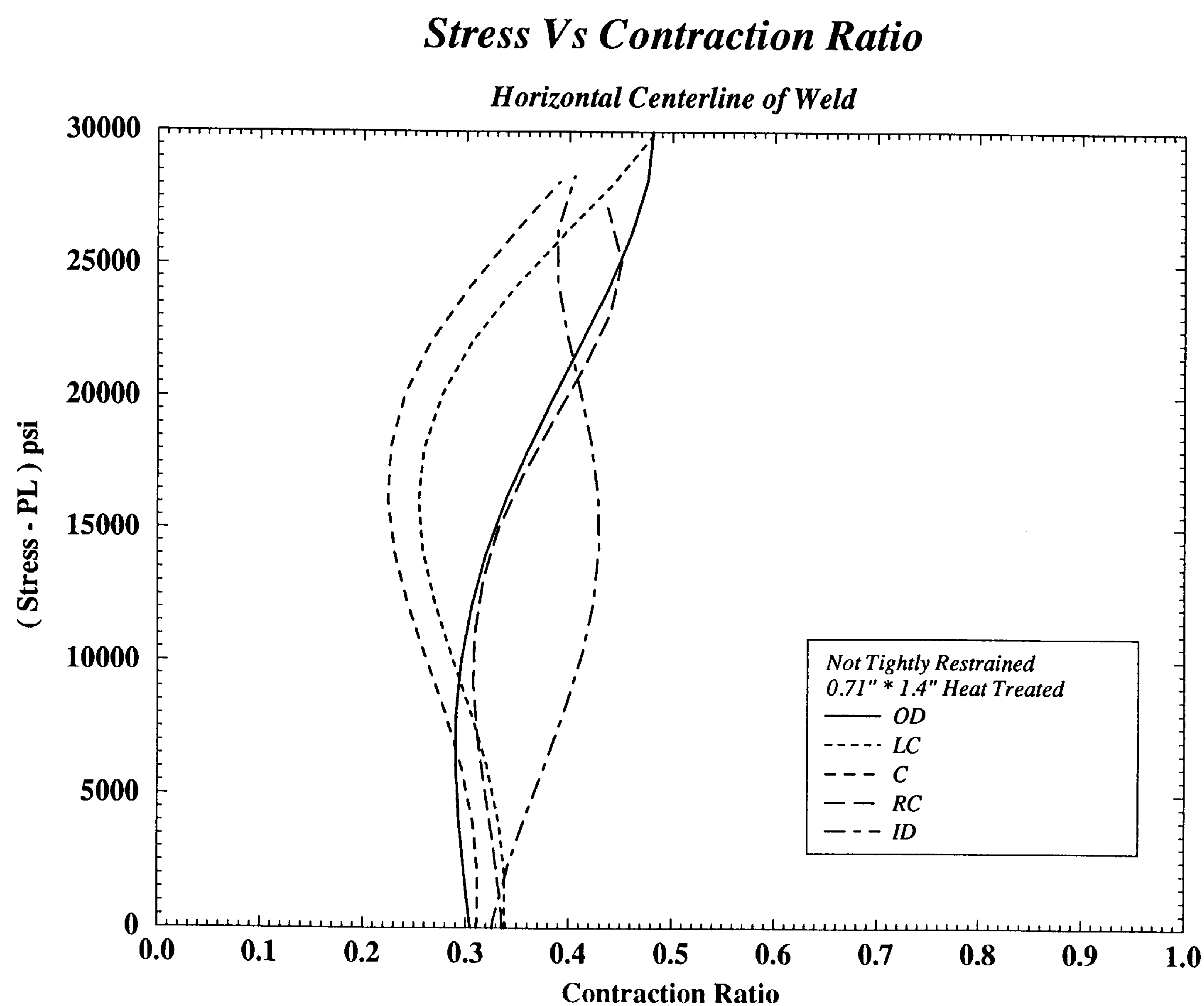

Figure 2-9. In-Plane Contraction Ratios, Horizontal Centerline, NTR

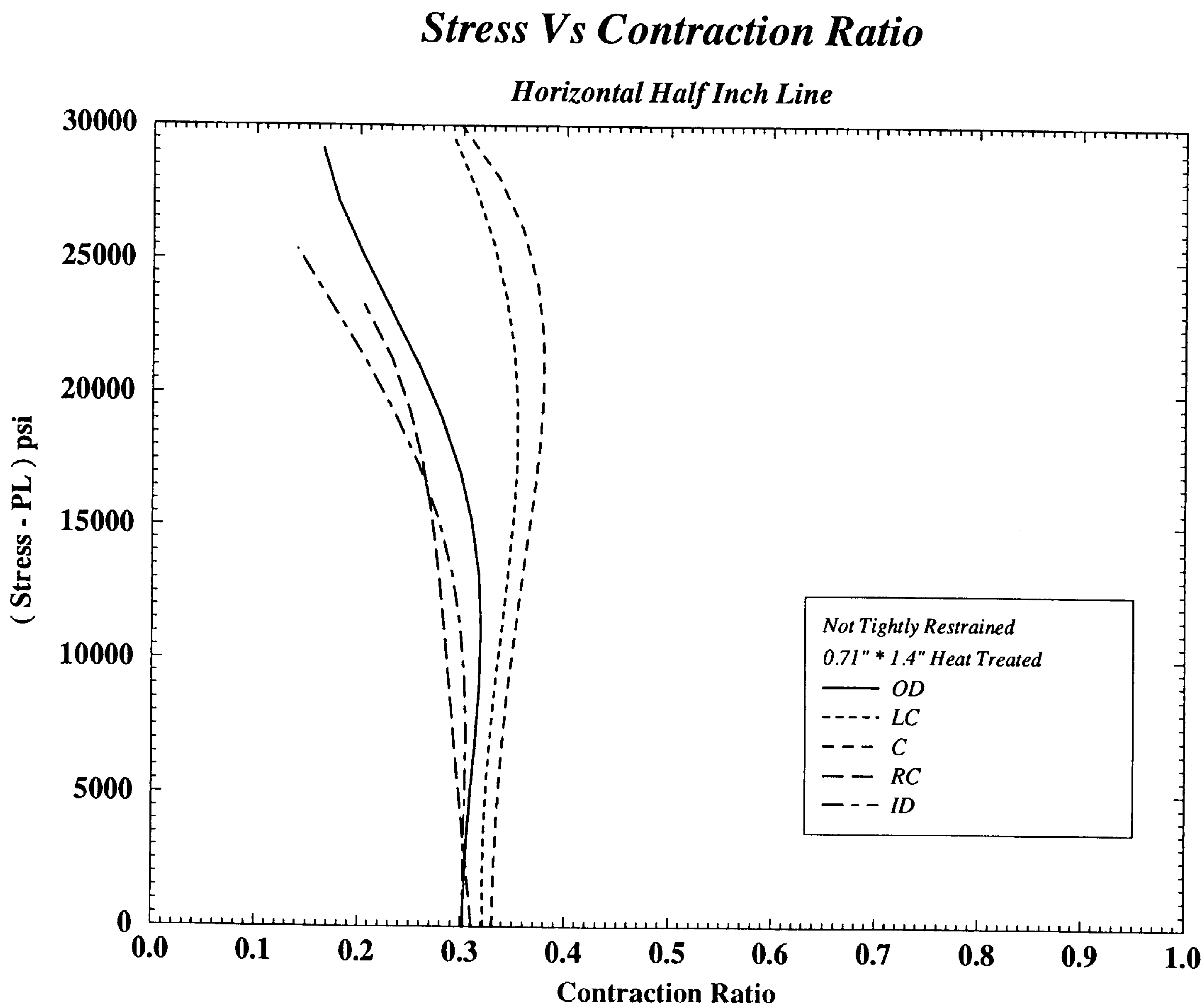

Figure 2-10. In-Plane Contraction Ratios, Half Inch Line, NTR

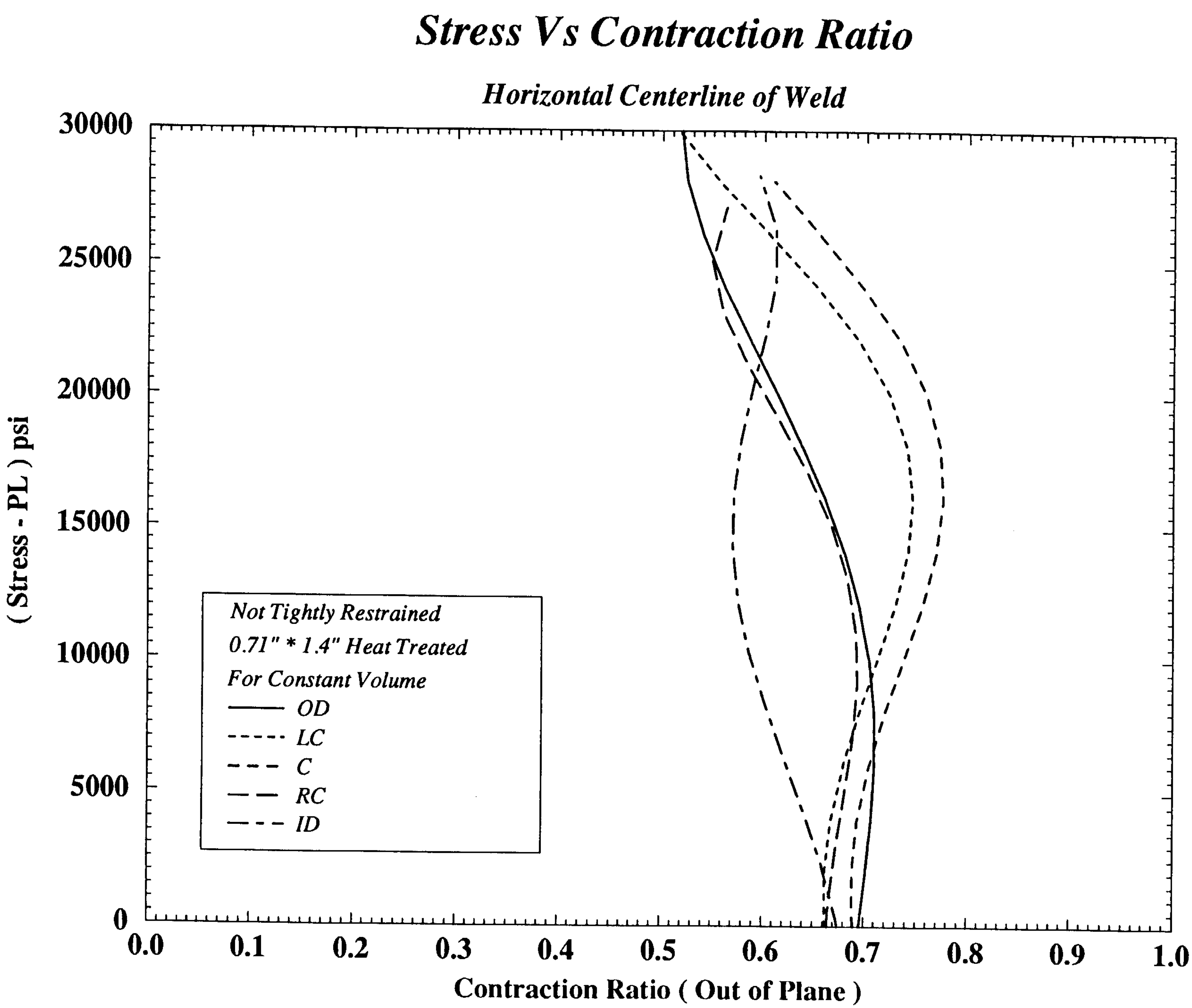

Figure 2-11. Out-of-Plane Contraction Ratios, Horizontal Centerline, NTR

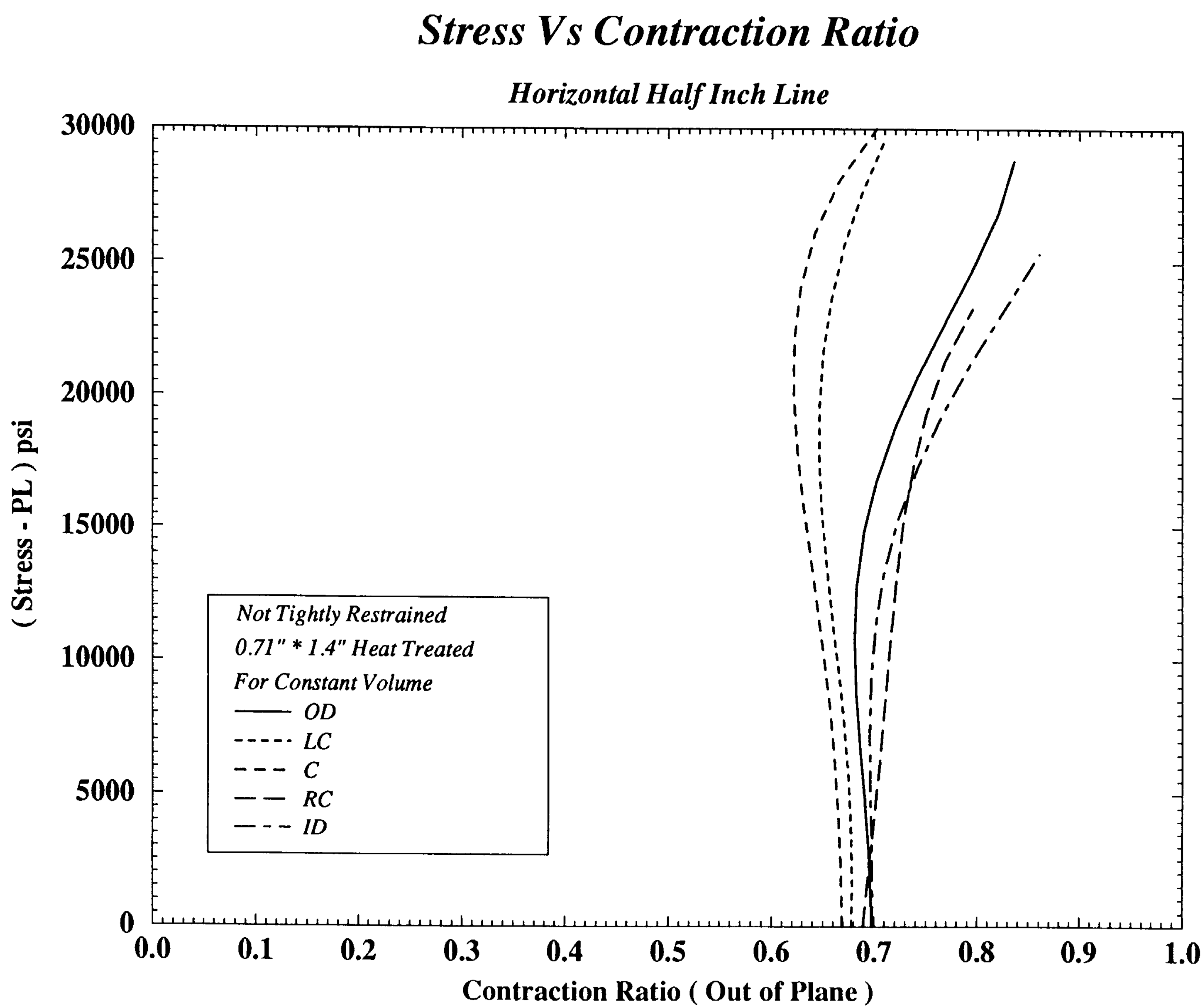

Figure 2-12. Out-of-Plane Contraction Ratios, Half Inch Line, NTR

more contraction perpendicular to the surfaces than there is within the surfaces.

Graphs showing the scatter of data for all tests of the 0.71" x 1.4" NTR specimens are presented in Appendix A.

B. Normal Weld Procedure

Specimens made by the normal welding procedure have been previously tested extensively and results have been reported in (2), (3), (4), and (5). However, these results did not include information on contraction ratios for 1.4" thick welded joints. Therefore, Task 2 was modified as explained previously in section E.2. General yielding behavior of specimens made by the normal welding procedure can be seen in Photo 1-4. Proportional limits in the normal weld specimens for the points identified in Figure 2-1 are given in the following:

Along the centerline..................	OD =	7,900 psi
	LC =	10,000 psi
	C =	12,200 psi
	RC =	11,400 psi
	ID =	16,800 psi
Along the 1/2" line...................	OD =	15,700 psi
	LC =	12,500 psi
	C =	10,000 psi
	RC =	20,700 psi
	ID =	13,500 psi

Figures 2-13 through 2-19 show stress-strain behavior at various locations in the joint. Effects of peaking in the joints are clearly seen in the figures as an offset on the strain axis at

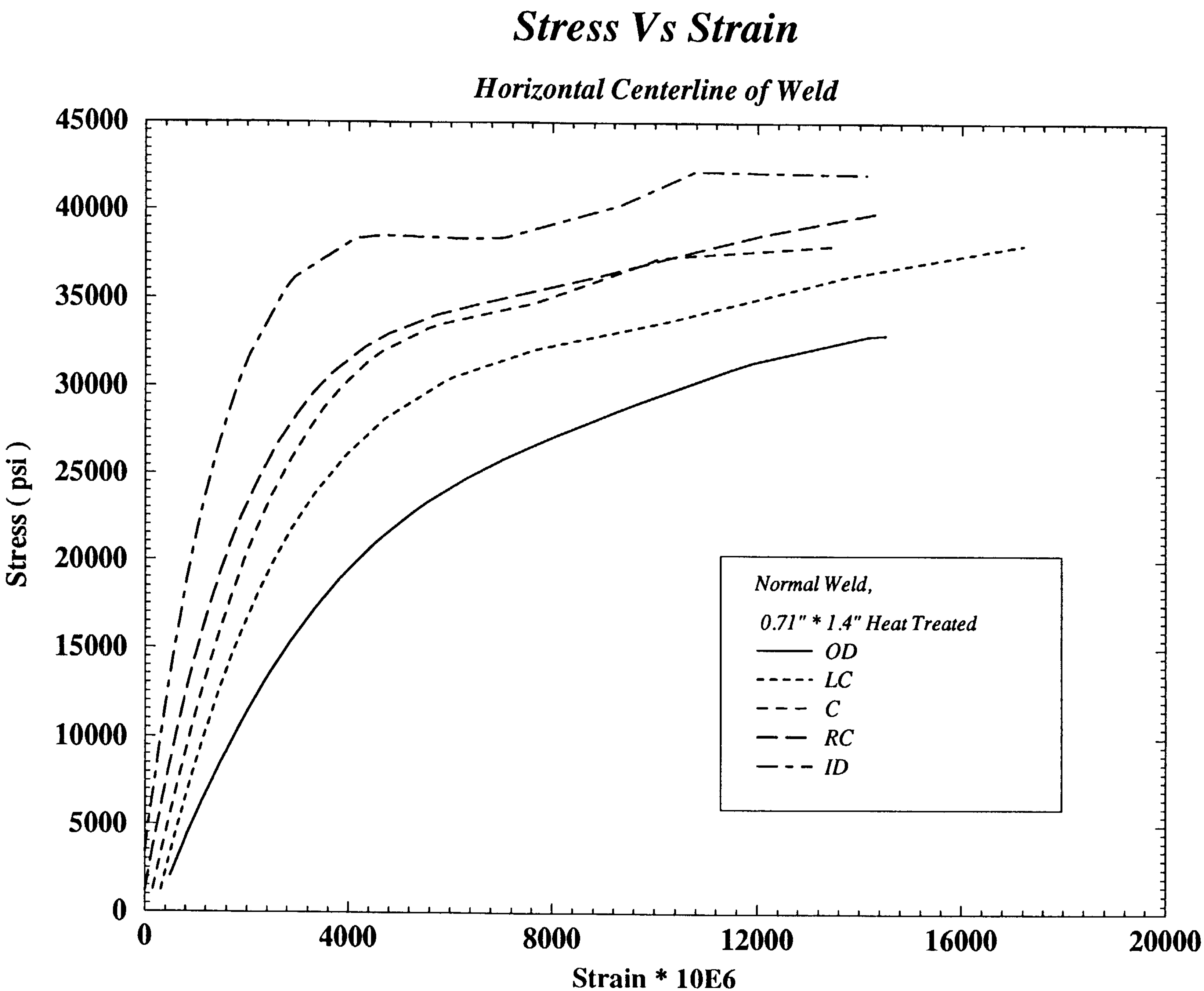

Figure 2-13. Material Behavior, Horizontal Centerline, NW

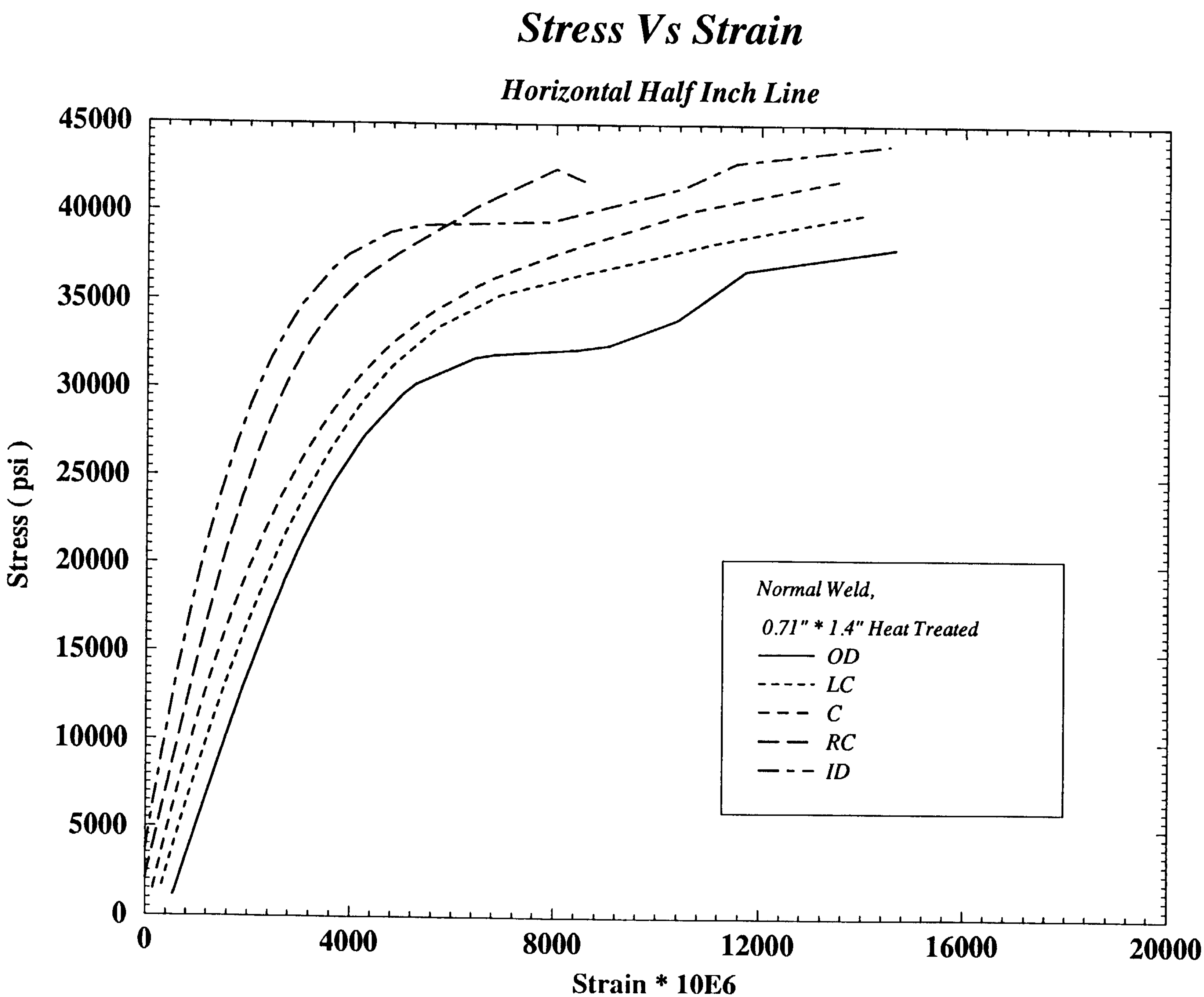

Figure 2-14. Material Behavior, Half Inch Line, NW

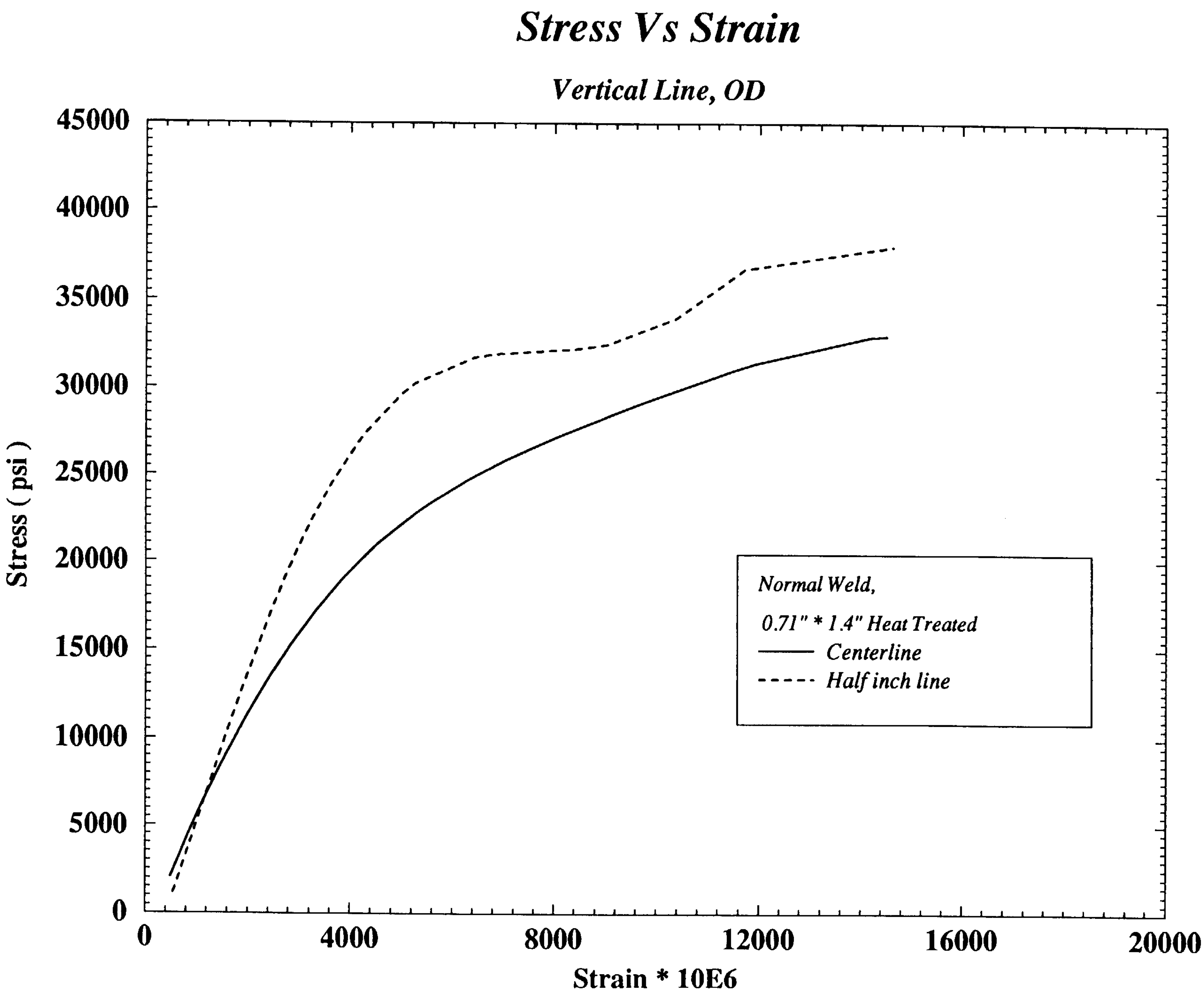

Figure 2-15. Material Behavior, Vertical OD Line, NW

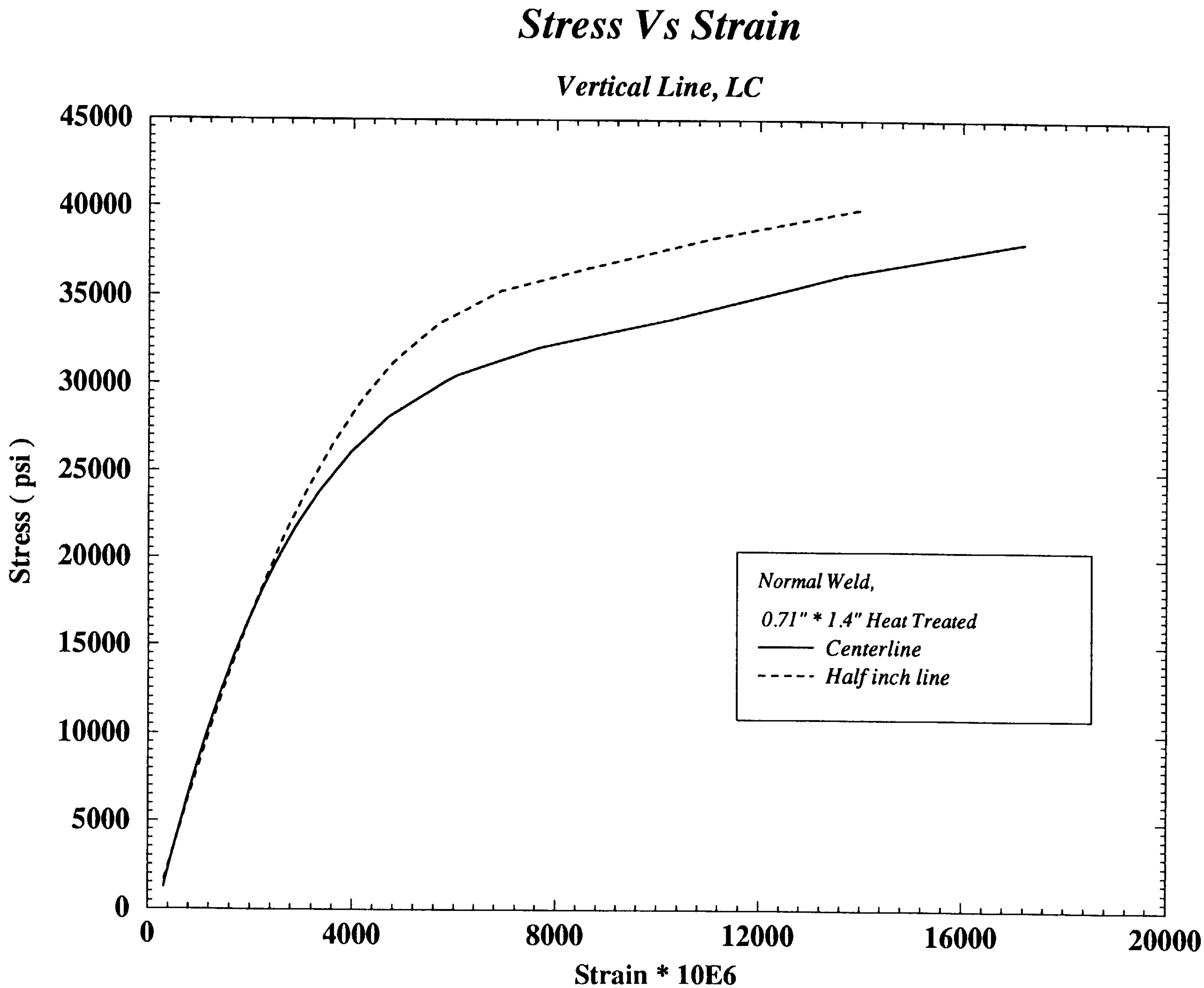

Figure 2-16. Material Behavior, Vertical LC Line, NW

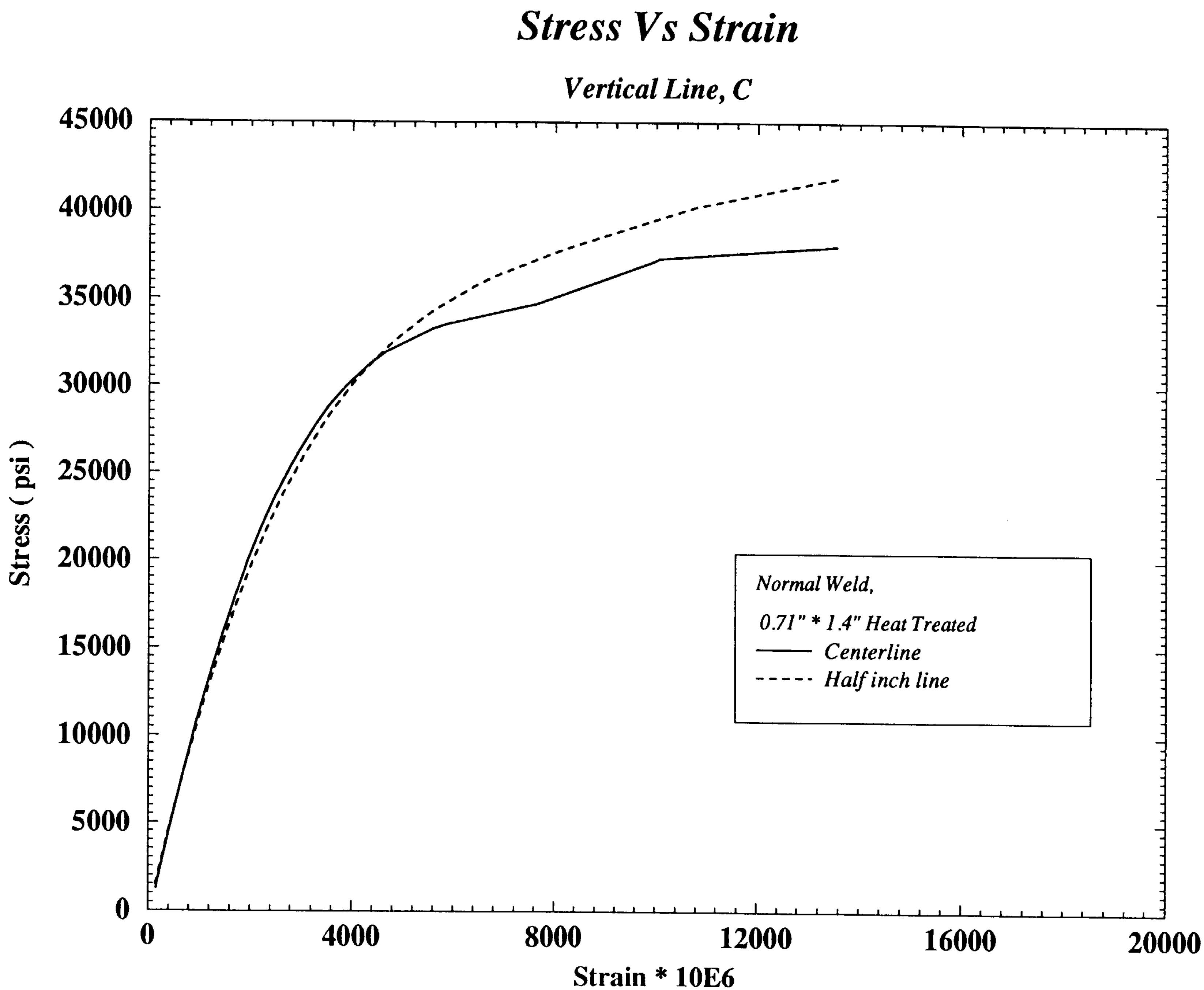

Figure 2-17. Material Behavior, Vertical C Line, NW

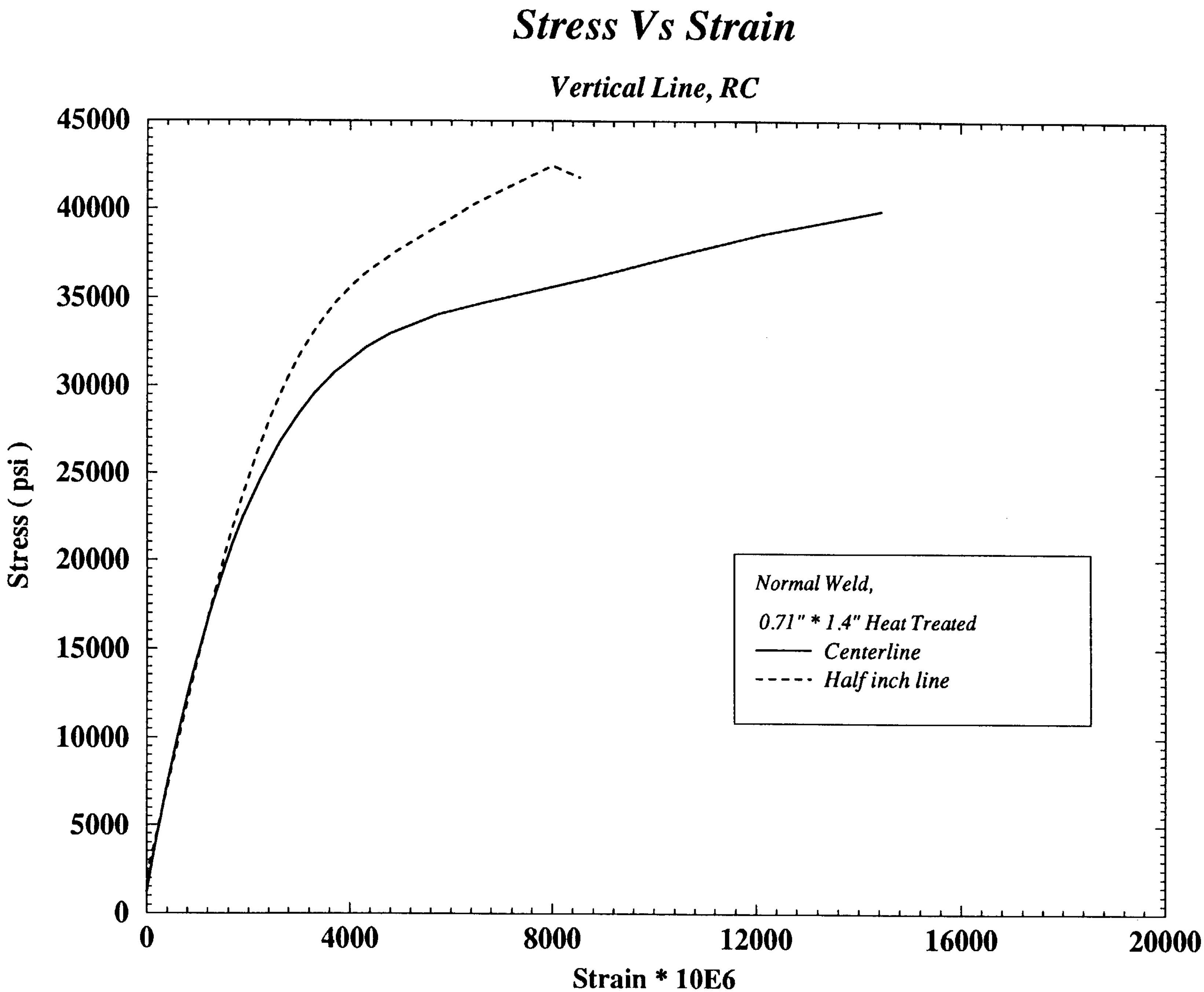

Figure 2-18. Material Behavior, Vertical RC Line, NW

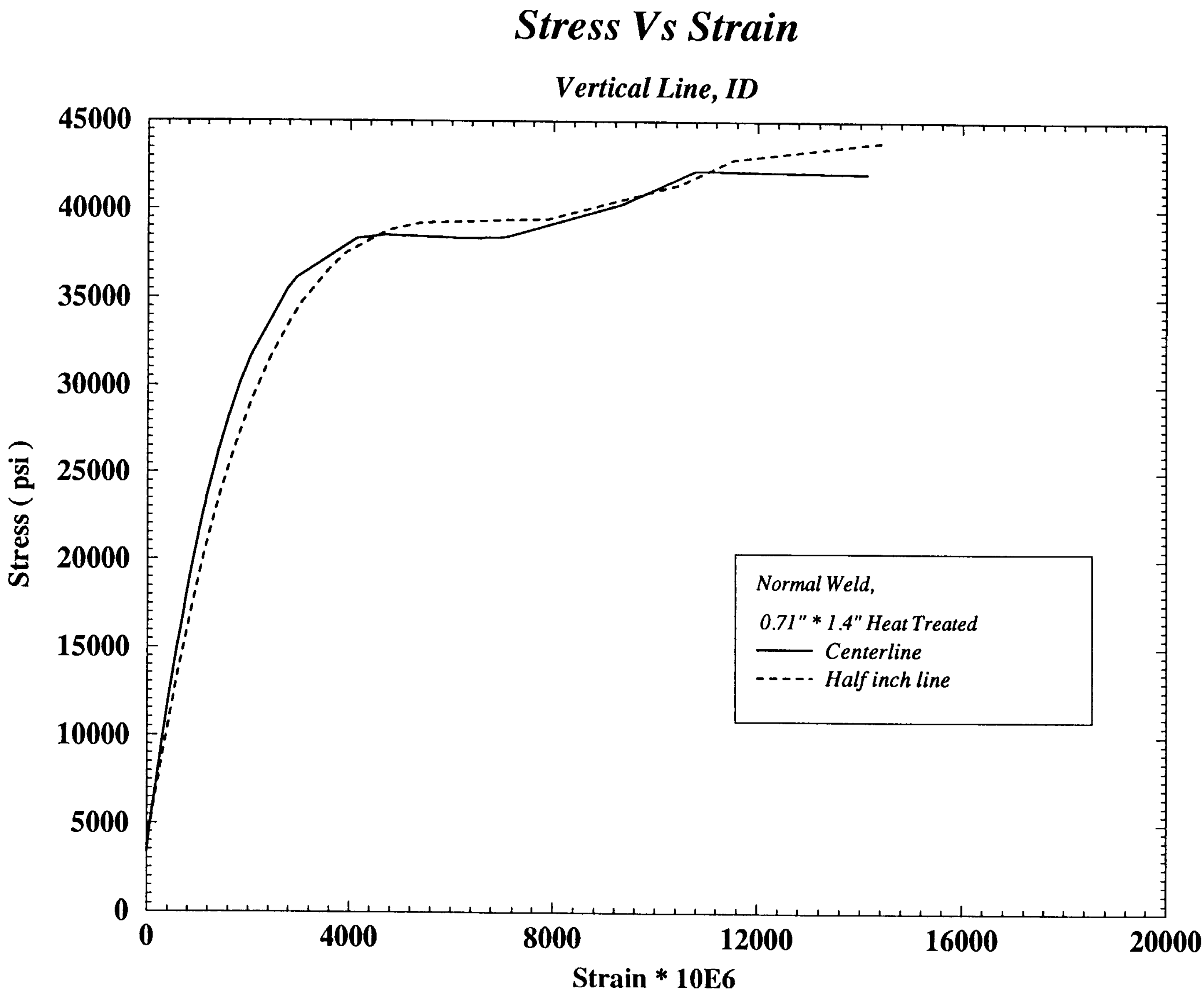

Figure 2-19. Material Behavior, Vertical ID Line, NW

zero stress. As in previous tests (2), and in current tests, the OD side of the joint was weaker and more ductile than the ID side. The general transition in strength and ductility from the OD to the ID side can be seen in Figures 2-13 and 2-14 for the centerline and half inch line respectively. Figures 2-15 through 2-19 indicate comparisons of material properties along vertical lines on the surfaces of the joint.

In Figure 2-19, it is seen that behavior at the two different points on the ID side of the joint is nearly identical. This same behavior was observed in previous tests on the ID side when Photostress, rather than strain gages, was used for measurement of strain (2). Referring to Photo 1-4, it may be noted that fringe orders on the ID side of the specimen at the centerline and the one-half inch line (lines zero and 2, respectively) are nearly the same at each stress value. Thus, Photostress fringe patterns on the through the weld surface are seen to validate measurements made by strain gages at the very near locations on the centerline and 1/2" line on the ID face of the joint.

Figures 2-20 and 2-21 show in-plane contraction ratios for various locations in the joint. At the ID point on the centerline of the weld (Figure 2-20), it is seen that the in-plane contraction ratio approaches 0.73 at approximately 21,000 psi plastic stress. Note the difference in contraction ratios between the OD point and the ID point on the centerline of the weld. There is much less in-plane contraction in the weaker material at the OD point than there is at the stronger ID point.

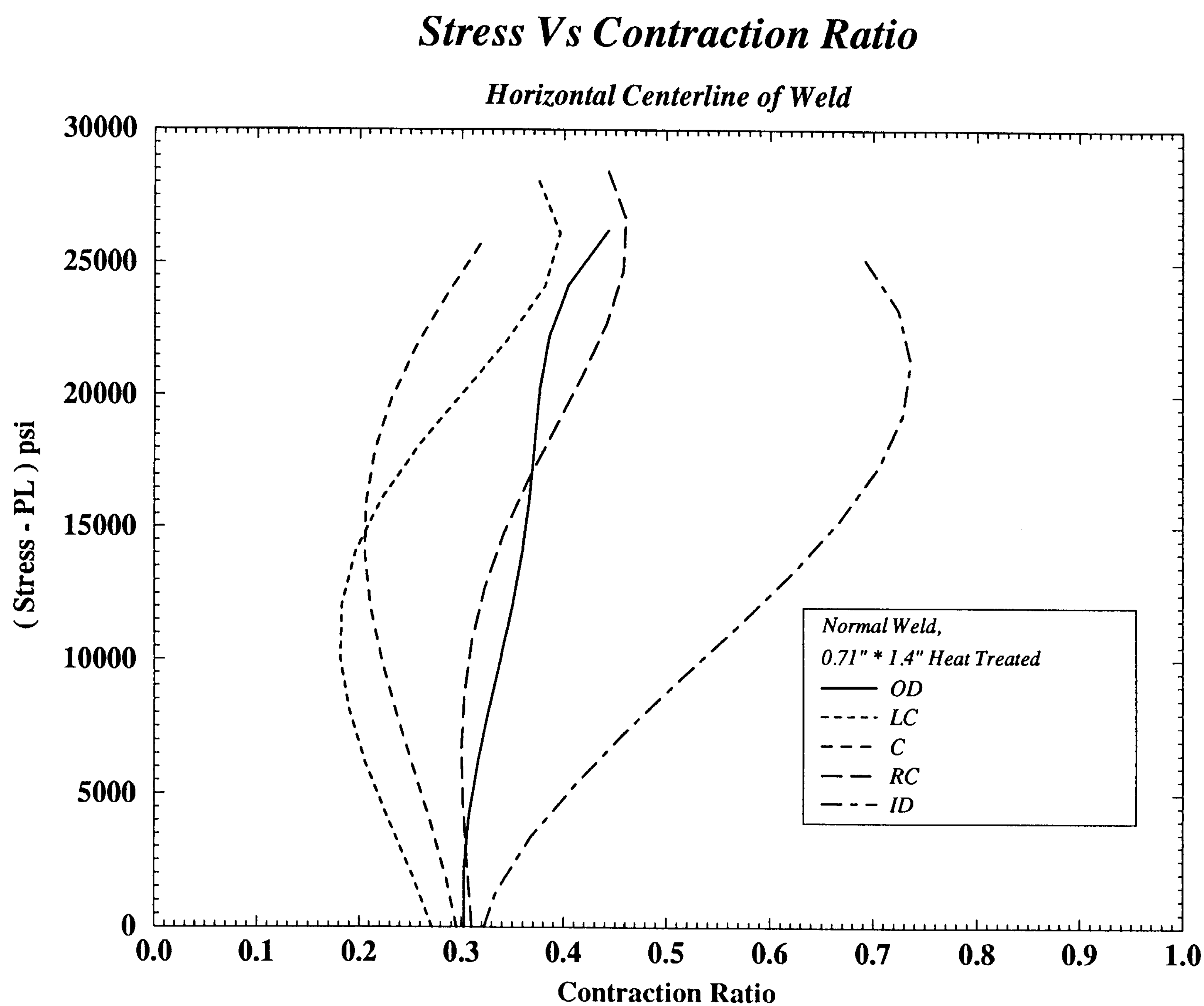

Figure 2-20. In-Plane Contraction Ratios, Horizontal Centerline, NW

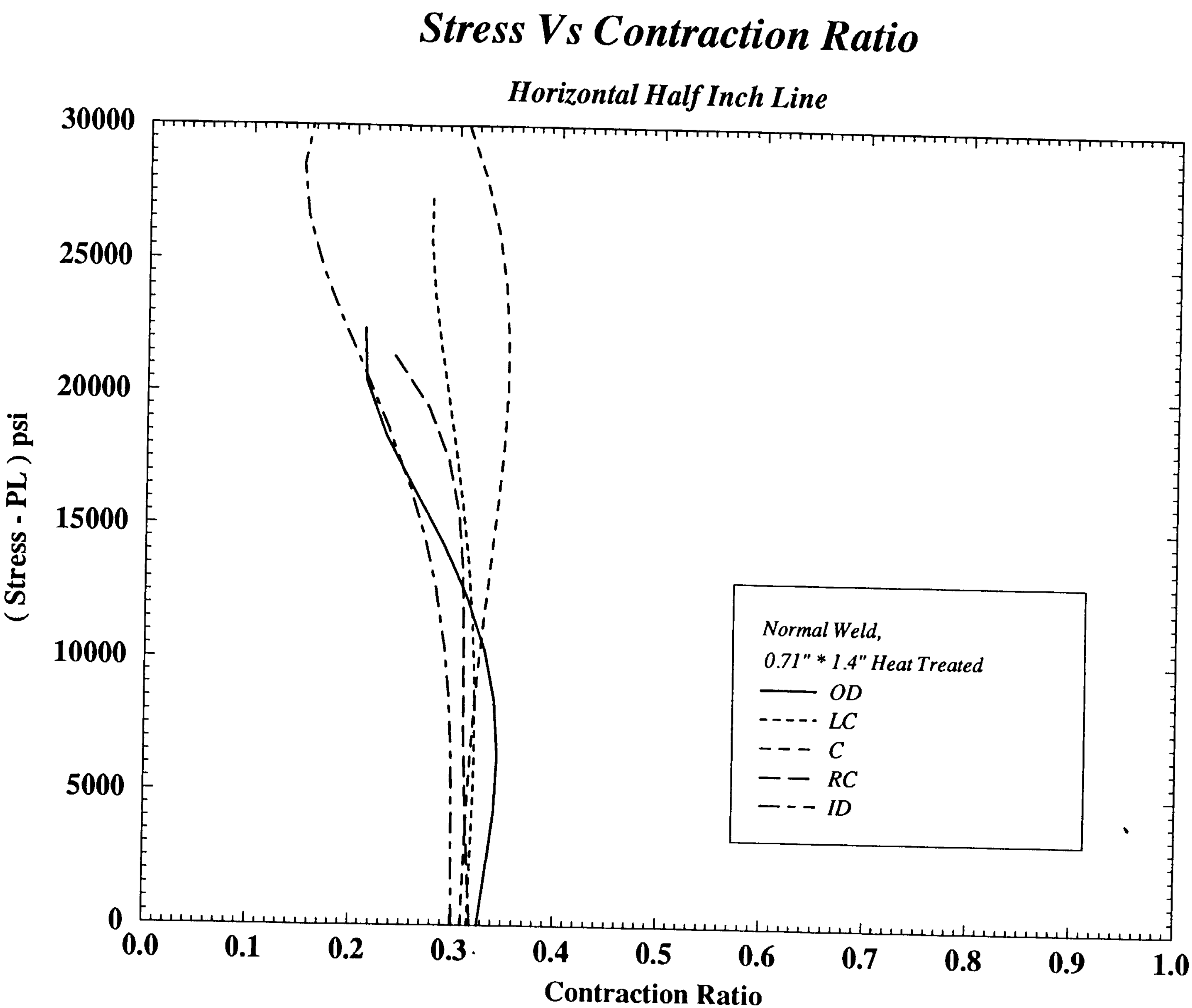

Figure 2-21. In-Plane Contraction Ratios, Half Inch Line, NW

As seen in Figure B15, data scatter was greater at the ID point than at other points with the greatest scatter being above a plastic stress of 13,000 psi. While there was more scatter, the trend seen in the data at the ID point from both specimens is the same and indicates quite large in-plane contraction at higher plastic stresses.

Out-of-plane contraction ratios are presented in Figures 2-22 and 2-23 for the horizontal centerline of the weld and the half inch line respectively. The smaller out-of-plane contraction ratios on the centerline at point ID can be seen in Figure 2-22 which correlate with the larger in-plane contraction ratios seen in Figure 2-20.

Graphs showing scatter of data for all tests of the 0.71" x 1.4" normal weld specimens are presented in Appendix B.

VII. RESULTS FROM TASK 3

A. Bending specimens

Panels made using normal welding procedures were machined into specimens for pure bending test (Figure 1). All specimens were peaked as seen in Photo 2 with the concavity being on the OD side. After receiving the panels from NASA, it was observed that parent material on the two sides of the weld had two different thicknesses, 1.375" and 1.410". During some part of the welding process, panels were apparently lined up on a flat surface thereby causing a shoulder to be formed across the top of the weld which connected the two pieces of parent material. Figure 3-1 is a sketch of the joint showing (a) the sloping shoulder across the top of the weld, (b) the centerlines of the two pieces

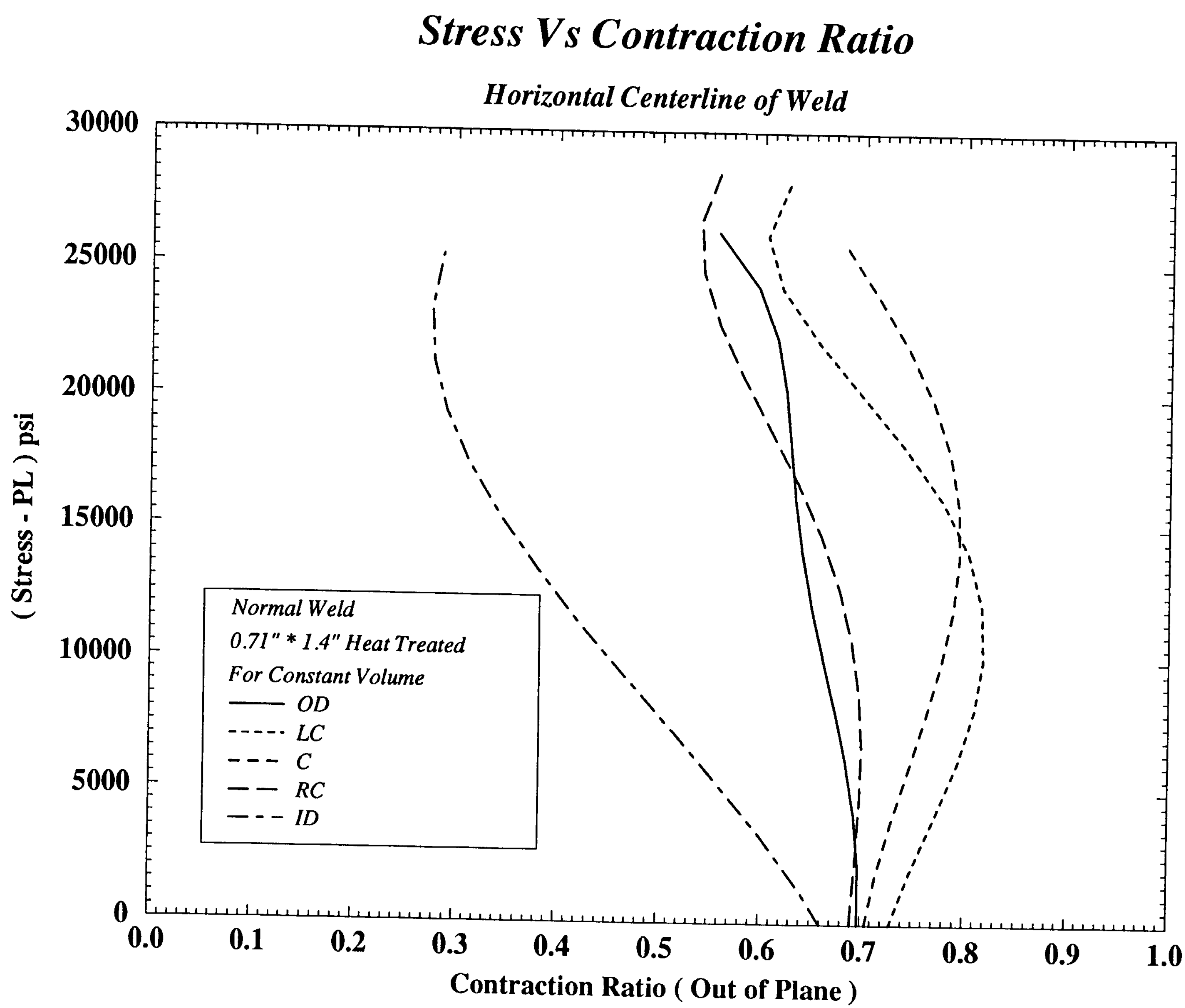

Figure 2-22. Out-of-Plane Contraction Ratios, Horizontal Centerline, NW

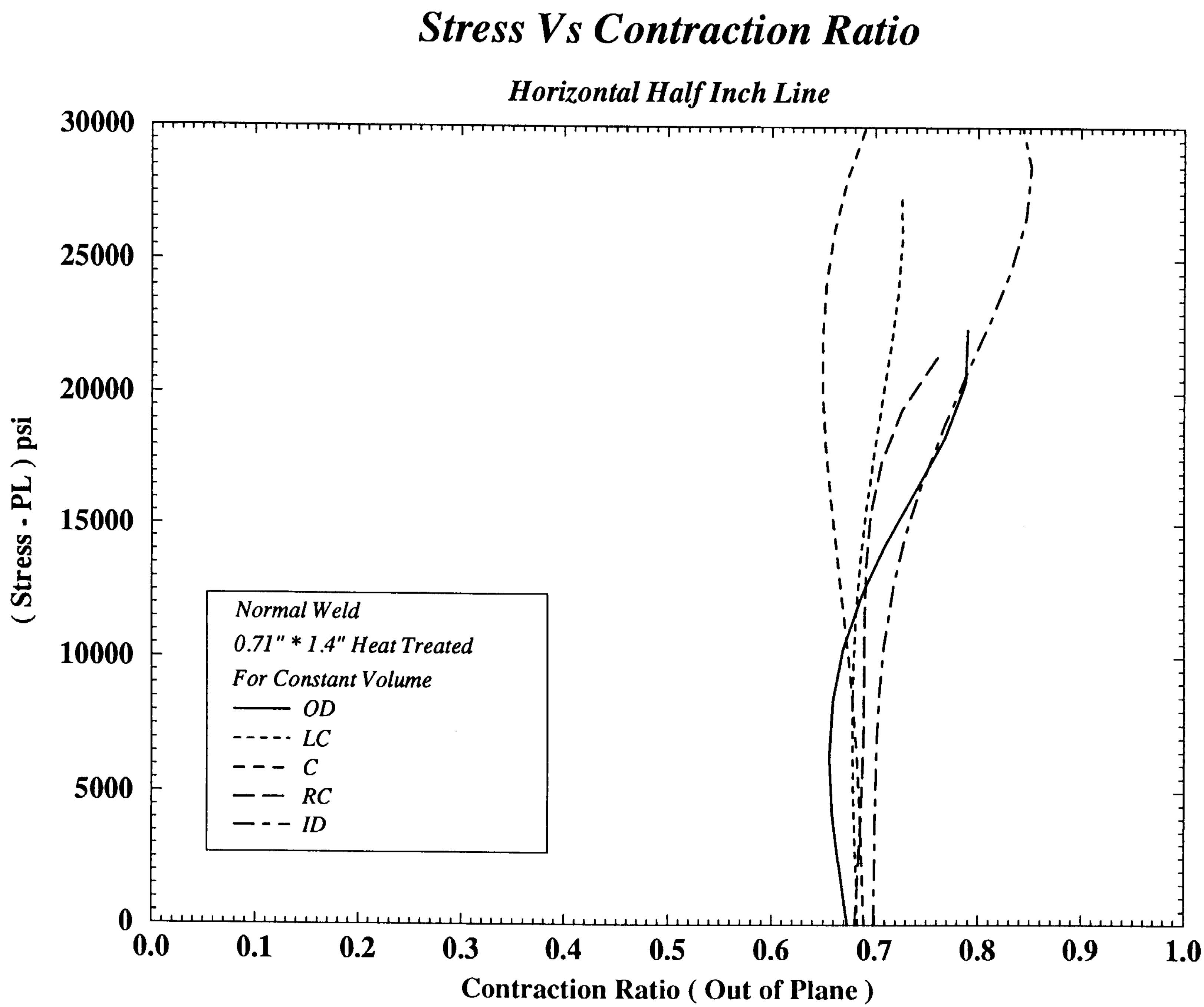

Figure 2-23. Out-of-Plane Contraction Ratios, Half Inch Line, NW

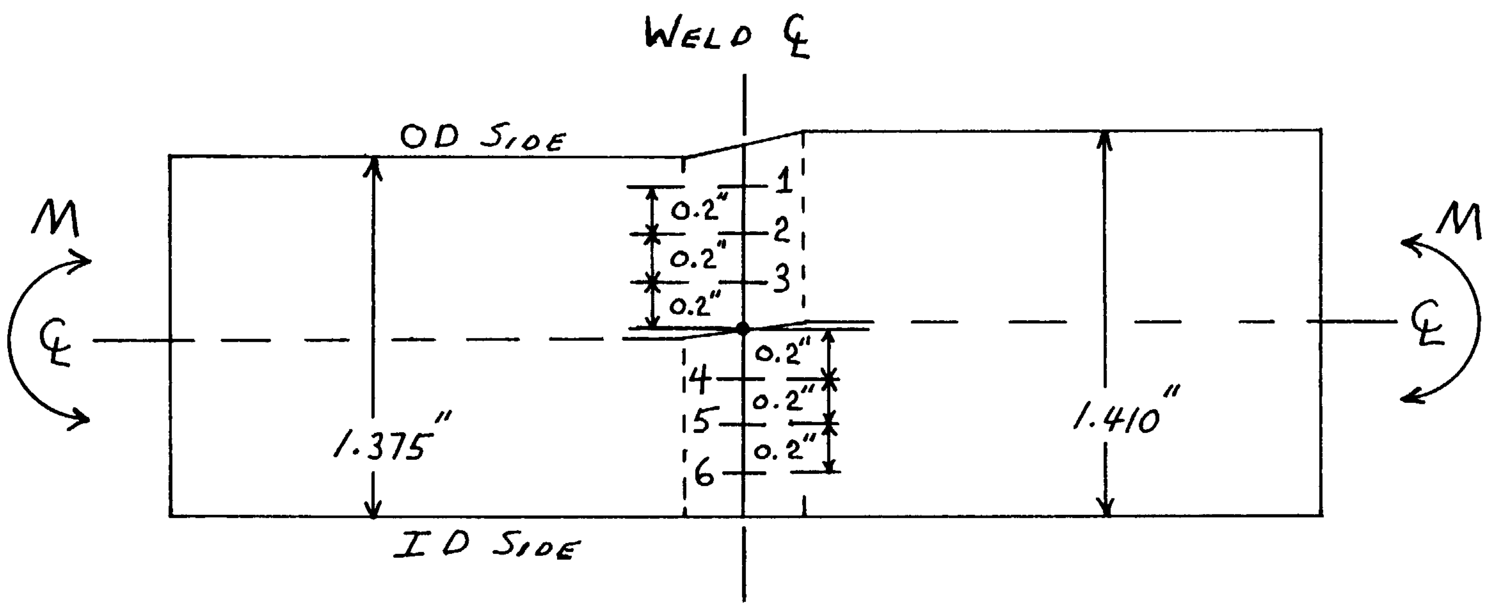

Figure 3-1. Sketch of Bending Specimen

of parent material, (c) the OD and ID sides in relation to the weld shoulder, (d) the directions of bending moment applied to the joint, (e) the approximate locations of the fusion boundaries (the vertical dotted lines), and (f) locations for data collection using Photostress. The point of reference for measurement to points where data were collected is the intersection of the vertical centerline of the weld with the sloping line connecting the two centerlines of each piece of parent material. All specimens had the weld shoulder on the OD side. The general shape of the fusion boundaries can be seen in Photo 1-3. Therefore, there was no clear, distinct division where weld and parent material joined as represented by the vertical dotted lines.

In graphs which follow, data collection points are always numbered 1 through 6. These numbers can also be seen in the photographs. Number 1 is always near the top of the specimen being tested for <u>both</u> conditions of the OD side in tension and the ID side in tension. As seen in Figure 3-1, points for data collection were equally spaced in 0.20 inch increments above and below the reference point. Thus, the topmost and bottommost points were approximately 0.10 inches from the upper and lower edges of each specimen respectively. In all tests, strains in material 1.375 inches thick at points along the fusion boundary near the intersection of the weld shoulder with the parent material were slightly larger than at similar points in 1.410" material.

B. OD Side in Tension

Figures 3-2 and 3-3 indicate behavior of weld material above and below the specimen centerline respectively. In the figures, the centerline is referred to as the "neutral axis." It can be seen that material at points above the specimen centerline (points 1,2,3) is more ductile than at corresponding points below the centerline (points 4,5,6). For reference, corresponding points are 1 and 6, 2 and 5, and 3 and 4 (See Figure 3-1). Figures 3-4 through 3-6 each show behavior at two corresponding points. If material in the weld exhibited the same behavior in both tension and compression, curves shown in Figures 3-4 through 3-6 would be coincident (or more nearly so). Figure 3-7 shows material behavior at the top (tension side) and bottom (compression side) of the specimen. Note also that measurements using strain gages indicate the difference in behavior between the weaker OD material and the stronger ID material.

Photo 3-1 shows fringe pattern development in specimen ODT-3 for moments between 6,120 and 17,895 inch pounds. Note the disappearance of the isotropic (black) line in the weld material as the moment increases. Photos 3-2 and 3-3 contain enlargements of fringe patterns in two different specimens, ODT-2 and ODT-3, at nearly the same moment. Note the similarities and differences in the patterns for the two specimens. The black isotropic point and isotropic line are clearly seen in these photographs. Also, note the difference in fringe patterns for points 4,5, and 6. In

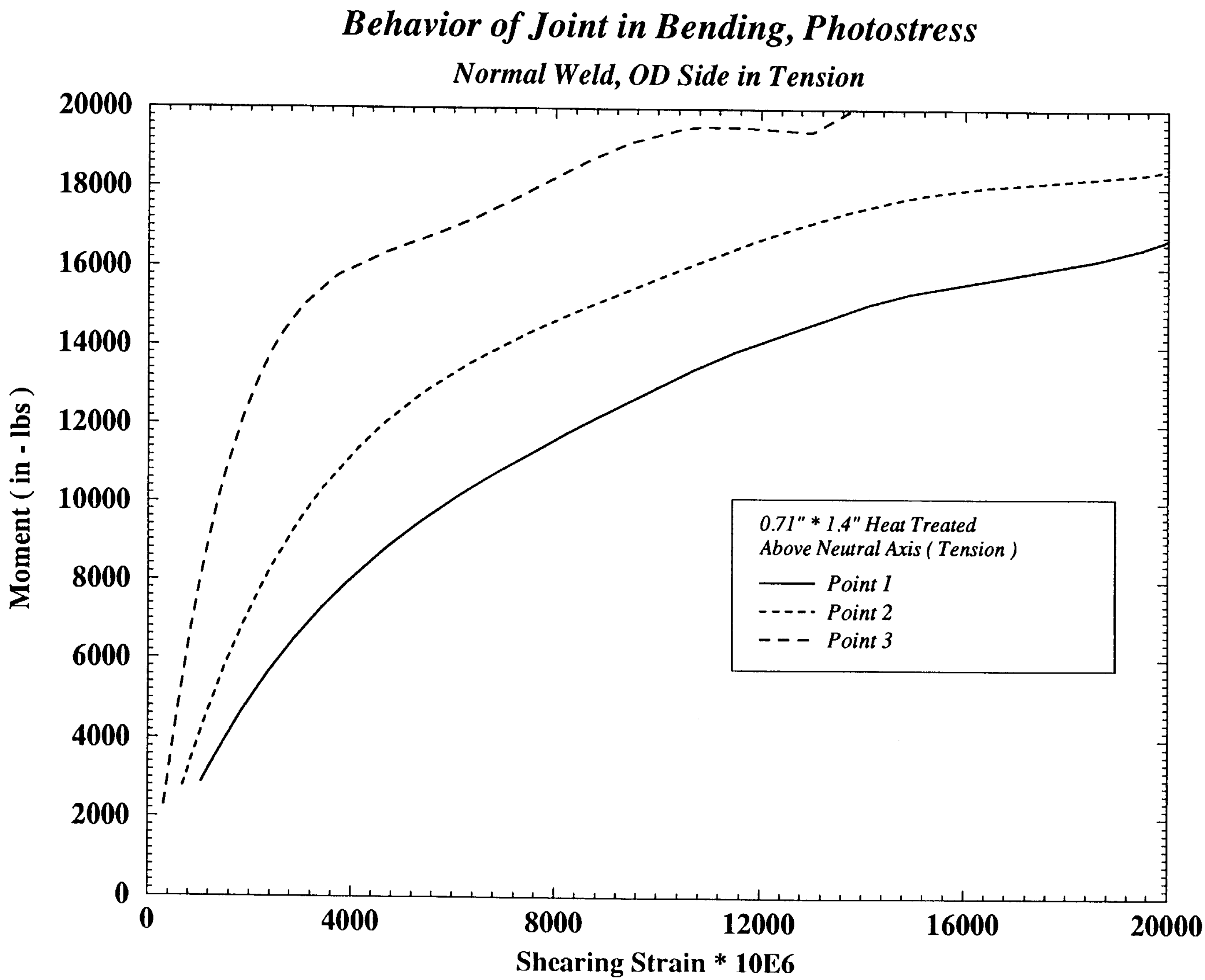

Figure 3-2. Material Behavior, OD Side Tension, Points 1,2,3.

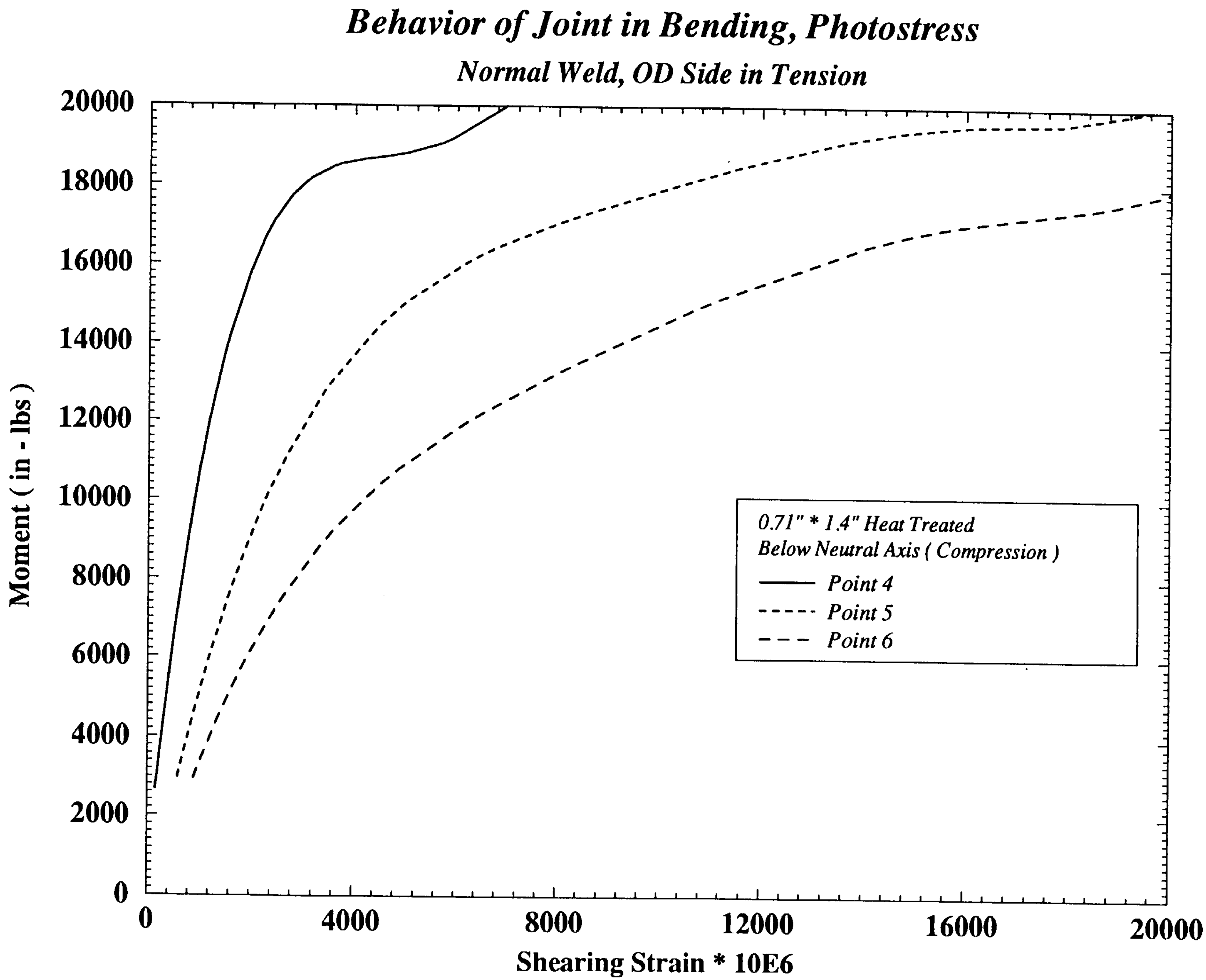

Figure 3-3. Material Behavior, OD Side Tension, Points 4,5,6

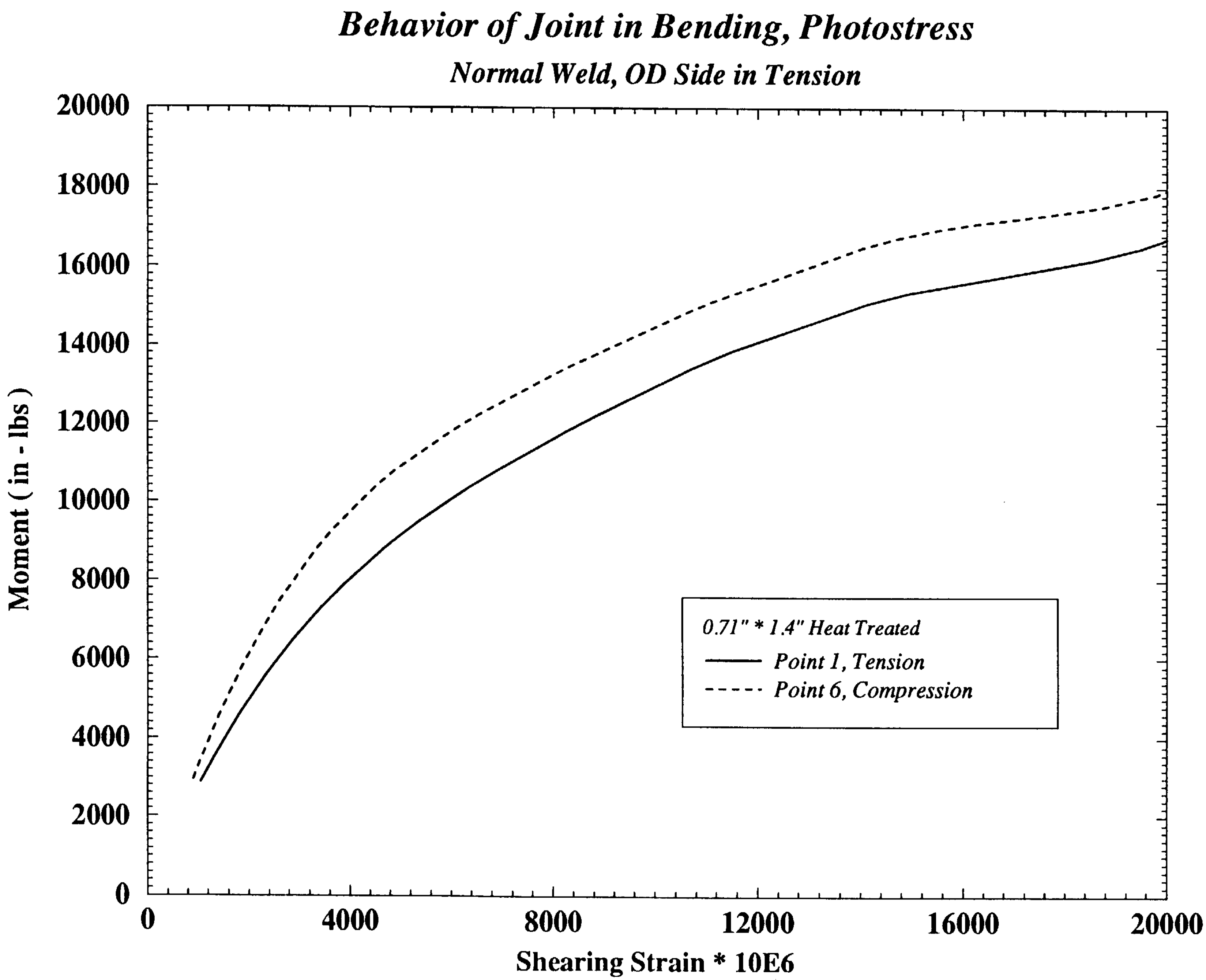

Figure 3-4. Material Behavior, OD Side Tension, Points 1,6

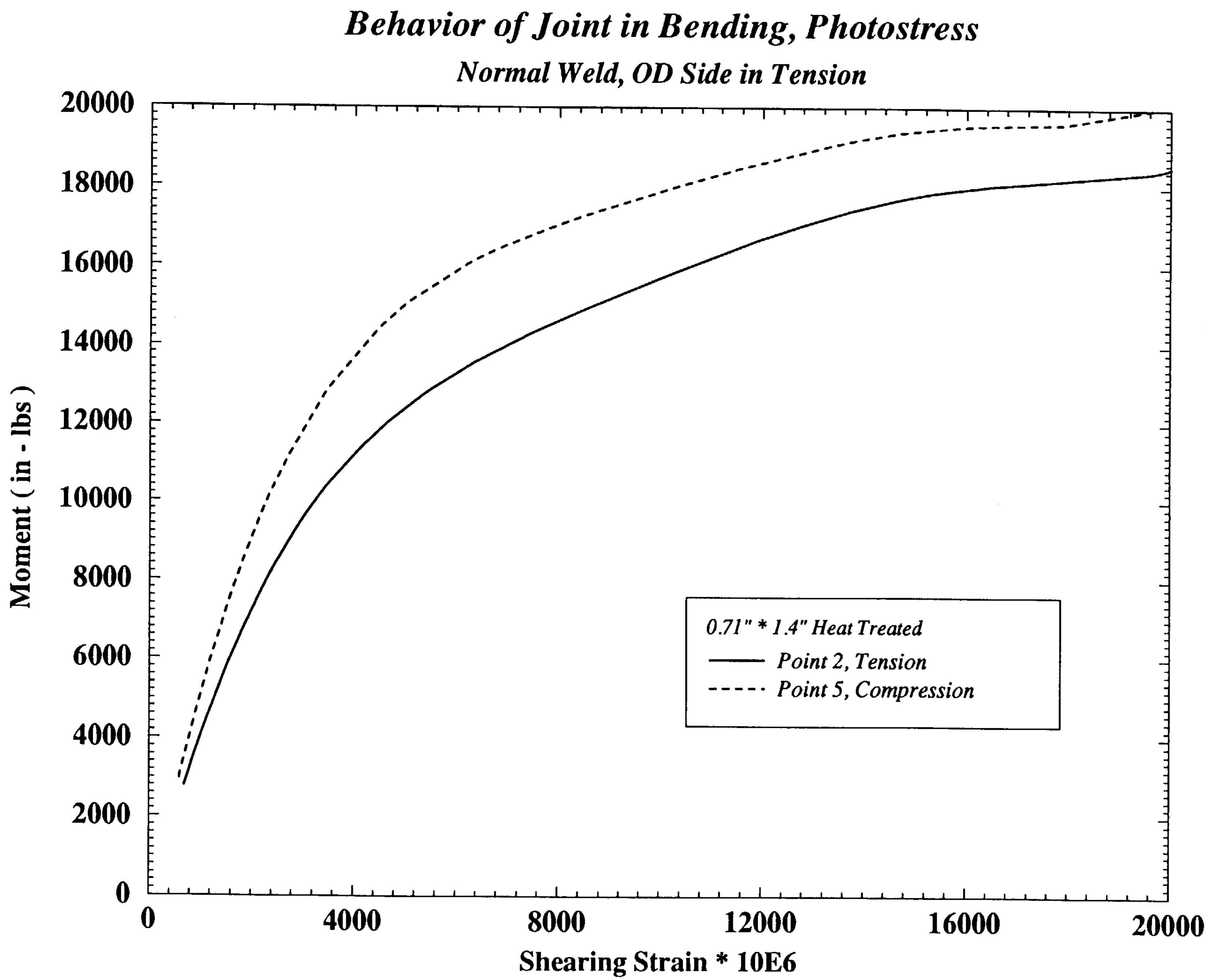

Figure 3-5. Material Behavior, OD Side Tension, Points 2,5

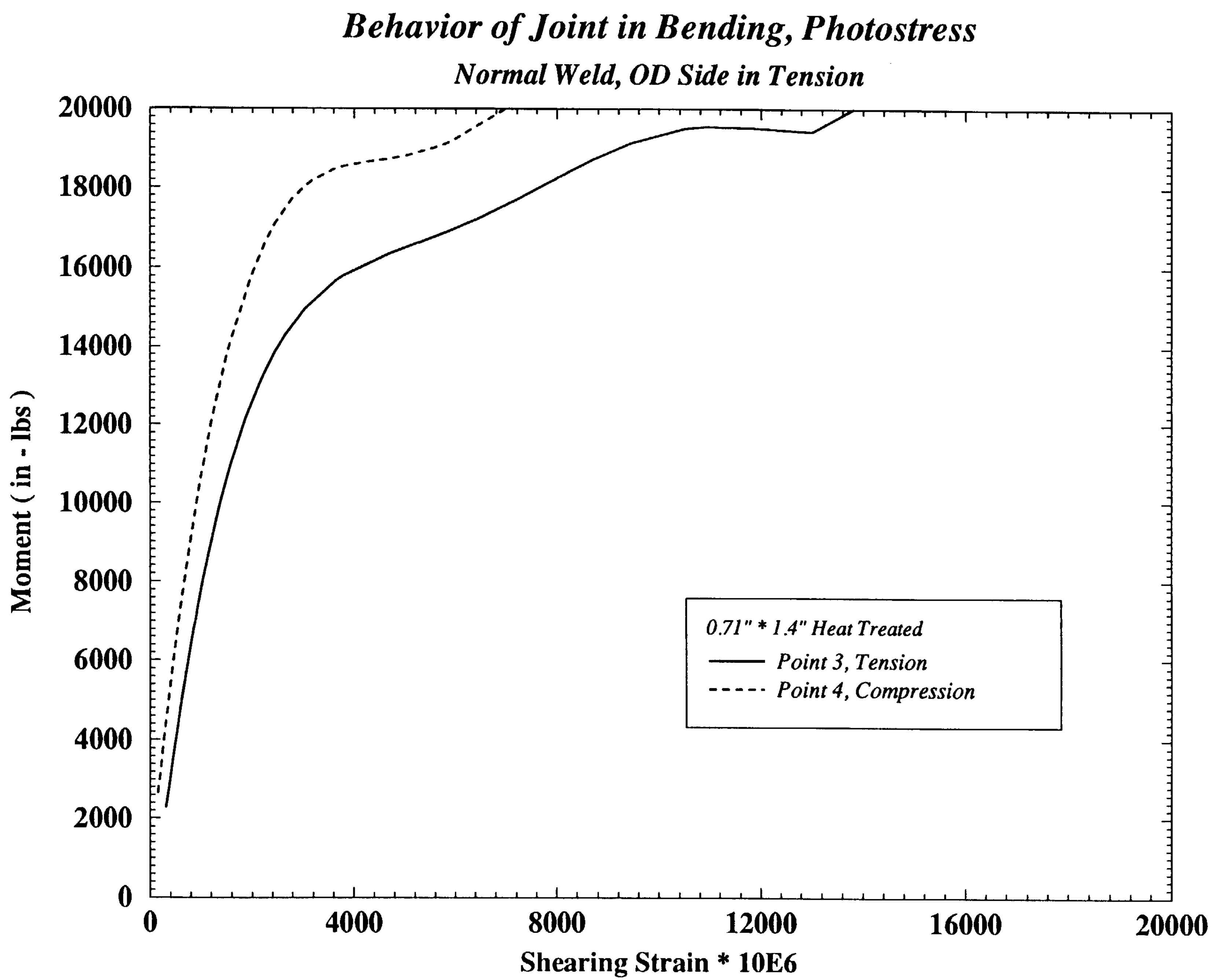

Figure 3-6. Material Behavior, OD Side Tension, Points 3,4

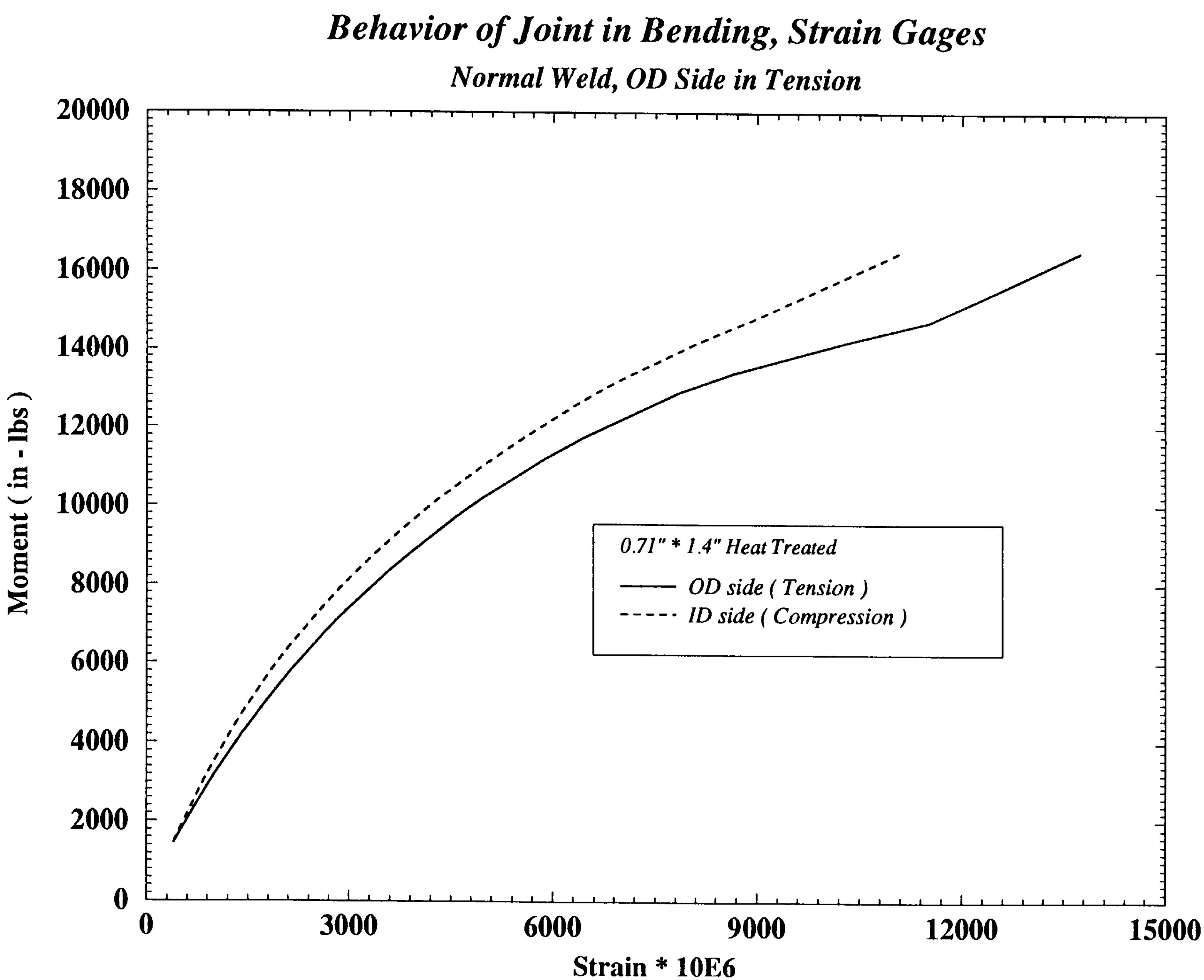

Figure 3-7. Material Behavior, OD Side Tension, OD and ID Sides

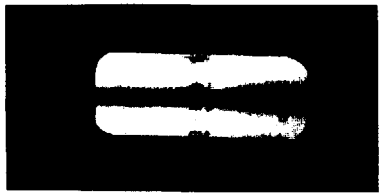

6,120 in-lbs

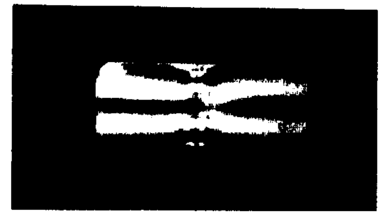

9,744 in-lbs

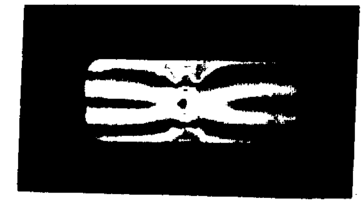

12,195 in-lbs

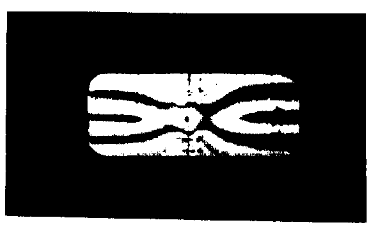

15,195 in-lbs

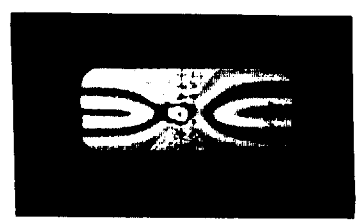

16,695 in-lbs

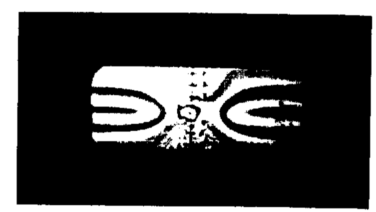

17,895 in-lbs

Photo 3-1. Fringe Pattern Development, Specimen ODT-3

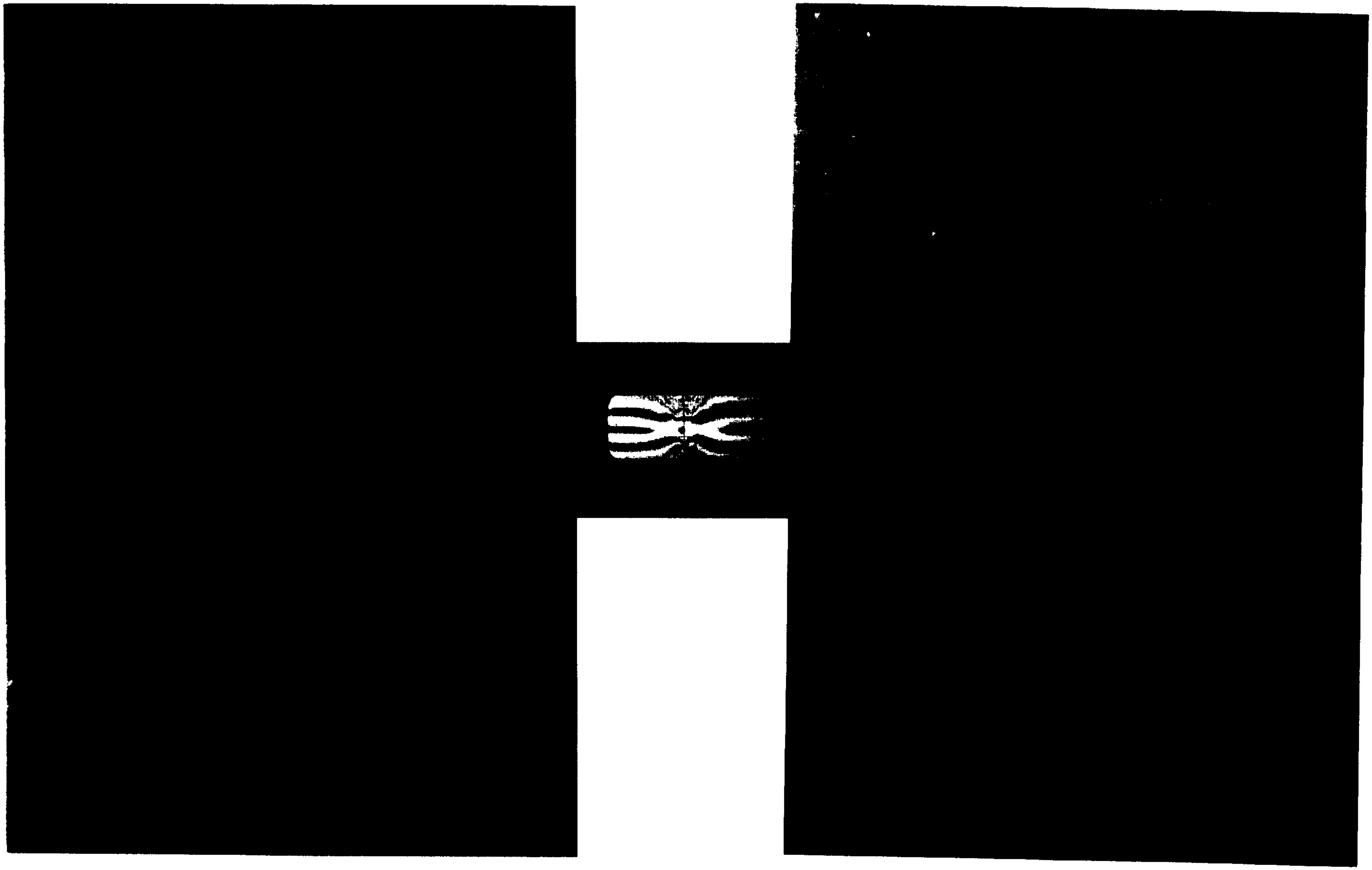

Photo 3-2. Fringe Pattern Detail, Specimen ODT-2, M=14,995 in-lbs

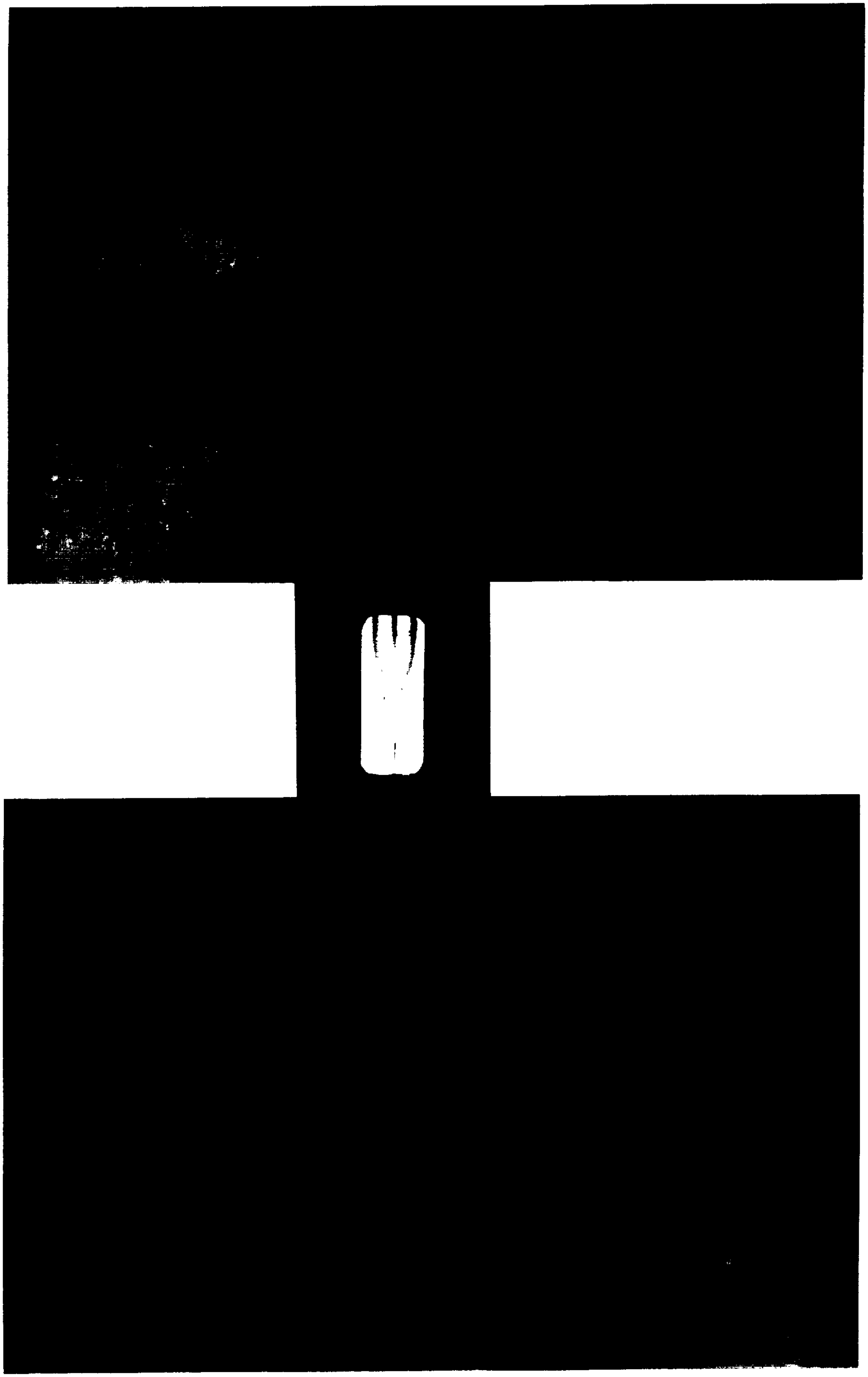

Photo 3-3. Fringe Pattern Detail, Specimen ODT-3, M=15,195 in-lbs

this region, strains in specimen ODT-3 are clearly larger than strains in specimen ODT-2 even though the moments are nearly the same.

C. ID Side in Tension

Figures 3-8 and 3-9 indicate behavior of weld material above and below the specimen centerline respectively. Again, it is seen that material in tension is somewhat more ductile than material in compression. However, Figures 3-10 through 3-12 indicate that, for the ID side in tension, there is less difference in behavior at corresponding points 1 and 6, 2 and 5, and 3 and 4 than there is for the OD side in tension. Therefore, placing the ID or strong side in tension has increased the uniformity in yielding of the joint. Figures 3-13 shows material behavior at the top and bottom of the specimens. Note that material in tension (the ID side) is more ductile than material in compression.

Photo 3-4 shows fringe pattern development in specimen IDT-1 for moments between 10,560 and 18,765 inch-pounds. Again, note that the isotropic line disappears as the moment increases leaving only the isotropic point on the weld centerline. Photos 3-5 and 3-6 present enlargements of fringe patterns in two different specimens, IDT-1 and IDT-2, at nearly the same moment. Note that these two photos are nearly identical indicating that tests having the ID or strong side in tension are somewhat more repeatable than tests having the OD or weak side in tension.

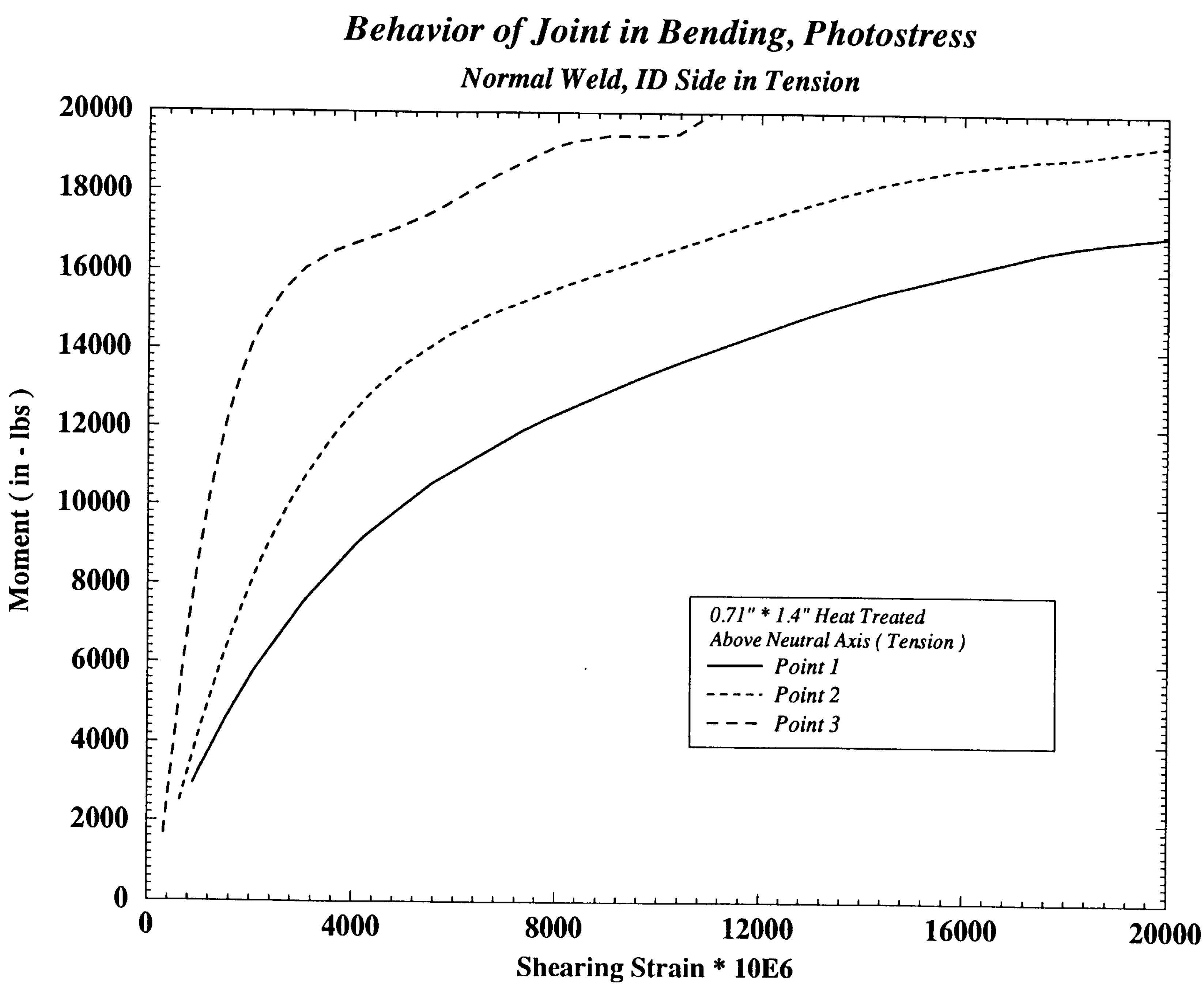

Figure 3-8. Material Behavior, ID Side Tension, Points 1,2,3

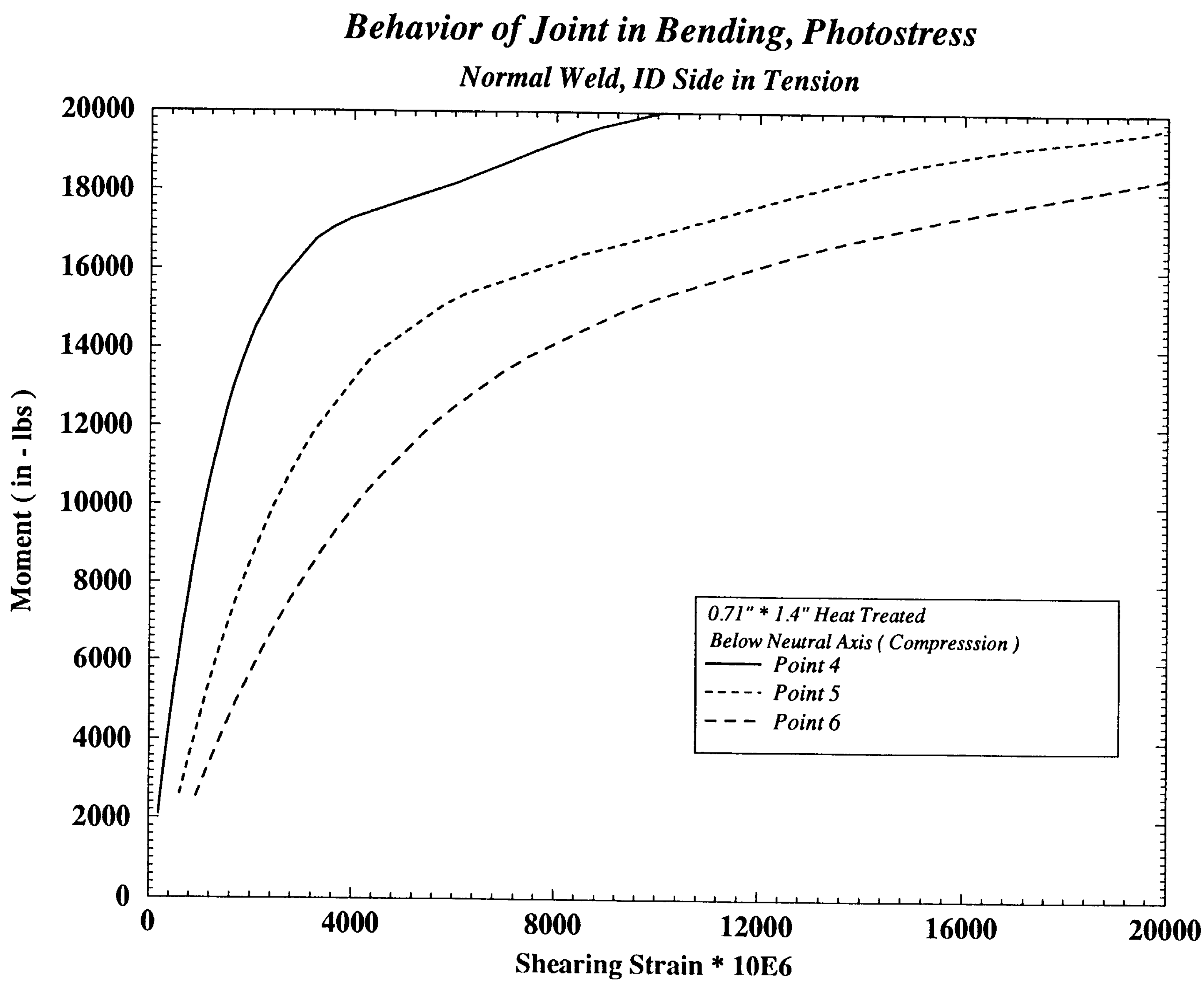

Figure 3-9. Material Behavior, ID Side Tension, Points 4,5,6

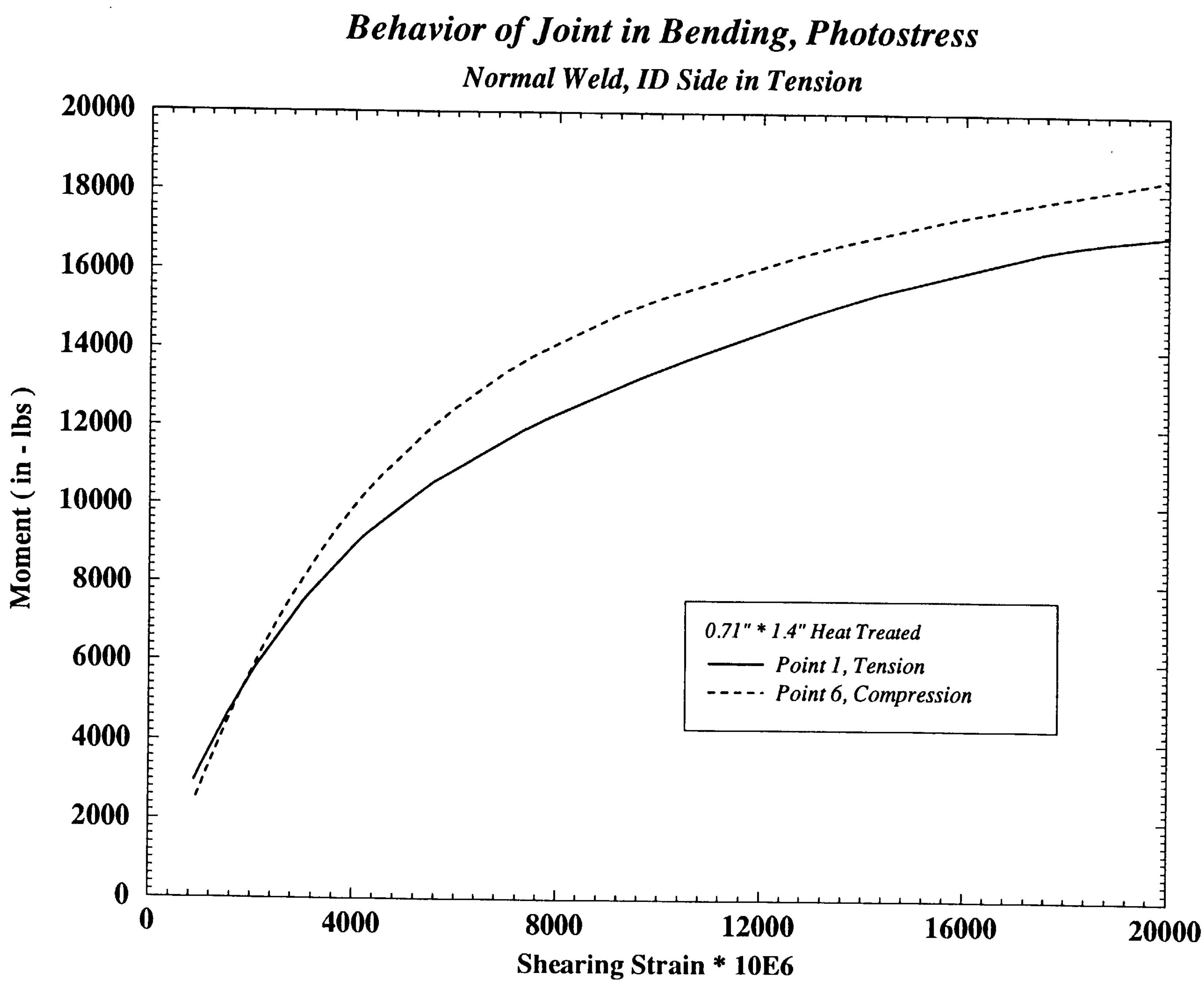

Figure 3-10. Material Behavior, ID Side Tension, Points 1,6

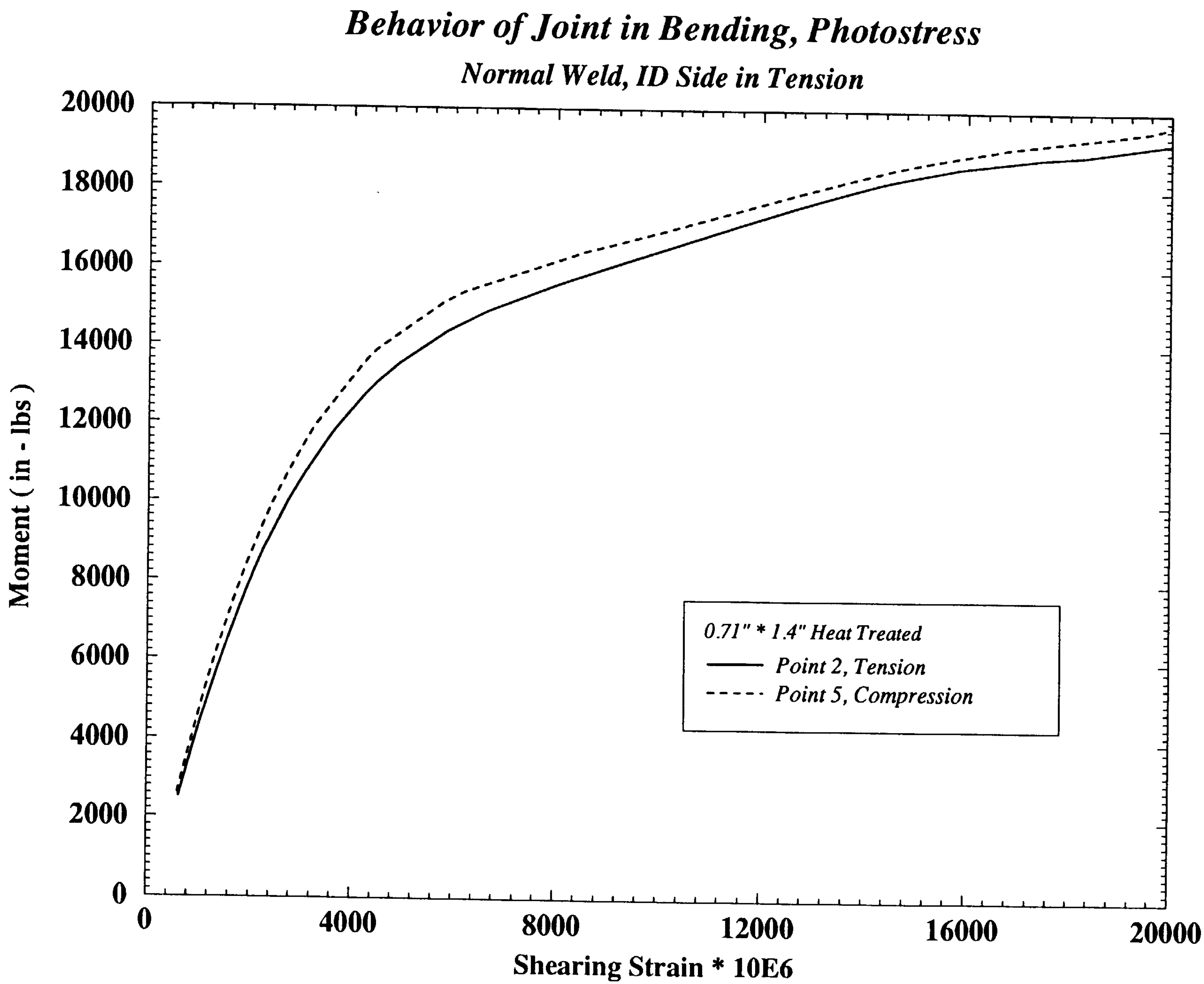

Figure 3-11. Material Behavior, ID Side Tension, Points 2,5

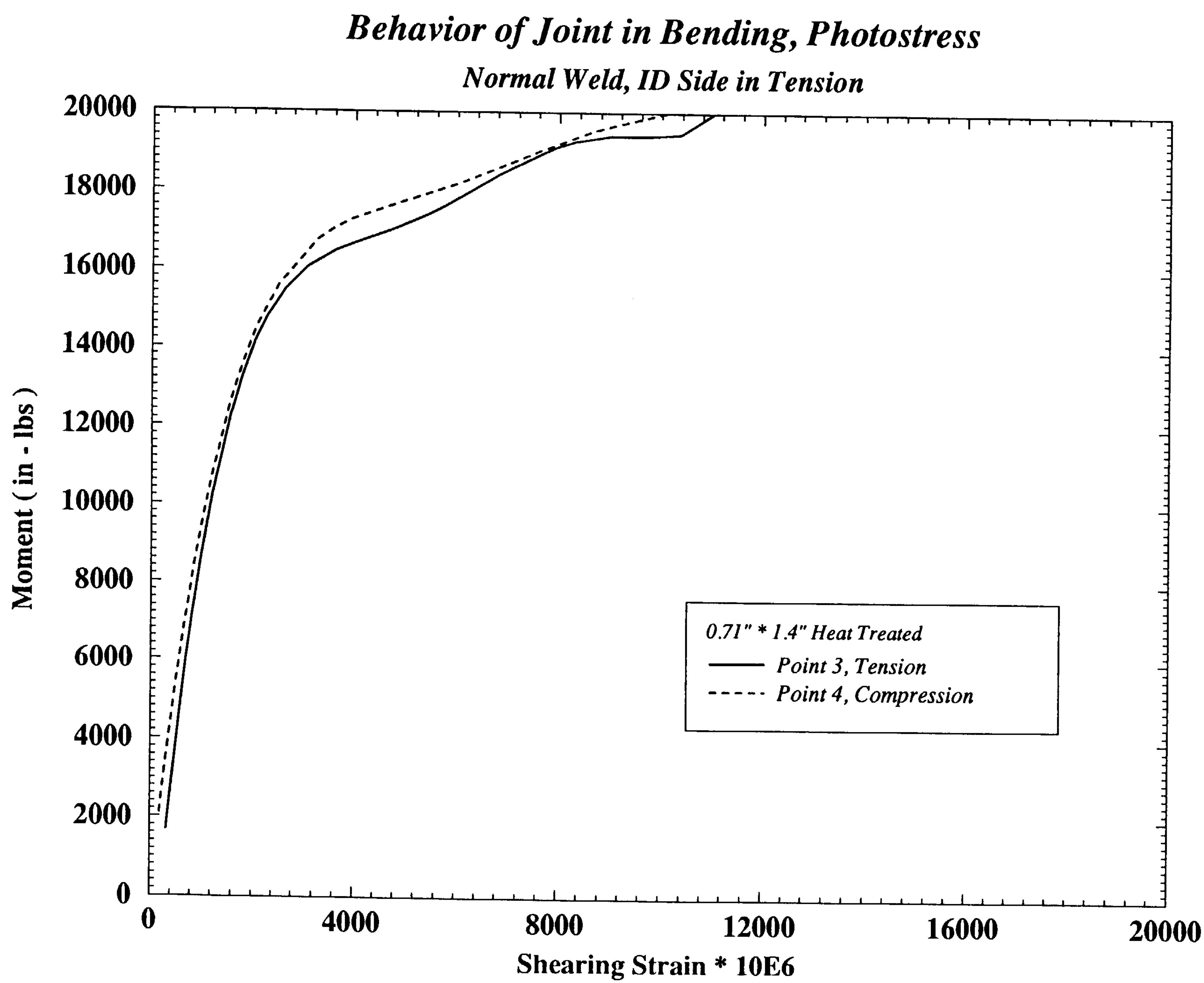

Figure 3-12. Material Behavior, ID Side Tension, Points 3,4

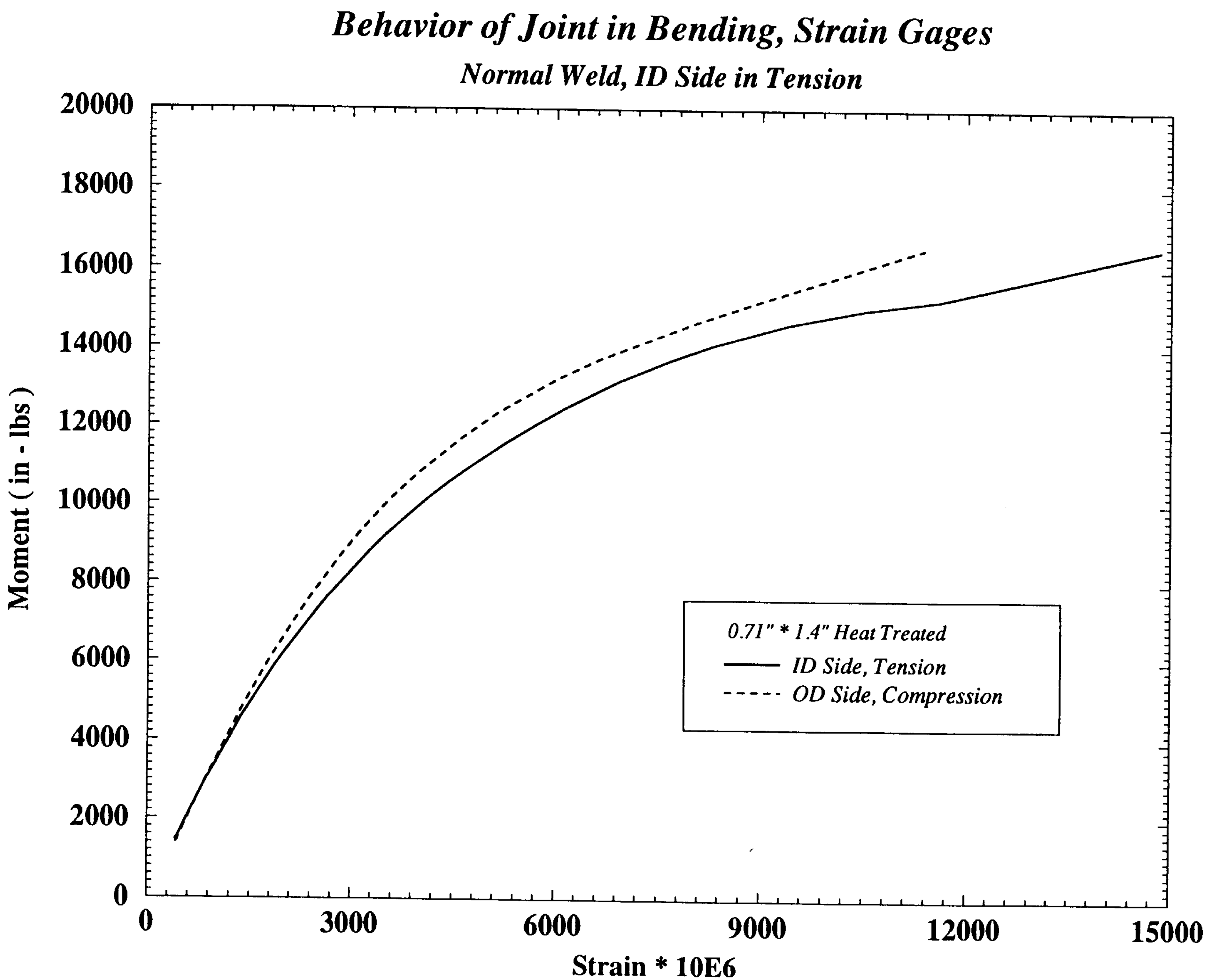

Figure 3-13. Material Behavior, ID Side Tension, OD and ID Sides

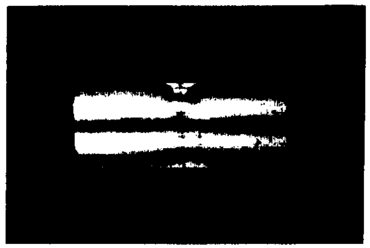

10,560 in-lbs

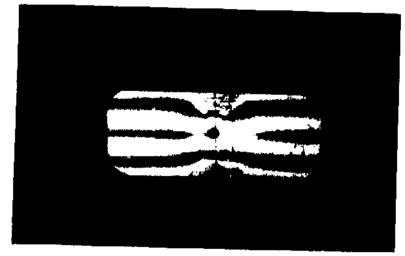

13,590 in-lbs

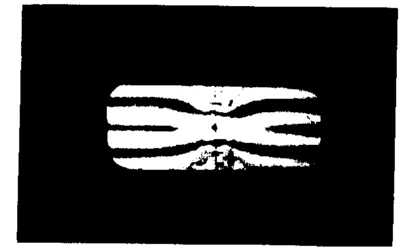

15,135 in-lbs

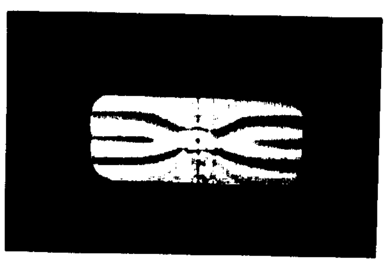

16,680 in-lbs

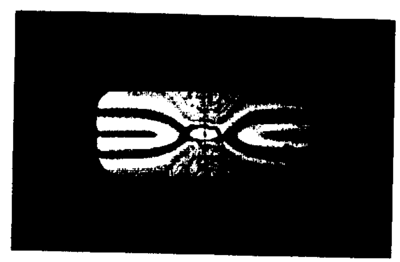

18,165 in-lbs

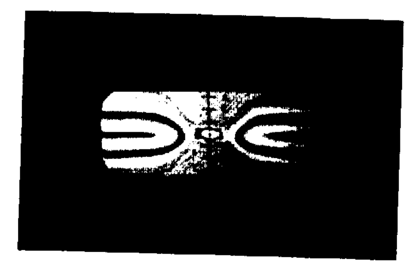

18,765 in-lbs

Photo 3-4. Fringe Pattern Development, Specimen IDT-1

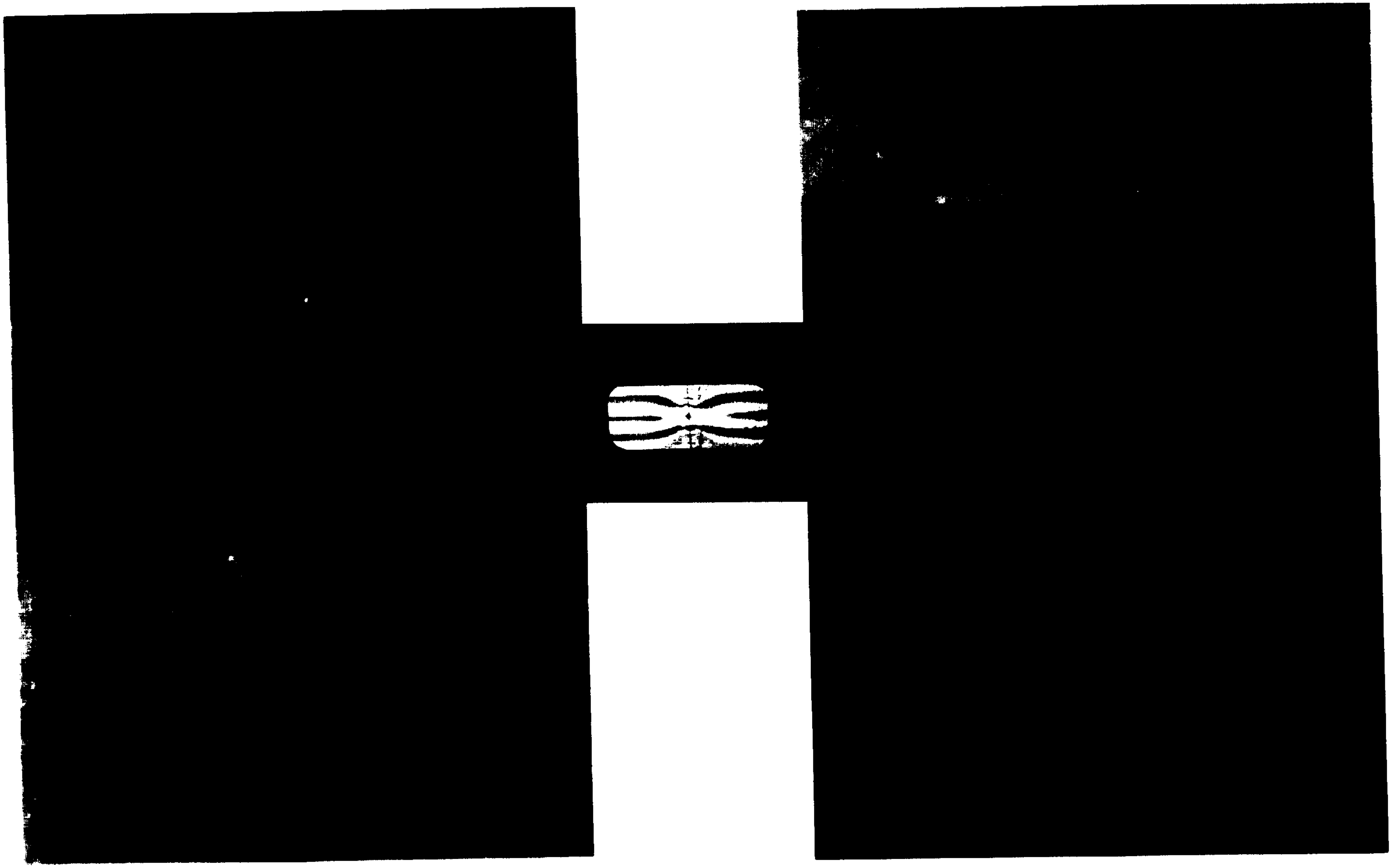

Photo 3-5. Fringe Pattern Detail, Specimen IDT-1, M=15,135 in-lbs

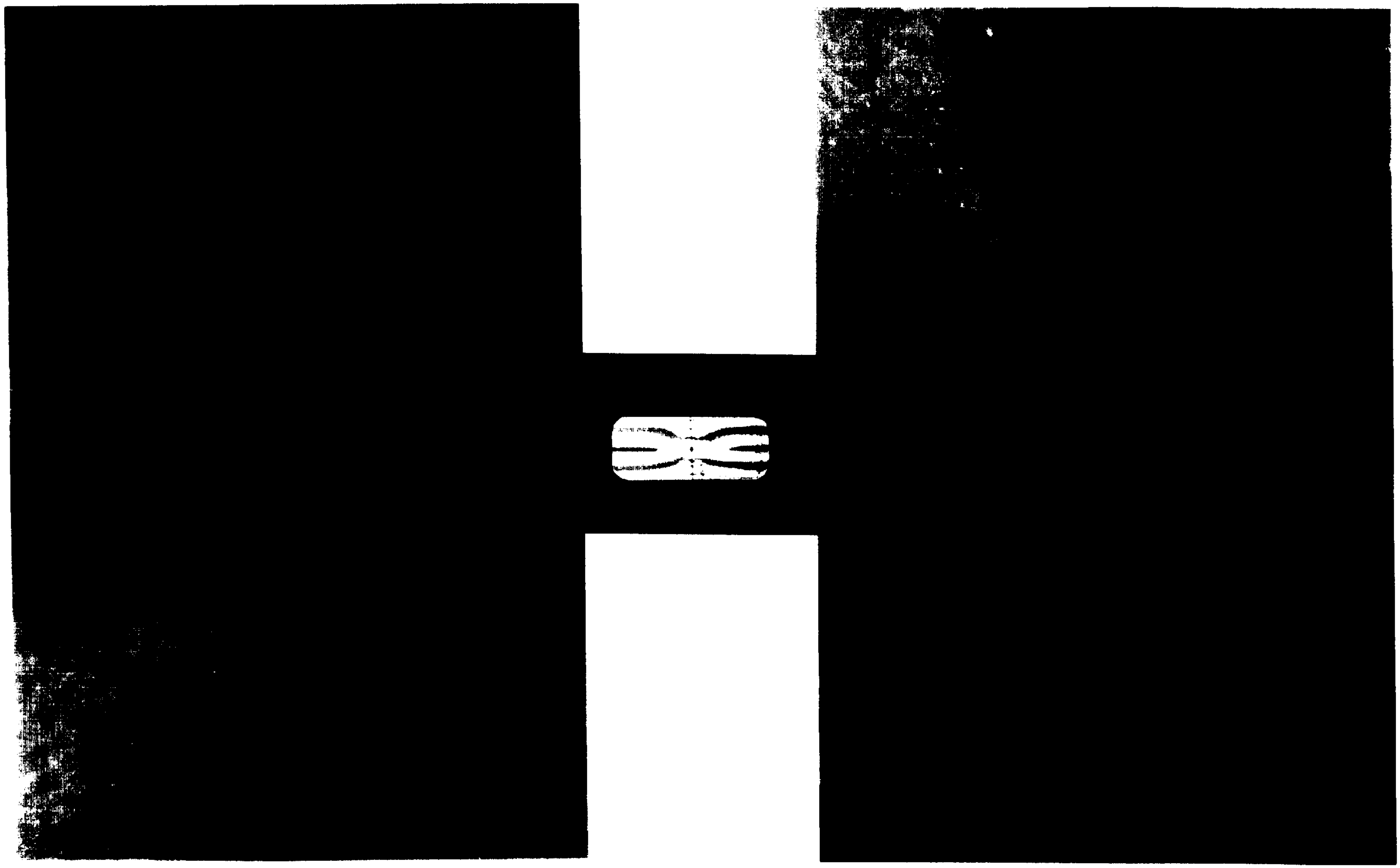

Photo 3-6. Fringe Pattern Detail, Specimen IDT-2, M=15,045 in-lbs

D. Comparison of OD and ID Behavior

Photo 3-7 from specimen ODT-3 can be compared with Photo 3-8 from specimen IDT-1 to see the effects of changing the weak side of the weld (the OD side) from a state of tensile stress to a state of compressive stress. In Photo 3-7, points 1, 2, and 3 are in tension. The first order fringe is located approximately at point 3 with several higher order fringes seen in the vicinity of points 2 and 1. In Photo 3-8, points 4, 5, and 6 (the same points as 1, 2, and 3 in Photo 3-7) are in compression. Note in Photo 3-8 that the first order fringe is located approximately half way between points 4 and 5 and that there are fewer higher order fringes in the vicinity of points 5 and 6. Therefore, as the photographs indicate, material on the weak side of the welded joint has higher strains when placed in tension (Photo 3-7) than it does when placed in compression (Photo 3-8).

In a similar manner, material on the strong side of the joint (points 4, 5, and 6 in Photo 3-7 and points 1, 2, and 3 in Photo 3-8) exhibits somewhat dissimilar fringe patterns that indicate the same trend. However, at the most strained points, point 6 in Photo 3-7 and point 1 in Photo 3-8, there are fringe orders of nearly equal value. Therefore, at these two points, tensile and compressive strains are more nearly the same.

Figures 3-14 through 3-16 indicate behavior at three separate points (1,2,3) in the weak OD side material in tension and compression. Note that, at all points, material is stronger and less ductile when placed in compression than it is when placed in tension. Figures 3-17 through 3-19 indicate that the

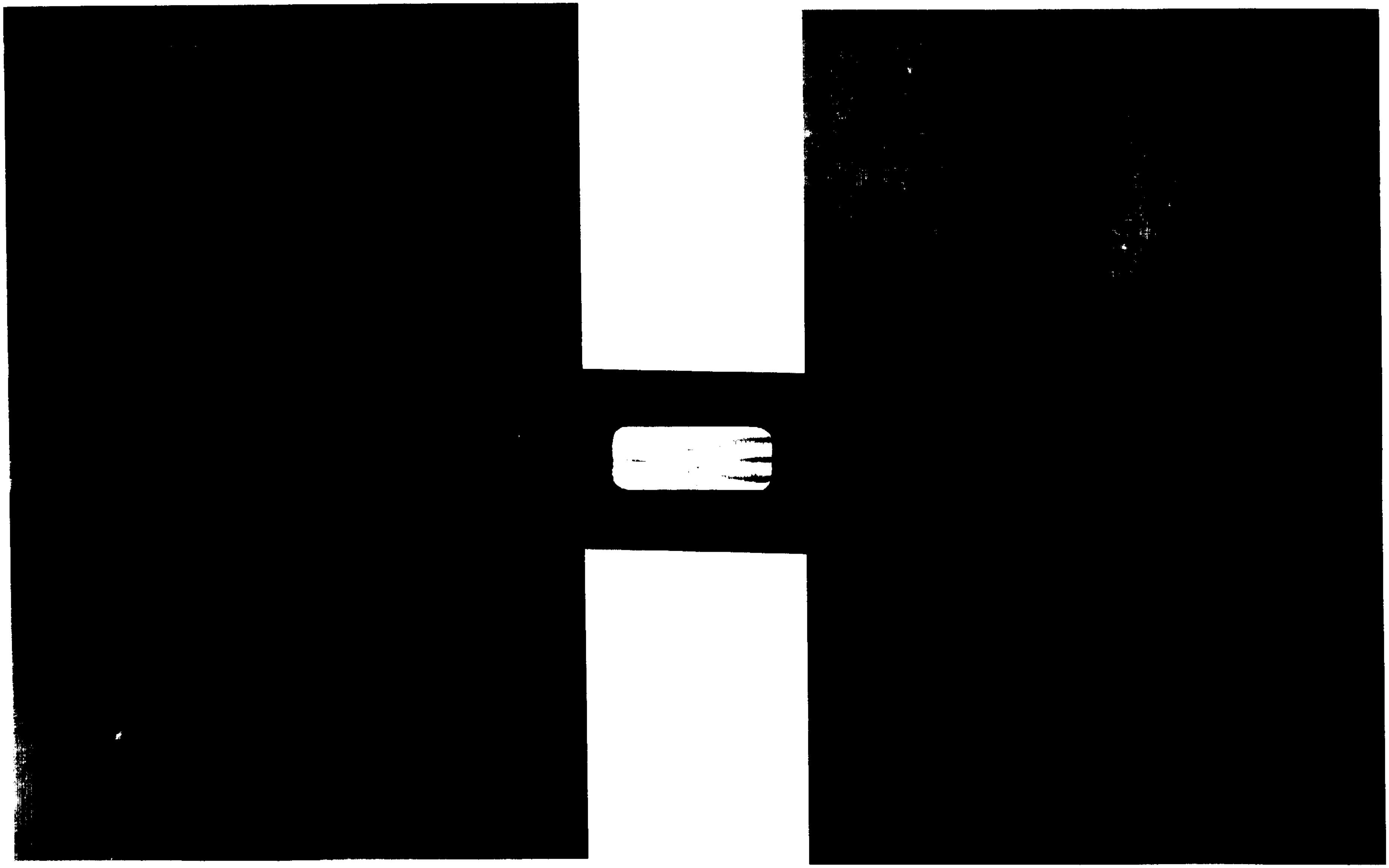

Photo 3-7. Fringe Pattern Detail, Specimen ODT-3, M=15,195 in-lbs

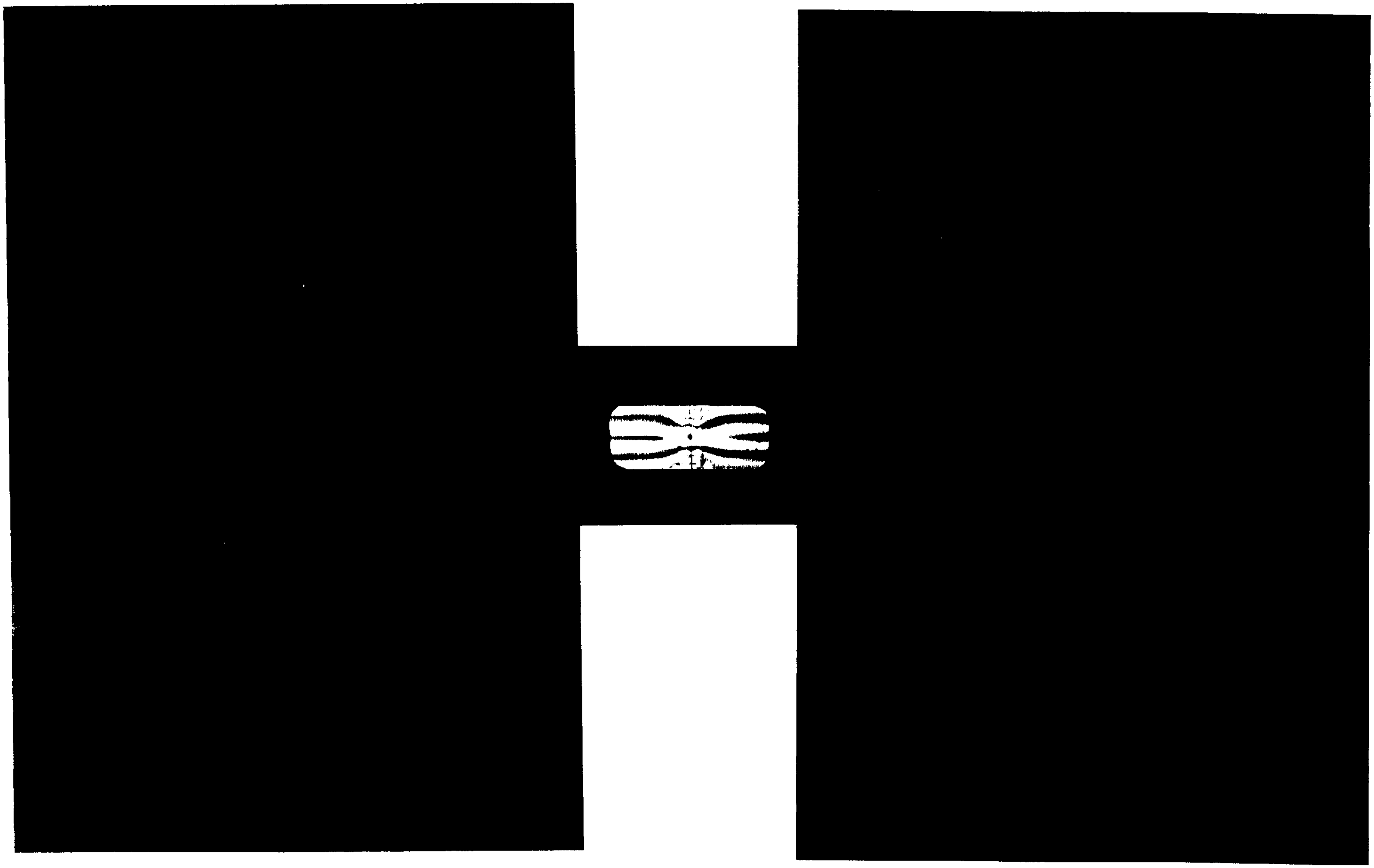

Photo 3-8. Fringe Pattern Detail, Specimen IDT-1, M=15,135 in-lbs

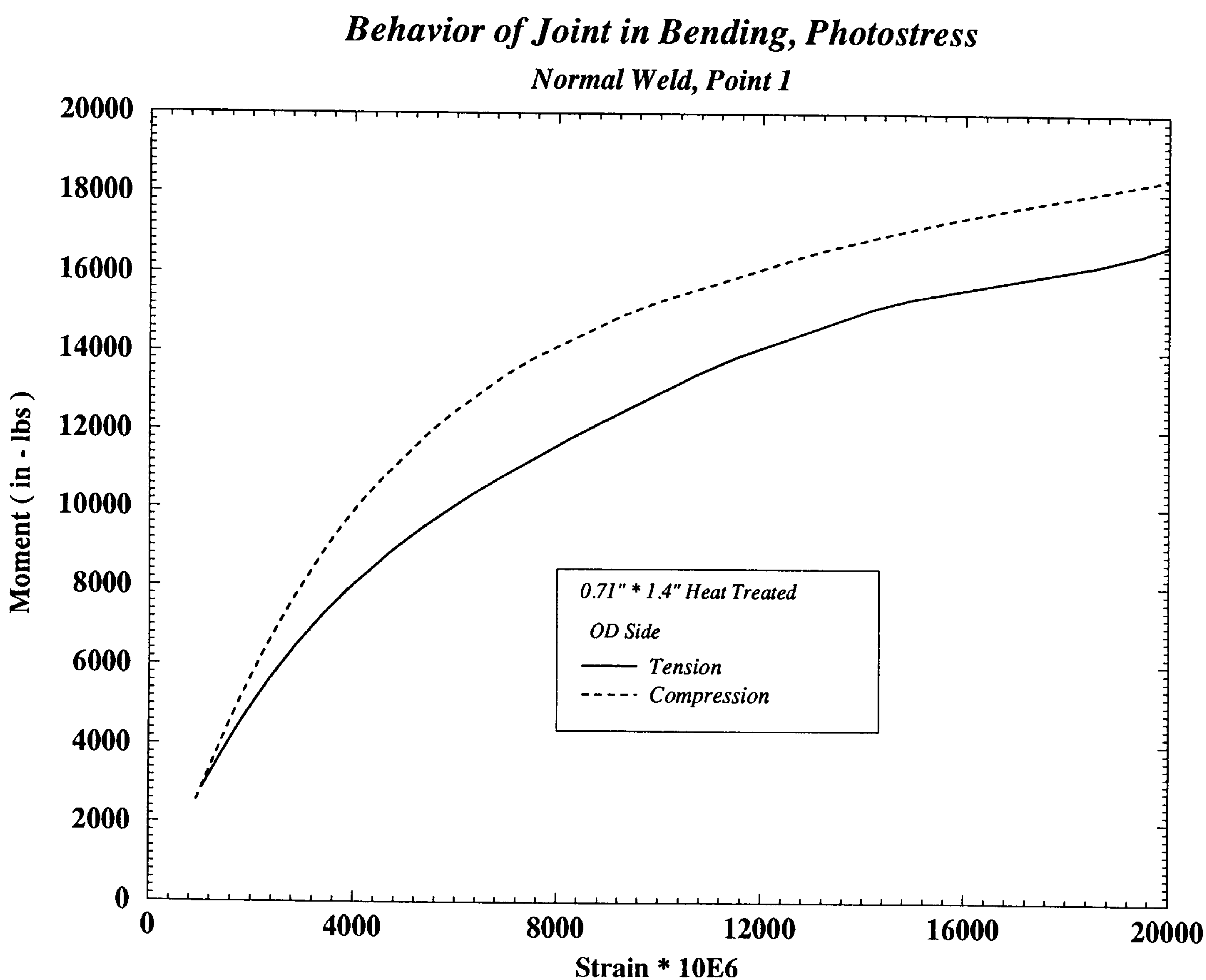

Figure 3-14. Comparison, OD Side, Point 1, Tension and Compression

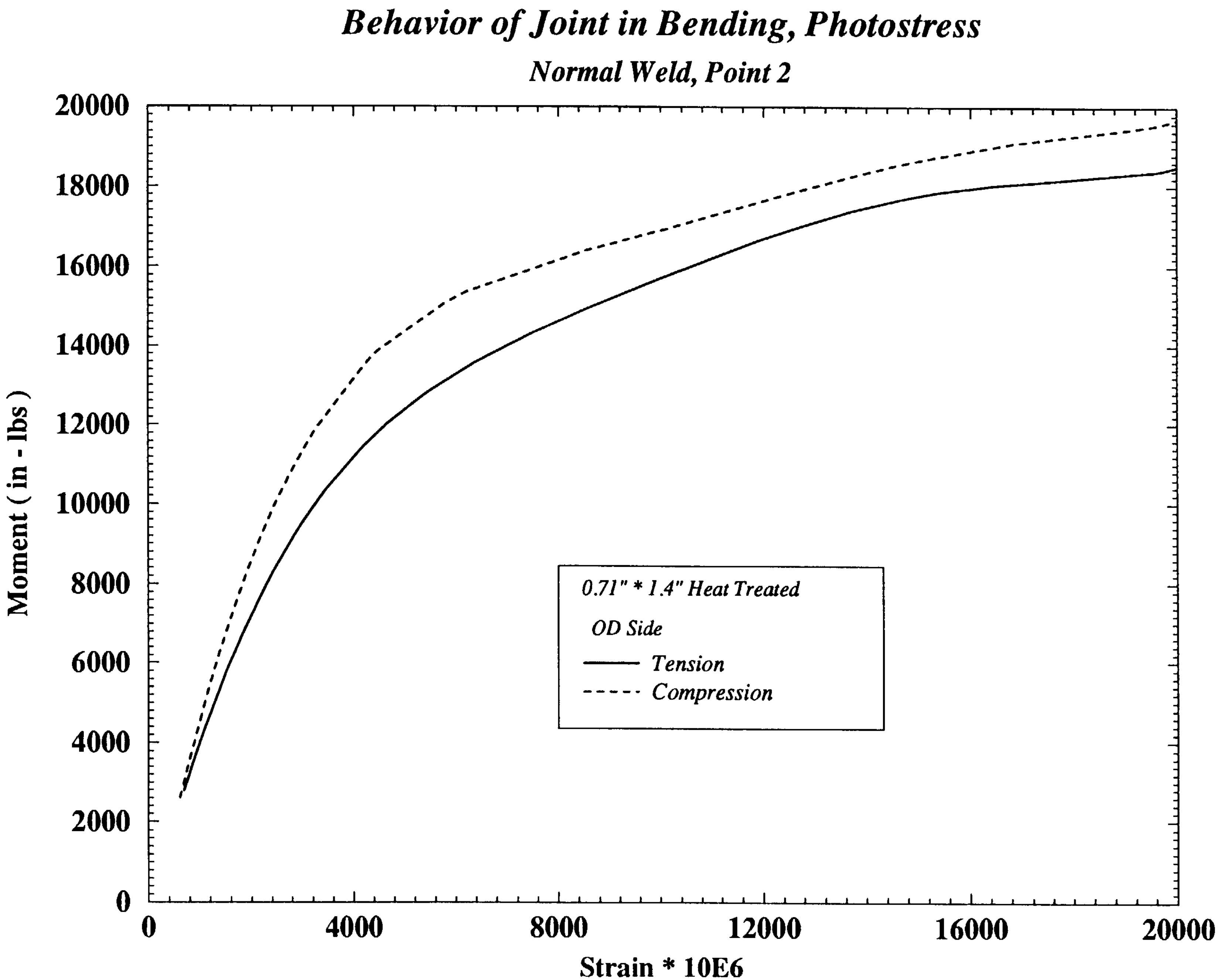

Figure 3-15. Comparison, OD Side, Point 2, Tension and Compression

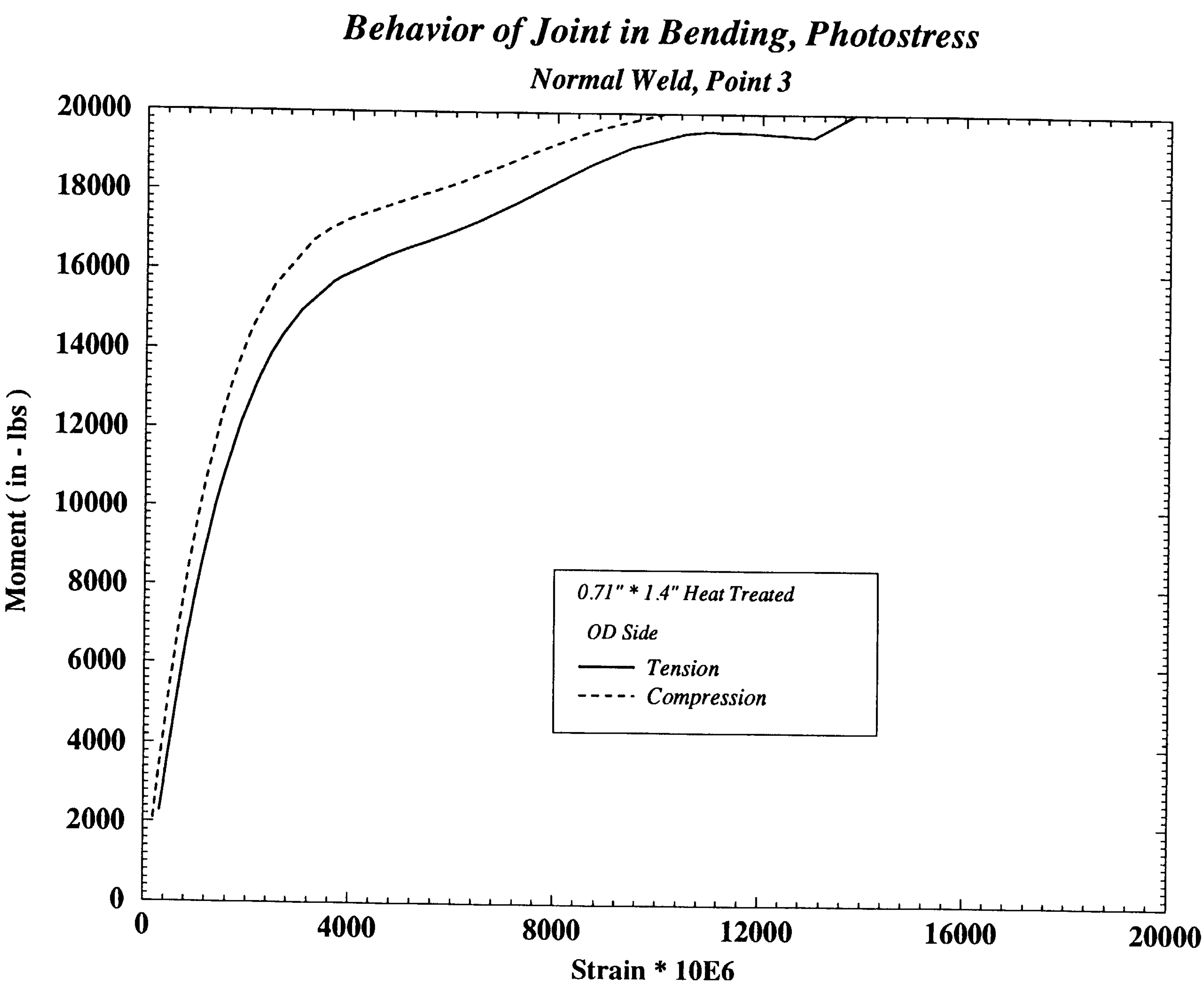

Figure 3-16. Comparison, OD Side, Point 3, Tension and Compression

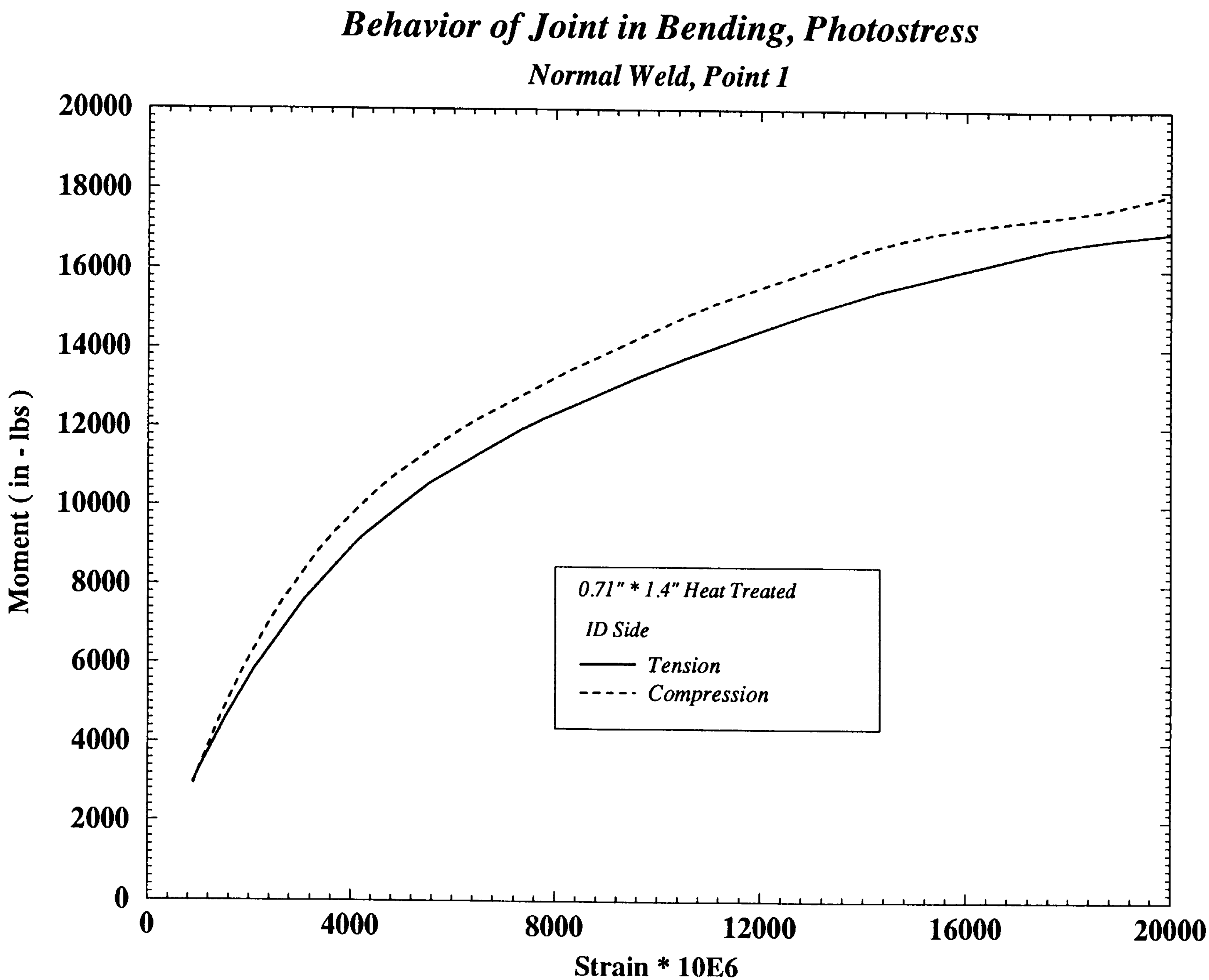

Figure 3-17. Comparison, ID Side, Point 1, Tension and Compression

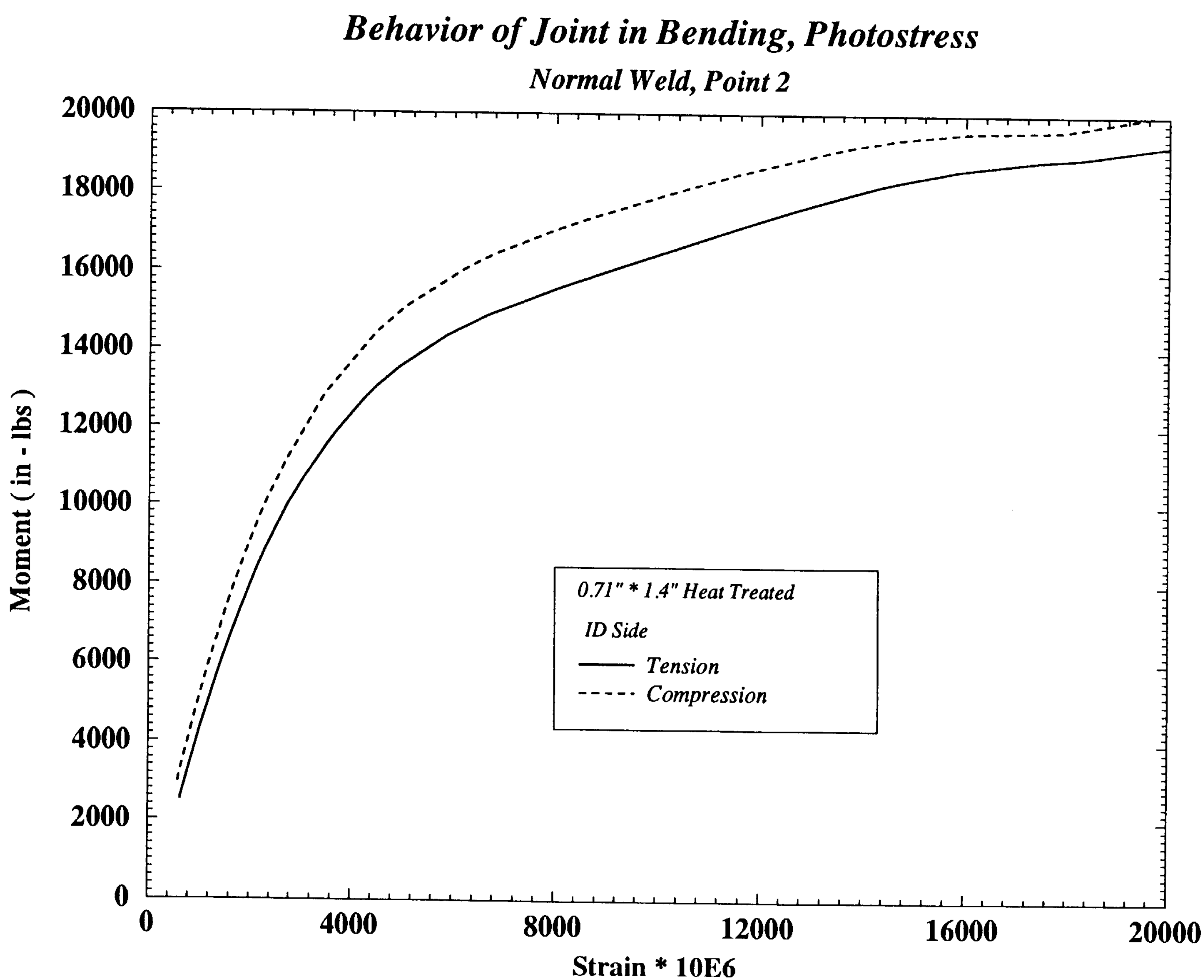

Figure 3-18. Comparison, ID Side, Point 2, Tension and Compression

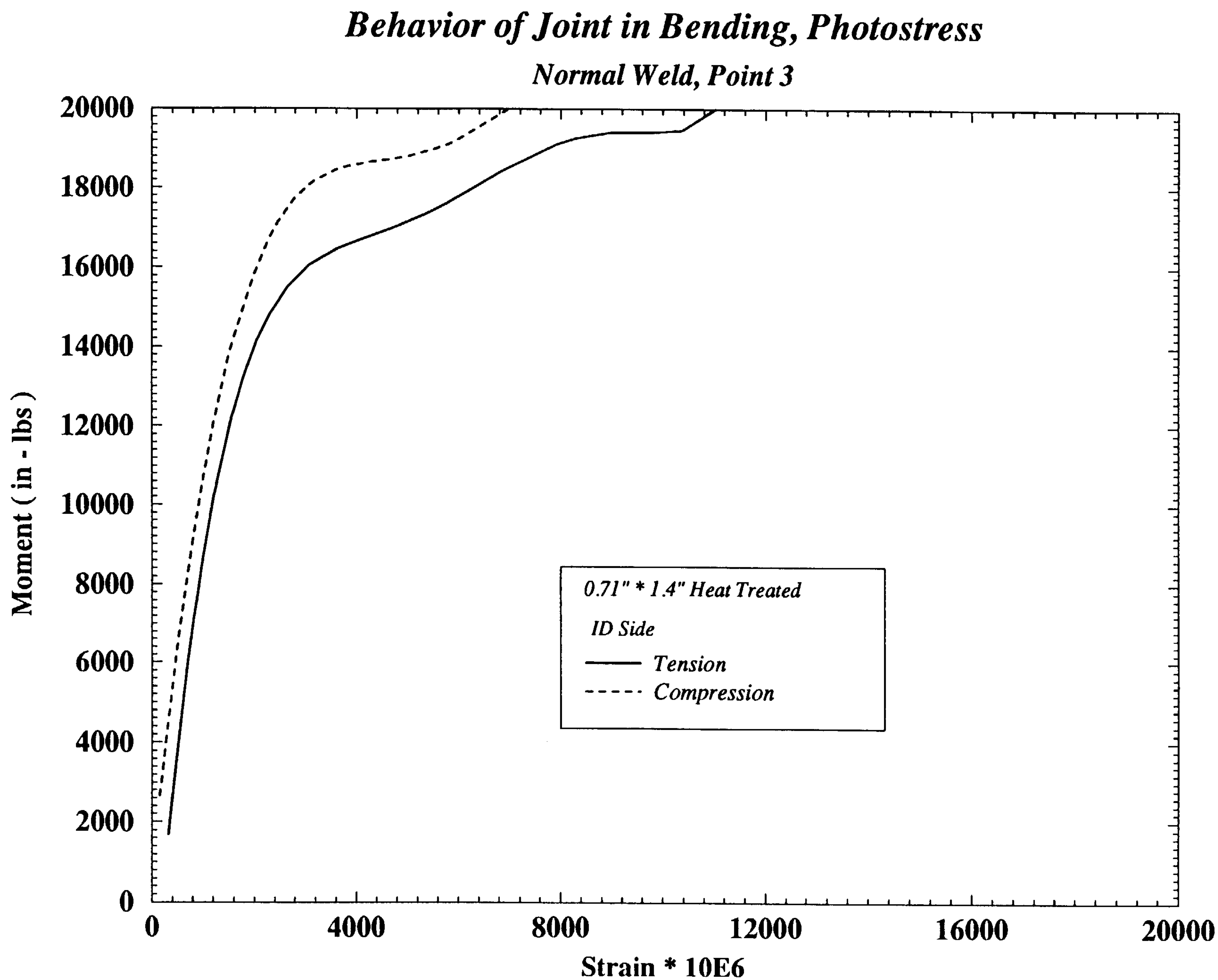

Figure 3-19. Comparison, ID Side, Point 3, Tension and Compression

same trend exists in the stronger ID side material where there is also less ductility and greater strength when the material is placed in compression. Figures 3-14 through 3-19 reflect trends seen in fringe patterns of Photos 3-7 and 3-8.

E. The "Neutral Axis"

In the context of the welded joint subjected to pure bending, the concept of a "neutral axis" exists only at lower applied moments. For example, Photos 3-1 and 3-4 indicate how the "neutral axis" disappears around the centerpoint of the weld as the moment increases leaving only a well defined isotropic point where the principal strains are of equal magnitude and the shearing strain vanishes. By comparison, the isotropic line, or neutral axis, remains intact in the parent material in a manner similar to that which occurs in specimens made from regular aluminum alloy having no welds. Photo 3-9 shows development of the shearing strain field in a 6061-T6 aluminum alloy specimen. Note that the black, center, isotropic line in Photo 3-9 does not change as the moment increases as it does in Photos 3-1 and 3-4 which show fringe patterns in the photoelastic coating applied to welded joint specimens.

Since the non-linear material in the weld near the upper and lower boundaries of the specimen yields non-uniformly at very low moment values, the stress distribution across the weld centerline must adjust to insure that $\Sigma F=0$ and $\Sigma M=0$. Therefore, the location of the isotropic point changes slightly as the applied moment changes. These slight changes can be seen by closely observing the position of the center of the black spot in the

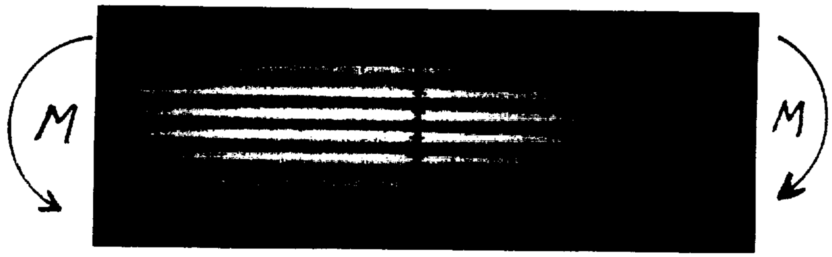

(15,815 psi)

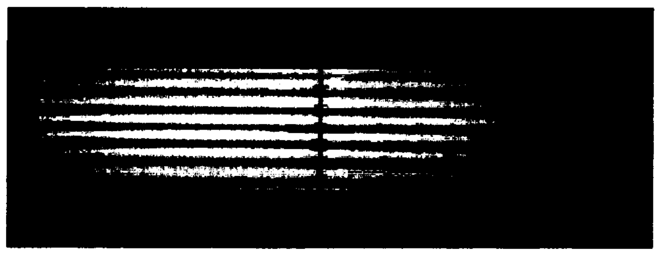

(25,564 psi)

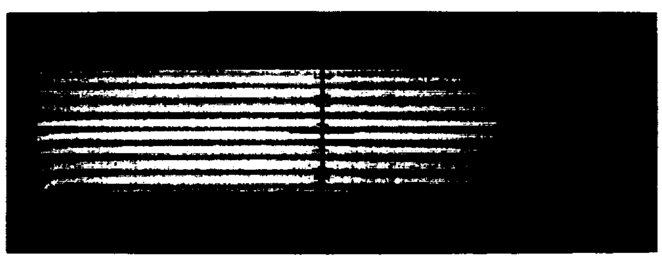

(31,854 psi)

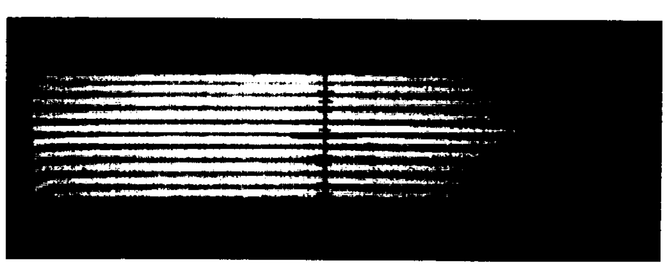

(35,000 psi)

Photo 3-9. Fringe Pattern Development, 6061-T6 Aluminum enlarged photographs. Recall that, at an isotropic point, only the maximum shearing strain is zero and one cannot assume that either the maximum or the minimum principal strain is zero. Thus, the location of the isotropic point may or may not be the location where the maximum and minimum principal strains are both zero as they are along the isotropic line in Photo 3-9 for the regular aluminum alloy specimen. Graphs showing scatter of data for all bending tests are presented in Appendix C.

VIII. RESULTS FROM TASK 4

To better define overall stress-strain and contraction ratio characteristics in the weld material and heat affected zone for the 1/2" x 2" as welded joints, a grid pattern of thirteen points (A through M), rather than just four points on a vertical centerline, was defined for data collection (see Figure 4-1). Vertical dimensions between horizontal lines were, on average,

CL to 1/2 FB.........................0.0875 inches,
CL to FB............................0.175 inches, and
CL to 1/2"...........................0.500 inches.

Figures 4-2 through 4-8 provide material behavior at each point. From these figures, except for points K, L, and M, it is seen that the material is highly ductile and non-linear with relatively small elastic ranges. Proportional limits at the points are:

A - 5,700 psi,	H - 6,300 psi,
B - 6,000 psi,	I - 5,700 psi,
C - 6,800 psi,	J - 8,800 psi,
D - 6,700 psi,	K - 11,500 psi,

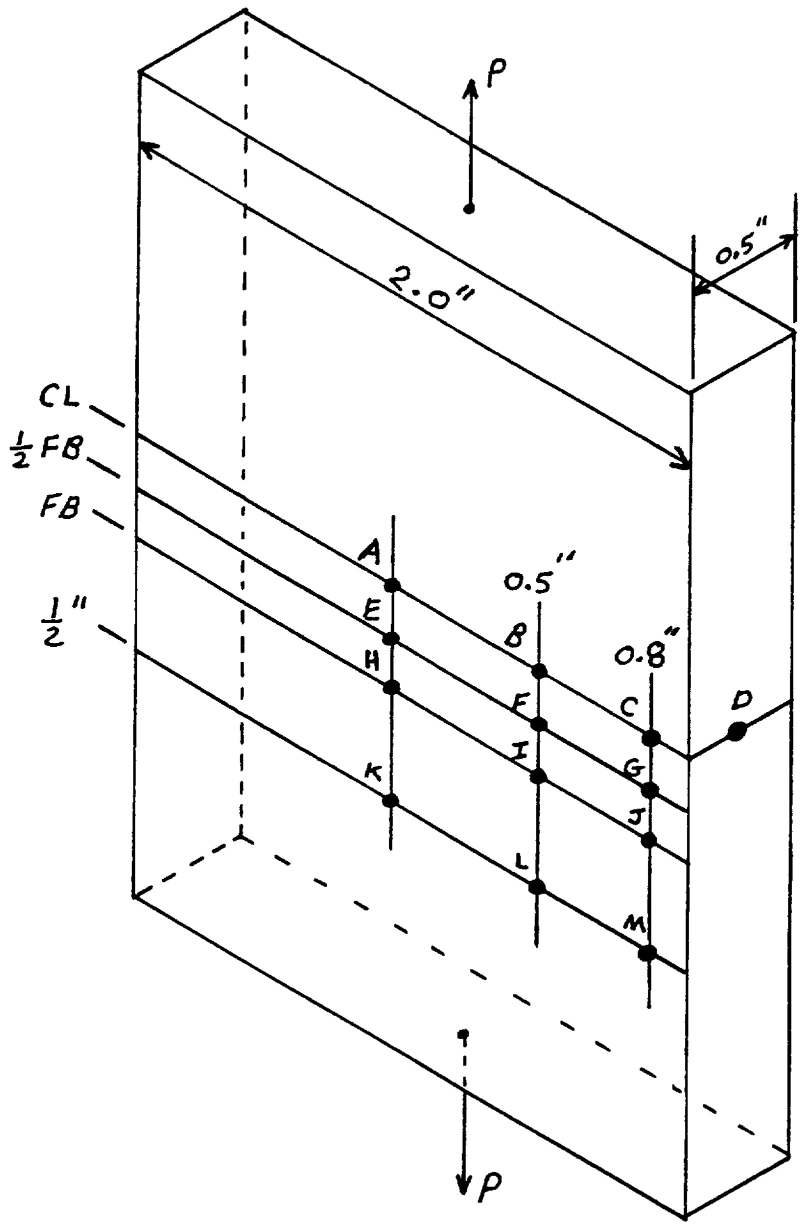

Figure 4-1. Grid Pattern, 1/2" x 2" Specimens

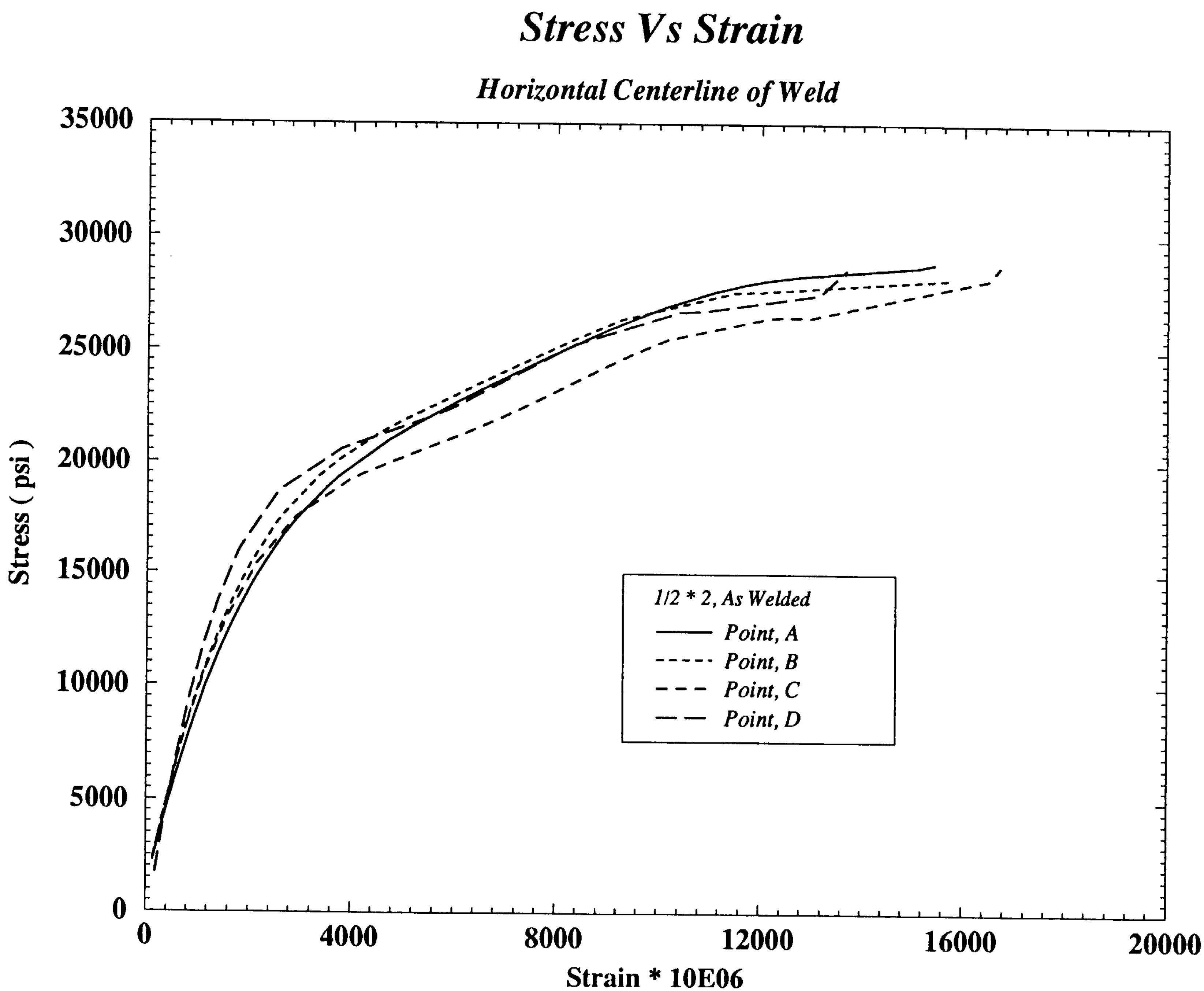

Figure 4-2. Material Behavior, Horizontal Centerline

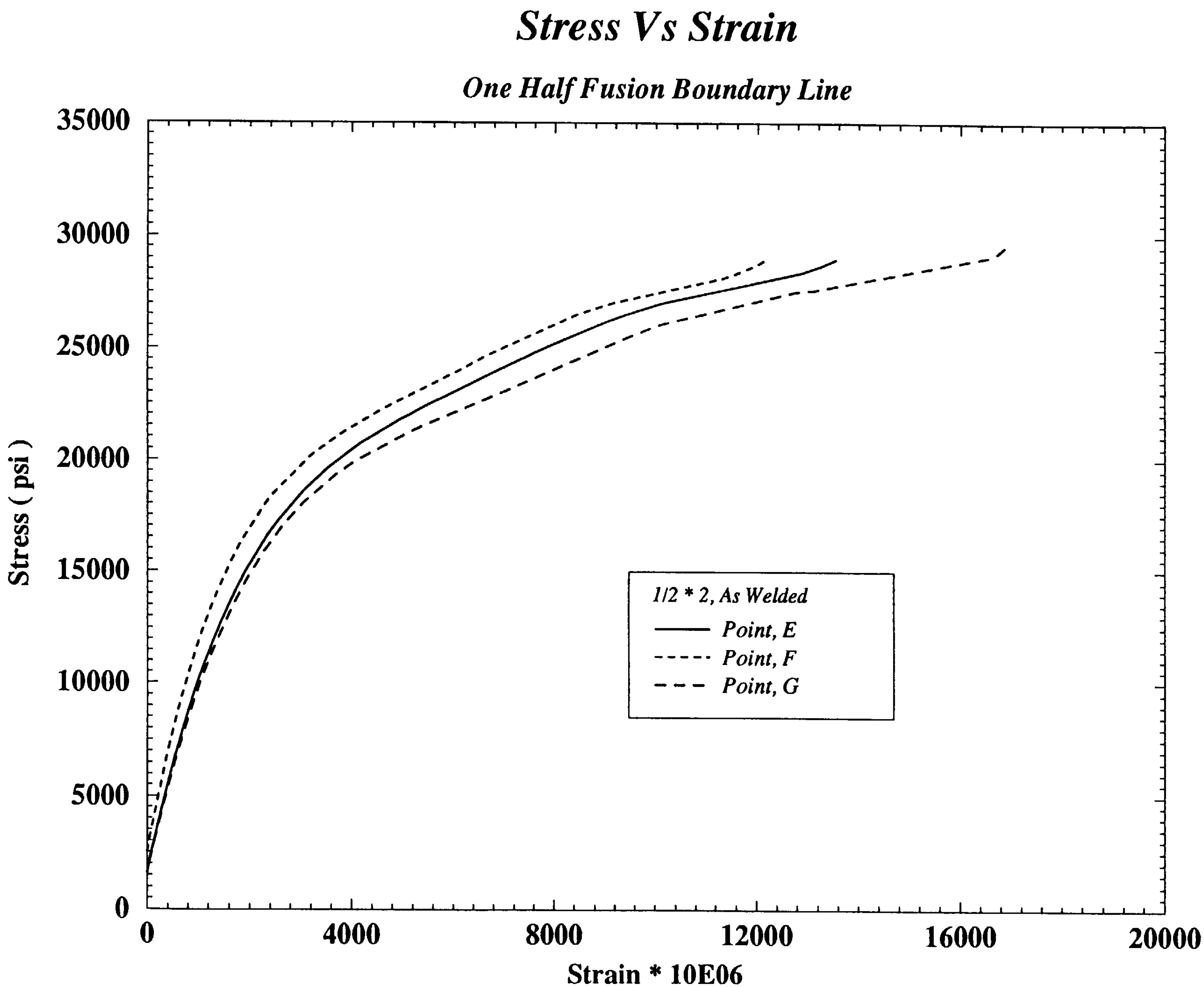

Figure 4-3. Material Behavior, Half Fusion Boundary

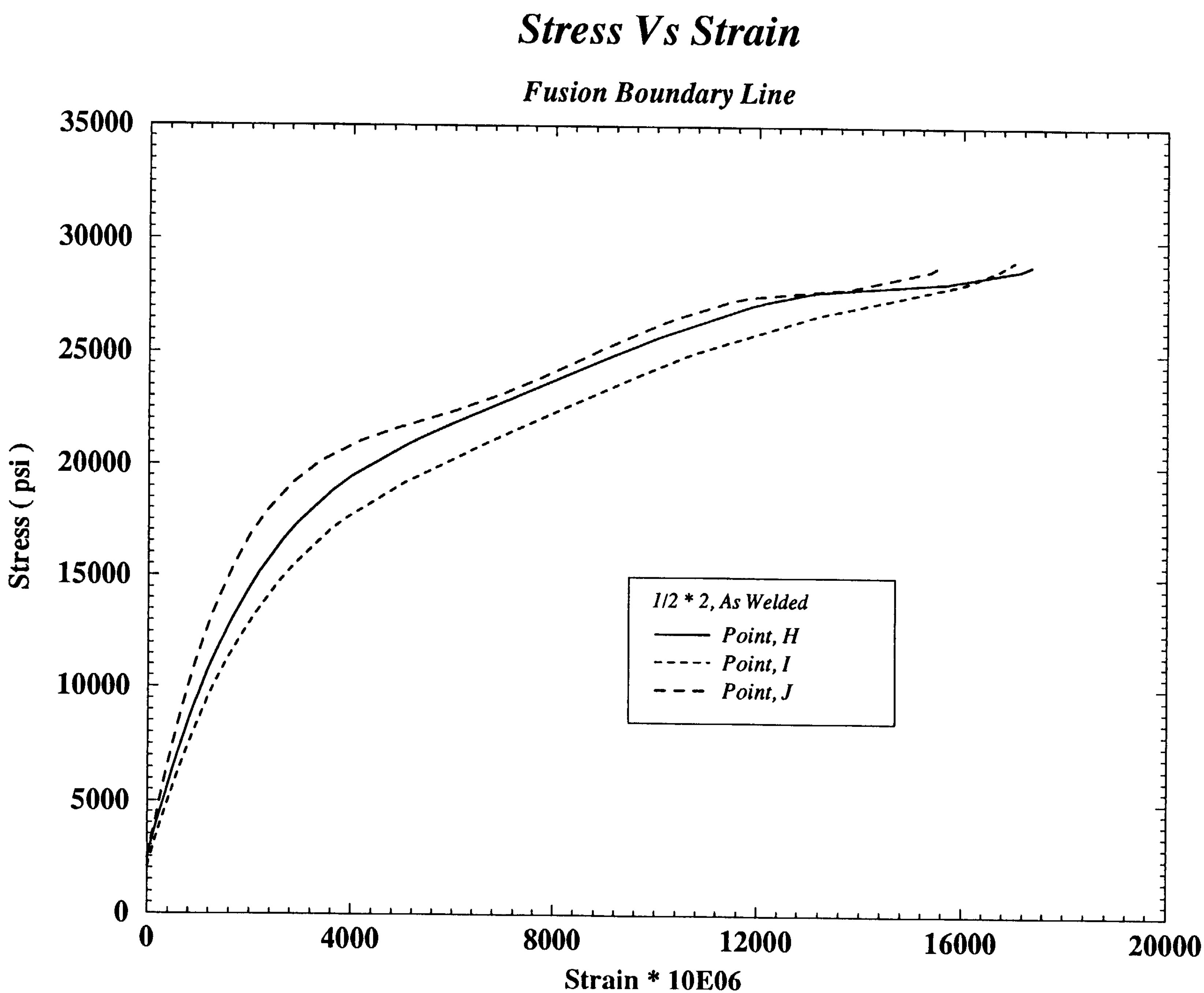

Figure 4-4. Material Behavior, Fusion Boundary

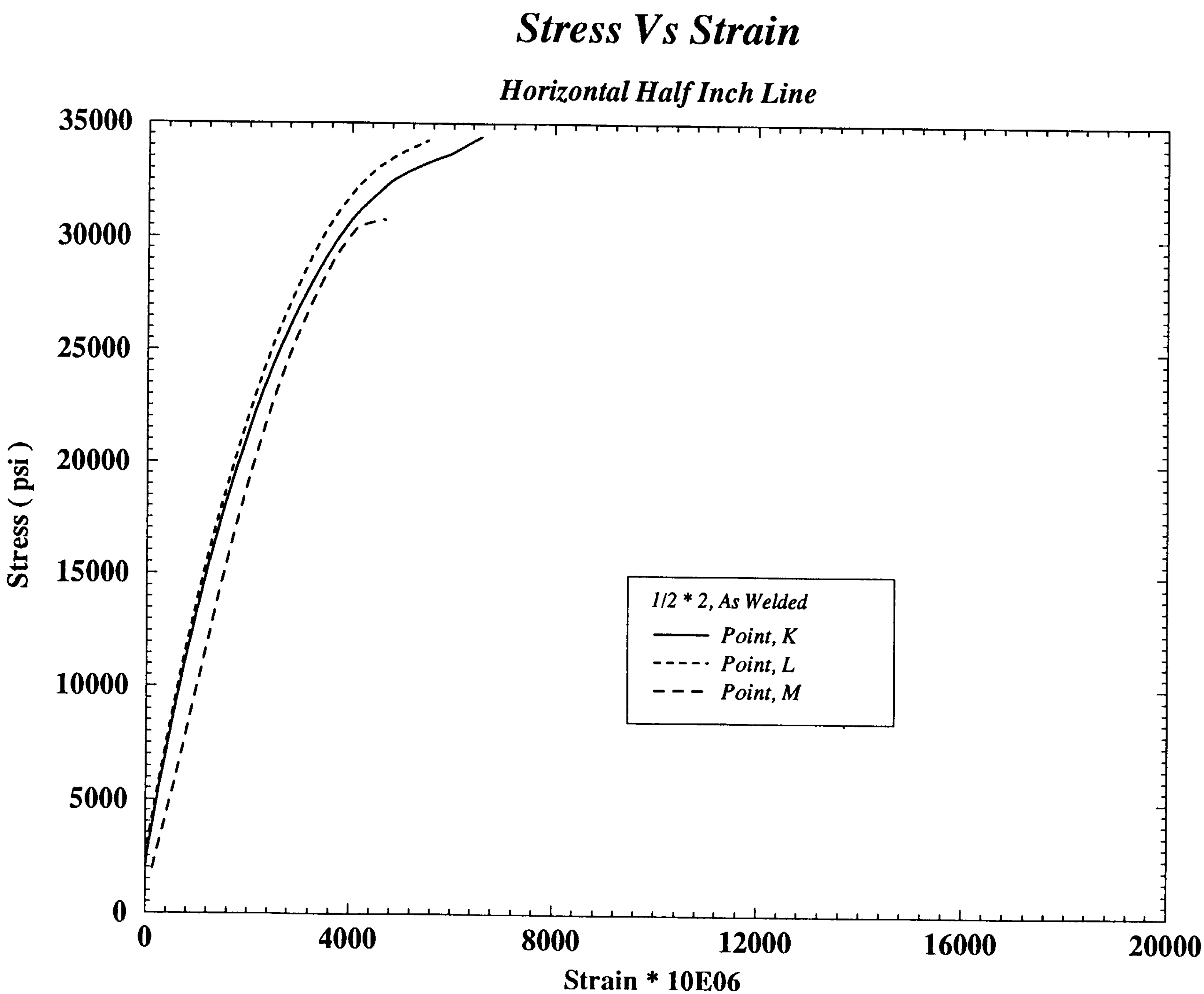

Figure 4-5. Material Behavior, Half Inch Line

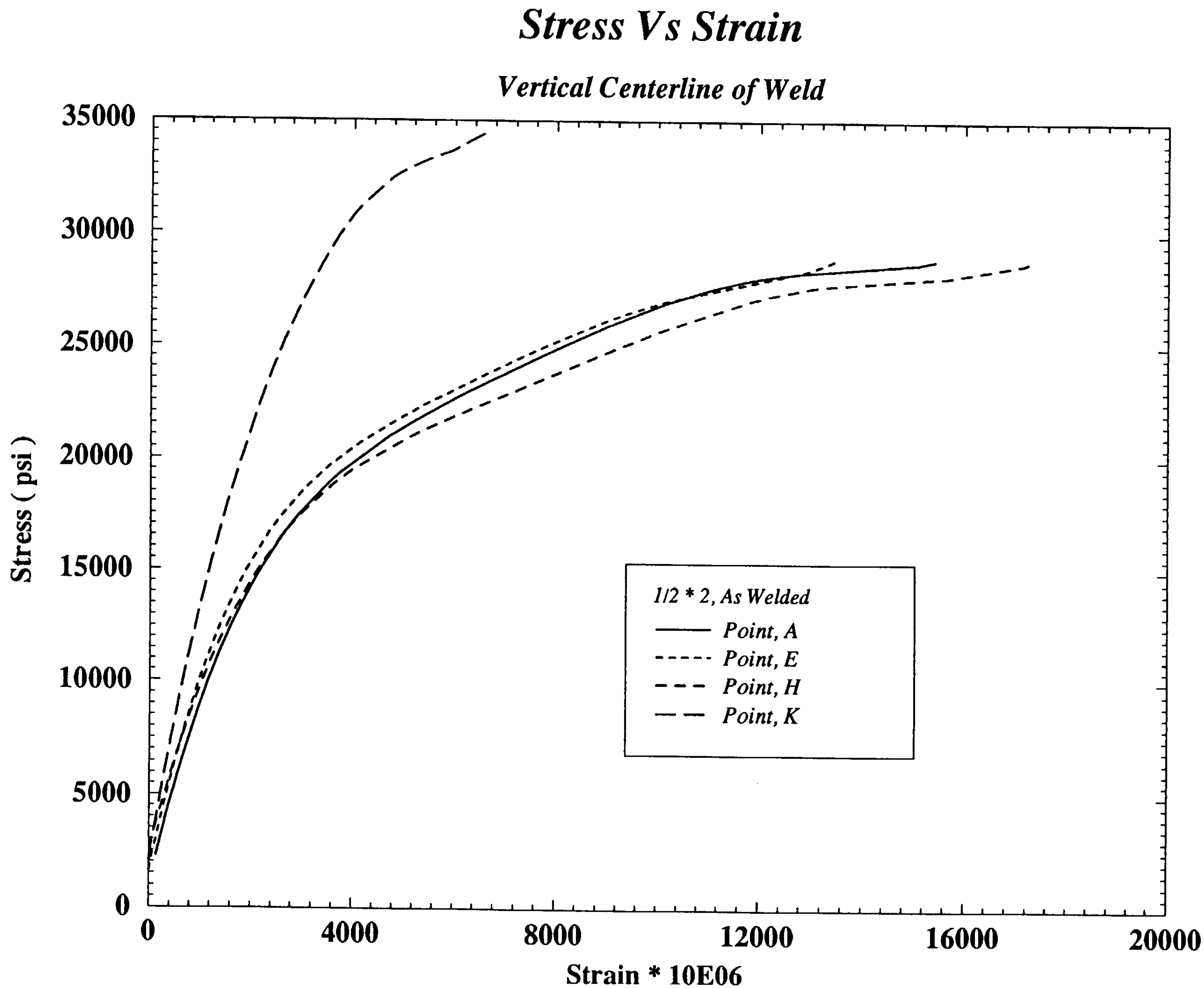

Figure 4-6. Material Behavior, Vertical Centerline

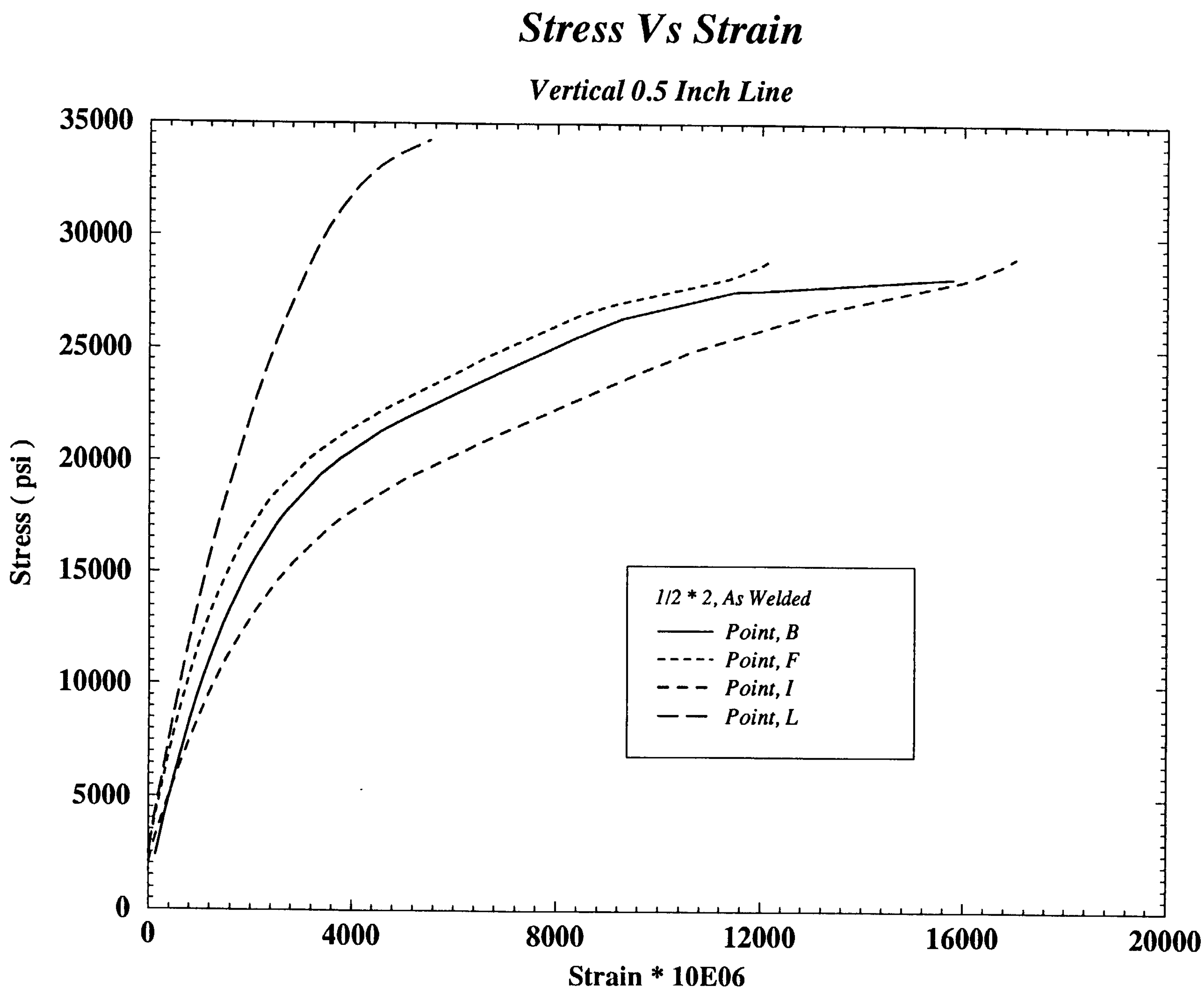

Figure 4-7. Material Behavior, Vertical 0.5" Line

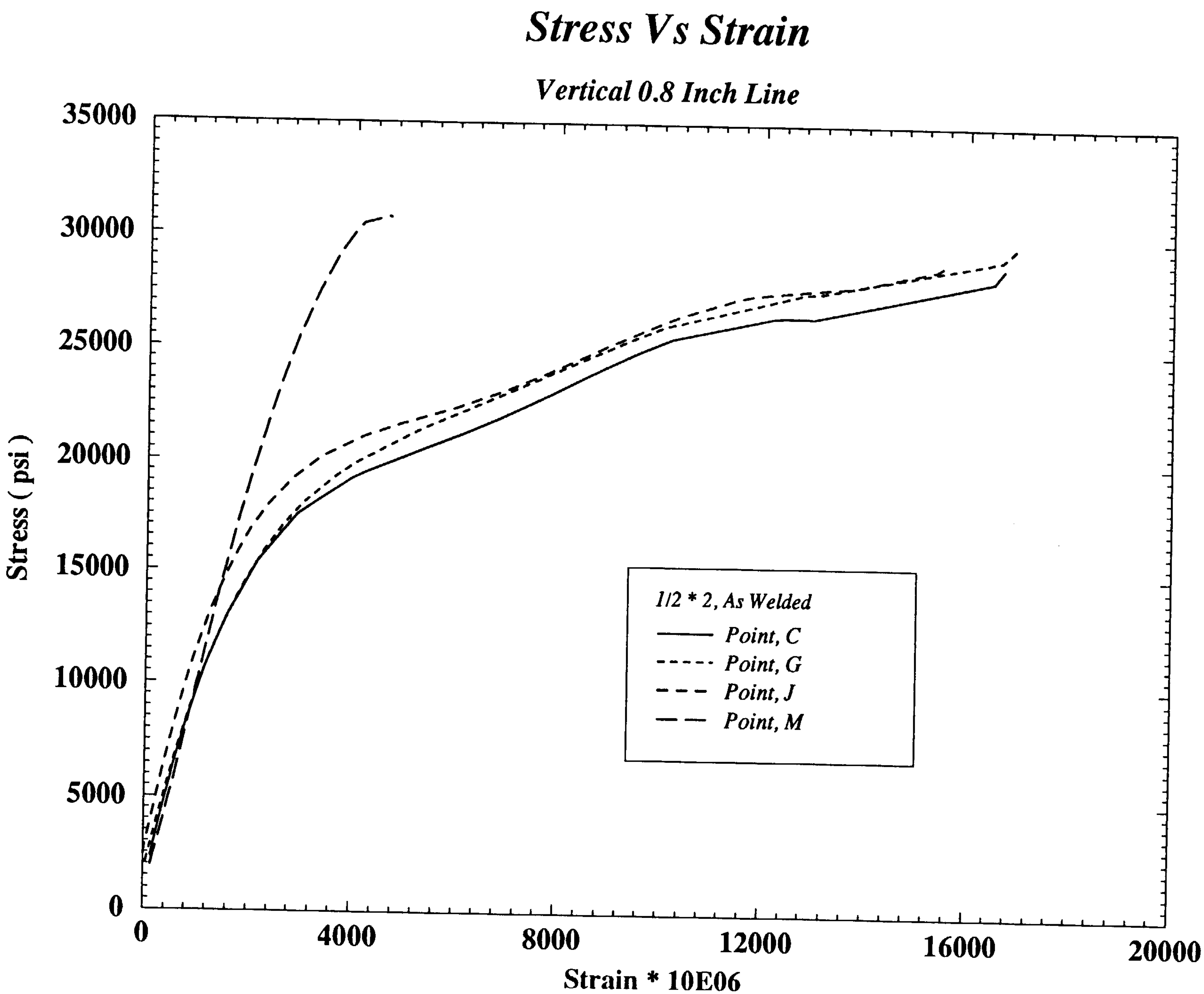

Figure 4-8. Material Behavior, Vertical 0.8" Line.

E - 7,000 psi,	L - 14,000 psi, and
F - 8,000 psi,	M - 17,600 psi.
G - 8,200 psi,	

Also, it may be seen that there are only small differences in stress-strain curves at points along horizontal lines A-D, E-G, H-J, and K-M and along vertical lines A-H, B-I, and C-J. Points K, L, and M along the line 1/2 inch from the weld centerline show considerably more elastic behavior than do other points in the grid.

With respect to in-plane contraction ratios at the several points, Figures 4-9 through 4-12 show that there is little correlation with Chakrabarty's plasticity theory for stresses above the proportional limit. This theory is based upon constant volume deformation of a standard tensile test specimen which is quite different from a welded test specimen. During tensile tests of the welded specimens, one can visually note large deformation occurring in the vicinity of the weld. It is unlikely that an assumption of a linear variation between 0.32 and 0.50 for the in-plane contraction ratio (which is sometimes done) would produce reliable results in efforts to mathematically model the welded joint. Point D on the 1/2 inch thick edge of the weld has a maximum in-plane contraction ratio of nearly 0.75 at a plastic stress of 20,000 psi. At other points, the in-plane contraction ratio varies with plastic stress but never becomes asymptotic to a value of 0.5 as predicted by the usual deformation theory. It appears that, in the weld and heat affected zone, strain in the direction of the tensile stress

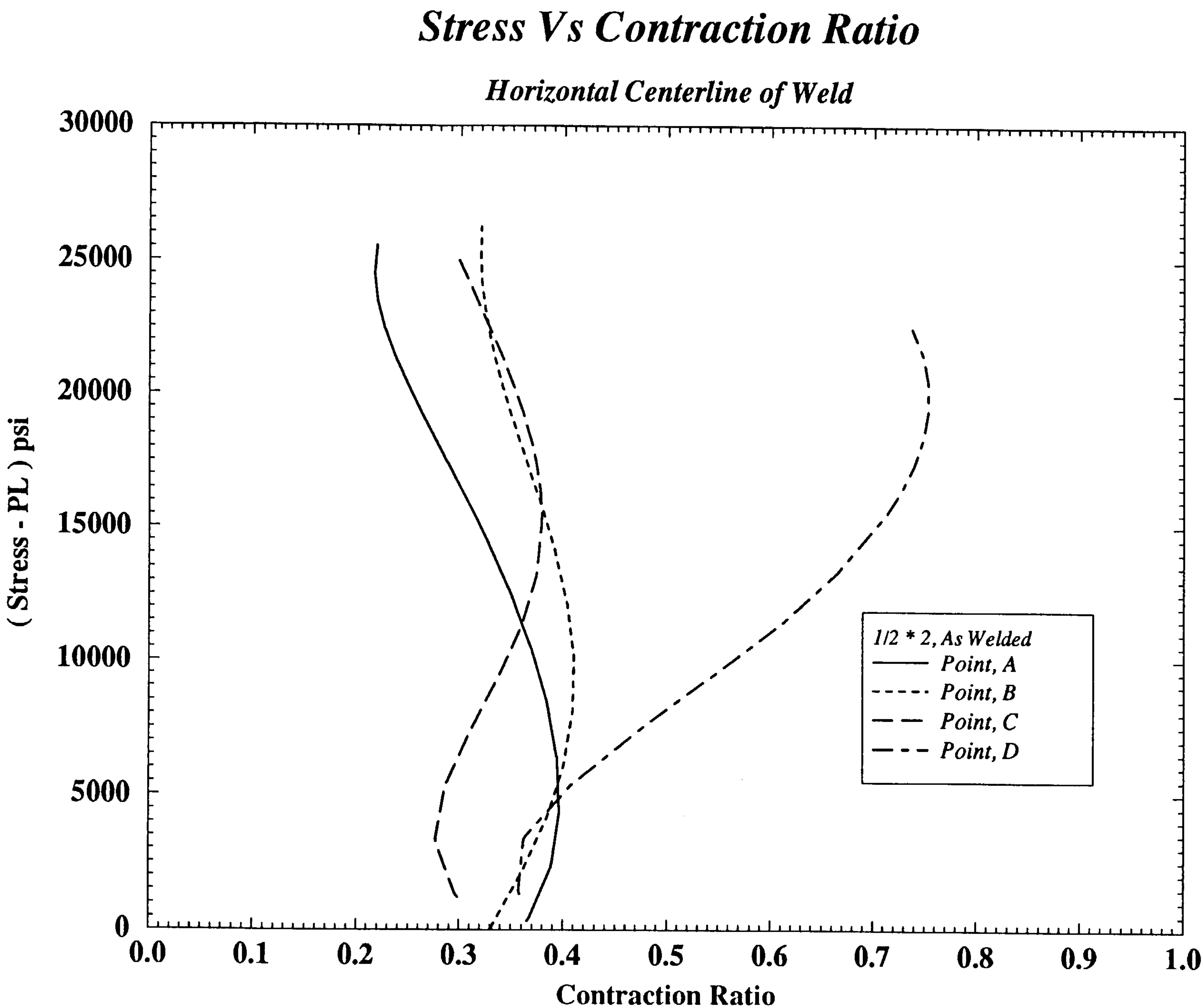

Figure 4-9. In-Plane Contraction Ratios, Horizontal Centerline

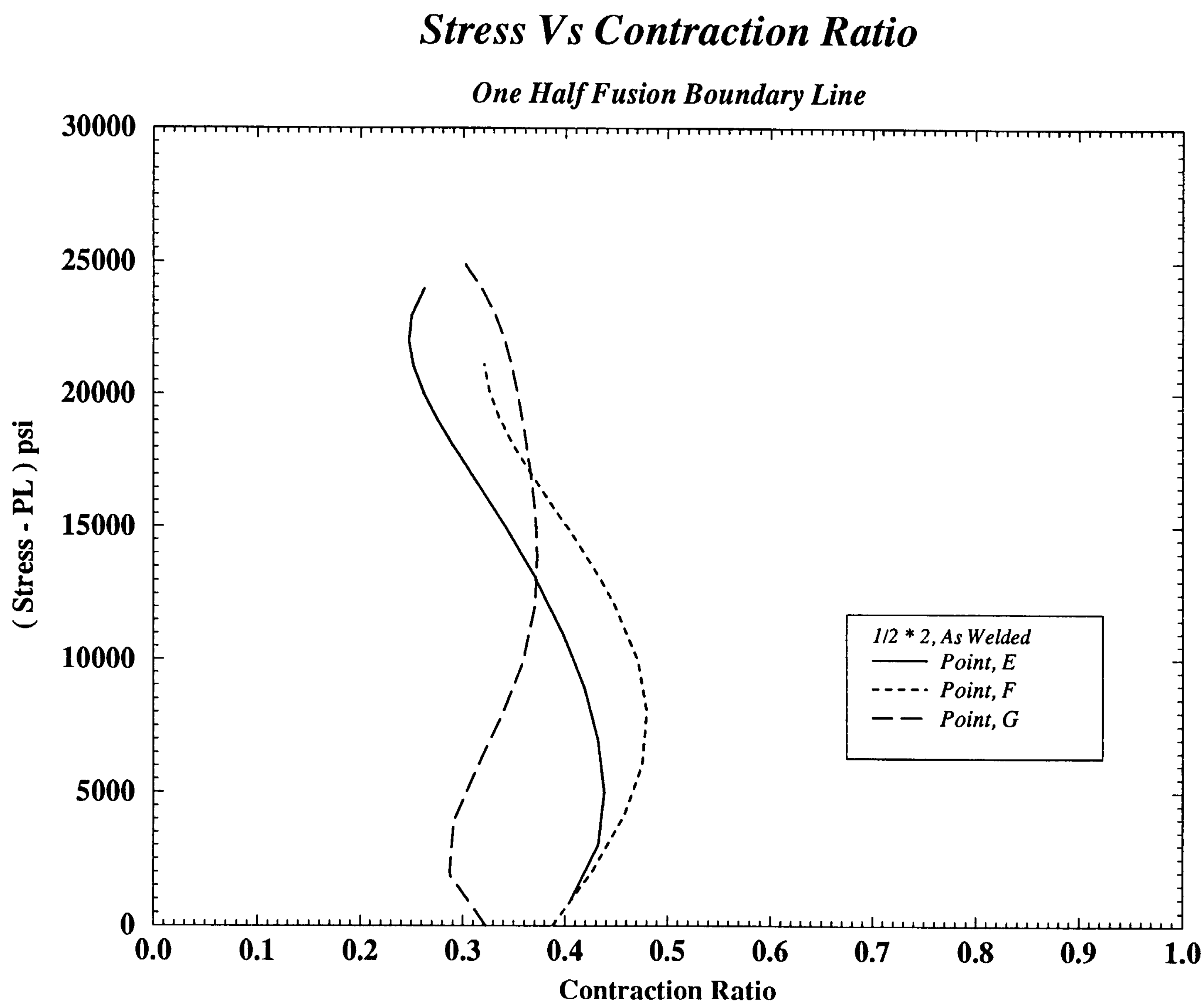

Figure 4-10. In-Plane Contraction Ratios, Half Fusion Boundary

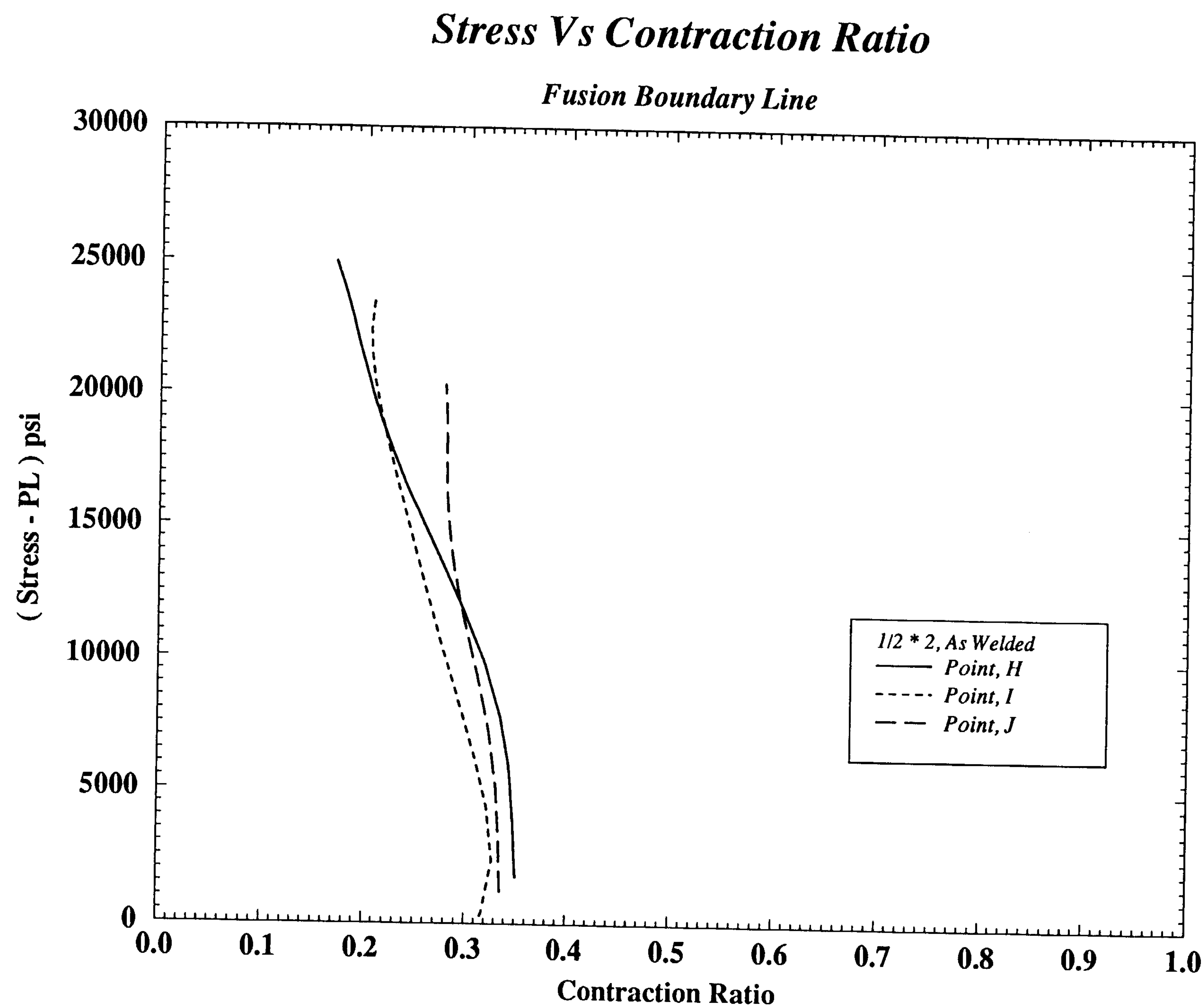

Figure 4-11. In-Plane Contraction Ratios, Fusion Boundary

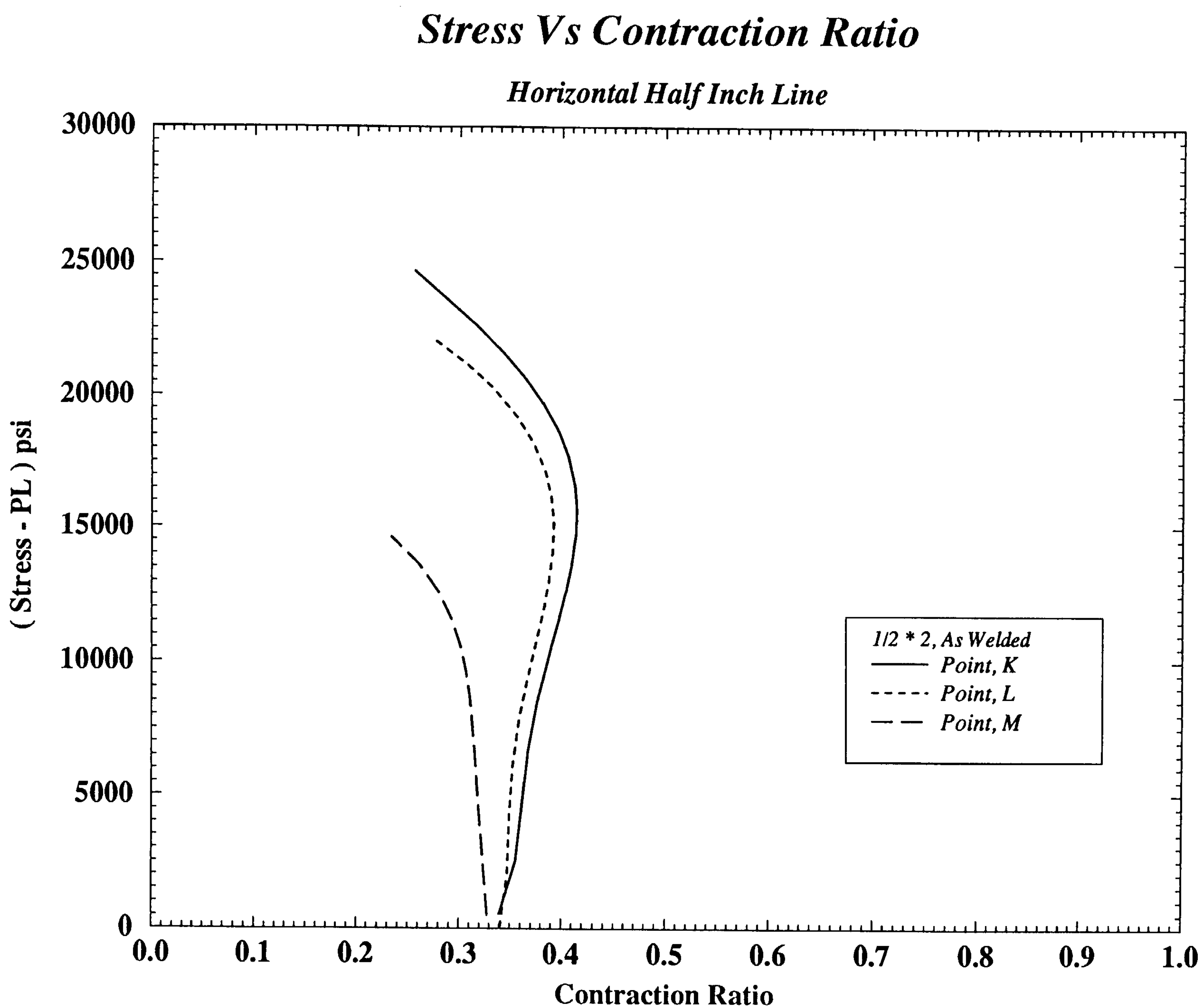

Figure 4-12. In-Plane Contraction Ratios, Half Inch Line

takes on larger values with respect to transverse strain than is expected under normal circumstances for all points except for point D. At point D, it appears that lack of constraint through the 1/2 inch thickness of the weld allows for transverse strain to greatly exceed that which would occur when testing a uniform specimen having no welded joint. Clearly, such a large transverse strain as was observed at point D cannot be predicted by a known theory. Since highly discontinuous yielding (2) was observed in all specimens above a stress of 21,000 psi, it is believed that such yielding at all points except point D contributed to the large strains measured in the direction of the applied stress whereas the measured transverse strain did not increase proportionately during the discontinuous yielding process.

Out-of-plane contraction ratios were calculated as indicated in section IV.D. and are presented in Figures 4-13 through 4-16 which give a good indication of the extent of deformation perpendicular to the surface of the specimen at all grid points. Note that, at point D, the very large in-plane contraction ratio (Figure 4-9) has resulted in a very small out-of-plane contraction ratio (Figure 4-13). At all points except point D, Figures 4-13 through 4-16 indicate that deformation of the joints perpendicular to the surface is relatively quite large when compared to transverse deformation in the surface.

It has been observed that discontinuous yielding is dependent upon the applied monotonic stress rate and upon the load increment and time at hold for a load-hold-load sequence.

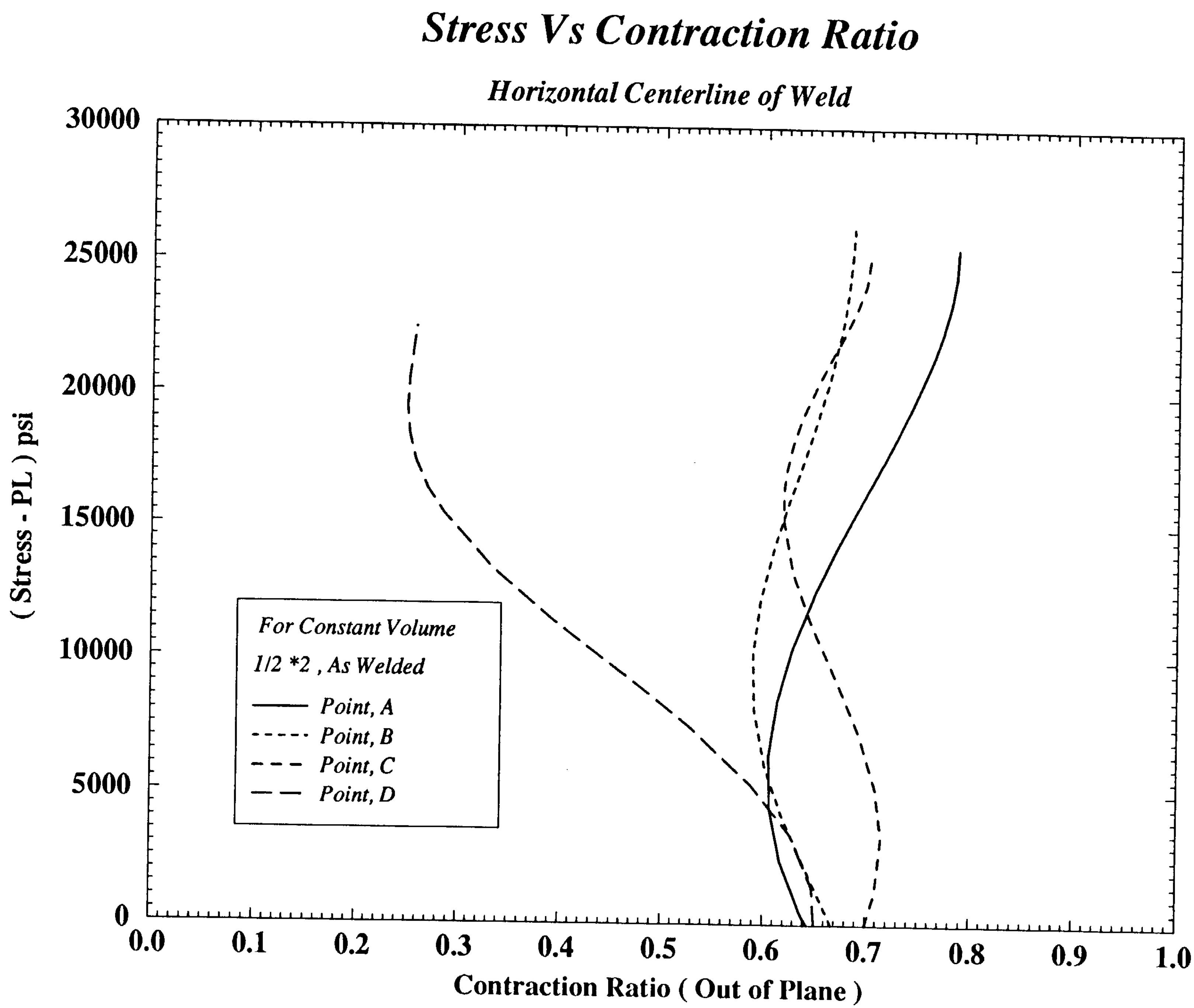

Figure 4-13. Out-of-Plane Contraction Ratios, Horizontal Centerline

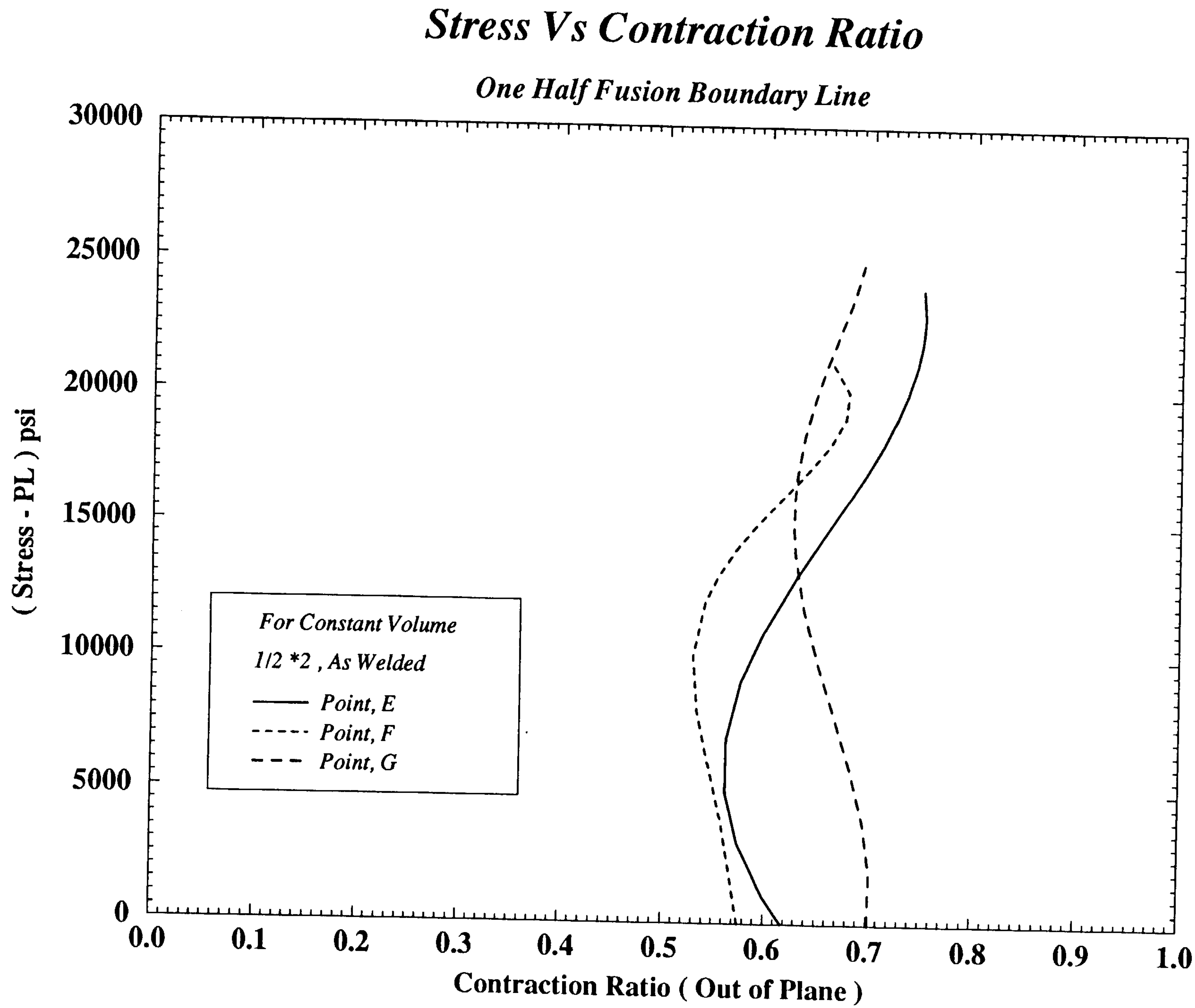

Figure 4-14. Out-of-Plane Contraction Ratios, Half Fusion Boundary

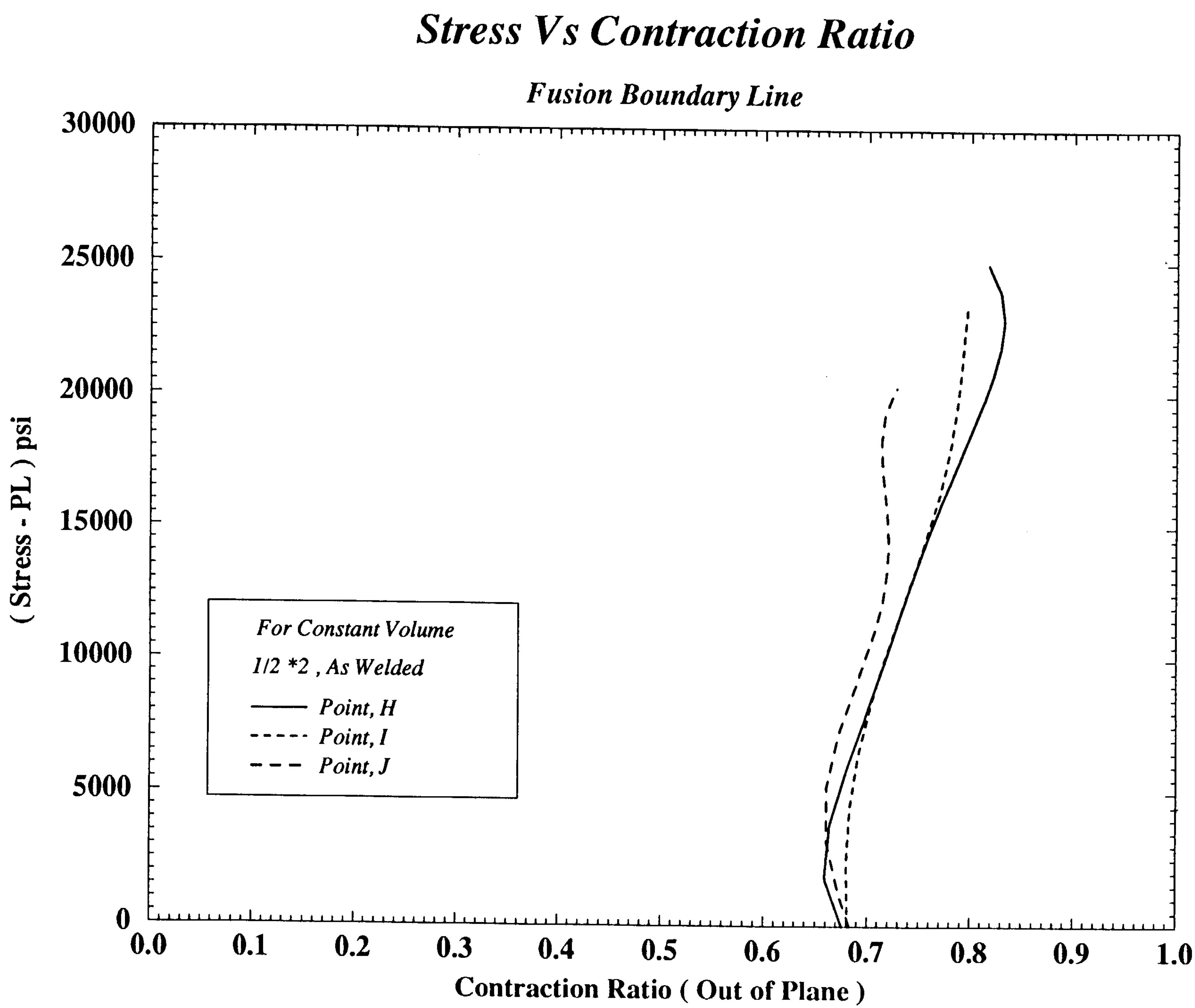

Figure 4-15. Out-of-Plane Contraction Ratios, Fusion Boundary

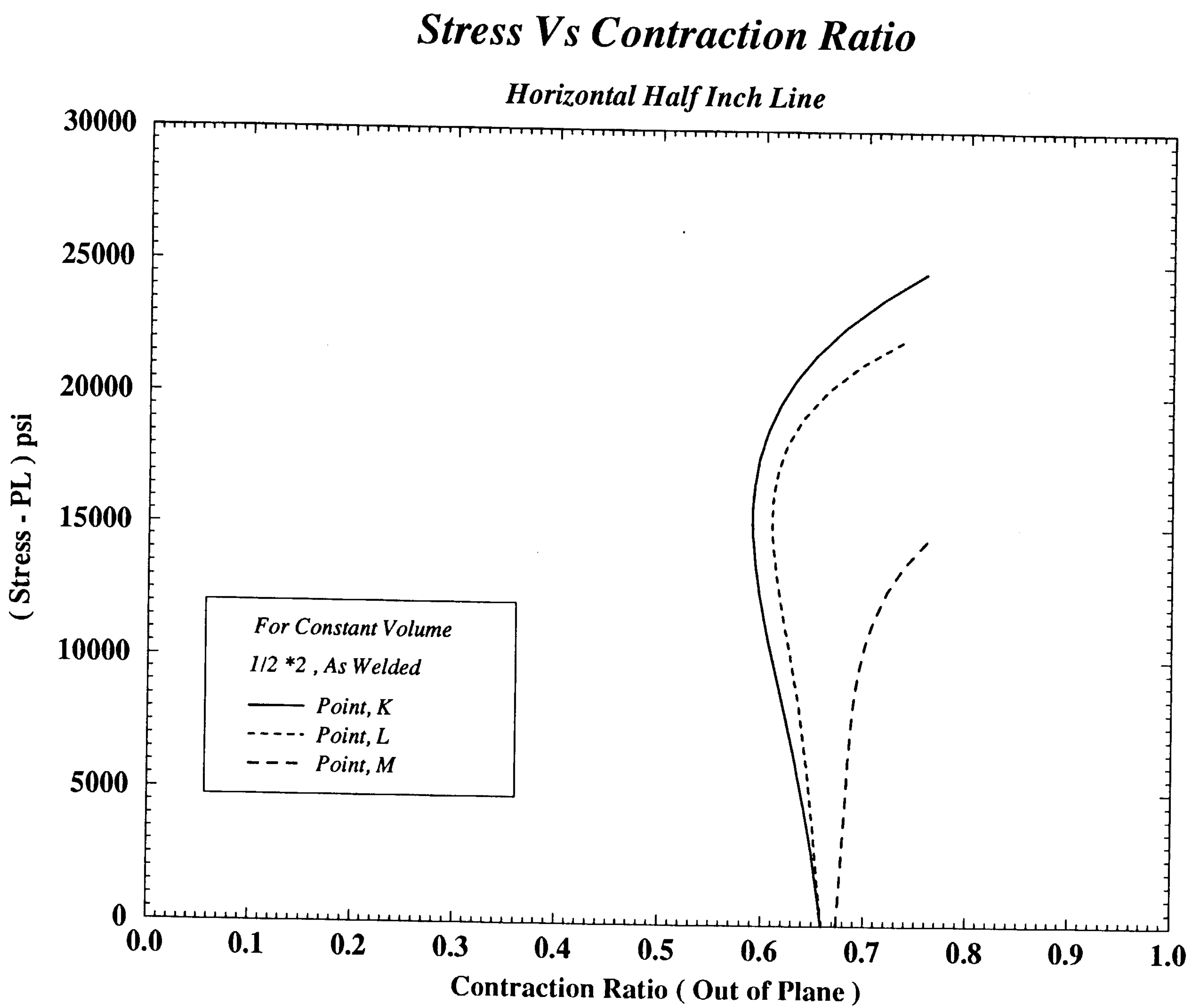

Figure 4-16. Out-of-Plane Contraction Ratios, Half Inch Line

Tests conducted using a monotonic stress rate from 4000 to 5000 psi per minute show two, or maybe three, discontinuous yields between 20,000 and 40,000 psi applied stress. However, when applying stress increments of 1000 psi at a rate of 4000 psi per minute and holding for one to one and one-half minutes between increments, tests show a discontinuous yield for every two 1000 psi increments between 20,000 and 40,000 psi applied stress. Therefore, contraction ratios may be somewhat different when obtained from a monotonic load sequence when compared to those obtained from a load-hold-load sequence. All contraction ratios presented in this report were obtained from a load-hold-load sequence.

All 1/" x 2" specimens were slightly "peaked" and, therefore, some initial bending was present during tensile tests. The effect of initial bending can be seen in several graphs as an offset on the strain axis at zero stress. In several specimens, strains measured in the direction of loading were initially compressive which then reverted back to tensile strains as the load increased.

During the Summer of 1992, (2), tests were conducted on 1/2" x 2" specimens made similar to those tested during the summer of 1993. To correlate data from the two different years, Figure 4-17 was produced using a data file for point A from tests one year apart. It may be seen that test specimens from both years behave in a similar manner with little or no significant difference.

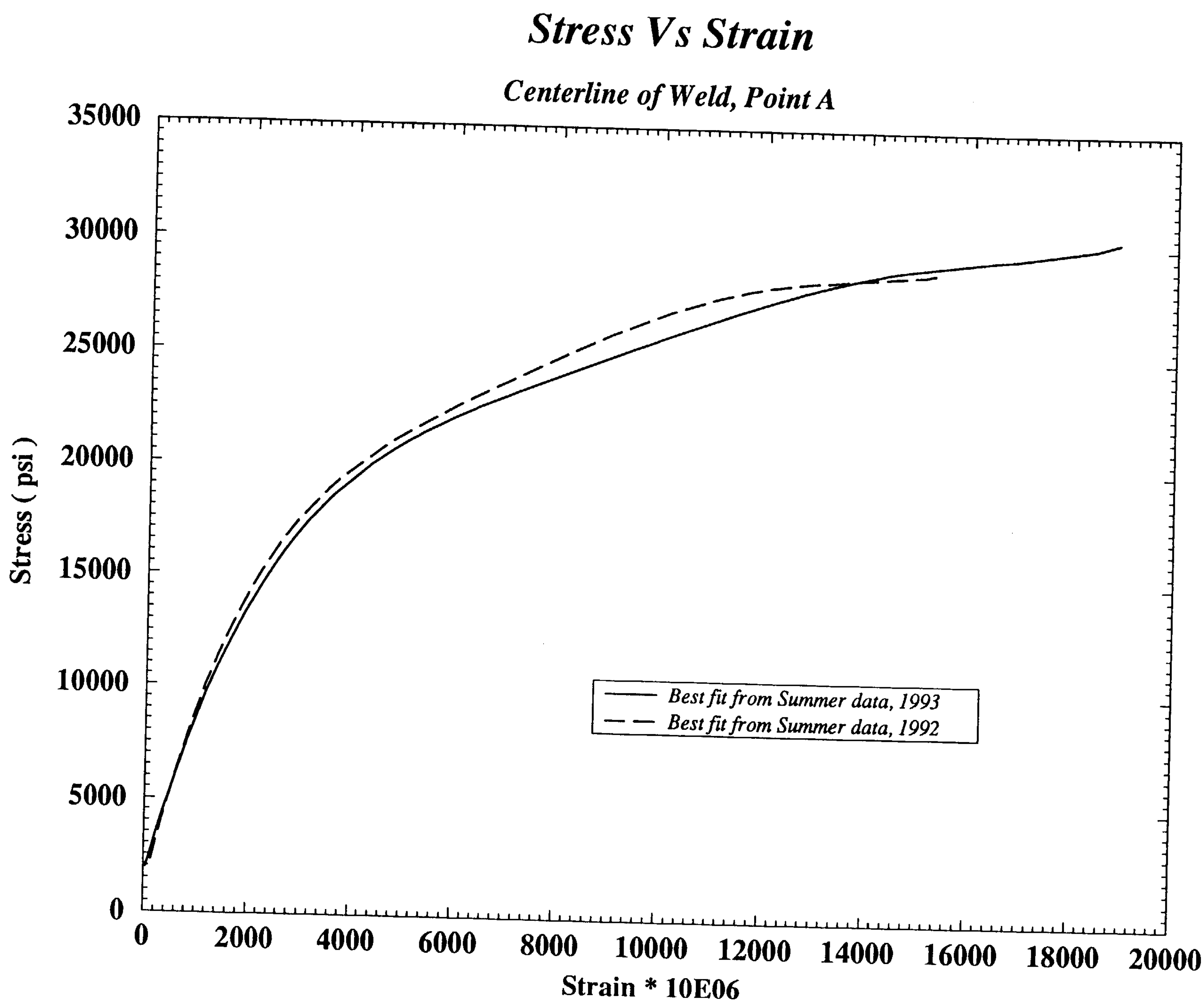

Figure 4-17. Material Behavior, Centerline, Centerpoint

Graphs showing scatter of data for all tests of the 1/2" thick by 2" wide as welded test specimens are presented in Appendix D.

IX. SUMMARY AND CONCLUSIONS

A. Summary

Four new procedures developed for welding 1.4" thick, heat treated, 2219-T87 parent material with 2319 filler material were evaluated to determine which procedure, if any, caused the welded joint to yield in a uniform manner. Dogbone tensile specimens were tested using Photostress and results were compared to similar tests on welded joints made by the normal weld procedure. One new procedure, called Not Tightly Restrained, was seen to be different from the other three and was tested extensively to determine its mechanical behavior characteristics.

Dogbone tensile specimens made from heat treated, 1.4" thick material were machined from panels welded using the normal welding procedure and were tested to determine mechanical properties and contraction ratios. Contraction ratios were seen to vary considerably from point to point in the welded joint and, at some points, exceeded 0.50.

Specimens machined from heat treated 1.4" thick material were tested in pure bending to determine mechanical properties of the weld material in tension and compression. The two conditions of the OD side in tension and the ID side in tension were examined. Tests indicated that material in the weld deformed in a non-linear, non-uniform manner as the bending moment increased.

Tensile tests were conducted on as welded dogbone specimens made from 0.5 inch thick material to determine mechanical properties and contraction ratios. Mechanical properties compared closely with those obtained in similar tests during previous research and contraction ratios varied from point to point, being near 0.75 when measured on the through the weld surface.

Tests on all 0.5" and 1.4" thick welded joints indicated that, for the first applied load, material in the weld and heat affected zone was non-linear, yielded in a non-uniform manner, and exhibited contraction ratios that varied from point to point and did not conform to Chakrabarty's plasticity theory. Upon applying a second load to the material, it becomes essentially elastic up to the stress applied during the first load.

B. Conclusions

1. None of the four newly developed procedures for welding the 1.4" thick 2219-T87 panels provided for improved, more uniform yielding of the joint. Yielding starts on one side of the weld and progresses through the weld in a non-uniform manner as the applied stress increases.
2. The new procedure called Not Tightly Restrained yields in a manner different from the other three in that yielding begins on the ID side of the joint rather than the OD side. Yielding progresses through the weld in a non-uniform manner similar to that seen in the other three procedures.

3. When placed in pure bending, material subjected to tensile stress is more ductile than material placed in compression. Material subjected to compressive stress is stronger than material placed in tension.
4. In bending tests, the concept of a "neutral axis" does not exist through the weld material since a very complex state of stress is developed in this region.
5. In-plane contraction ratios in the 0.5" and 1.4" thick material are different at different points, are a function of the applied plastic stress, and exceed 0.50 at some points in the weld material. Chakrabarty's approximation for contraction ratios is not valid when applied to 2219-T87 welded specimens.
6. Out-of-plane contraction ratios indicate that, for constant volume deformation, strains normal to the specimen surface are greater than transverse strains within the surface.
7. Weld material 0.50 and 1.50 inches thick exhibits near perfect strain hardening upon application of the second load.

X. REFERENCES

1. Gambrell, S. C., Jr., "Use of Photostress to Characterize the Mechanical Behavior of Weldments," Summary of Work, NASA/ASEE Summer Fellowship Program, Metallurgy Research Branch, Metallic Materials Division, Materials and Processes Laboratory, MSFC, May 28-August 2, 1991.
2. Gambrell, S. C., Jr., "Use of Photostress to Characterize the Mechanical Behavior of Weldments," Final Report, Contract No. NAG8-212, SUB92-195, University of Alabama in Huntsville/NASA, BER Report No. 570-97, September, 1992.
3. Gambrell, S. C., Jr., "Use of Photostress to Characterize the Mechanical Behavior of Weldments," Proceedings of the VII International Congress on Experimental Mechanics, SEM, June, 1992, Session 22, pp. 543-549.
4. Gambrell, S. C., Jr., "Use of Photostress to Characterize the Mechanical Behavior of Weldments," Experimental Techniques, Vol. 17, No. 1, Jan/Feb 1993, pp. 15-18.
5. Gambrell, S. C., Jr., and Kavikondala, K., "Yield Detection in Aluminum Welded Joints Using Photostress," Proceedings of the 1993 SEM 50th Anniversary Conference on Experimental Mechanics, Session 27, June 1993, pp. 653-649.
6. Chakrabarty, J., Theory of Plasticity, McGraw-Hill, 1987.
7. "Photostress Instrumentation," Measurements Group Inc. Literature, Raleigh, NC, Bulletin 315-B, 1989.
8. "How to Select Photoelastic Coatings," Measurements Group Inc. Literature, Raleigh, NC, TN-704, 1978.

9. "Automatic Data Acquisition," ADA-1 through ADA-8, Measurements Group Inc. Literature, Raleigh NC.

10. "Operating Instructions and Technical Manual-Strain Measurement with the 030-Series Reflection Polariscope," Measurements Group Inc. Literature, Raleigh, NC.

11. "Instructions for Bonding Flat and Contoured Photoelastic Sheets to Test-Part Surfaces," Measurements Group Inc. Literature, Raleigh, NC, IB-223-F, 1982.

12. "Instructions for Using PC-8 Adhesive," Measurements Group Inc. Literature, Raleigh, NC, IB-231, 1982.

13. Catalog 500, Part A - Strain Gage Listings, Measurements Group Inc. Literature, Raleigh, NC, 1988.

14. "Strain Gage Installations with M-Bond 200 Adhesive," Measurements Group Inc. Literature, Raleigh, NC, IB 127-12, 1979.

15. "Errors Due to Wheatstone Bridge Nonlinearity," Measurements Group Inc. Literature, Raleigh, NC, TN-507, 1982.

16. "Errors Due to Transverse Sensitivity in Strain Gages," Measurements Group Inc. Literature, Raleigh, NC, TN-509, 1982.

XI. APPENDICES

Scatter of data collected for various specimens and tests is given in Figures A1 through D40. Scatter is presented in four appendices as follows:

Appendix A. Task 2, Tensile Tests, New NTR Weld Procedure, 0.71" x 1.4" Material

Appendix B. Task 2, Tensile Tests, Normal Weld Procedure, 0.71" x 1.4" Material

Appendix C. Task 3, Bending Tests, Normal Weld Procedure, 0.71" x 1.4" Material

Appendix D. Task 4, Tensile Tests, 0.5" x 2.0" Material

APPENDIX A

Task 2

Tensile Tests

New NTR Weld Procedure

0.71" x 1.4" Material

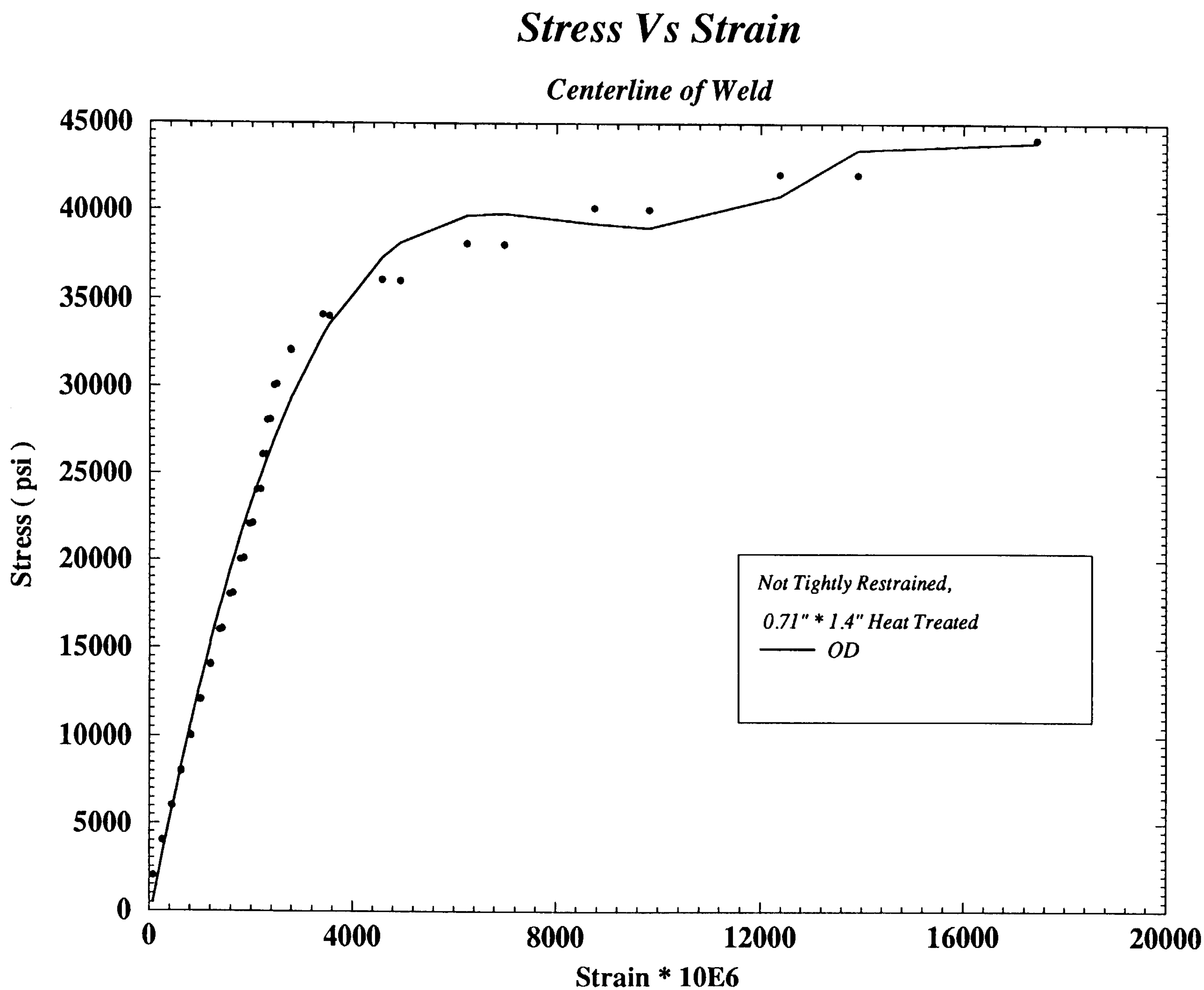

Figure A1. Material Behavior, Centerline, OD Point

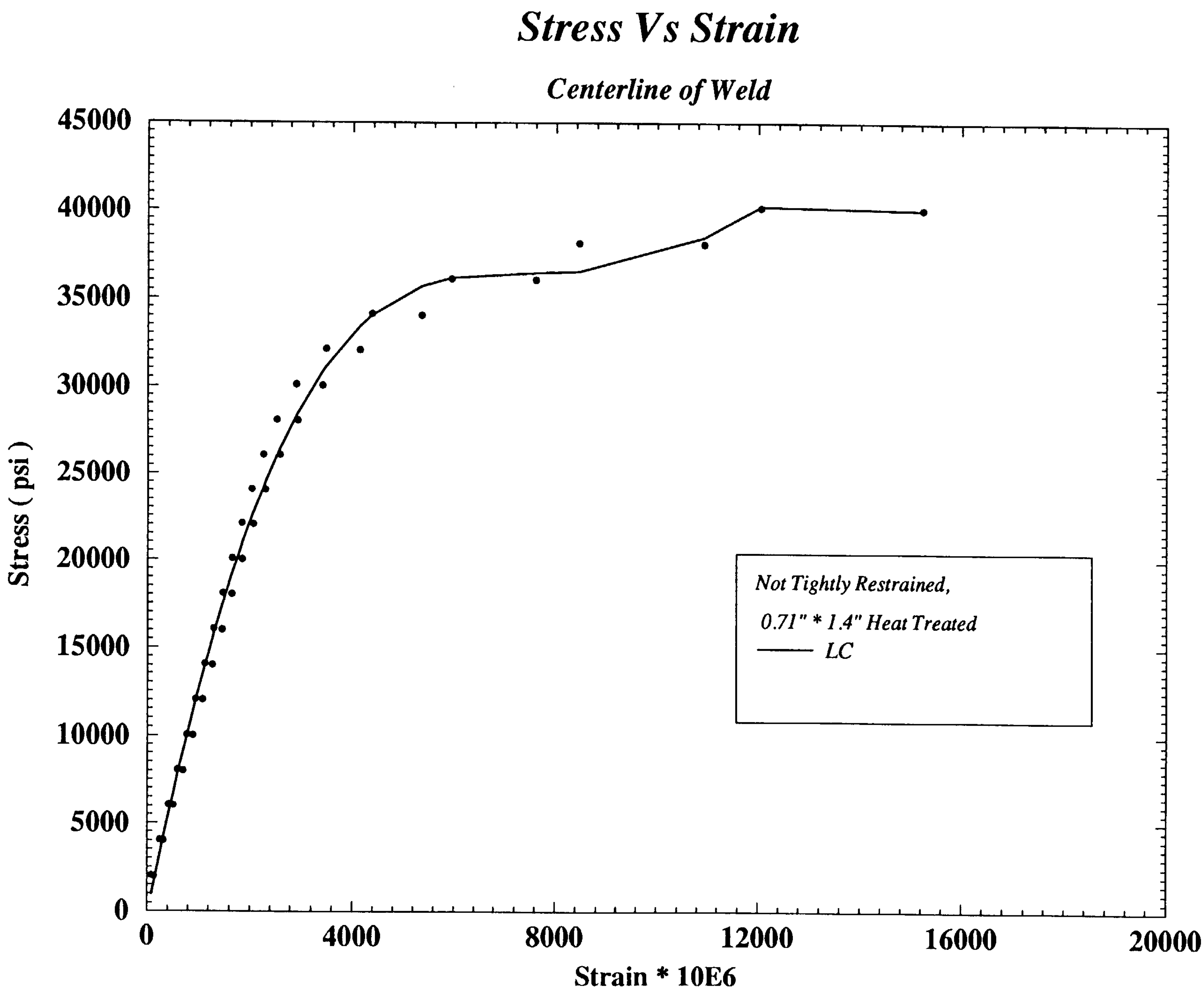

Figure A2. Material Behavior, Centerline, LC Point

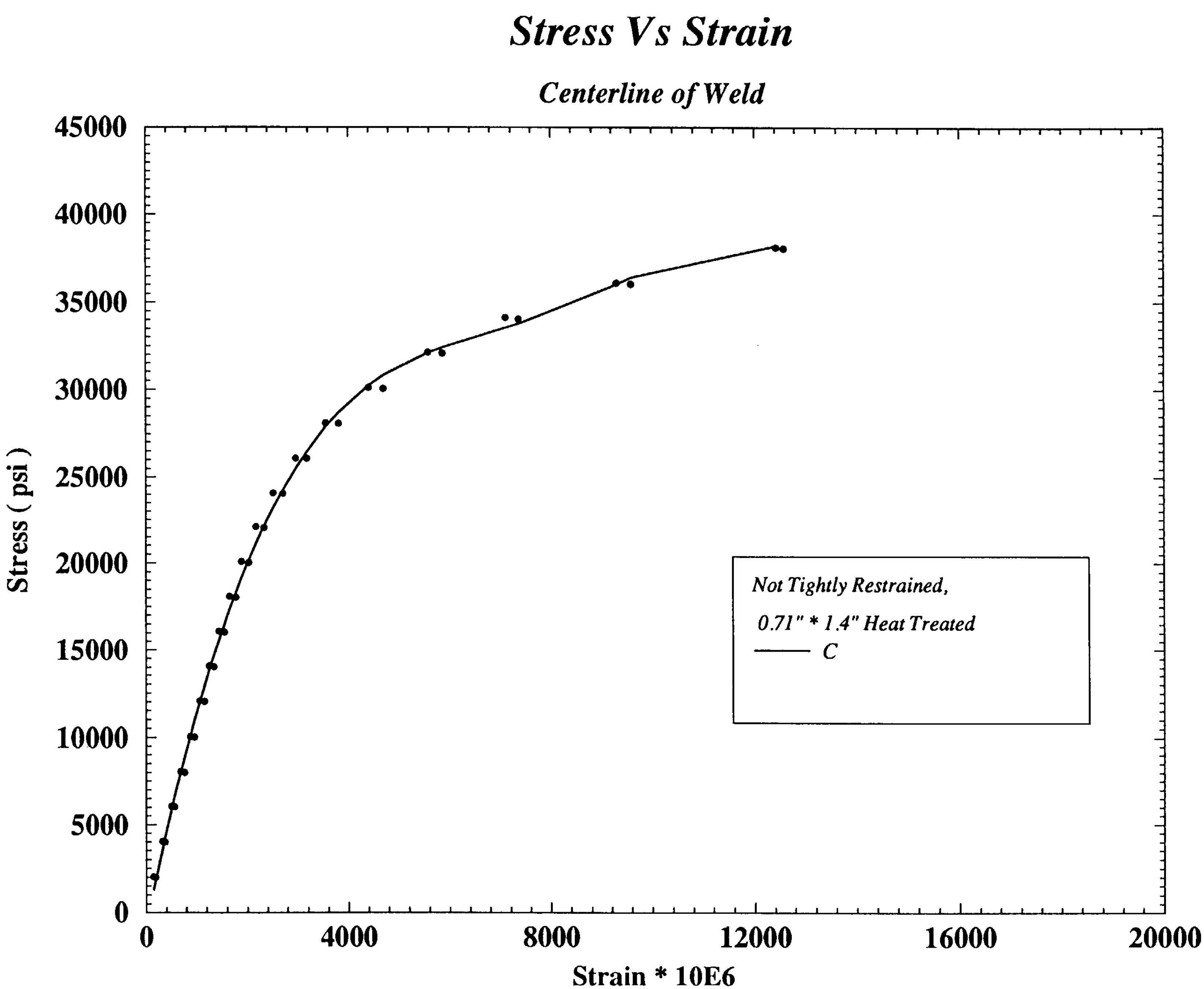

Figure A3. Material Behavior, Centerline, C Point

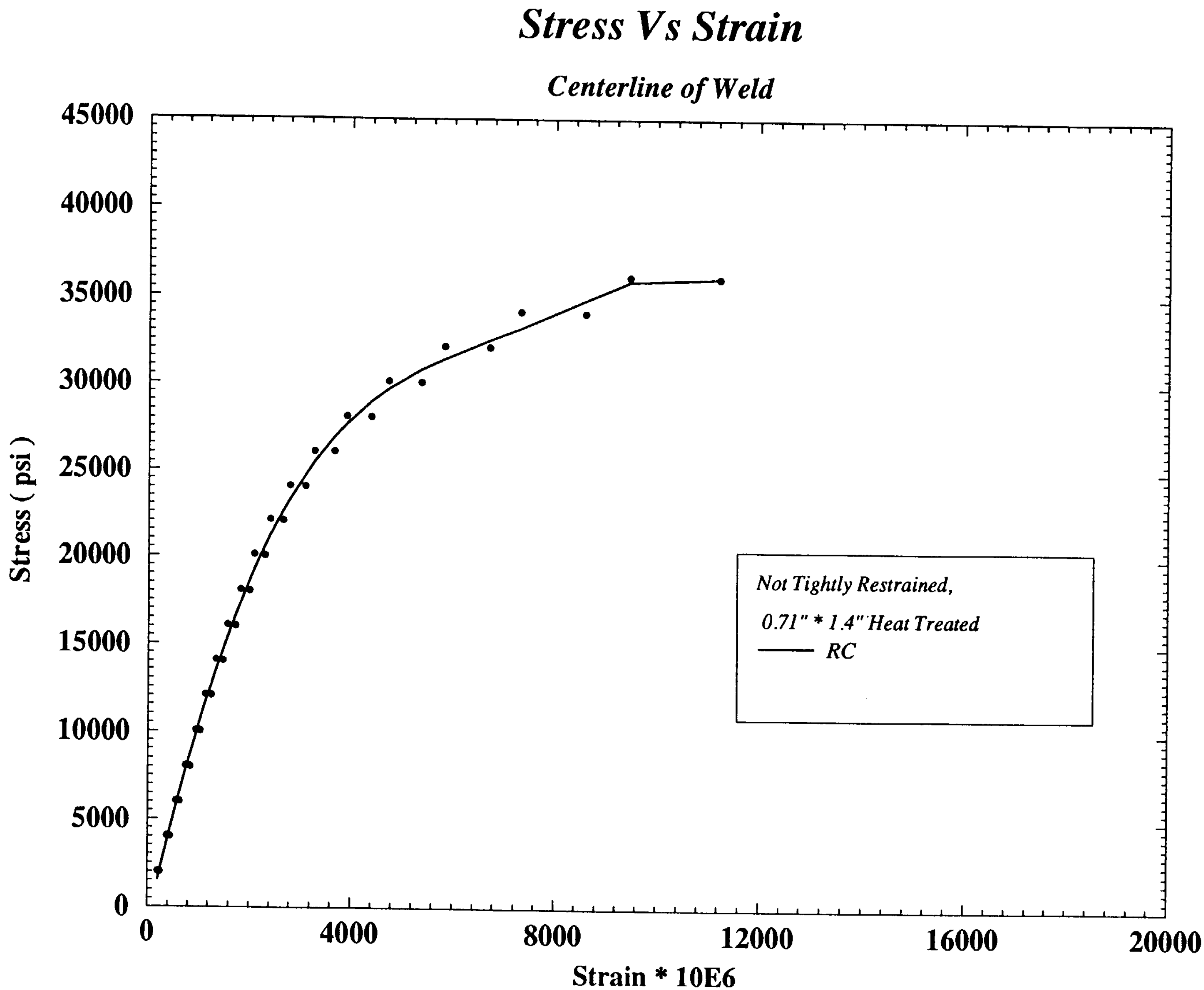

Figure A4. Material Behavior, Centerline, RC Point

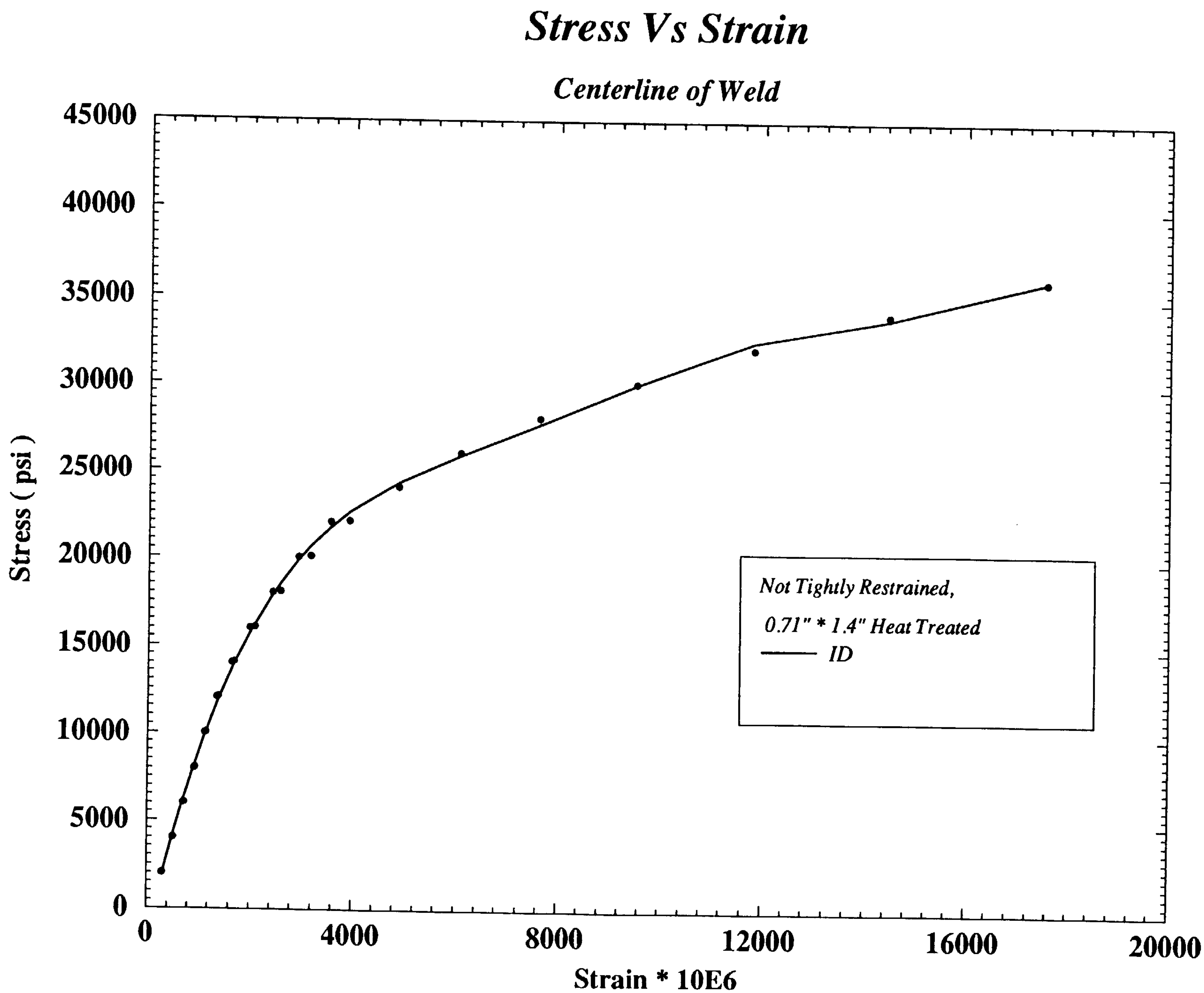

Figure A5. Material Behavior, Centerline, ID Point

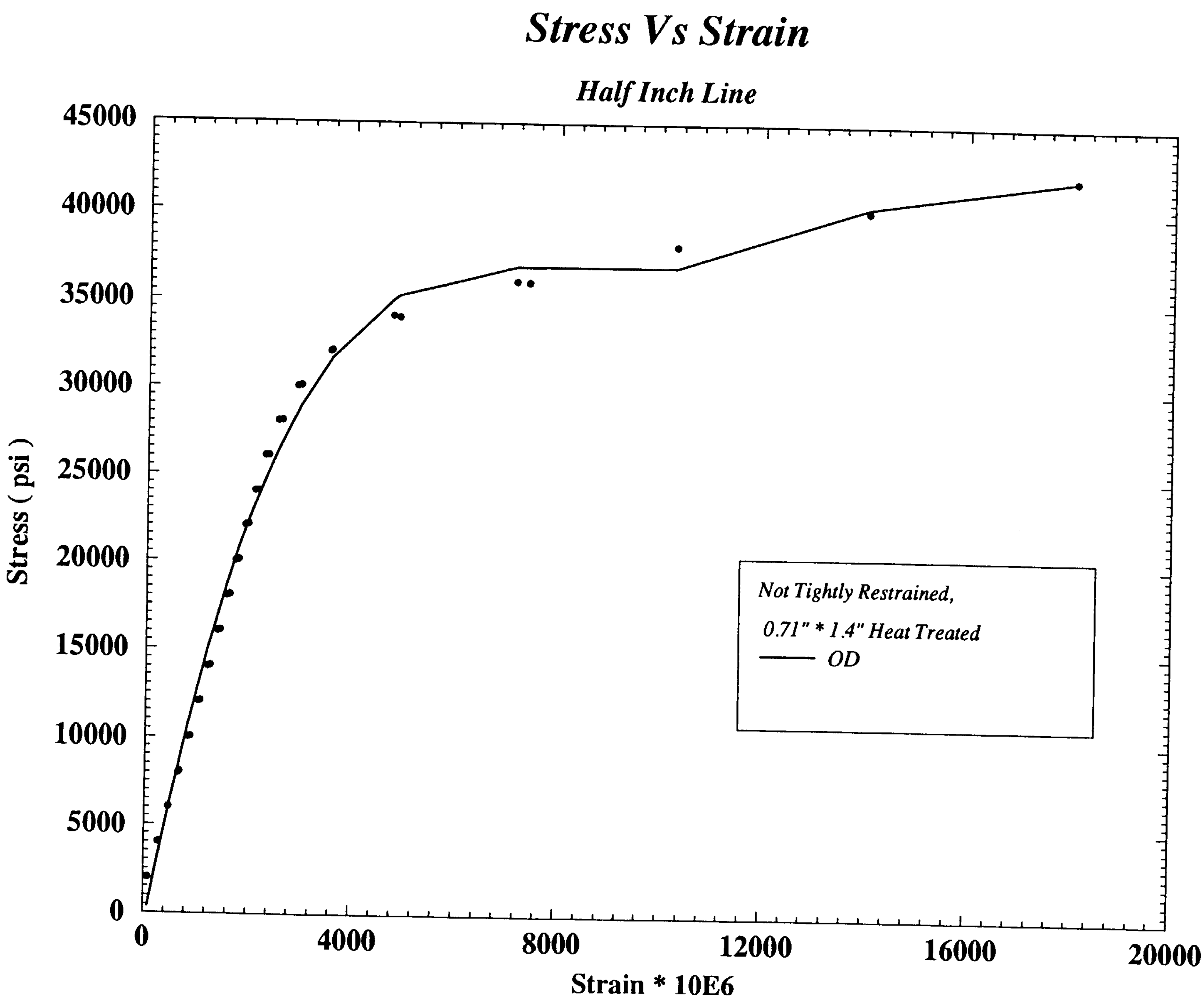

Figure A6. Material Behavior, Half Inch Line, OD Point

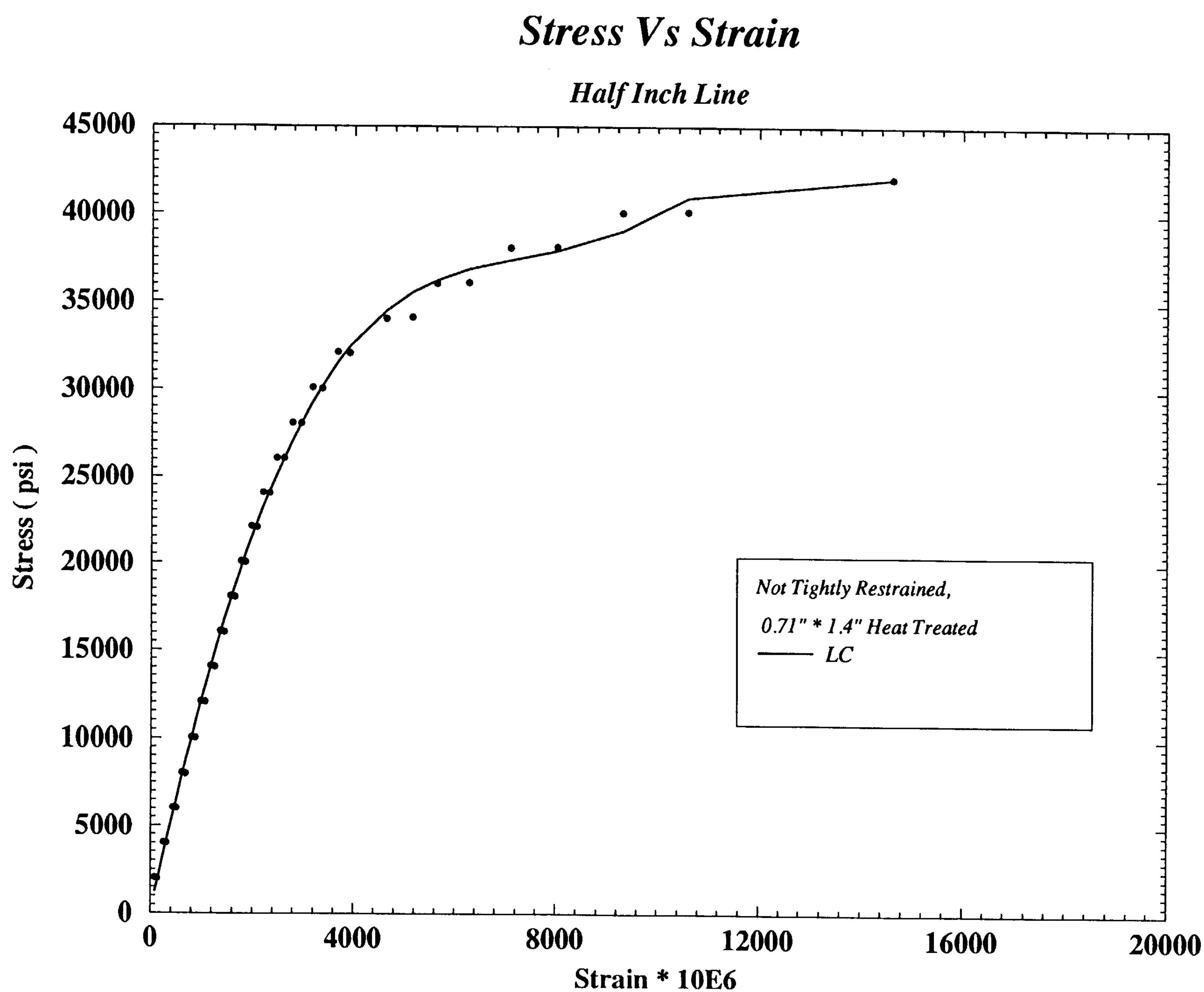

Figure A7. Material Behavior, Half Inch Line, LC Point

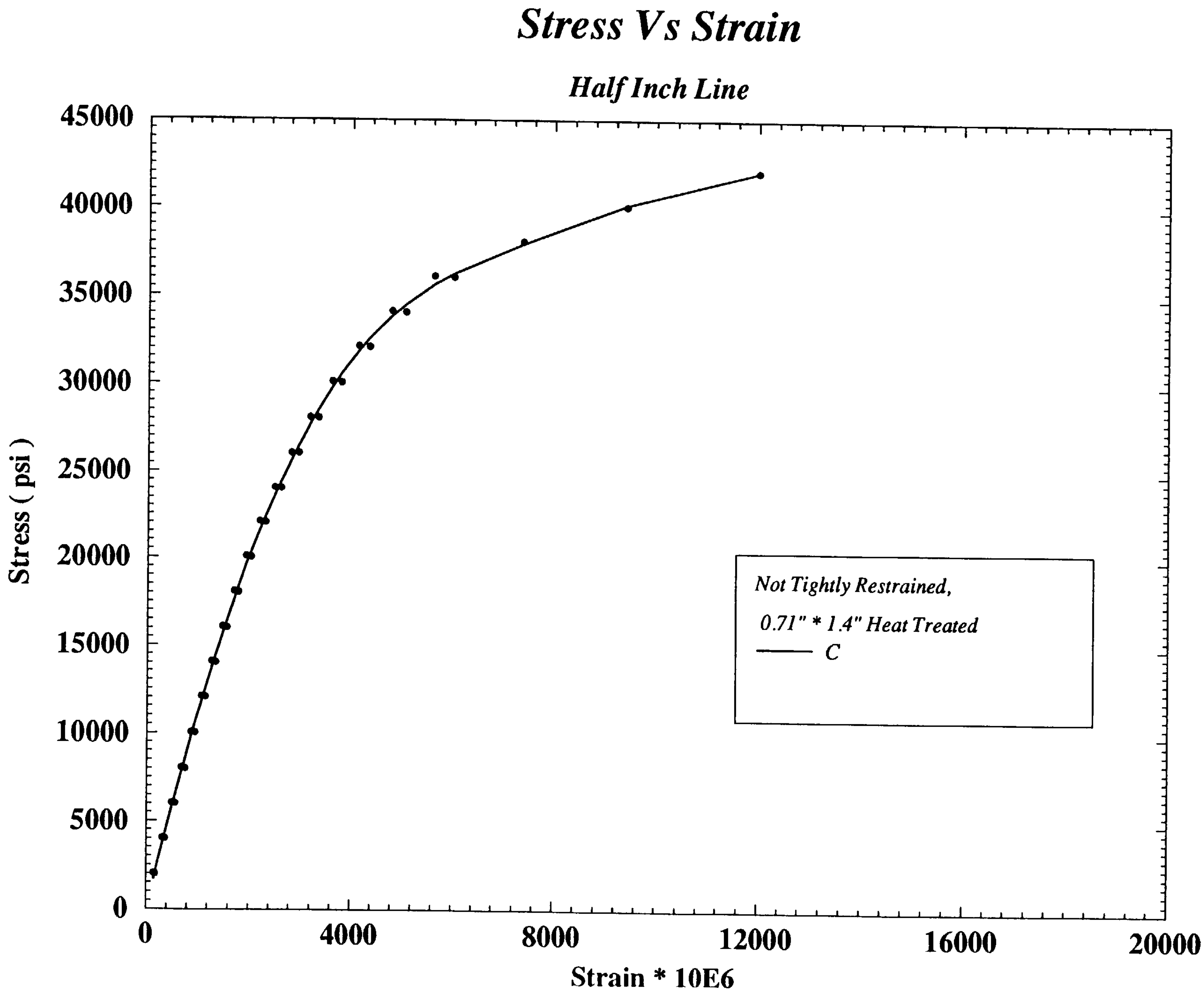

Figure A8. Material Behavior, Half Inch Line, C Point

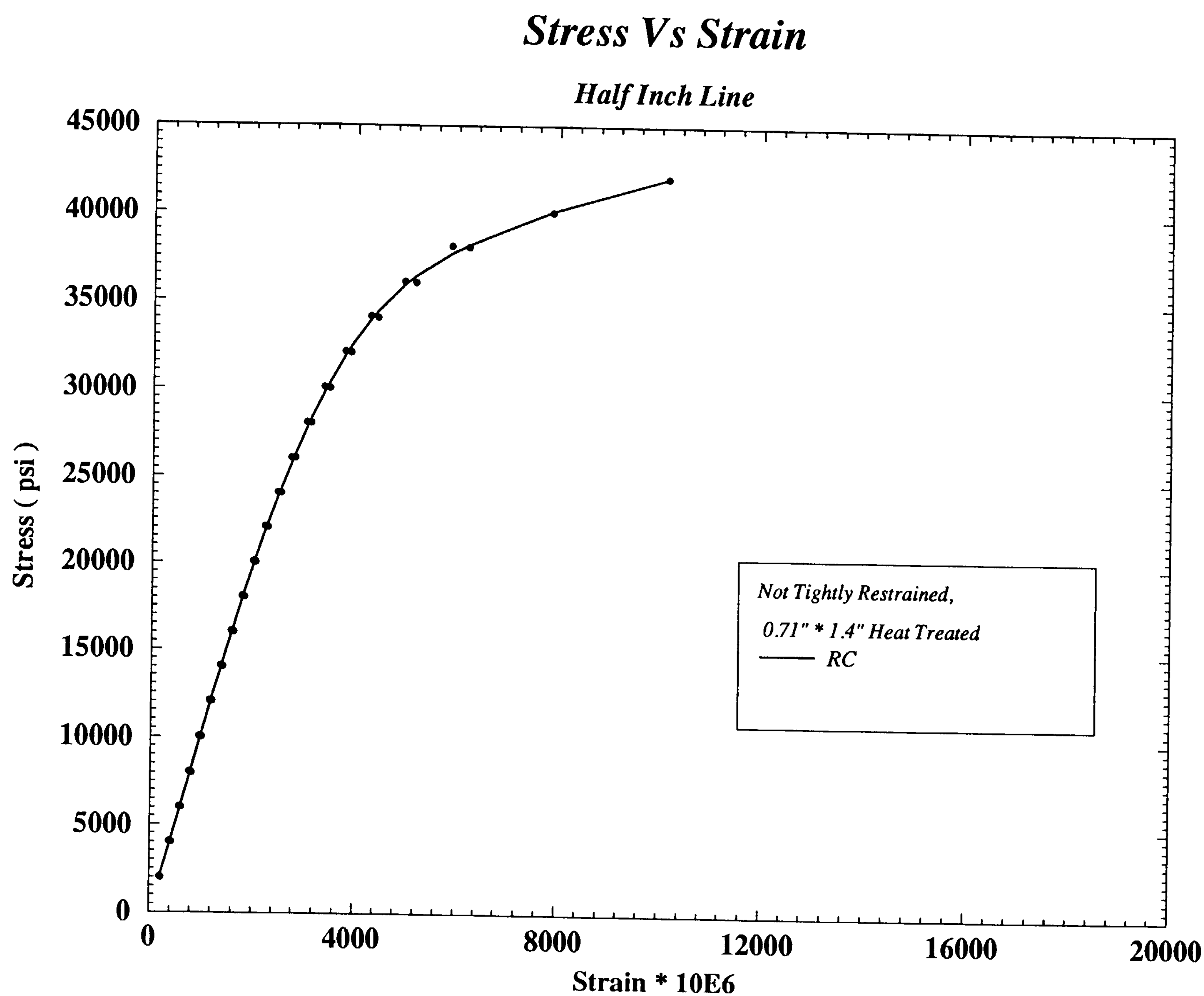

Figure A9. Material Behavior, Half Inch Line, RC Point

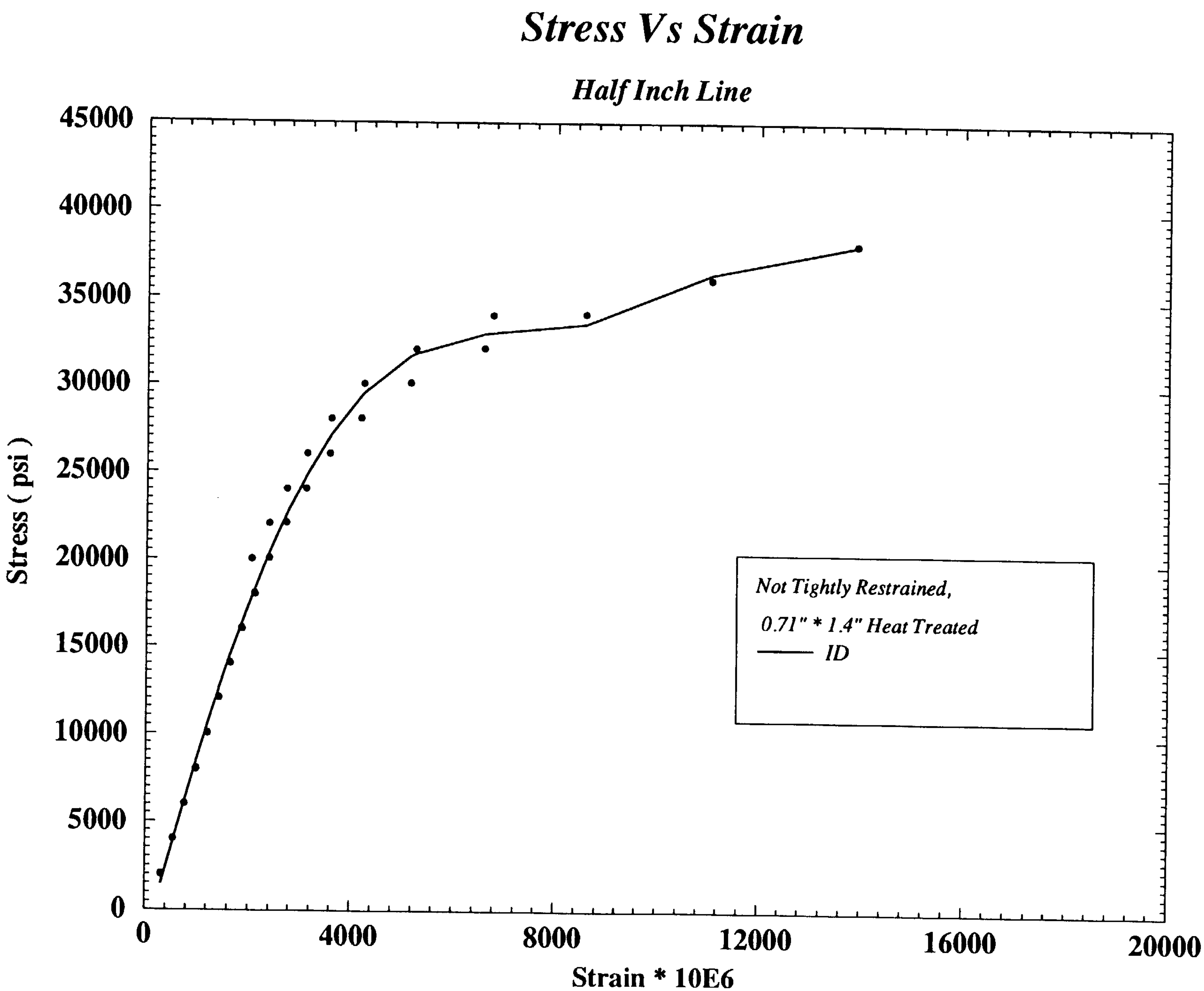

Figure A10. Material Behavior, Half Inch Line, ID Point

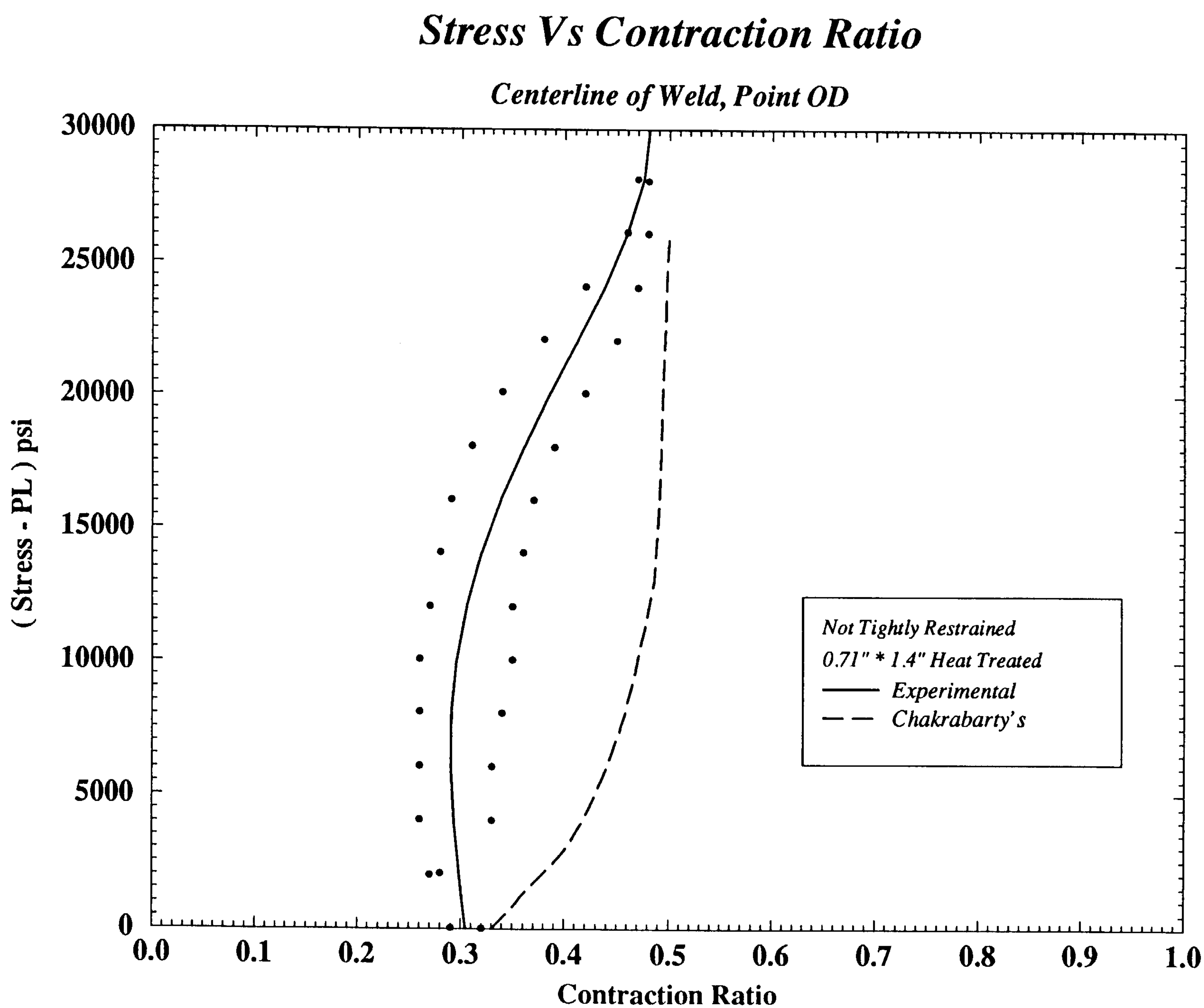

Figure A11. In-Plane CR, Centerline, OD Point

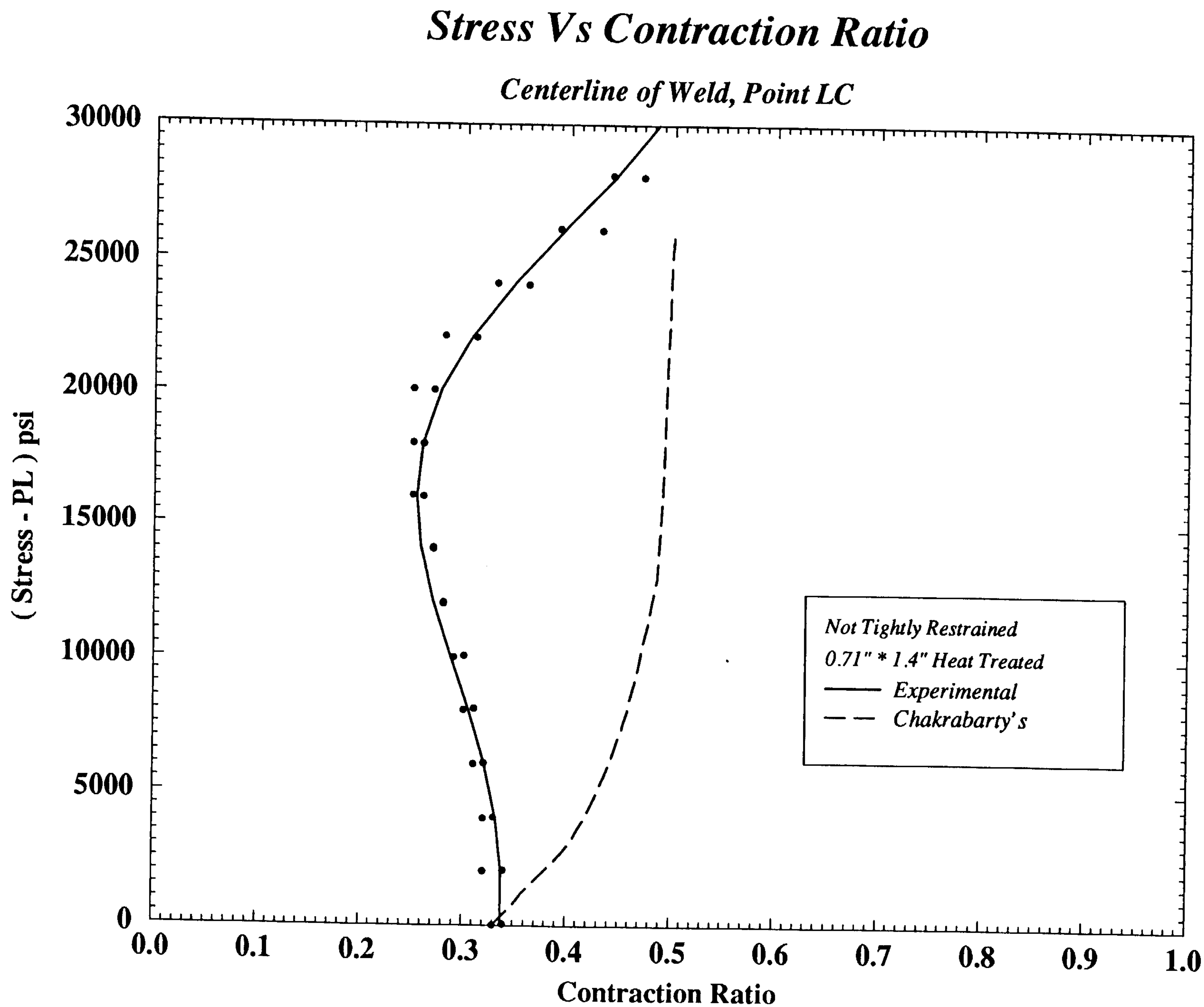

Figure A12. In-Plane CR, Centerline, LC Point

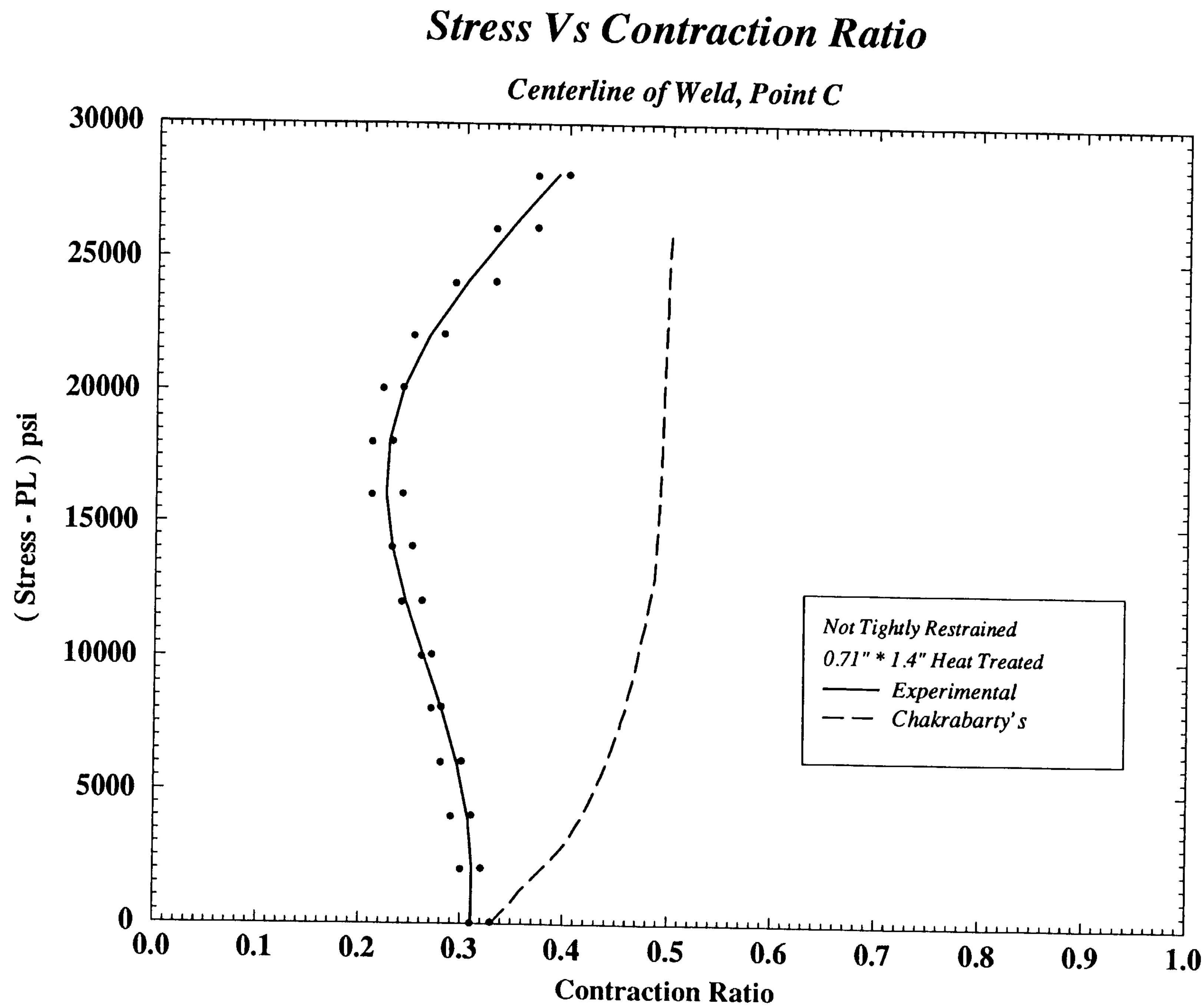

Figure A13. In-Plane CR, Centerline, C Point

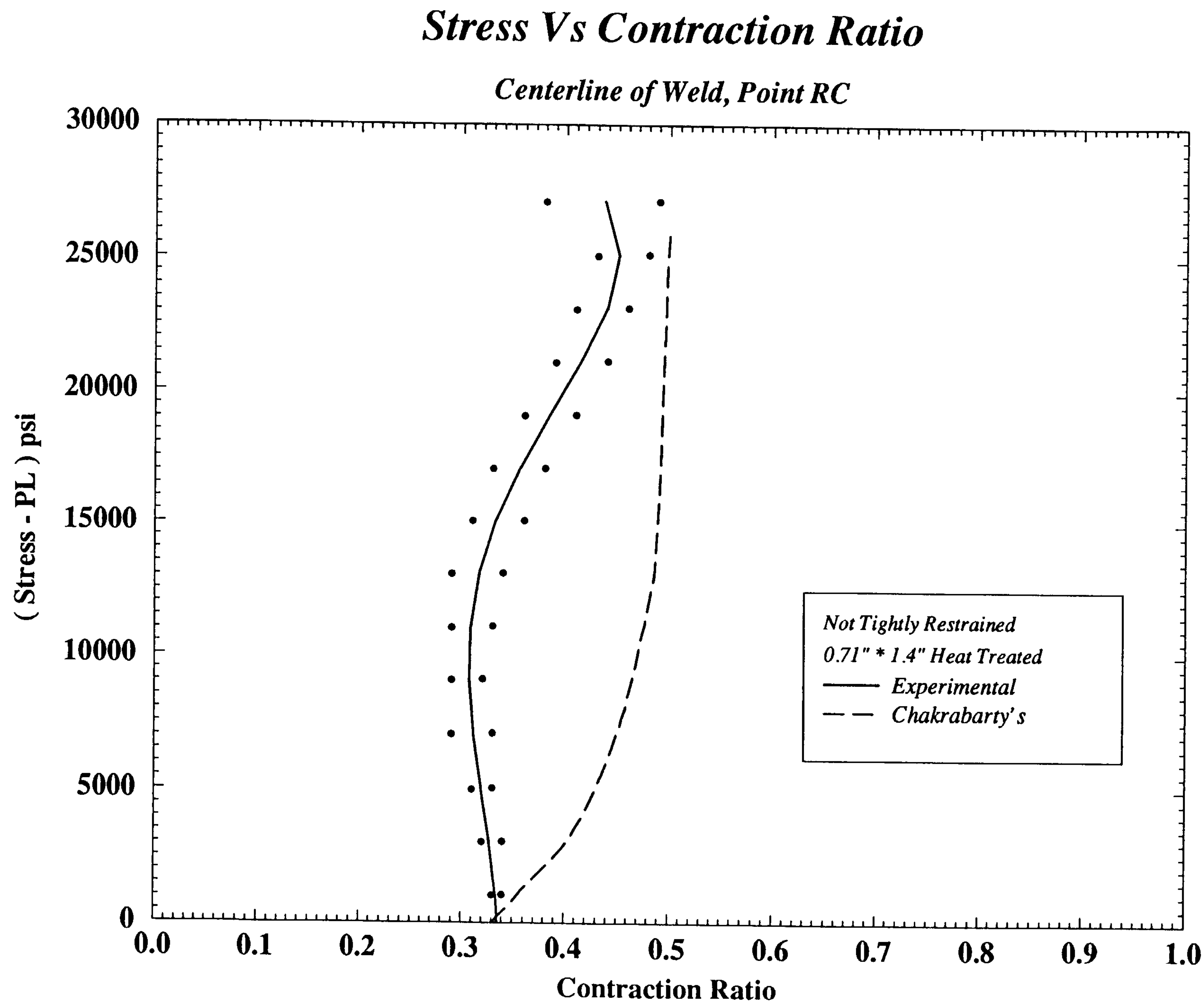

Figure A14. In-Plane CR, Centerline, RC Point

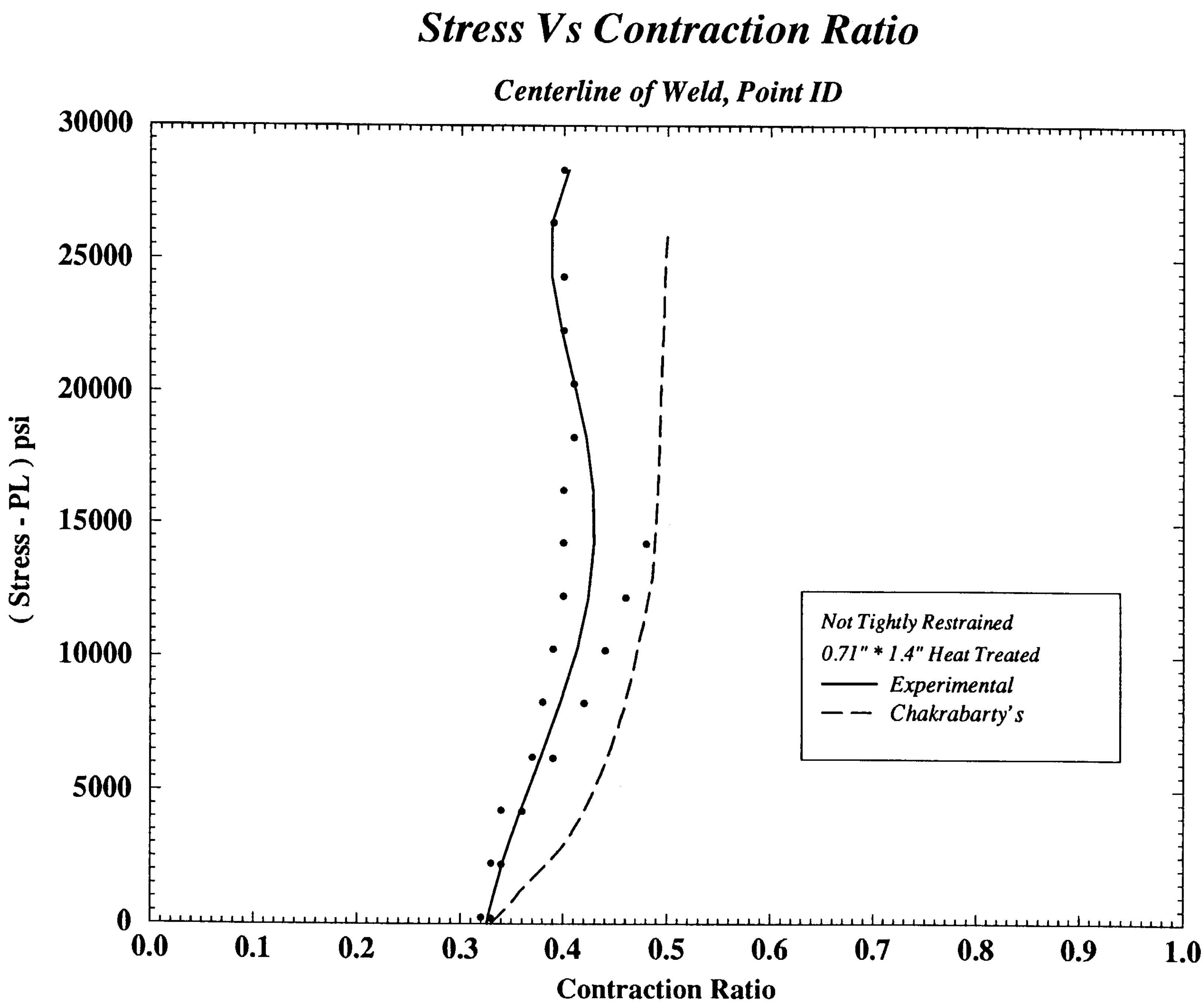

Figure A15. In-Plane CR, Centerline, ID Point

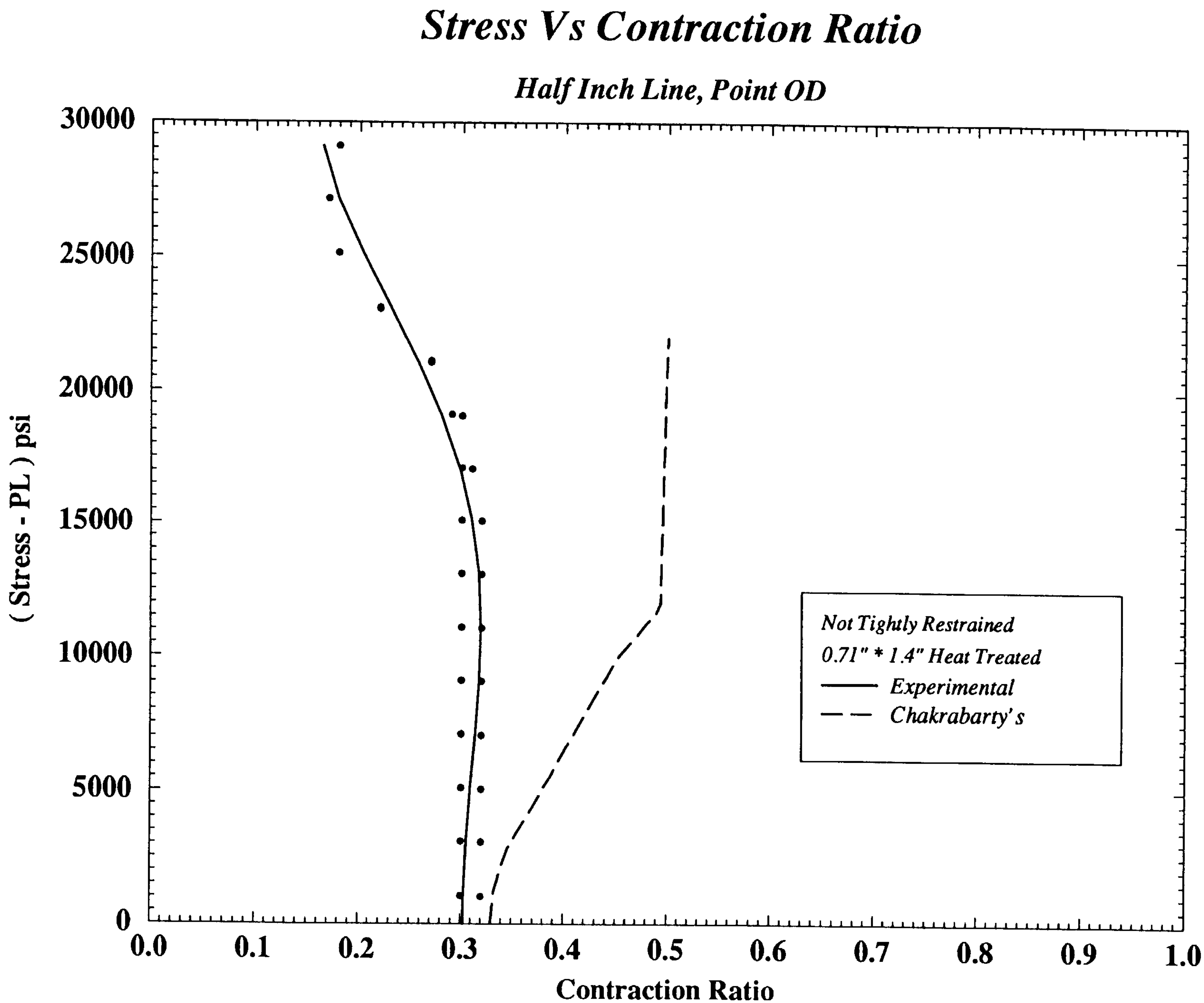

Figure A16. In-Plane CR, Half Inch Line, OD Point

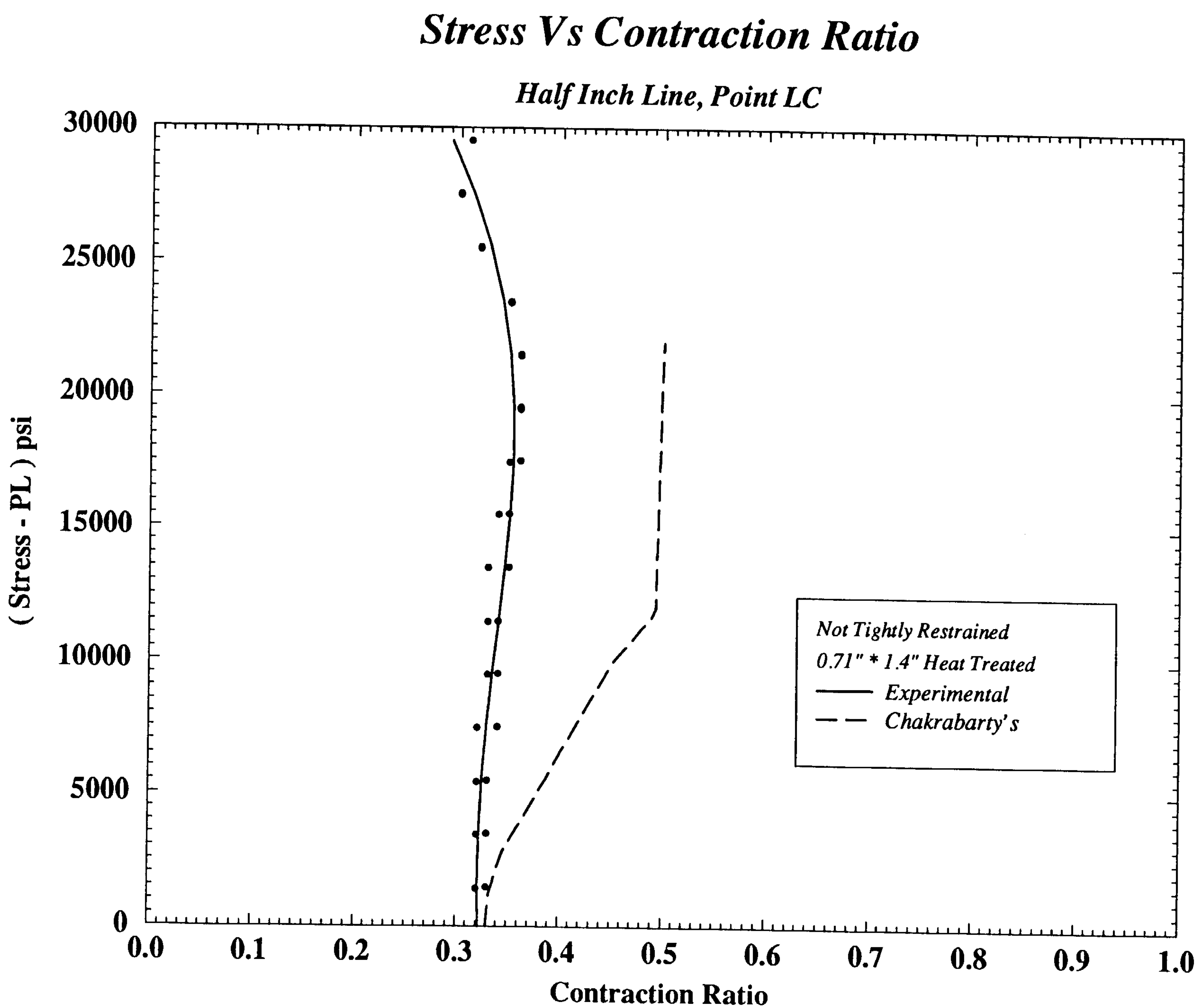

Figure A17. In-Plane CR, Half Inch Line, LC Point

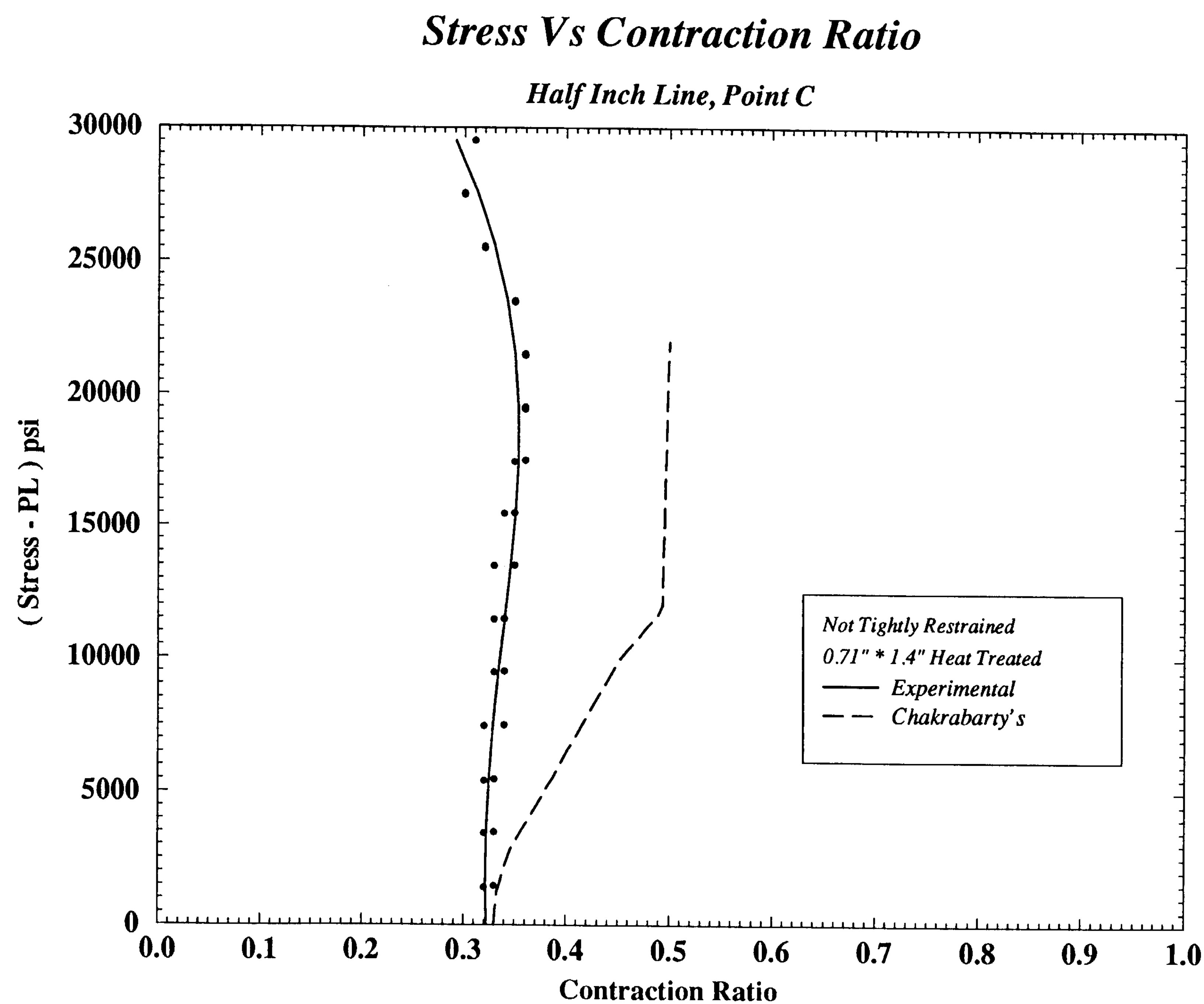

Figure A18. In-Plane CR, Half Inch Line, C Point

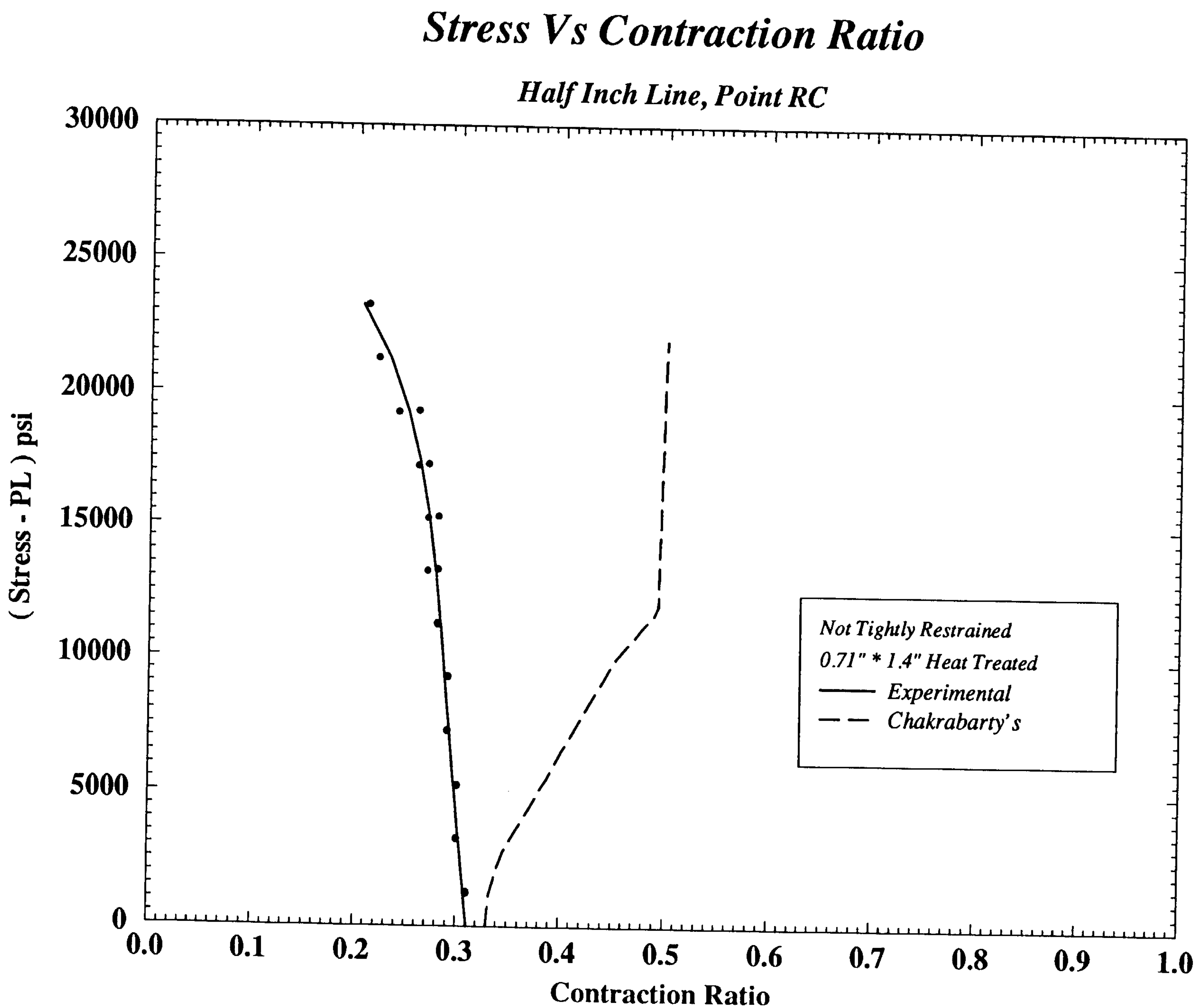

Figure A19. In-Plane CR, Half Inch Line, RC Point

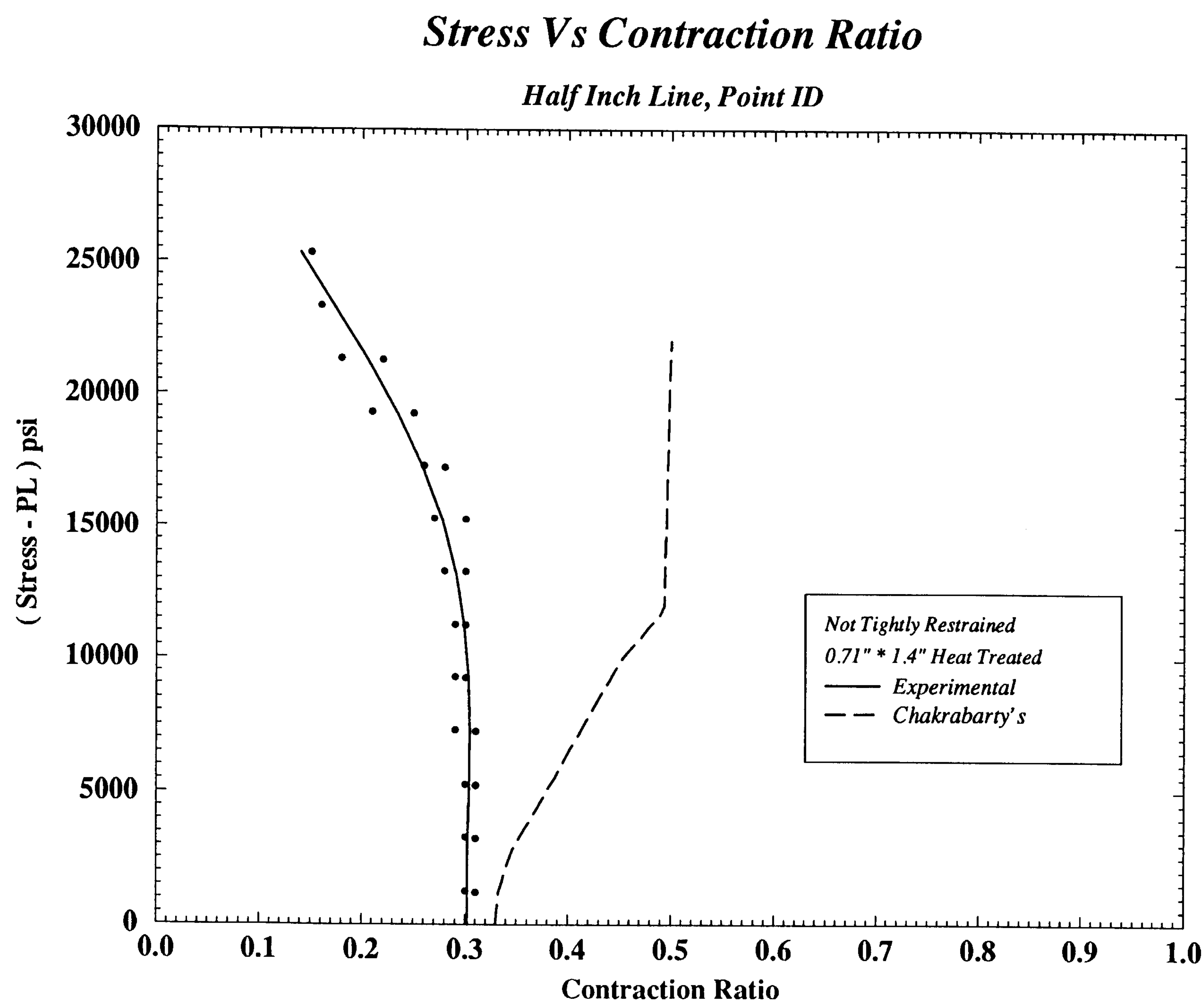

Figure A20. In-Plane CR, Half Inch Line, ID Point

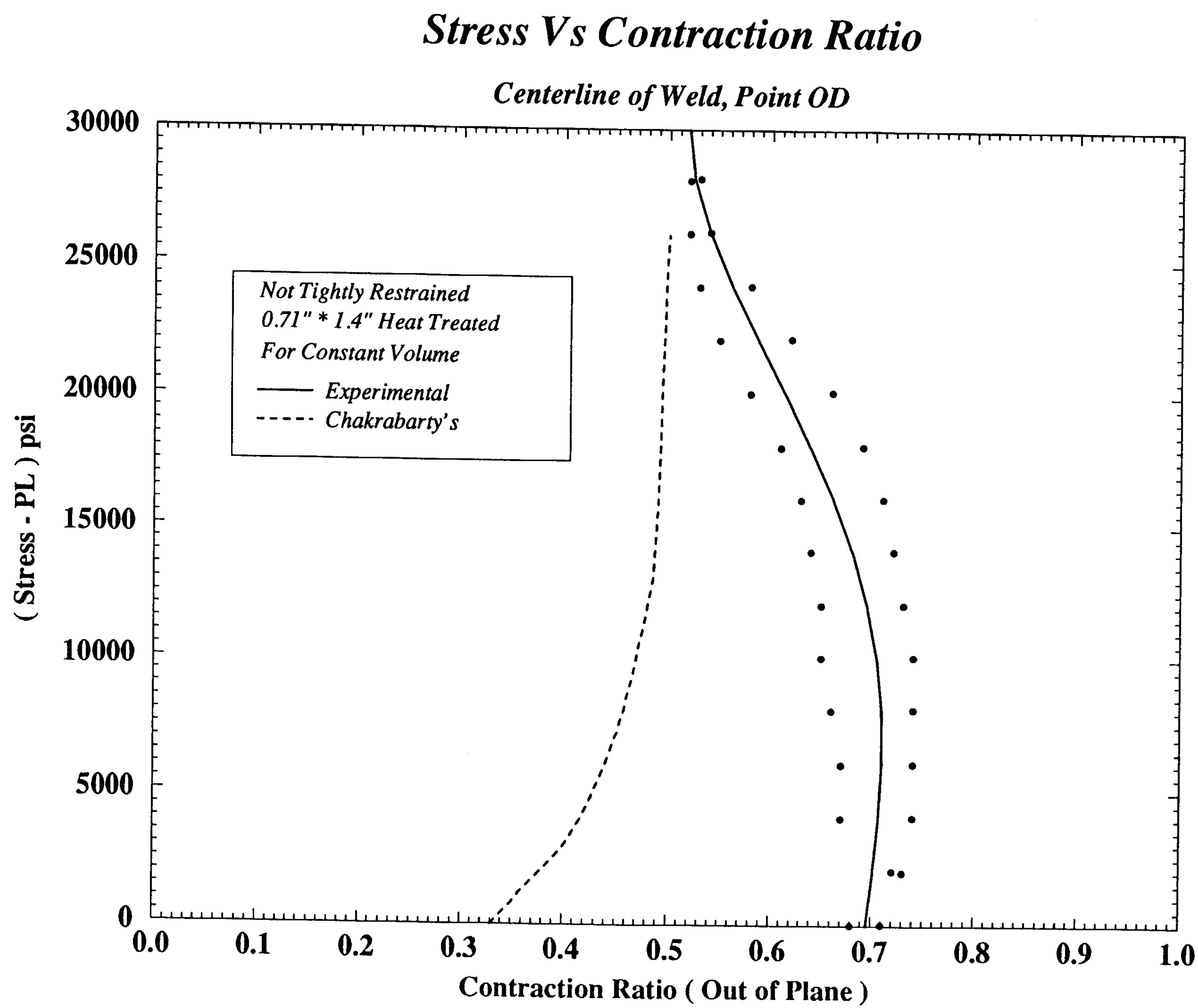

Figure A21. Out-of-Plane CR, Centerline, OD Point

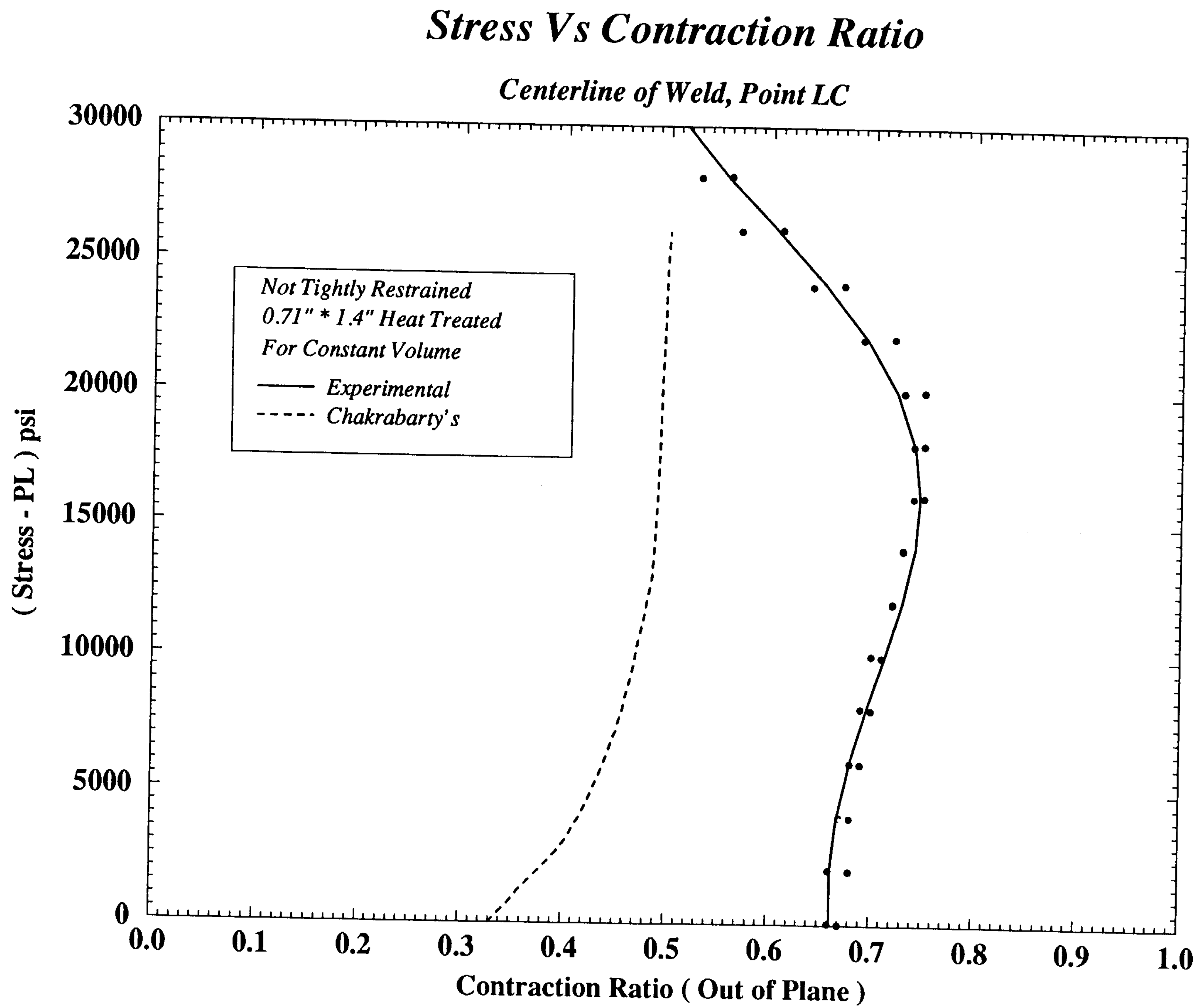

Figure A22. Out-of-Plane CR, Centerline, LC Point

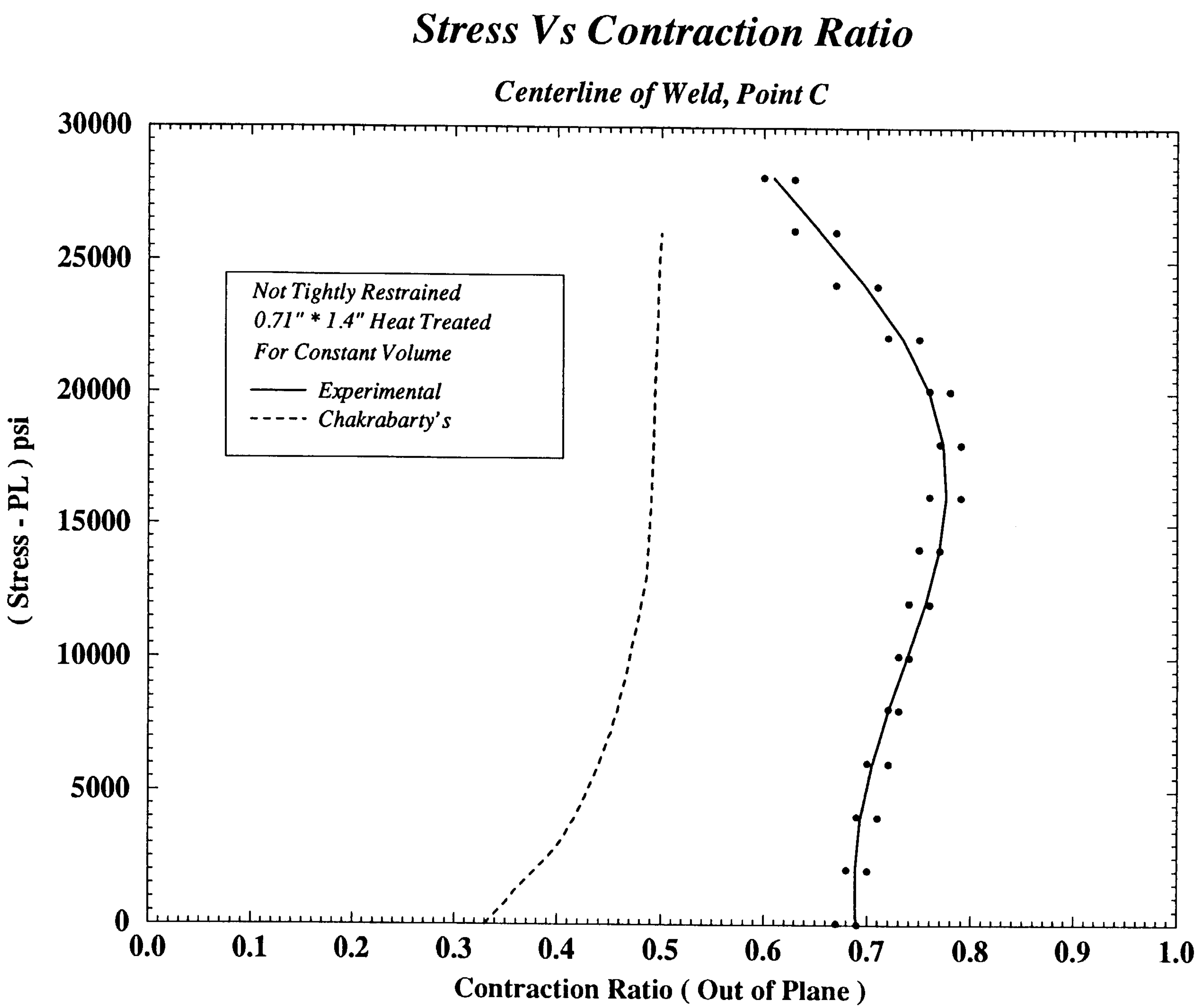

Figure A23. Out-of-Plane CR, Centerline, C Point

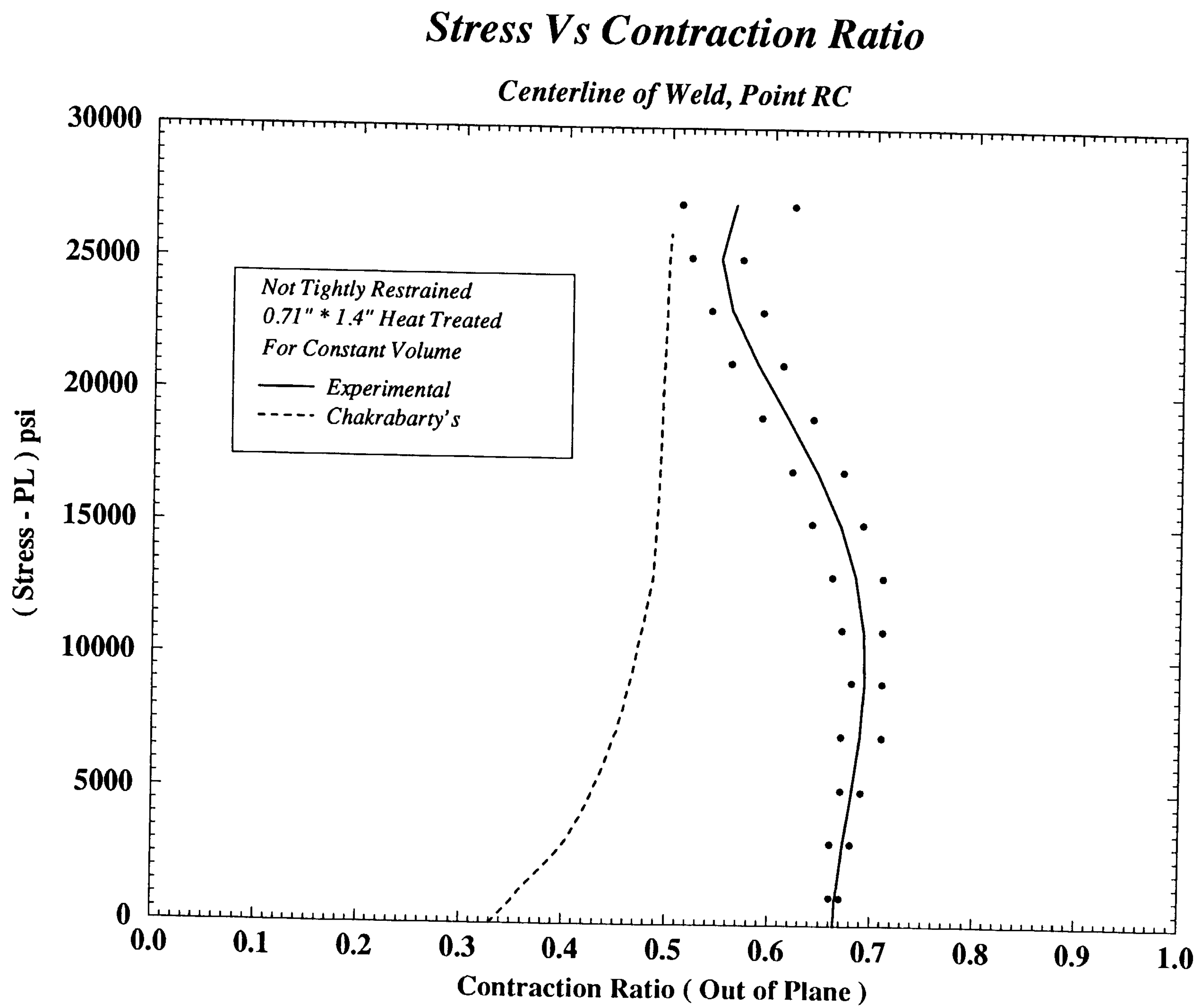

Figure A24. Out-of-Plane CR, Centerline, RC Point

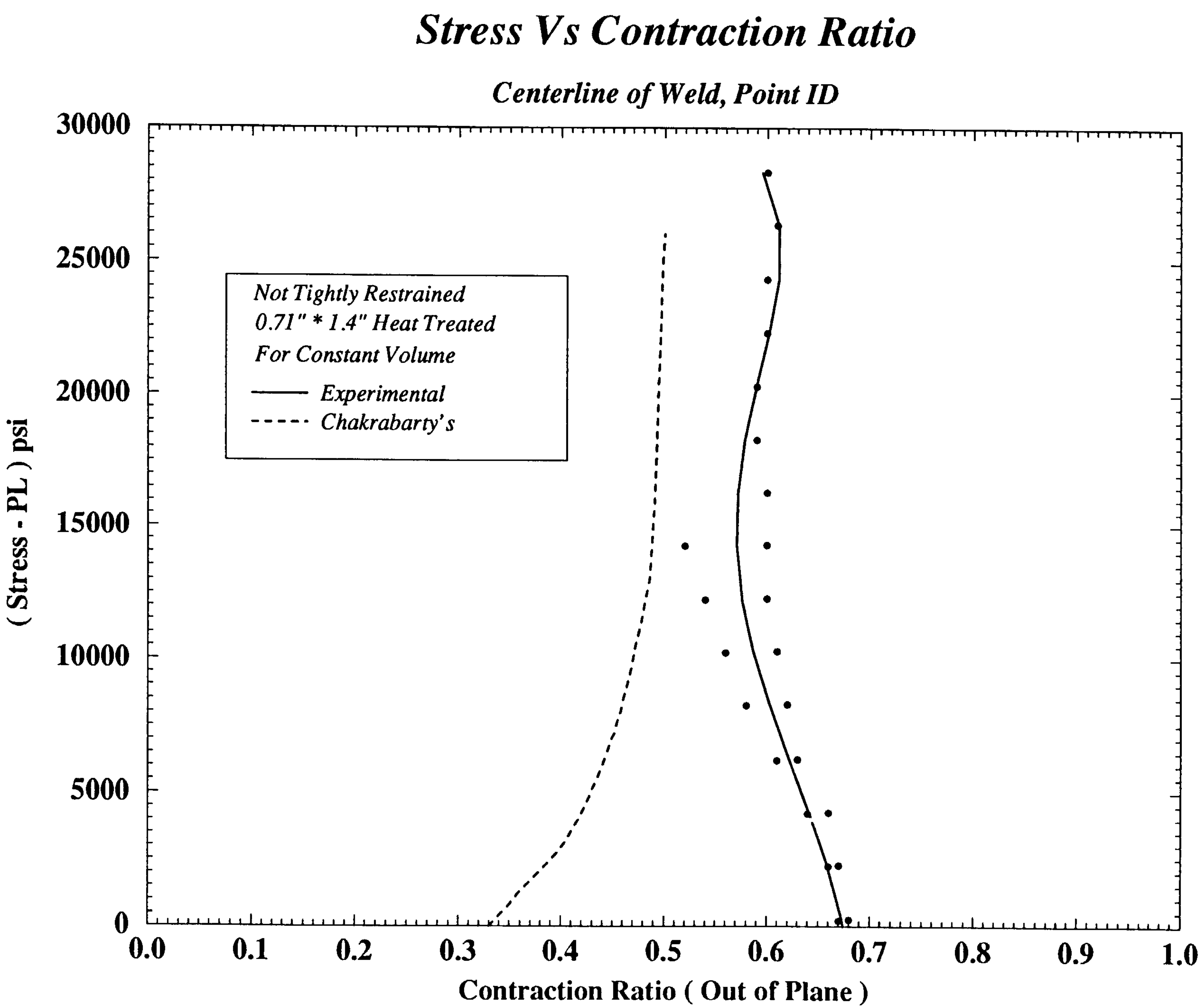

Figure A25. Out-of-Plane CR, Centerline, ID Point

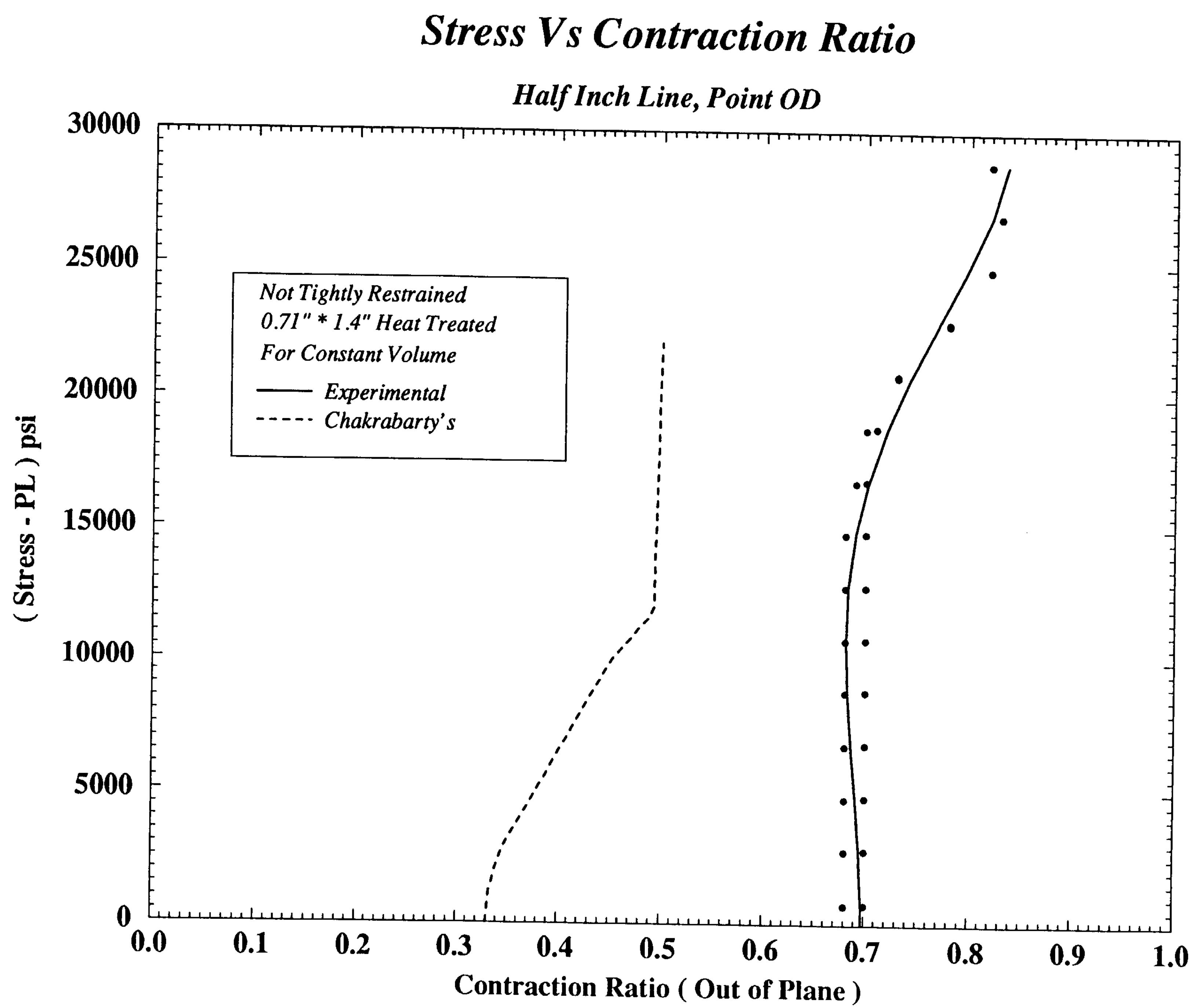

Figure A26. Out-of-Plane CR, Half Inch Line, OD Point

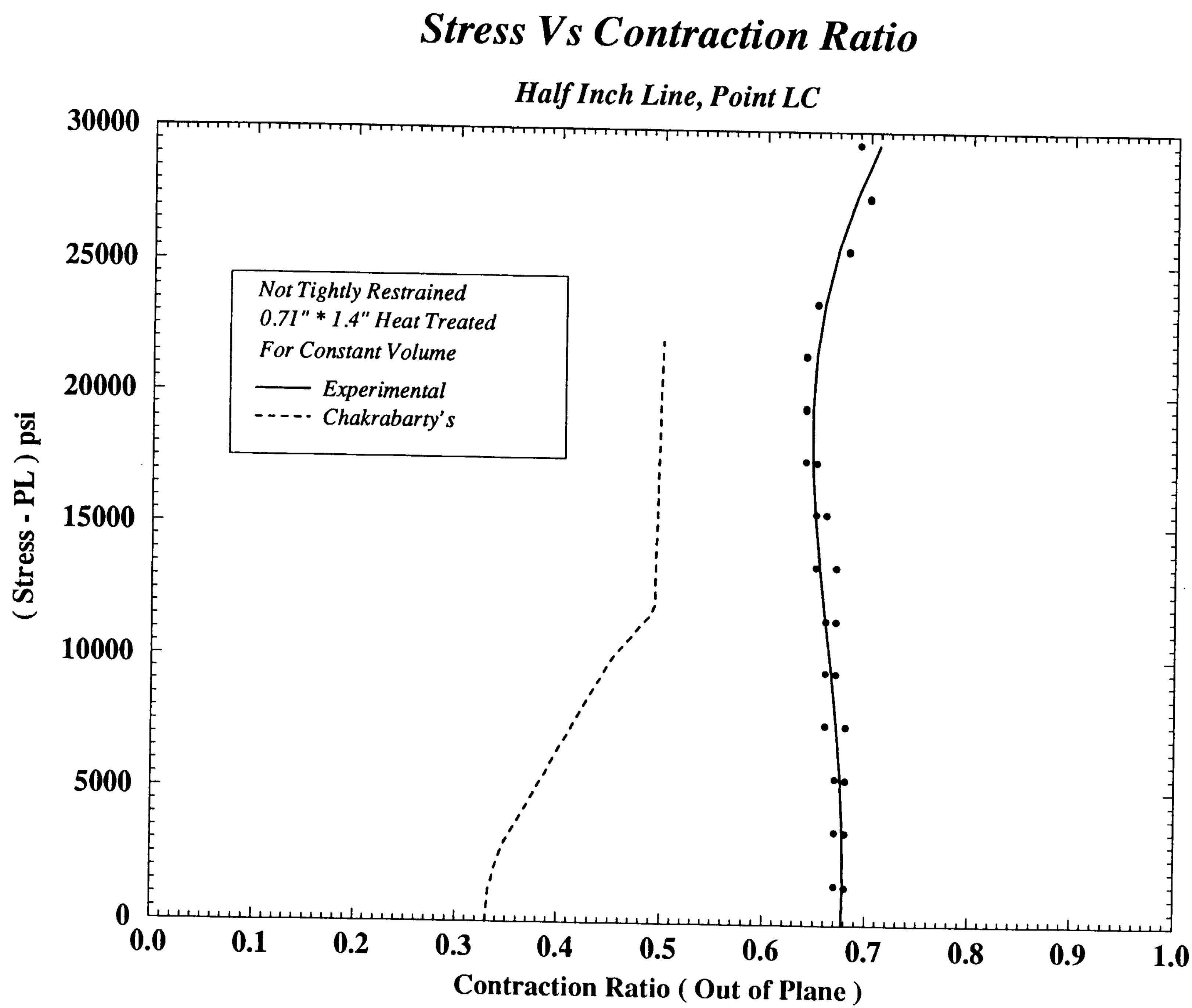

Figure A27. Out-of-Plane CR, Half Inch Line, LC Point

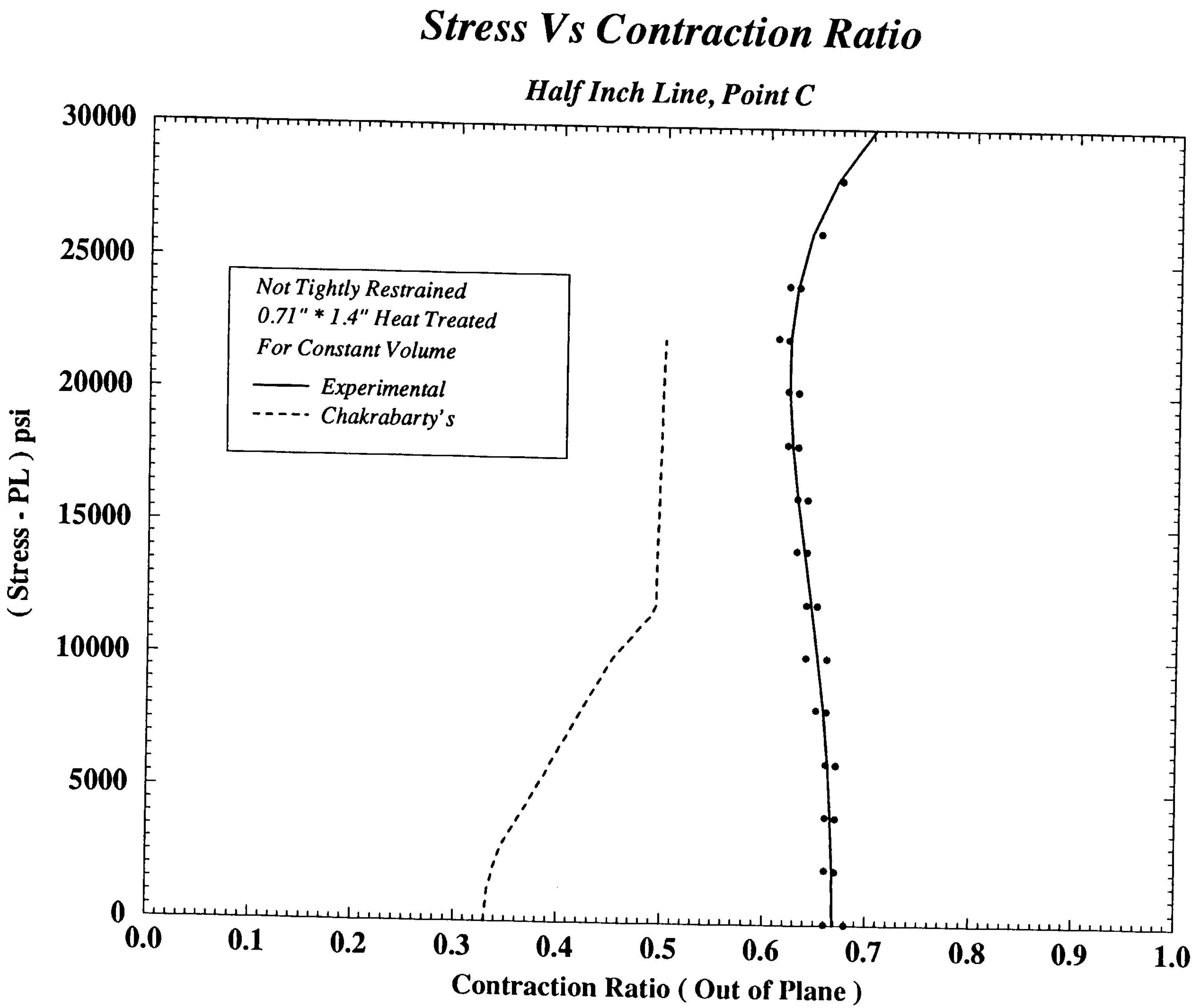

Figure A28. Out-of-Plane CR, Half Inch Line, C Point

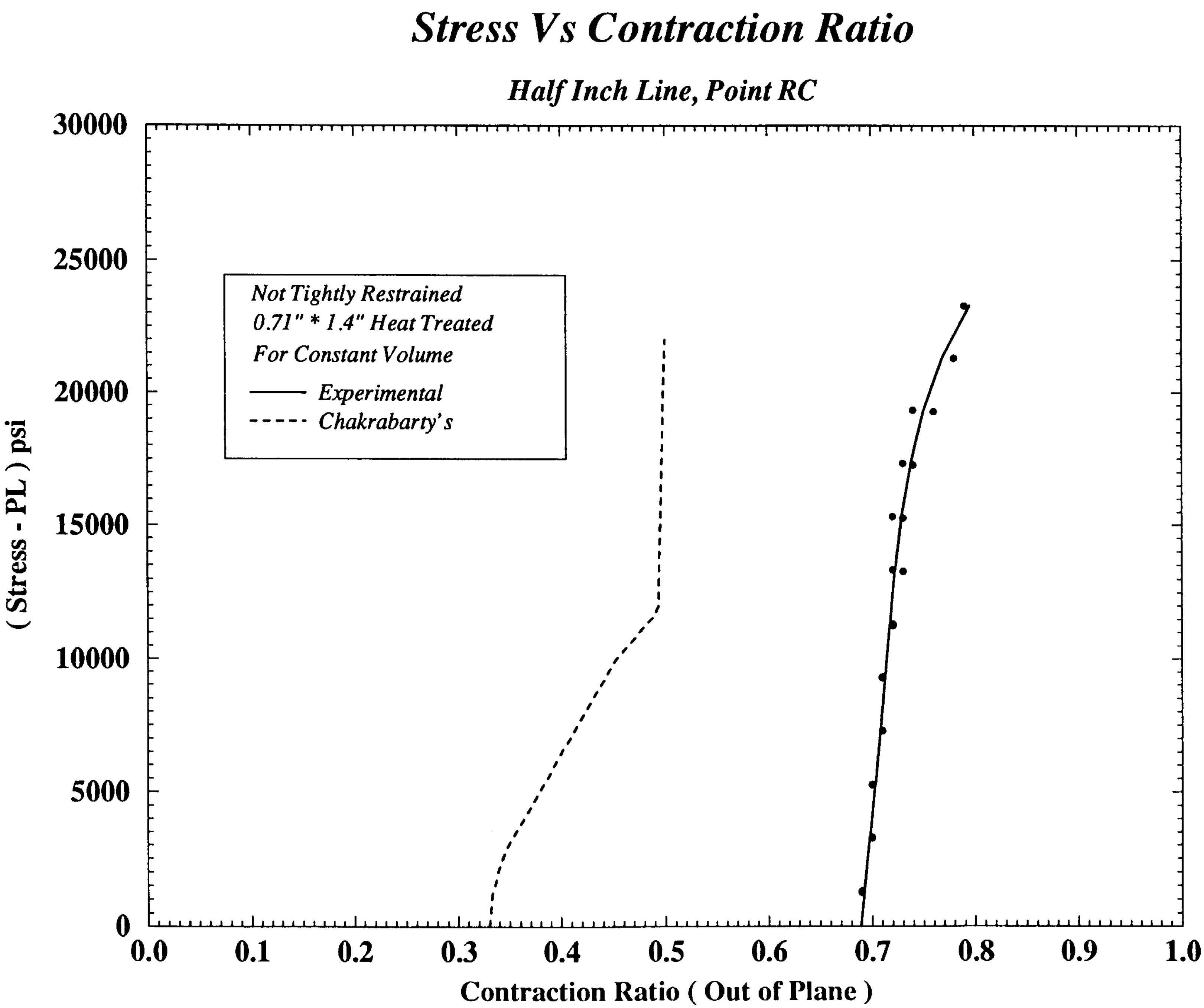

Figure A29. Out-of-Plane CR, Half Inch Line, RC Point

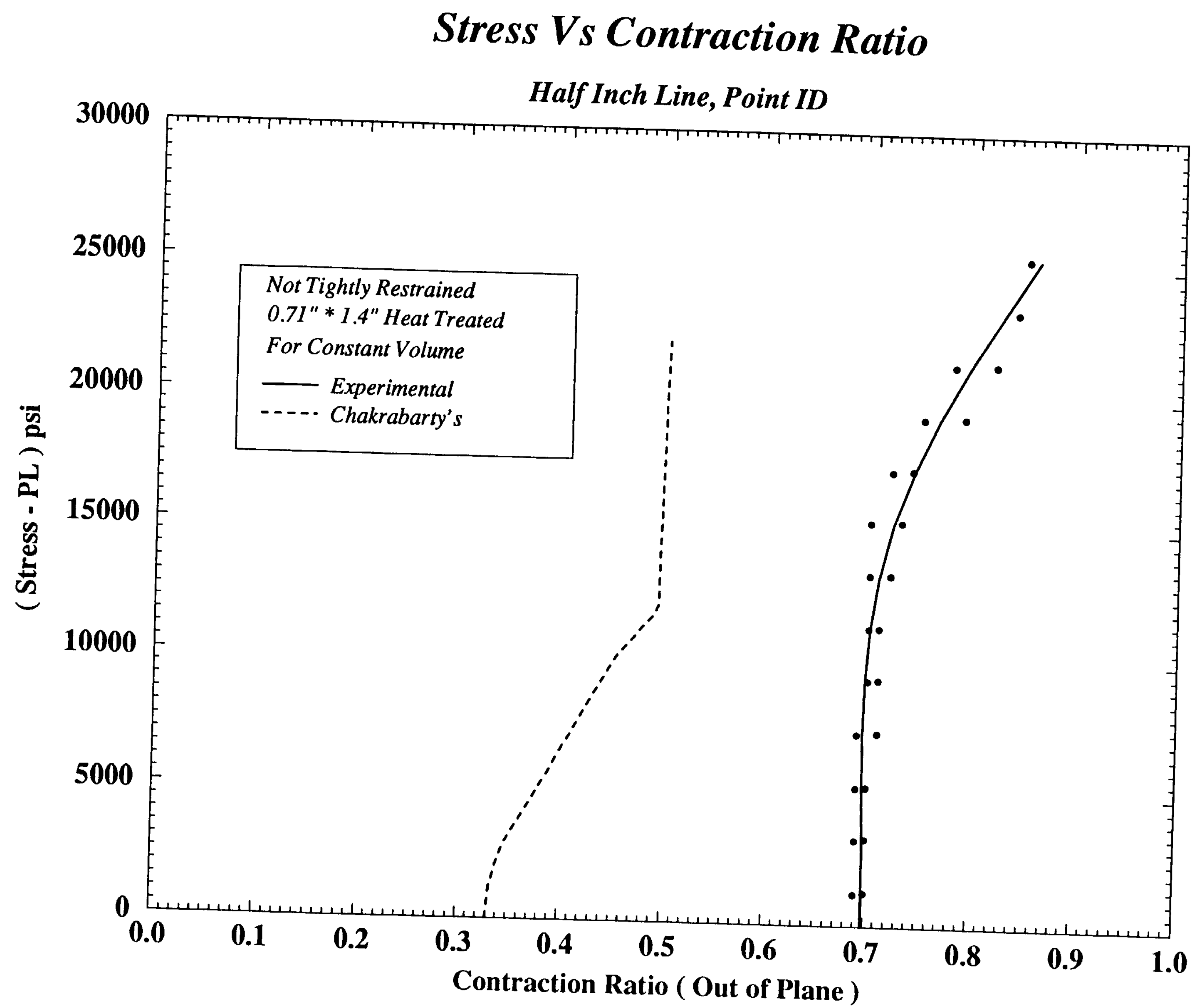

Figure A30. Out-of-Plane CR, Half Inch Line, ID Point

APPENDIX B

Task 2

Tensile Tests

Normal Weld Procedure

0.71" x 1.4" Material

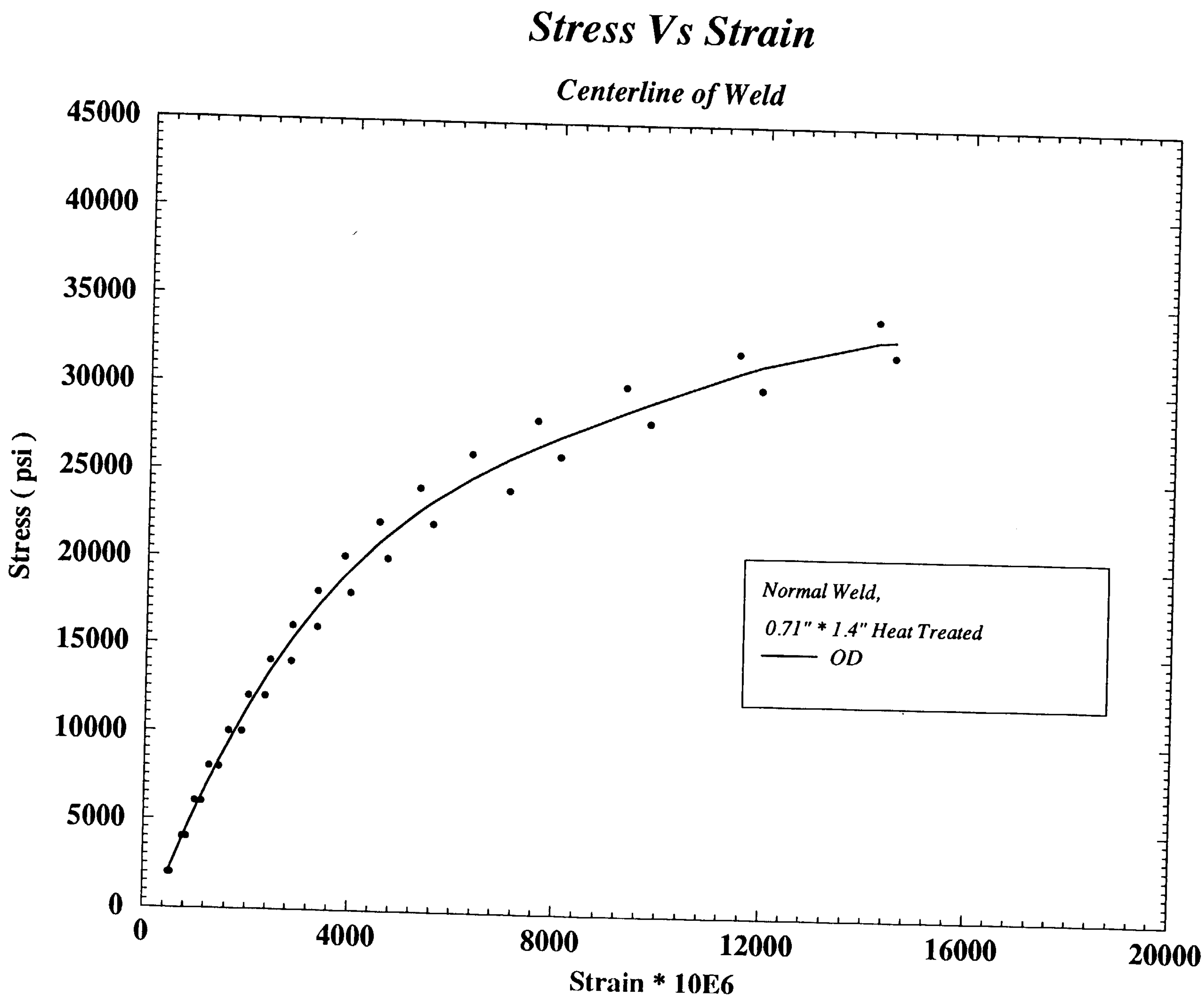

Figure B1. Material Behavior, Centerline, OD Point

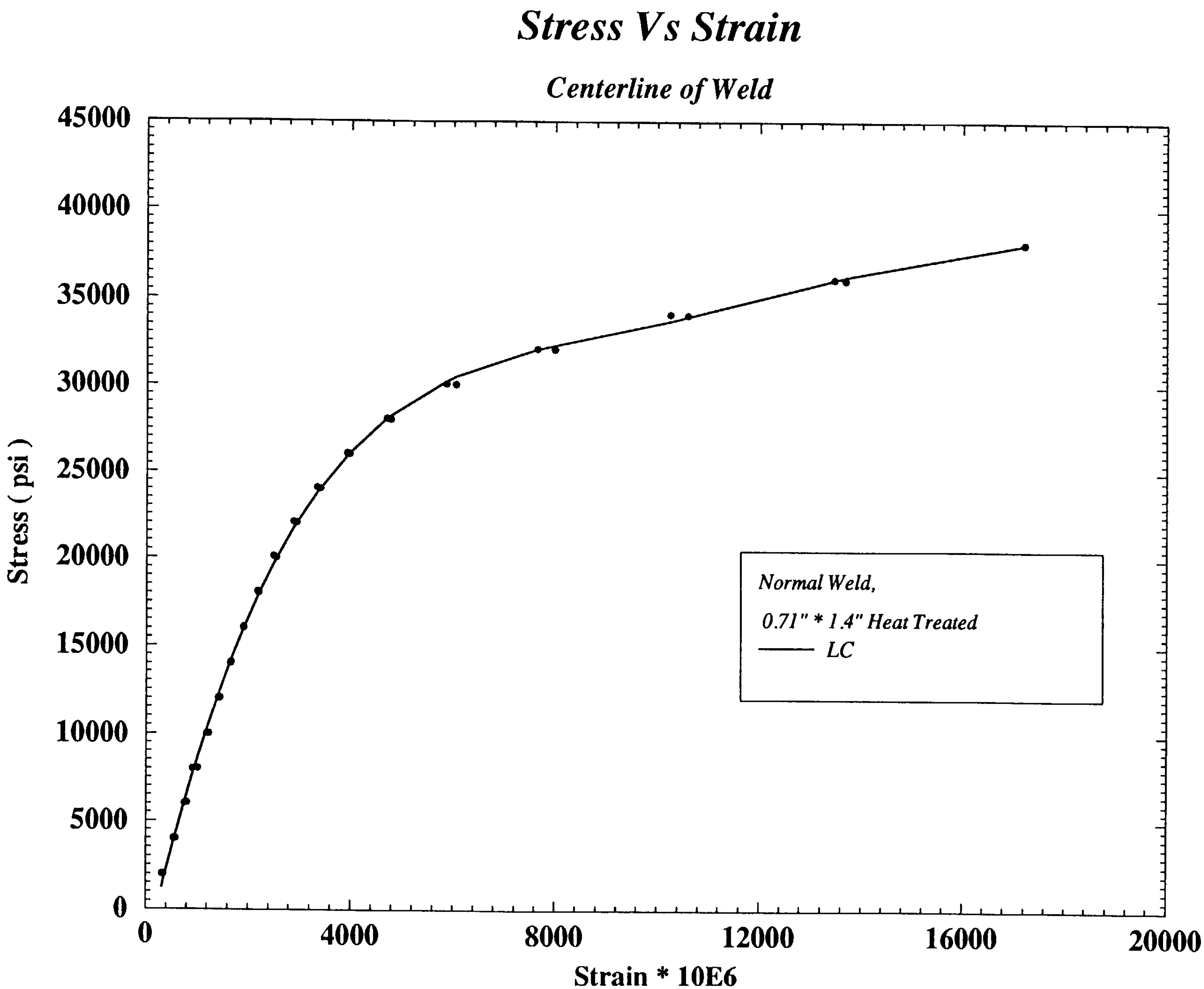

Figure B2. Material Behavior, Centerline, LC Point

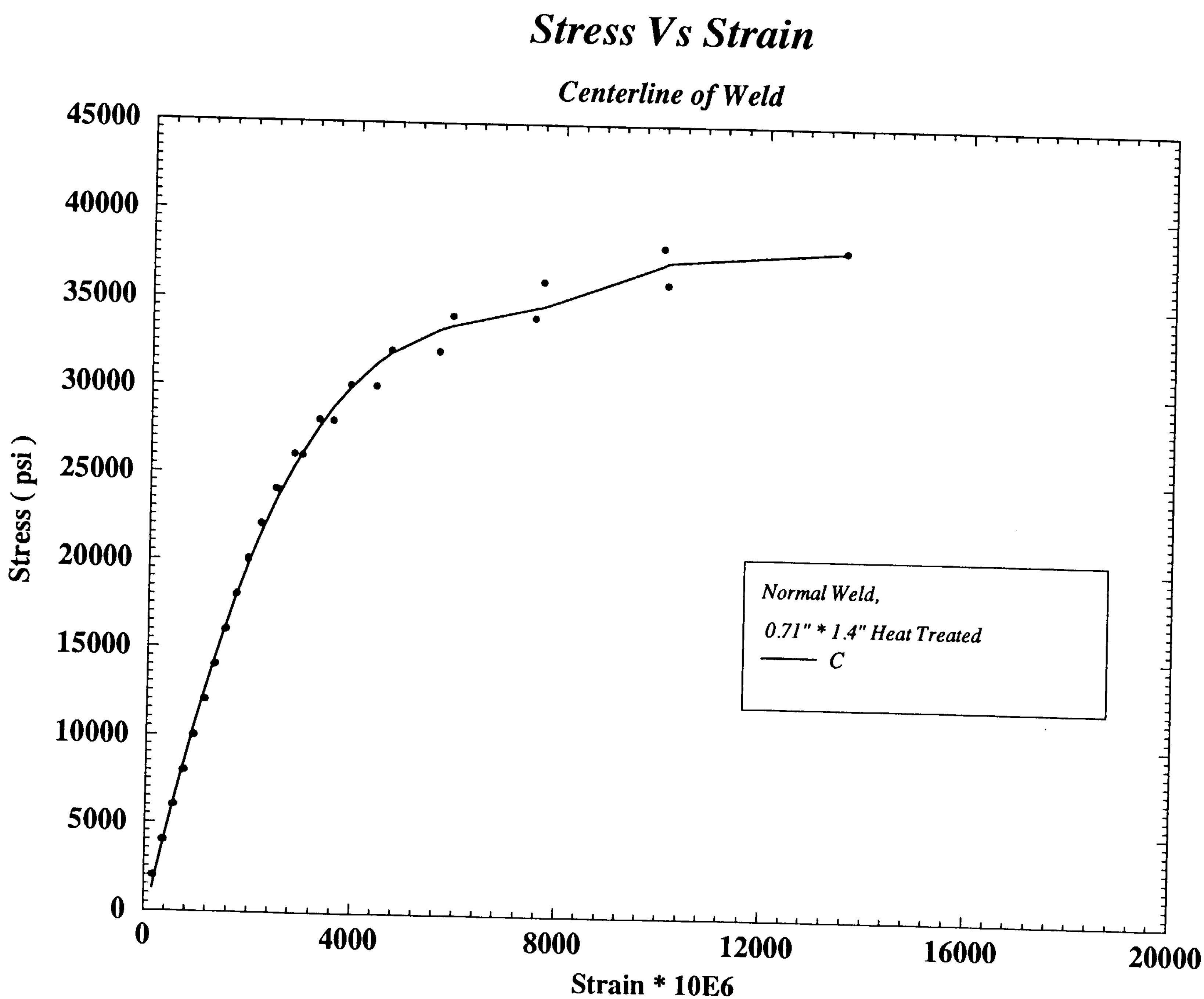

Figure B3. Material Behavior, Centerline, C Point

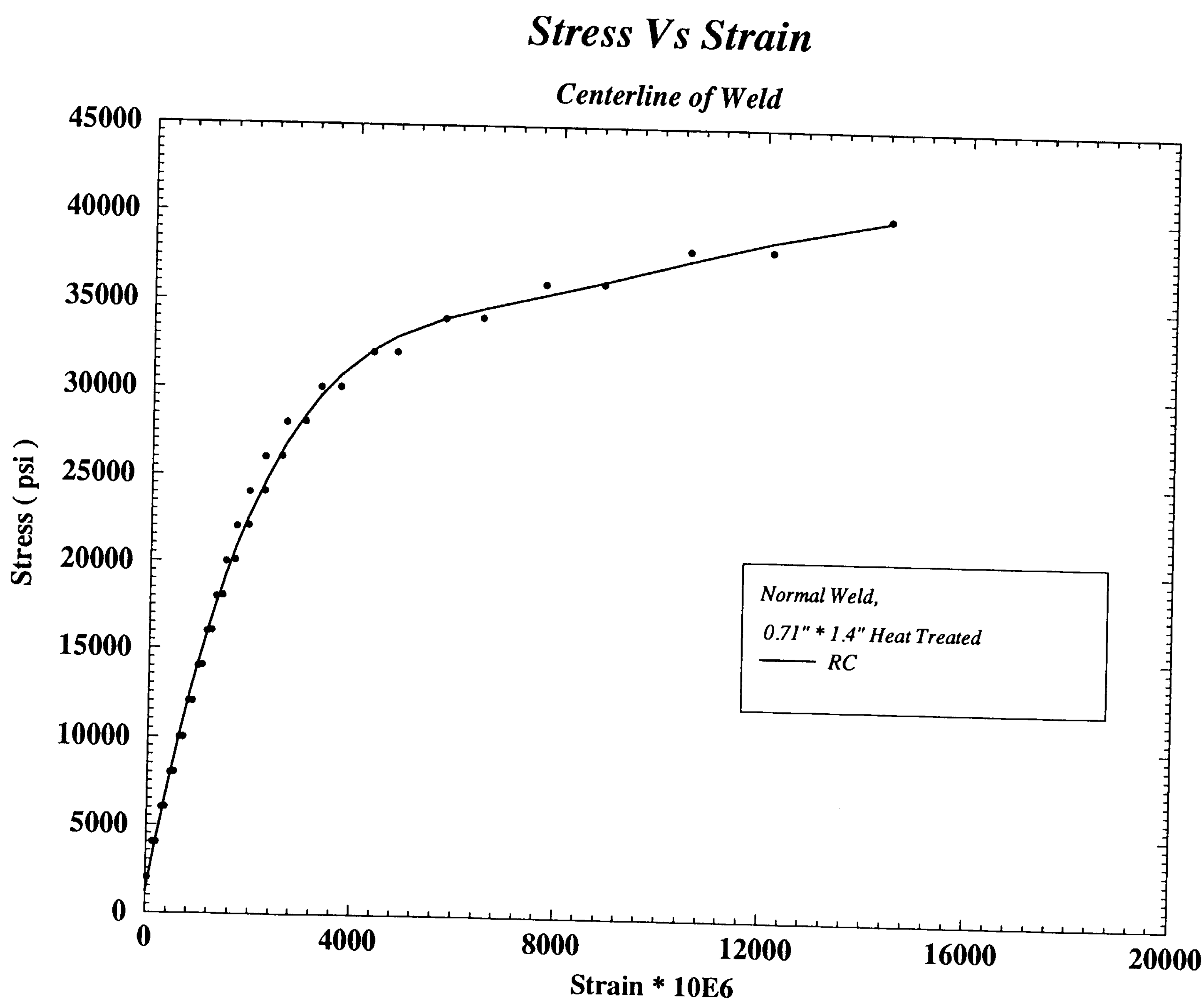

Figure B4. Material Behavior, Centerline, RC Point

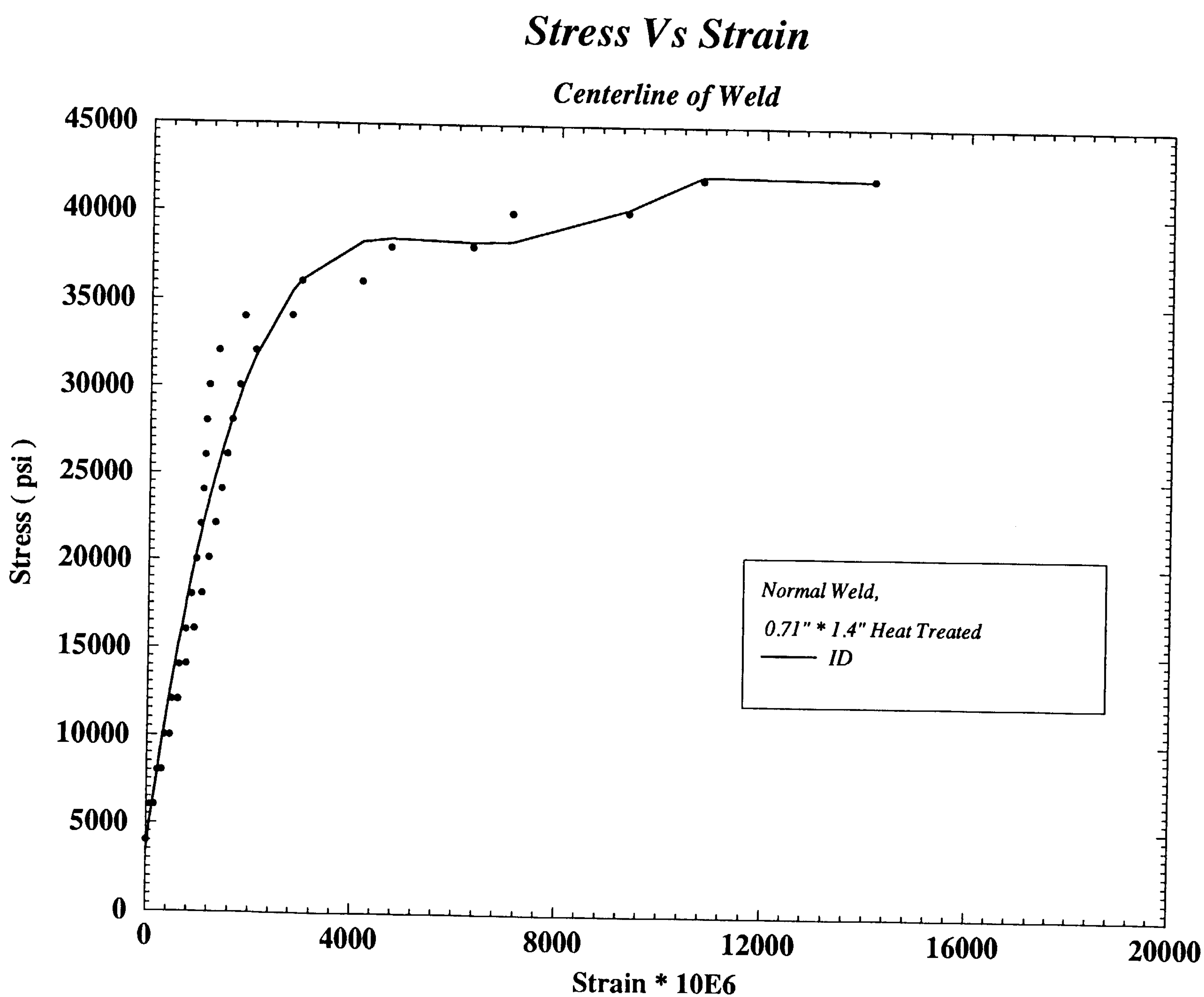

Figure B5. Material Behavior, Centerline, ID Point

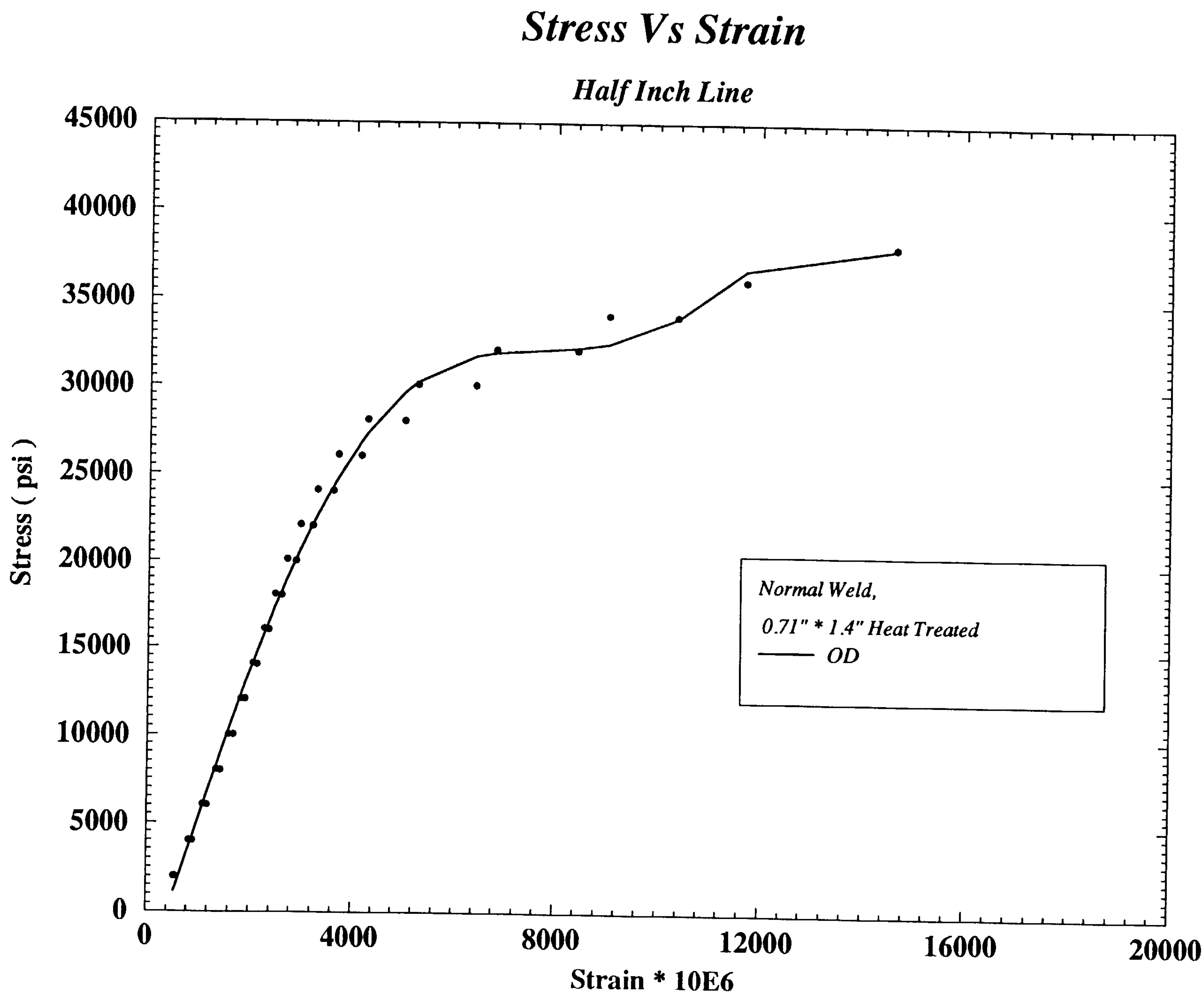

Figure B6. Material Behavior, Half Inch Line, OD Point

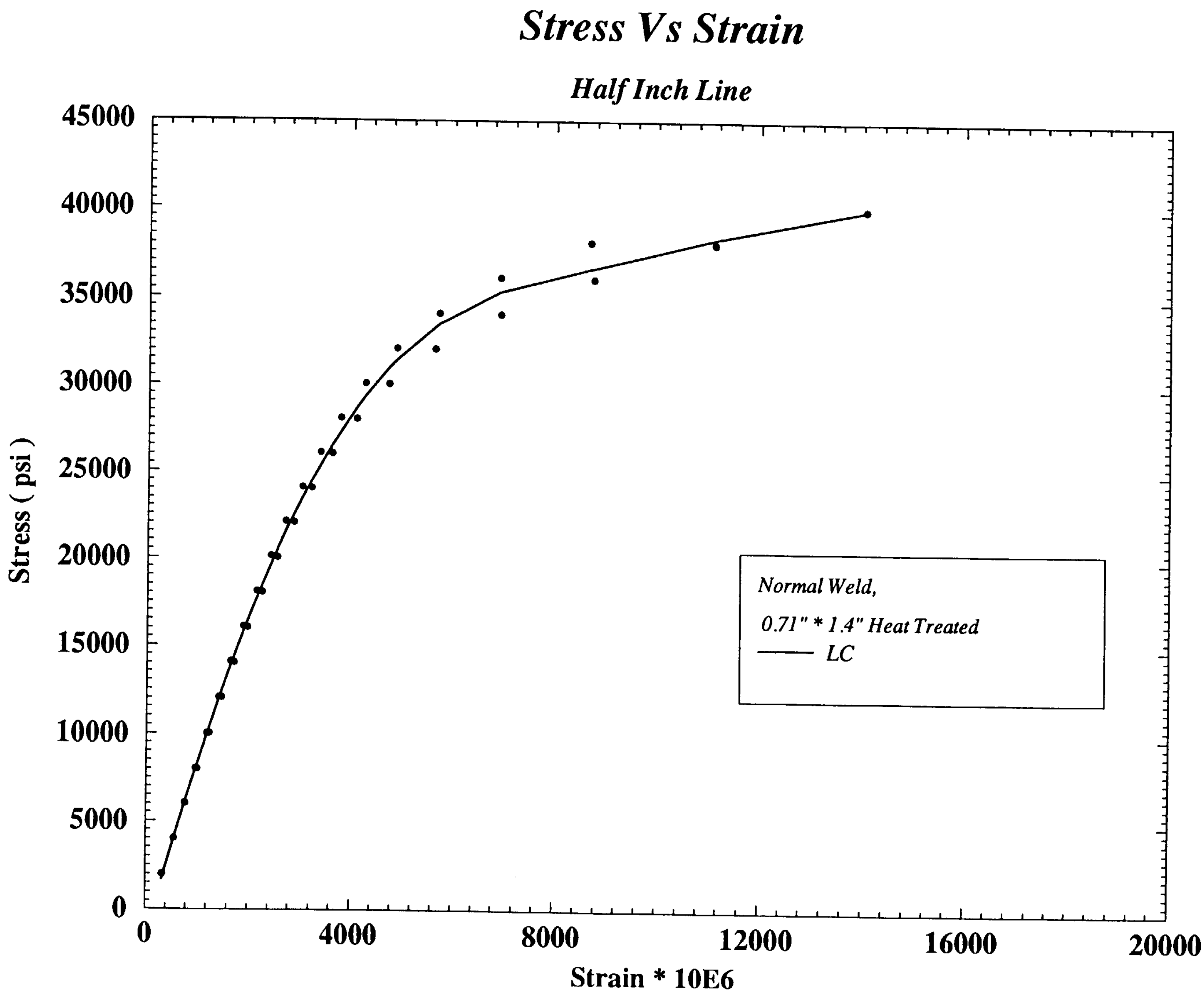

Figure B7. Material Behavior, Half Inch Line, LC Point

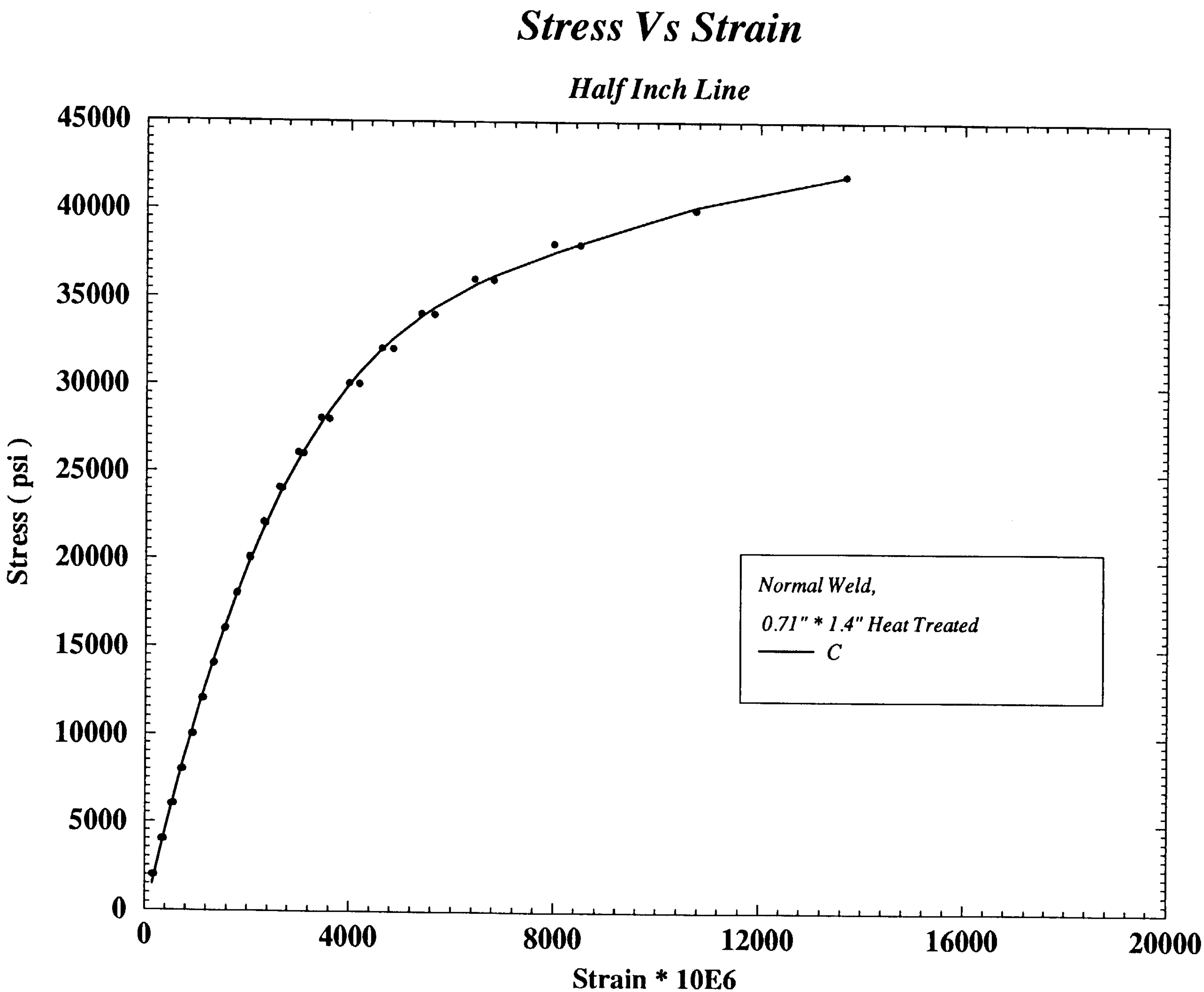

Figure B8. Material Behavior, Half Inch Line, C Point

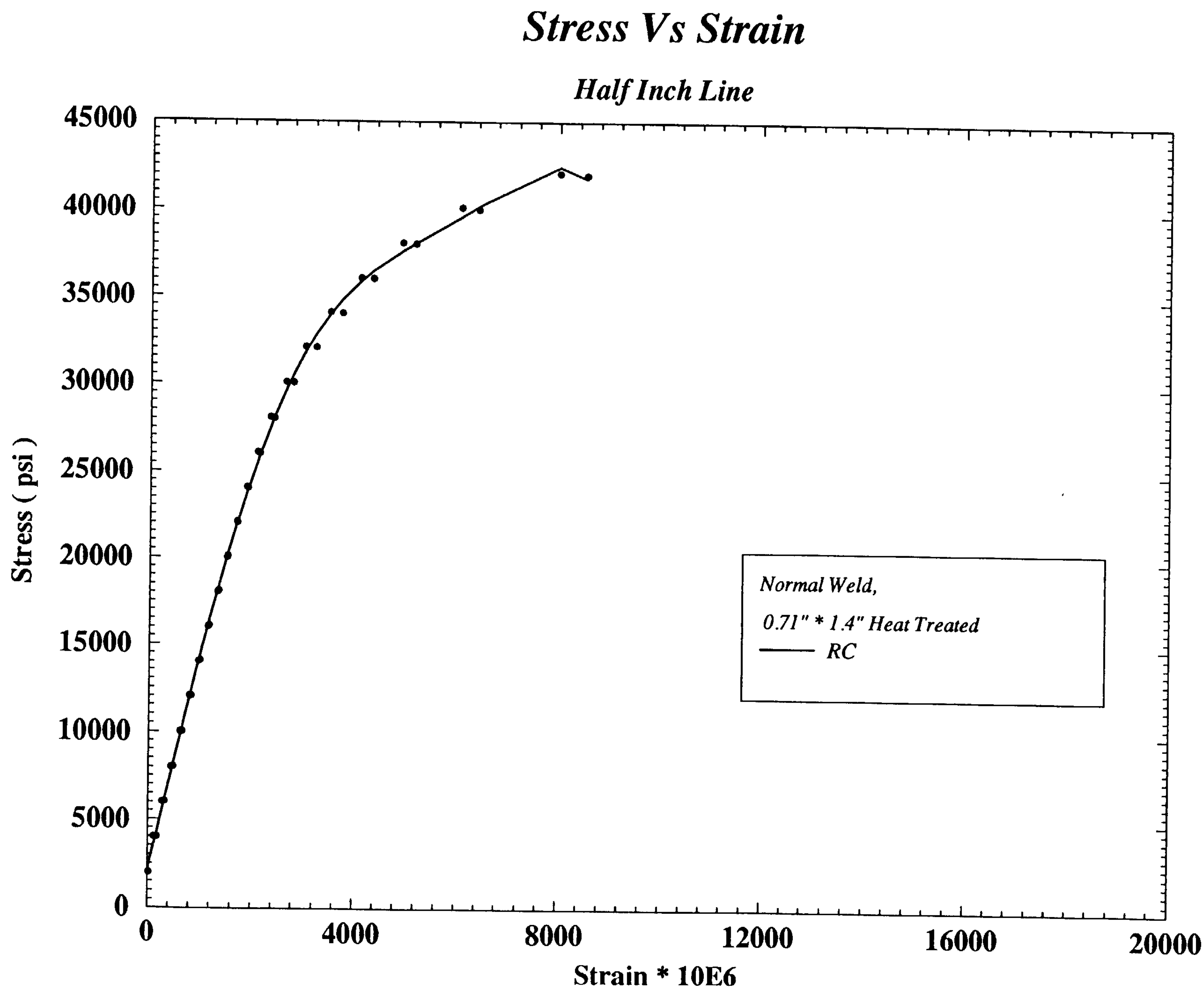

Figure B9. Material Behavior, Half Inch Line, RC Point

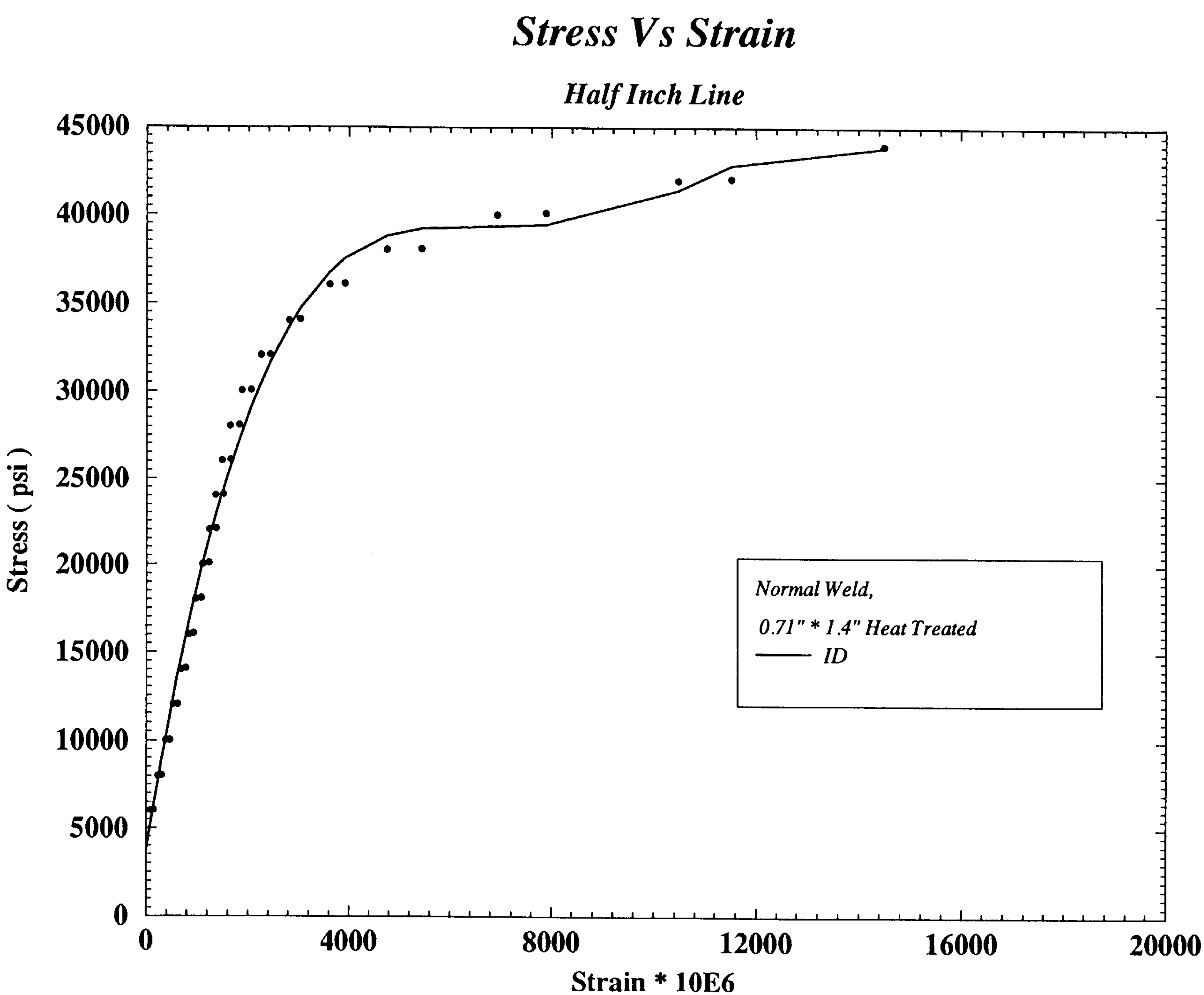

Figure B10. Material Behavior, Half Inch Line, ID

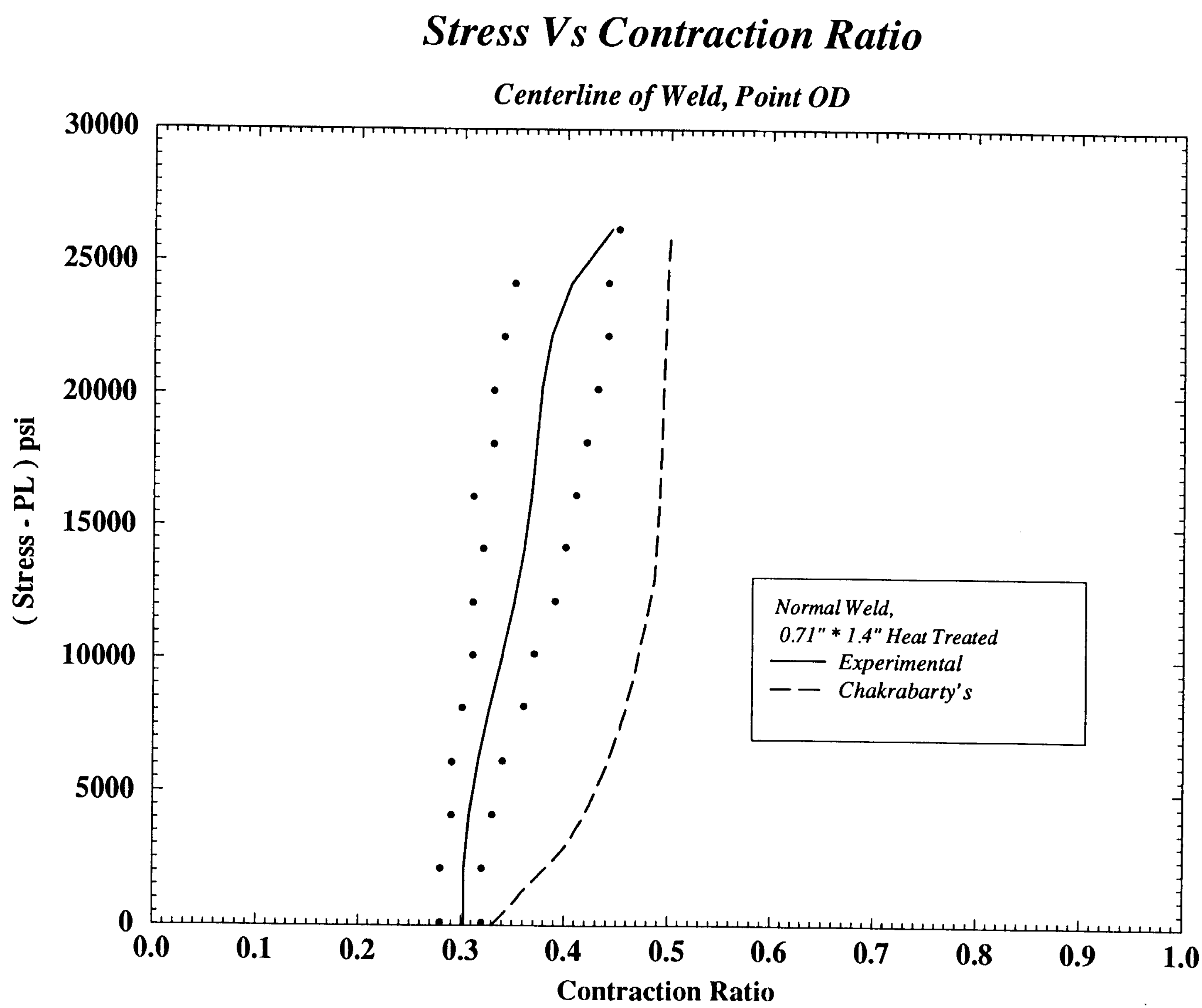

Figure B11. In-Plane CR, Centerline, OD Point

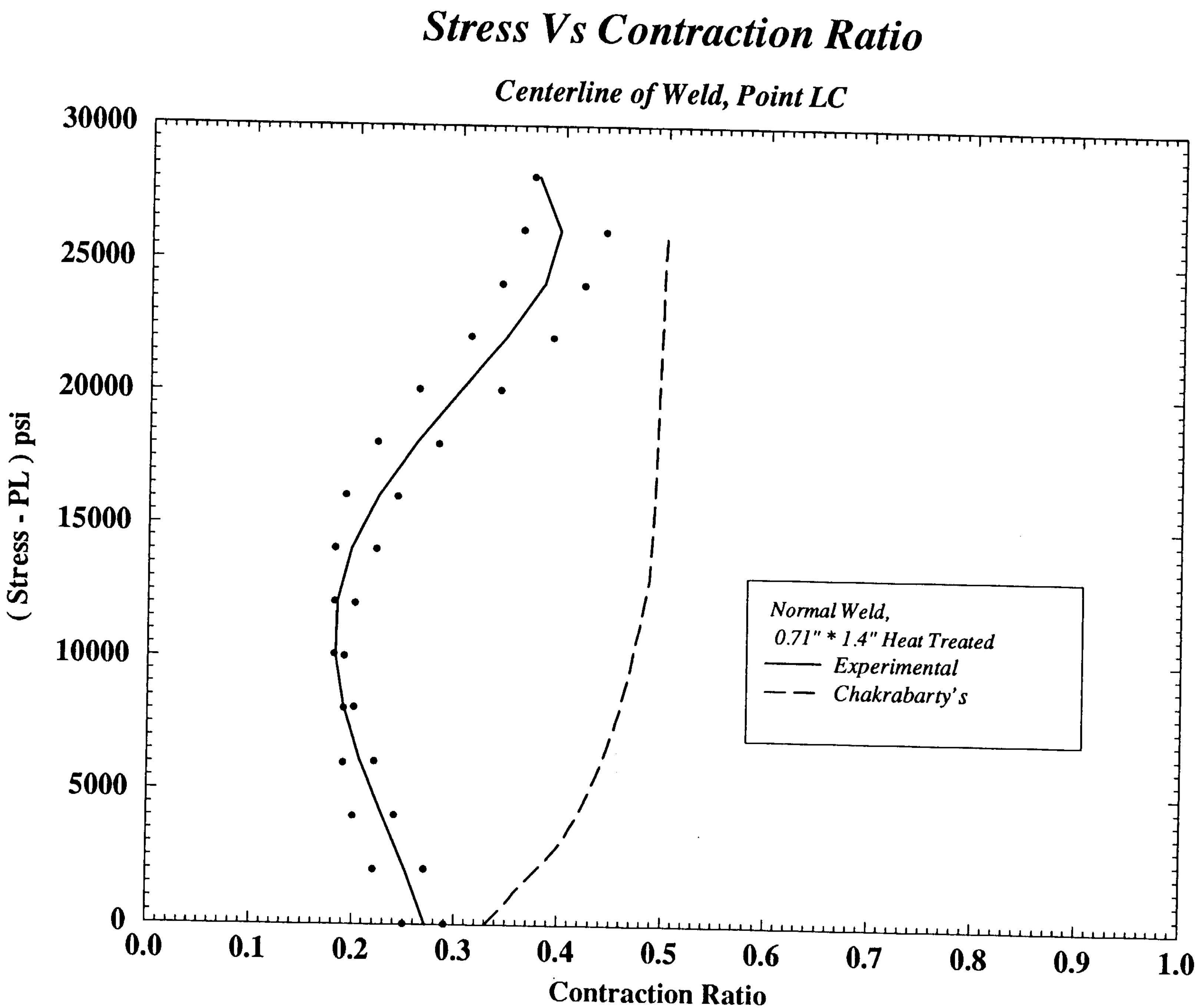

Figure B12. In-Plane CR, Centerline, LC Point

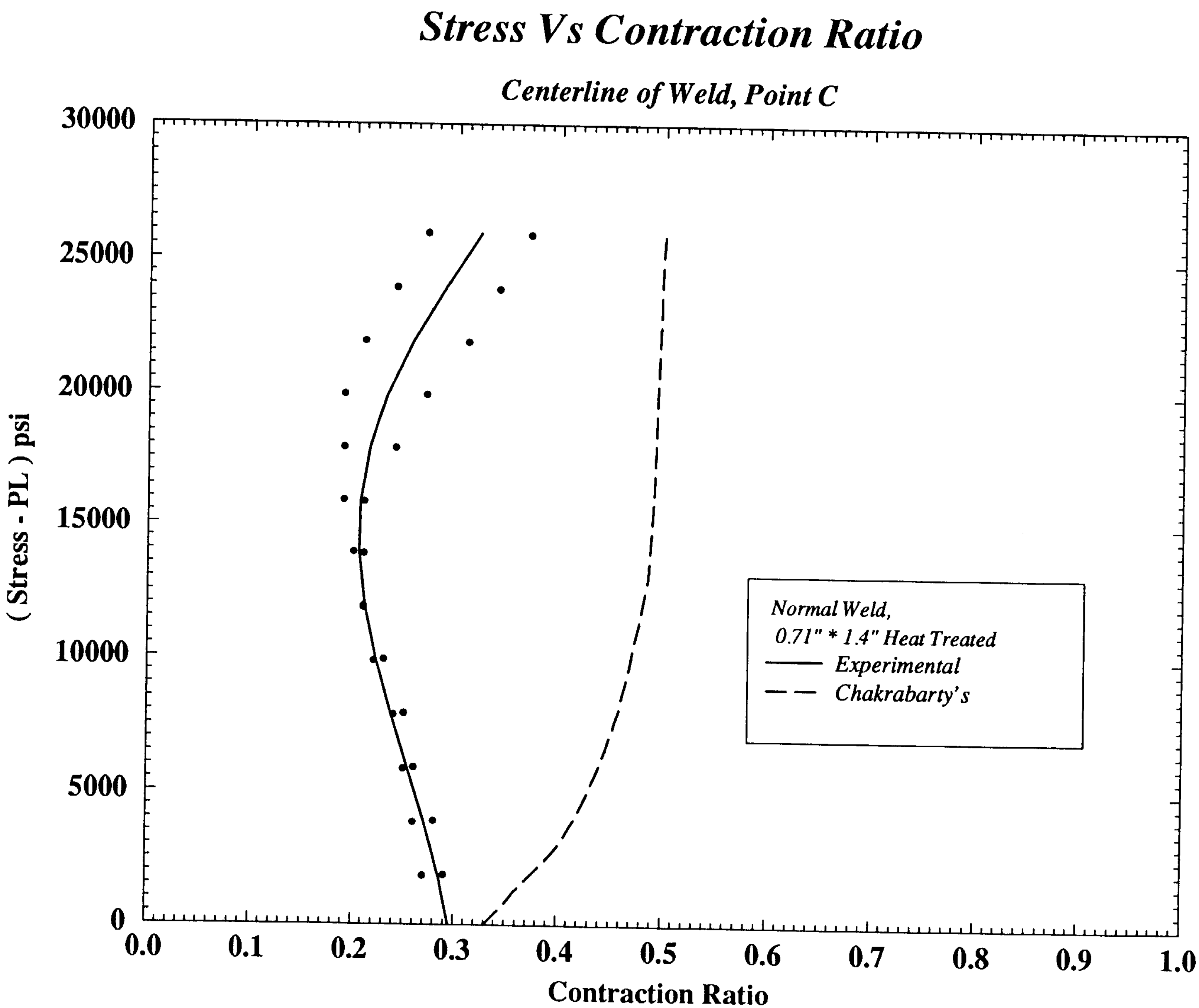

Figure B13. In-Plane CR, Centerline, C Point

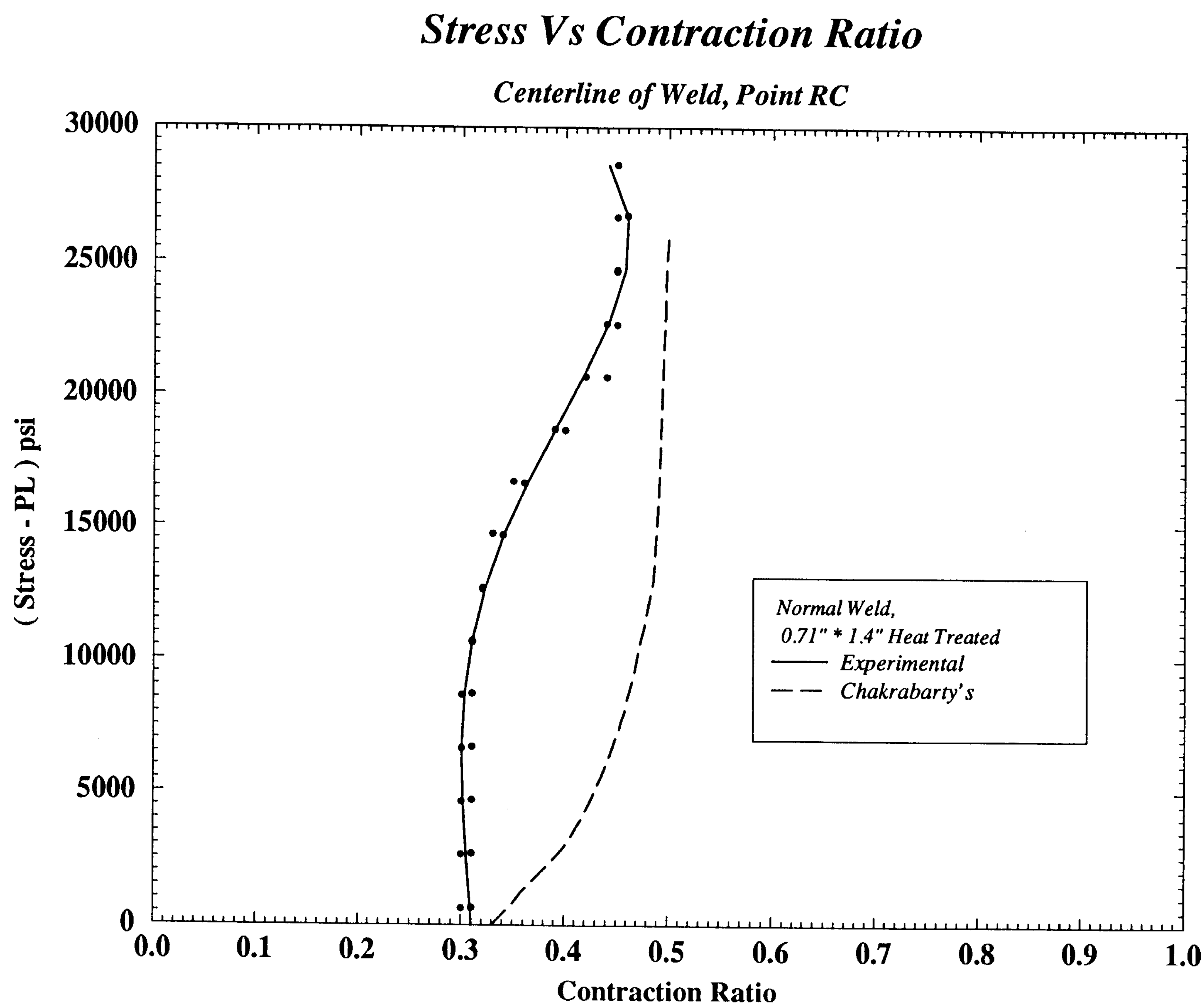

Figure B14. In-Plane CR, Centerline, RC Point

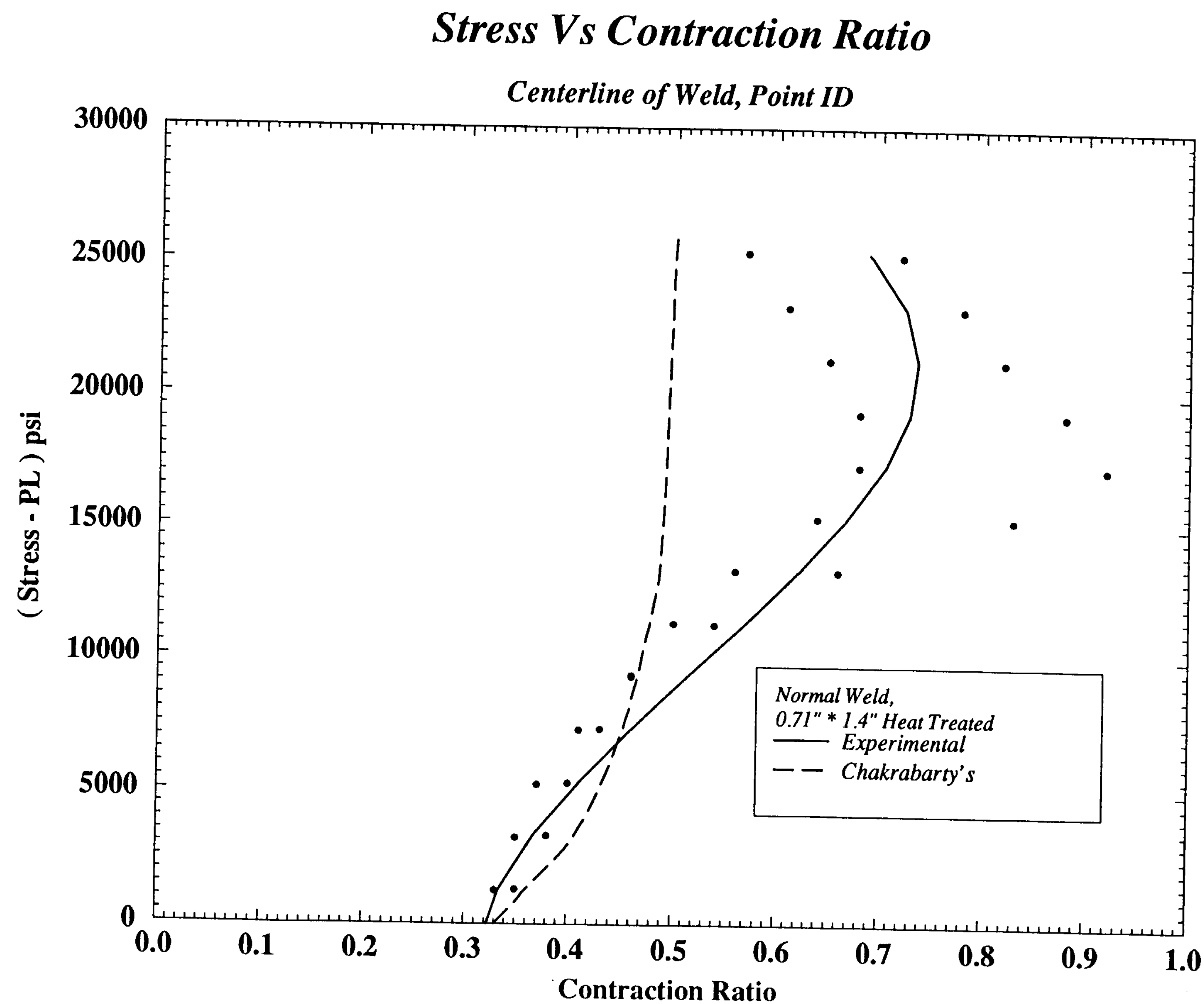

Figure B15. In-Plane CR, Centerline, ID Point

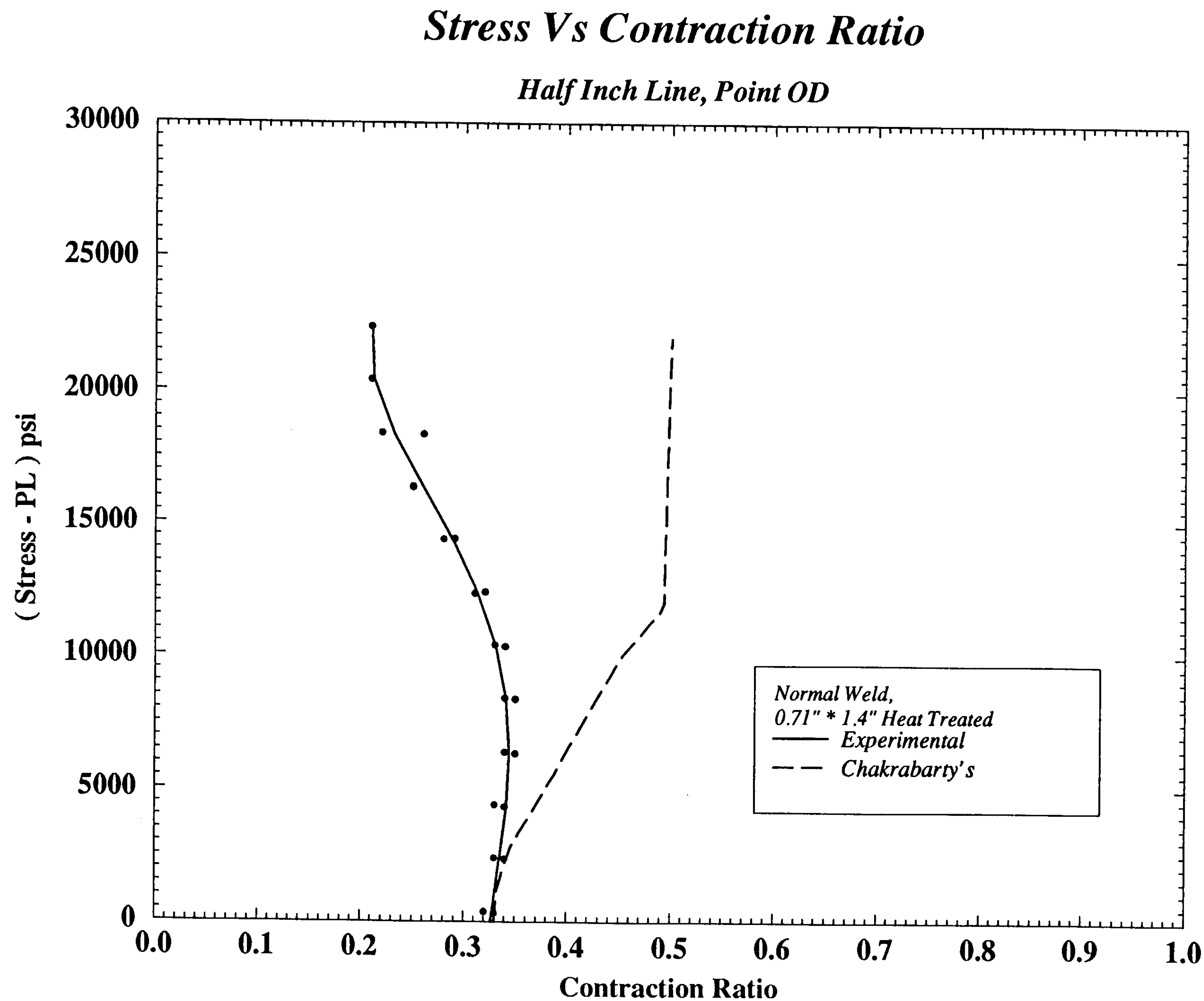

Figure B16. In-Plane CR, Half Inch Line, OD Point

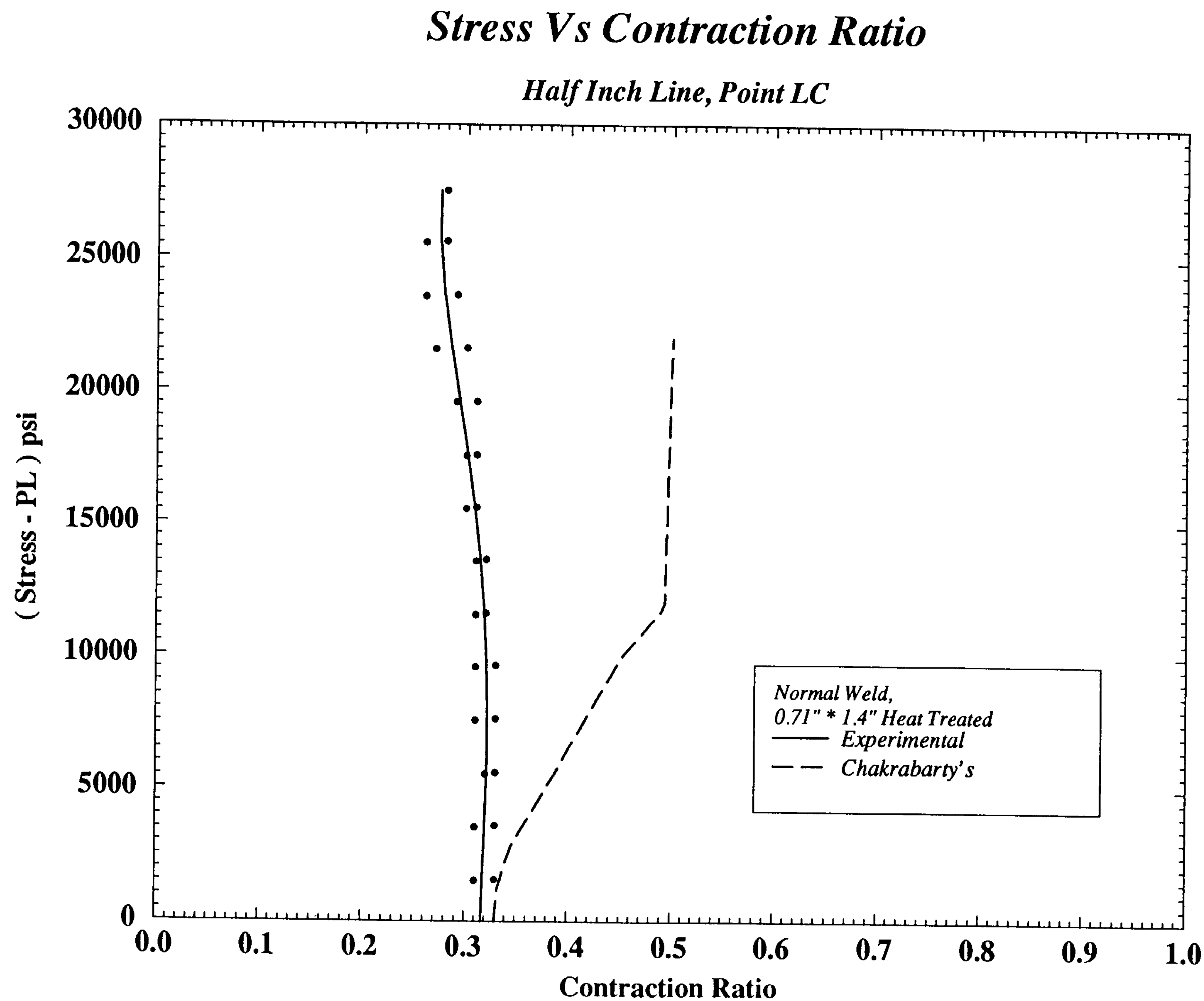

Figure B17. In-Plane CR, Half Inch Line, LC Point

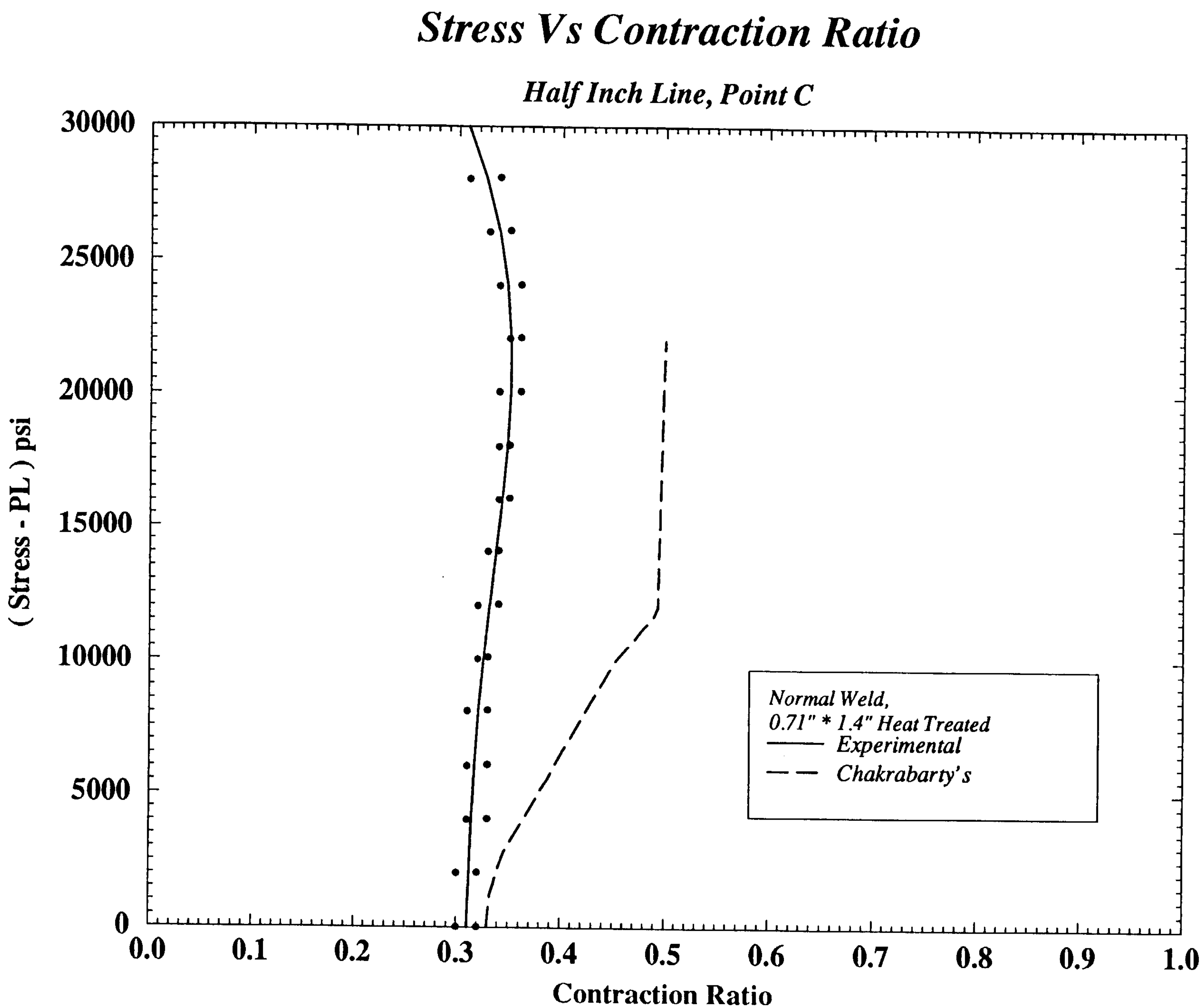

Figure B18. In-Plane CR, Half Inch Line, C Point

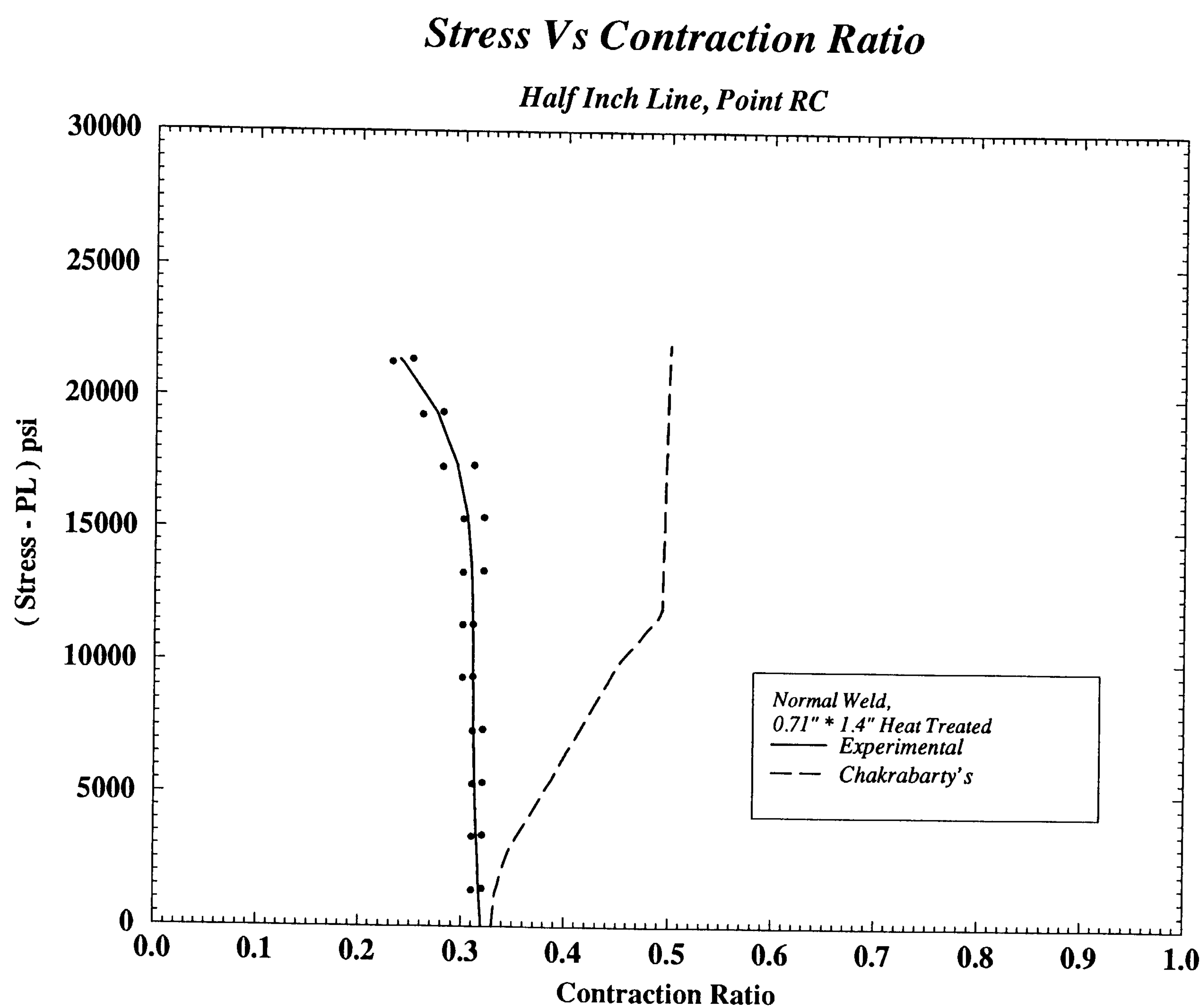

Figure B19. In-Plane CR, Half Inch Line, RC Point

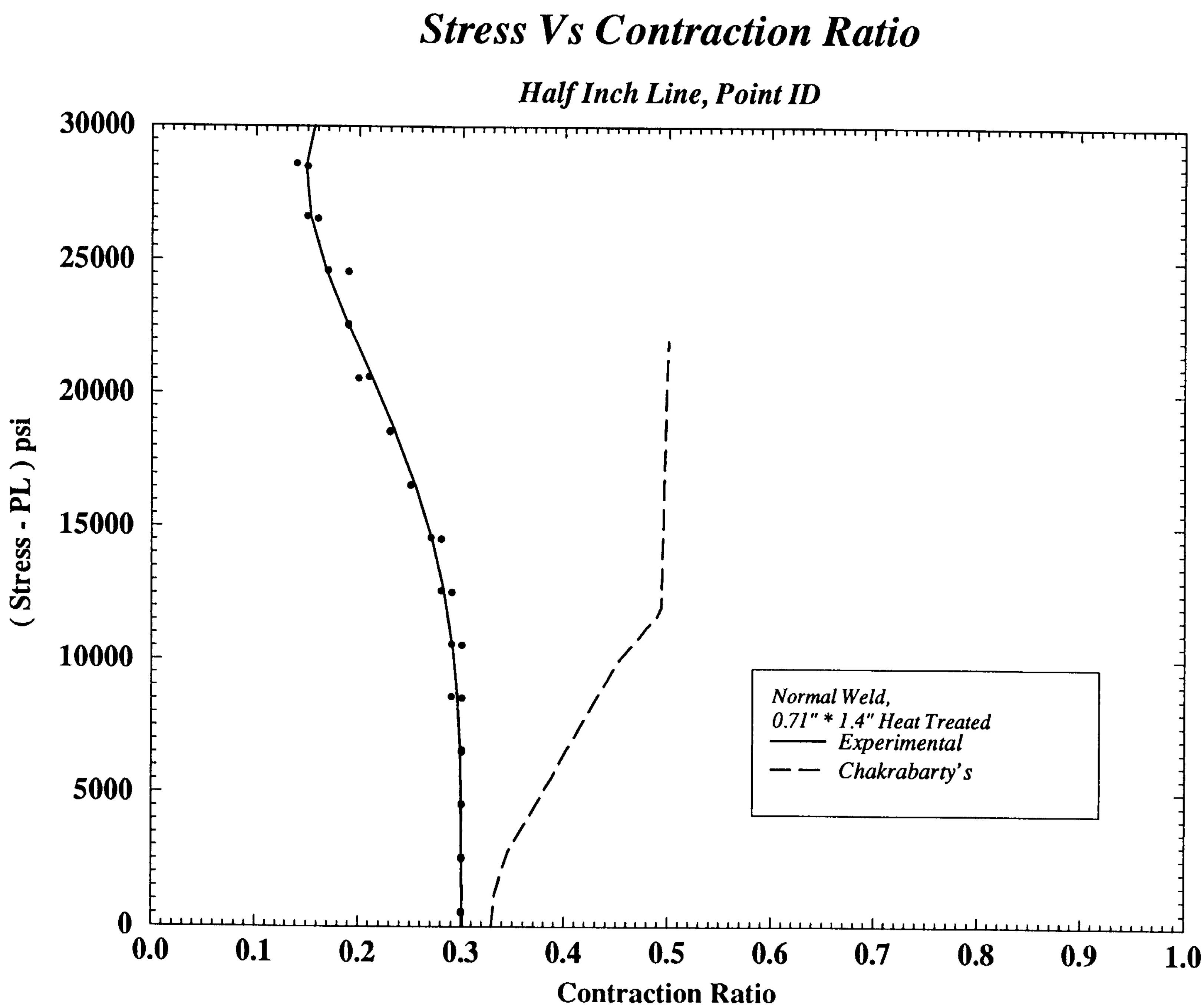

Figure B20. In-Plane CR, Half Inch Line, ID Point

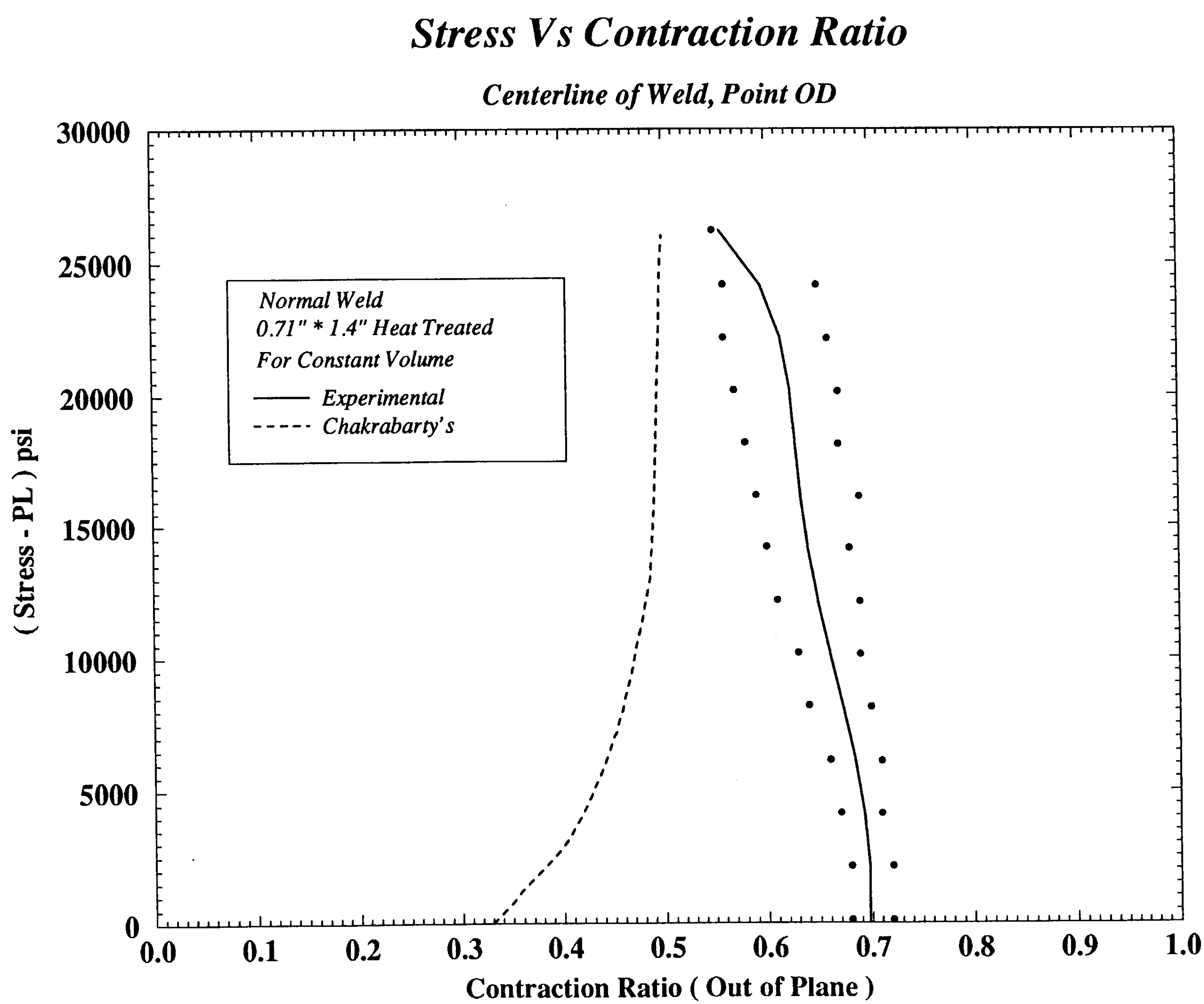

Figure B21. Out-of-Plane CR, Centerline, OD Point

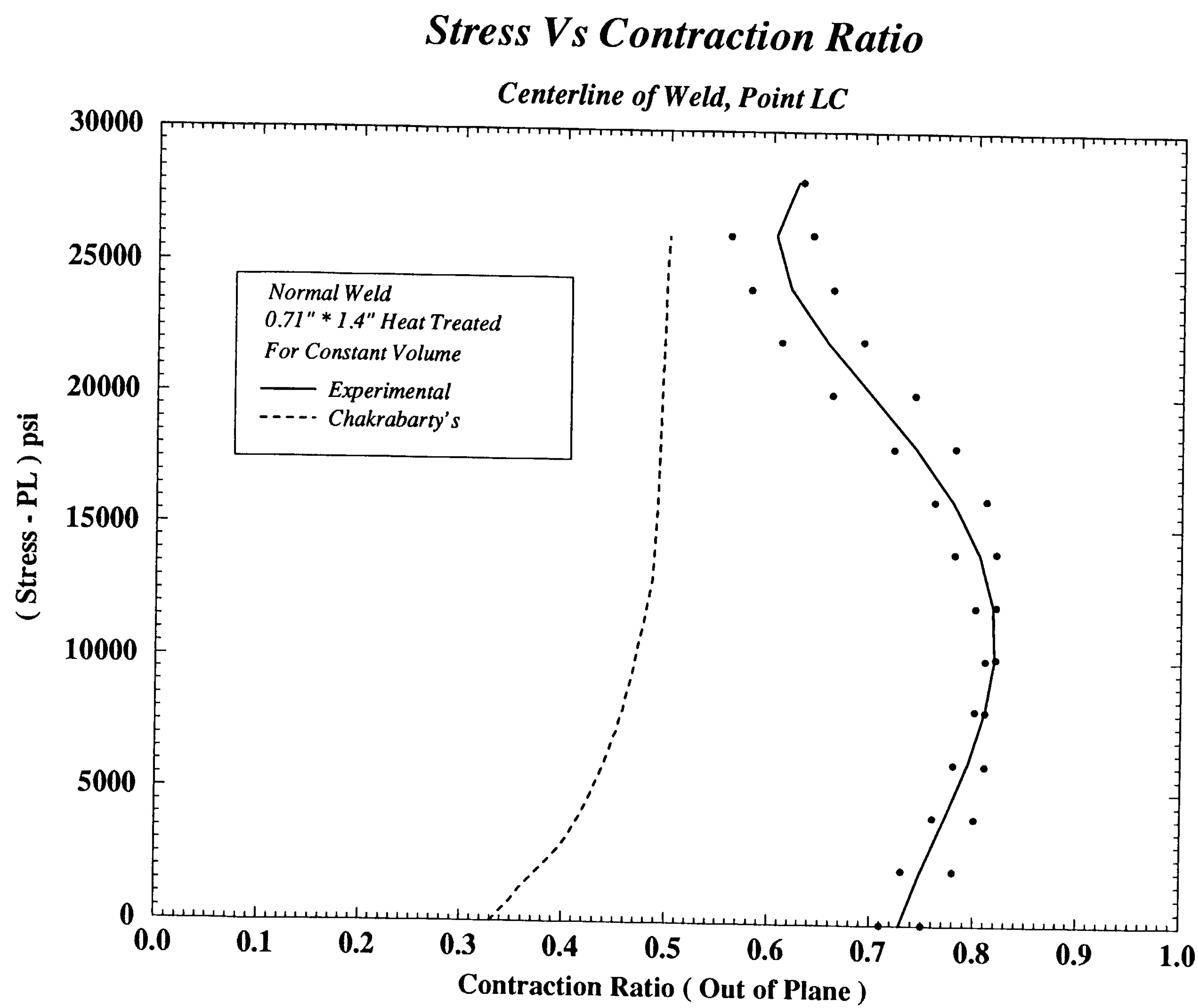

Figure B22. Out-of-Plane CR, Centerline, LC Point

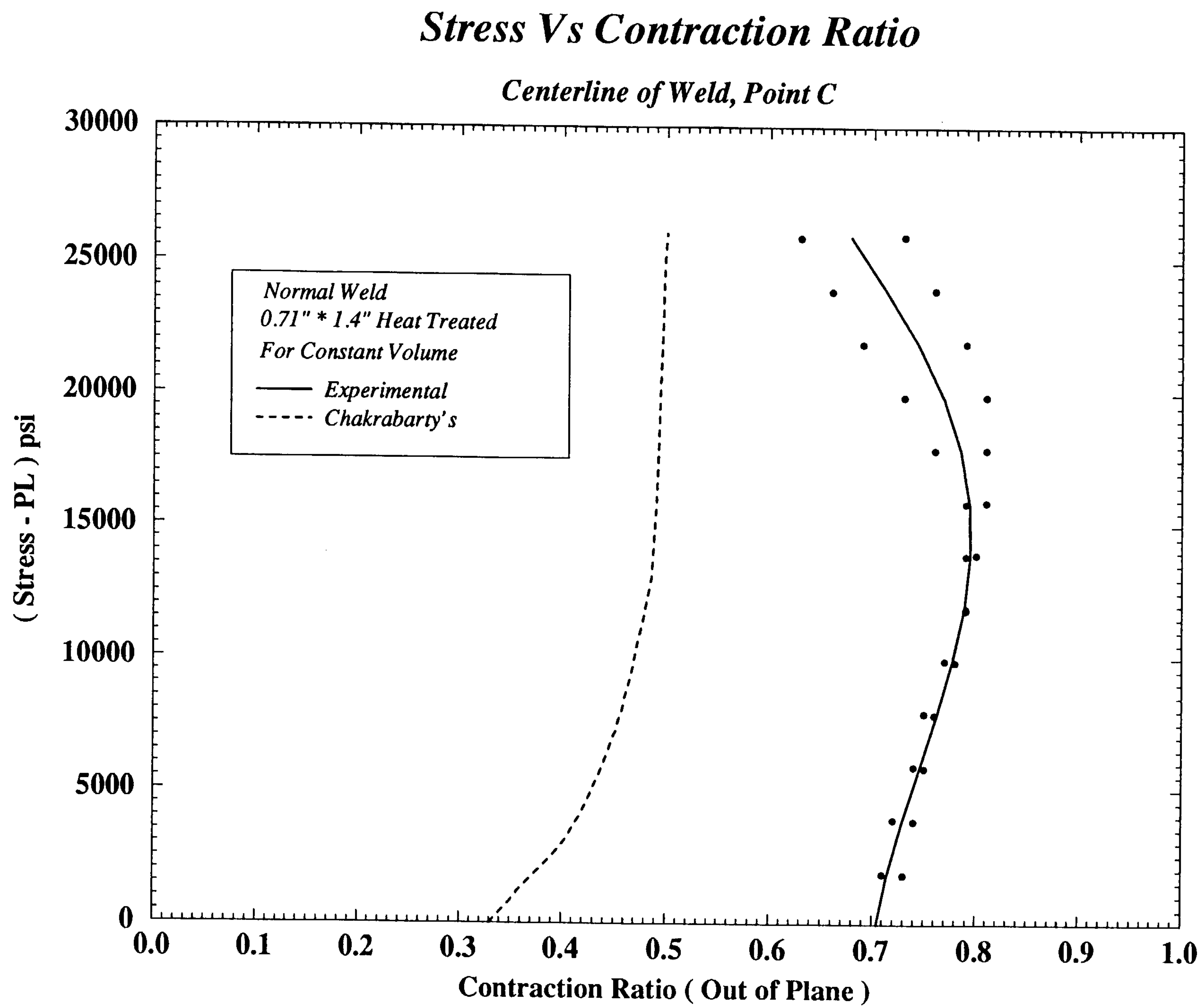

Figure B23. Out-of-Plane CR, Centerline, C Point

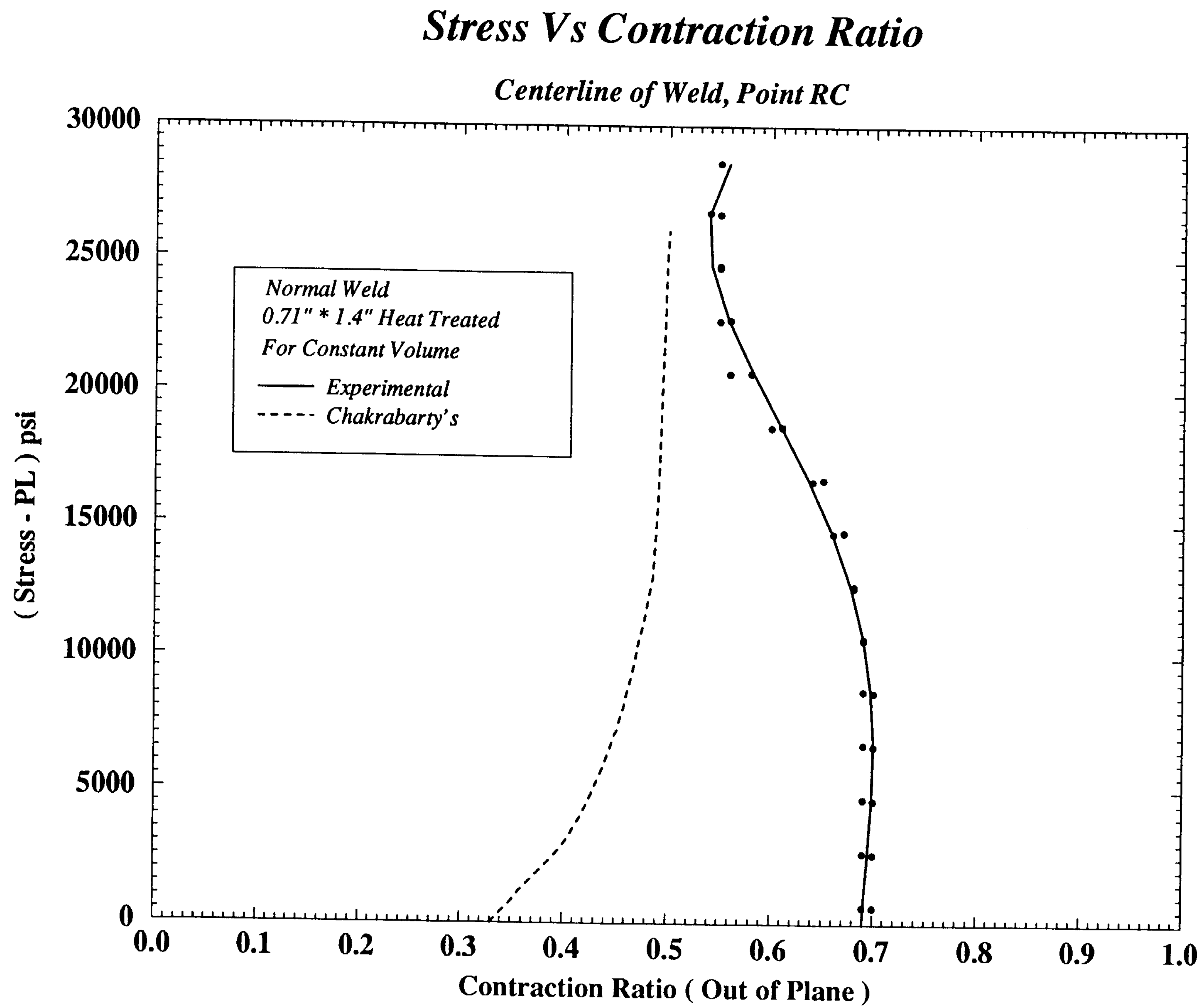

Figure B24. Out-of-Plane CR, Centerline, RC Point

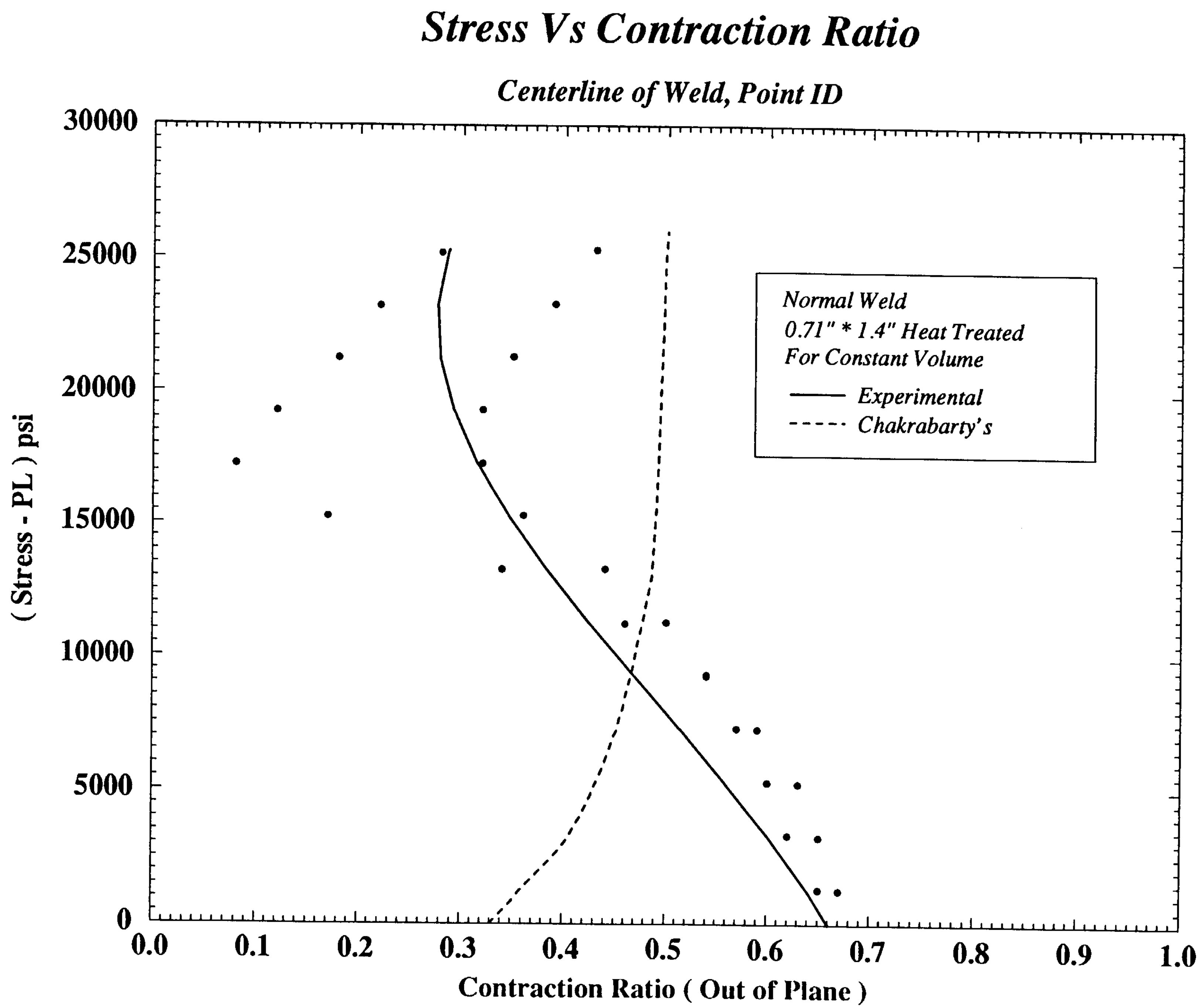

Figure B25. Out-of-Plane CR, Centerline, ID Point

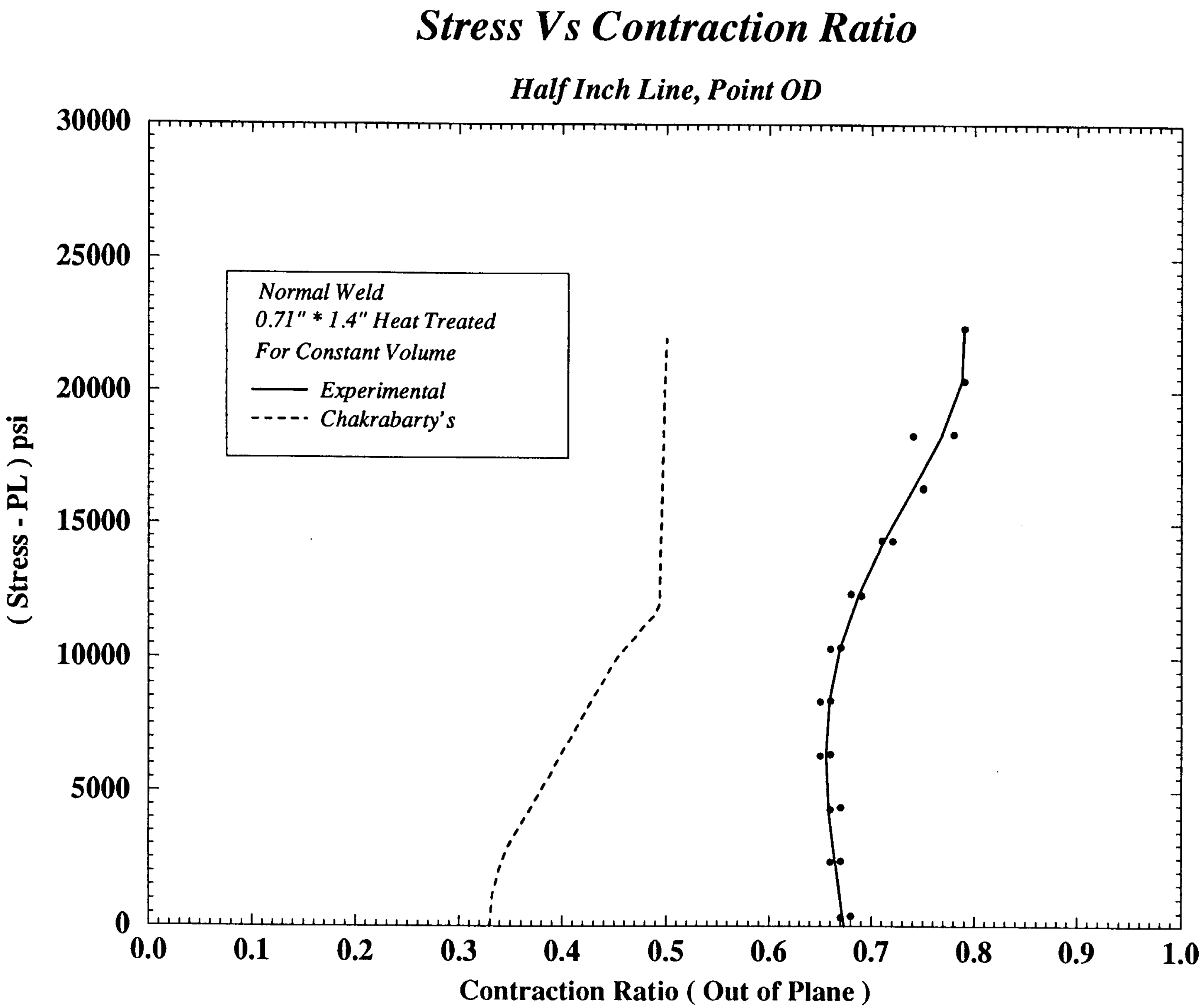

Figure B26. Out-of-Plane CR, Half Inch Line, OD Point

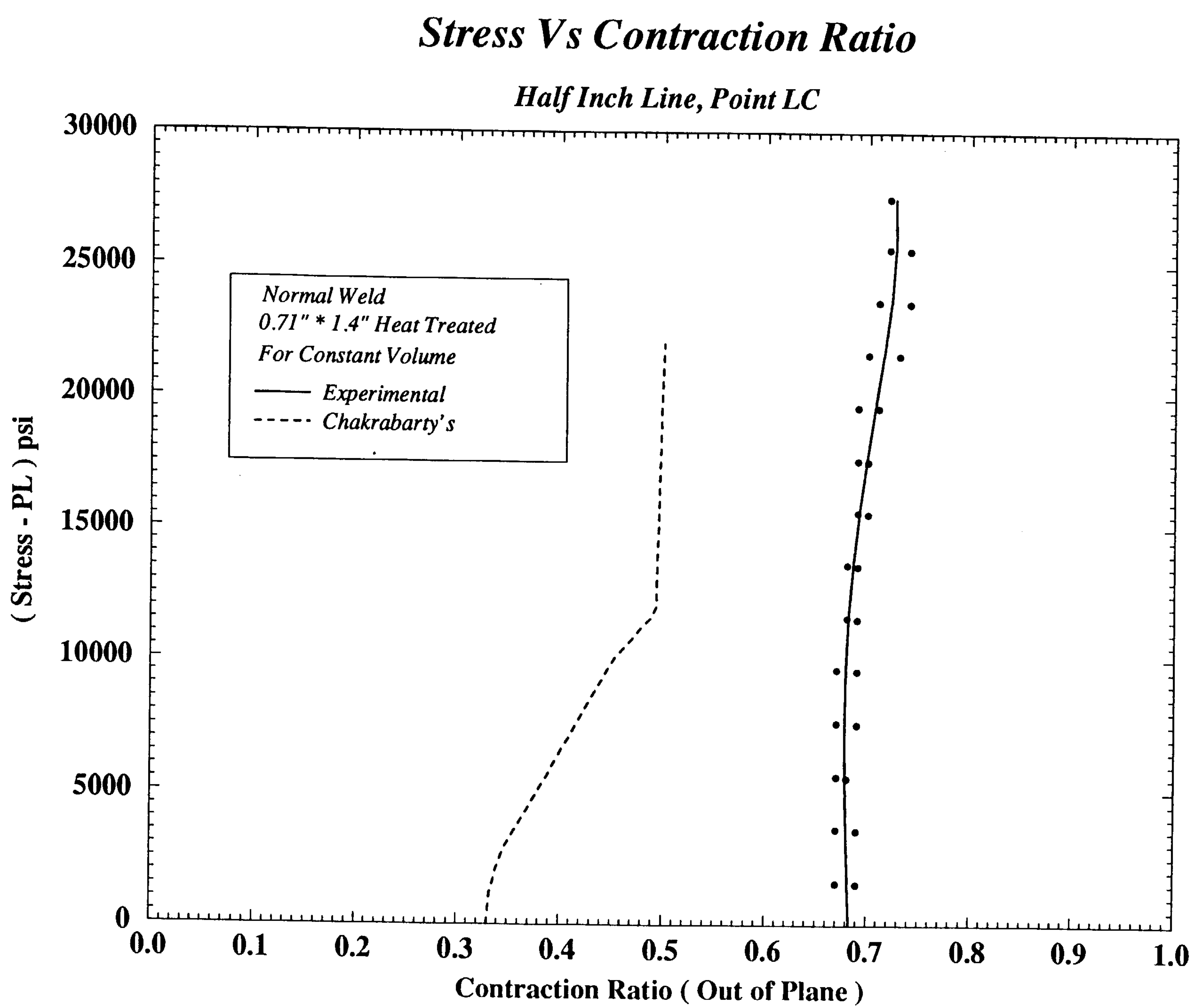

Figure B27. Out-of-Plane CR, Half Inch Line, LC Point

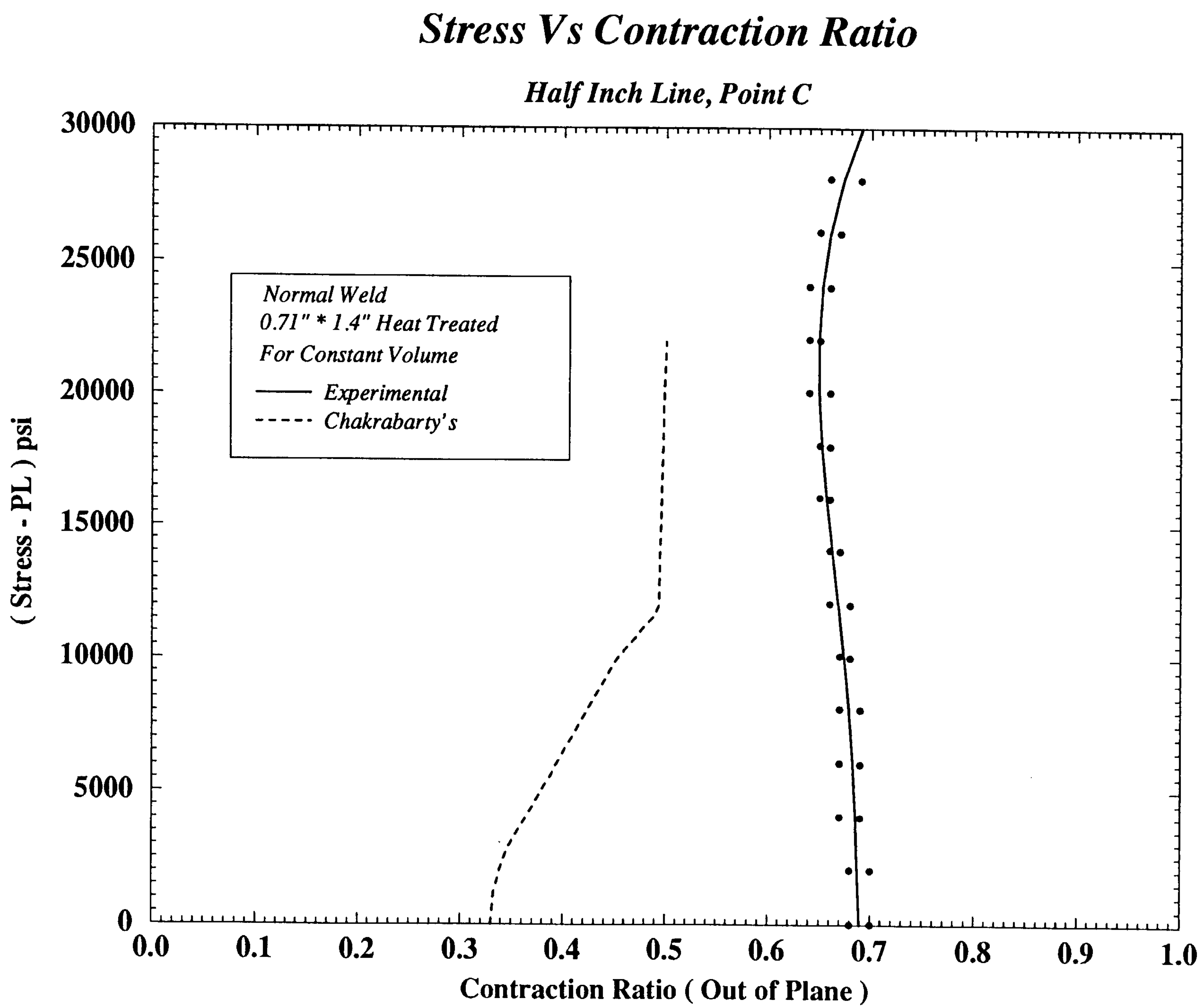

Figure B28. Out-of-Plane CR, Half Inch Line, C Point

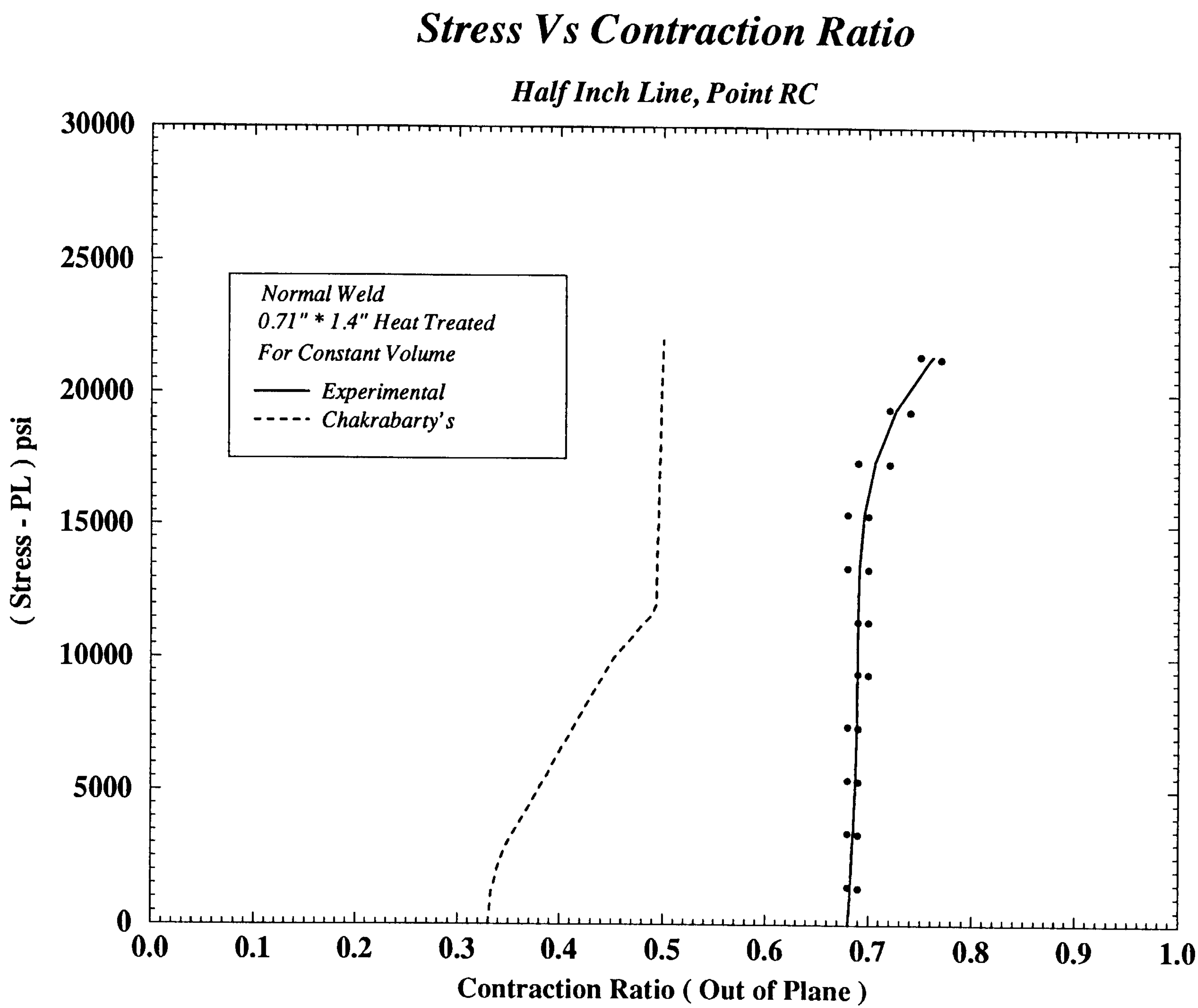

Figure B29. Out-of-Plane CR, Half Inch Line, RC Point

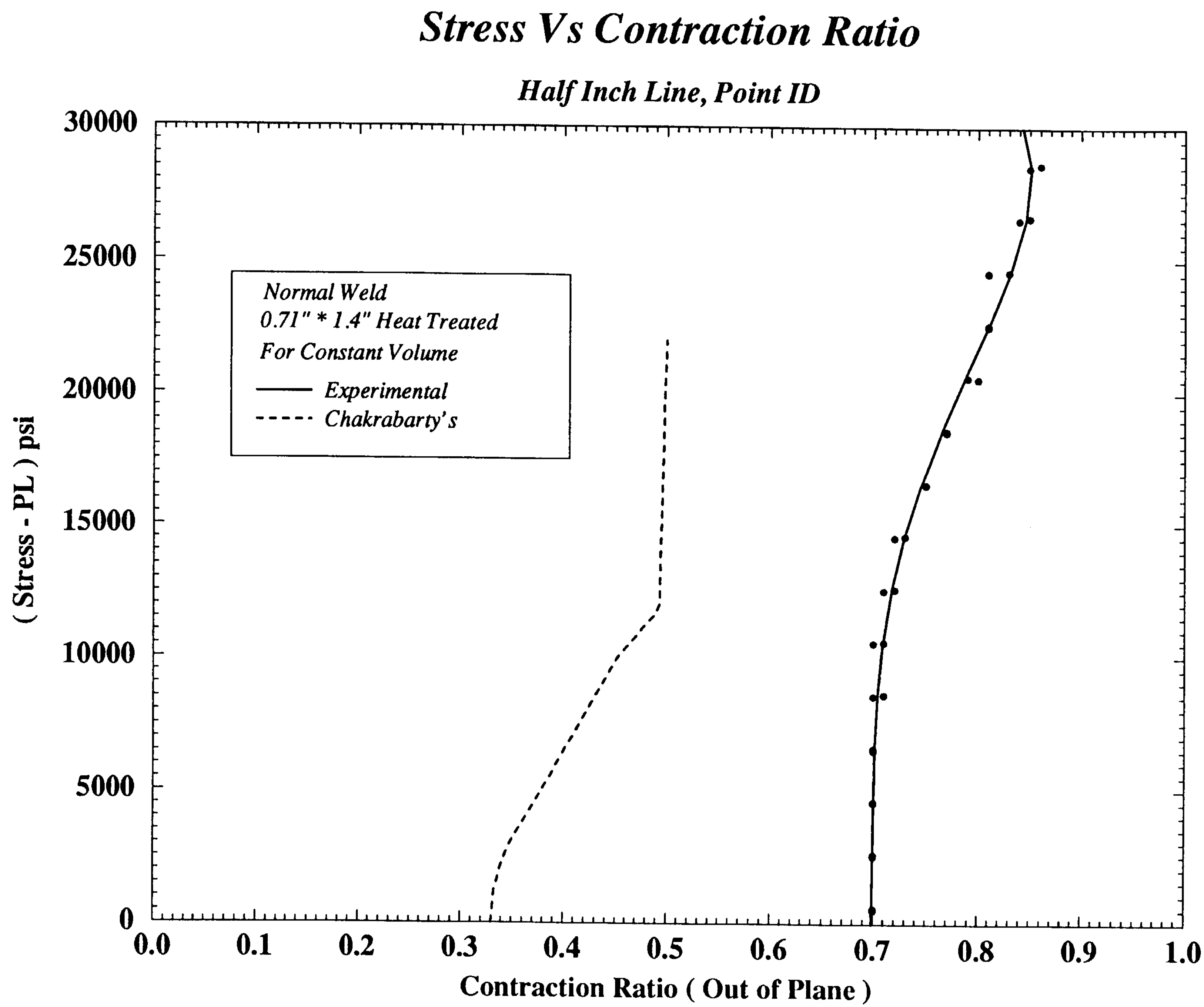

Figure B30. Out-of-Plane CR, Half Inch Line, ID Point

APPENDIX C

Task 3

Bending Tests

Normal Weld Procedure

0.71" x 1.4" Material

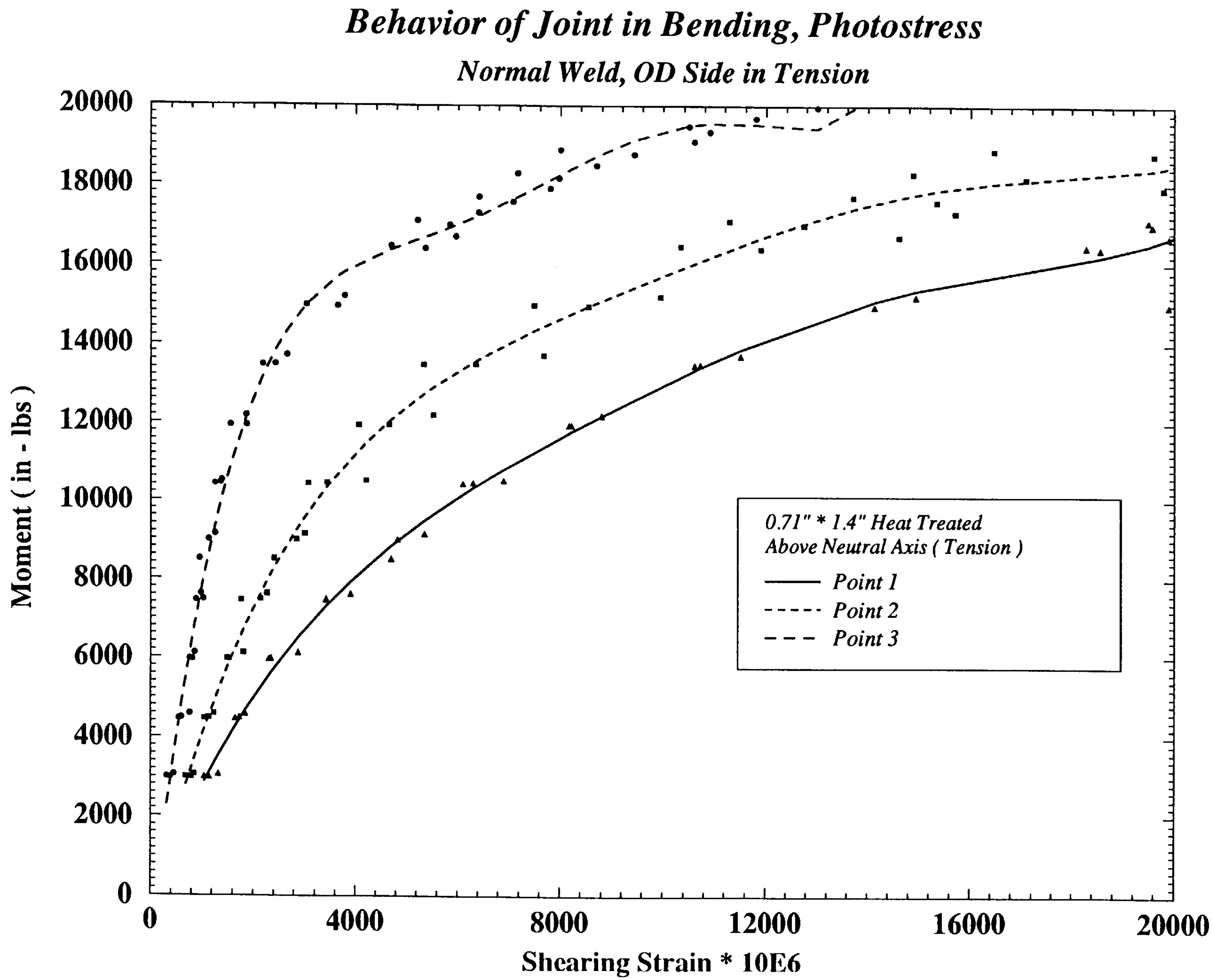

Figure C1. Material Behavior, OD Side Tension, Above NA

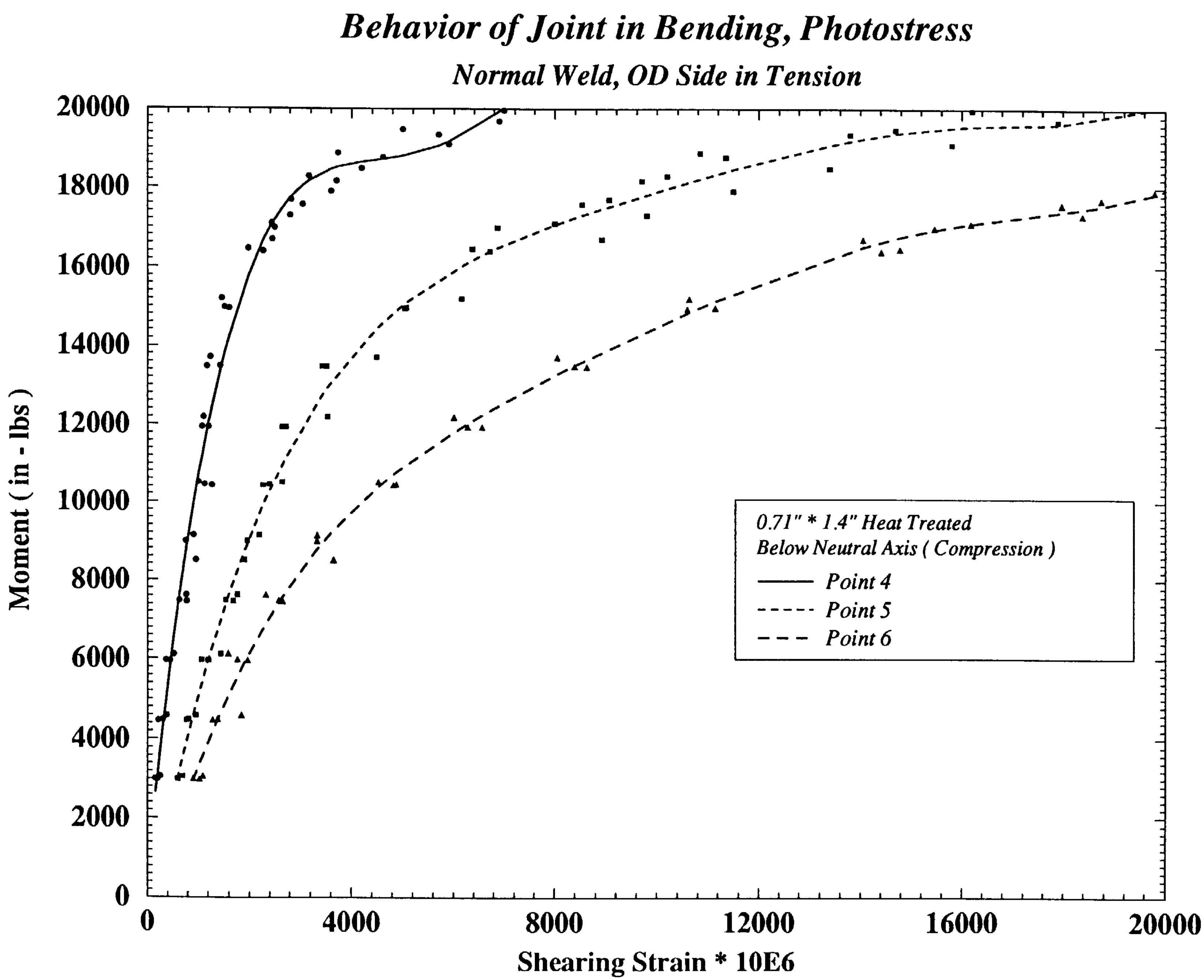

Figure C2. Material Behavior, OD Side Tension, Below NA

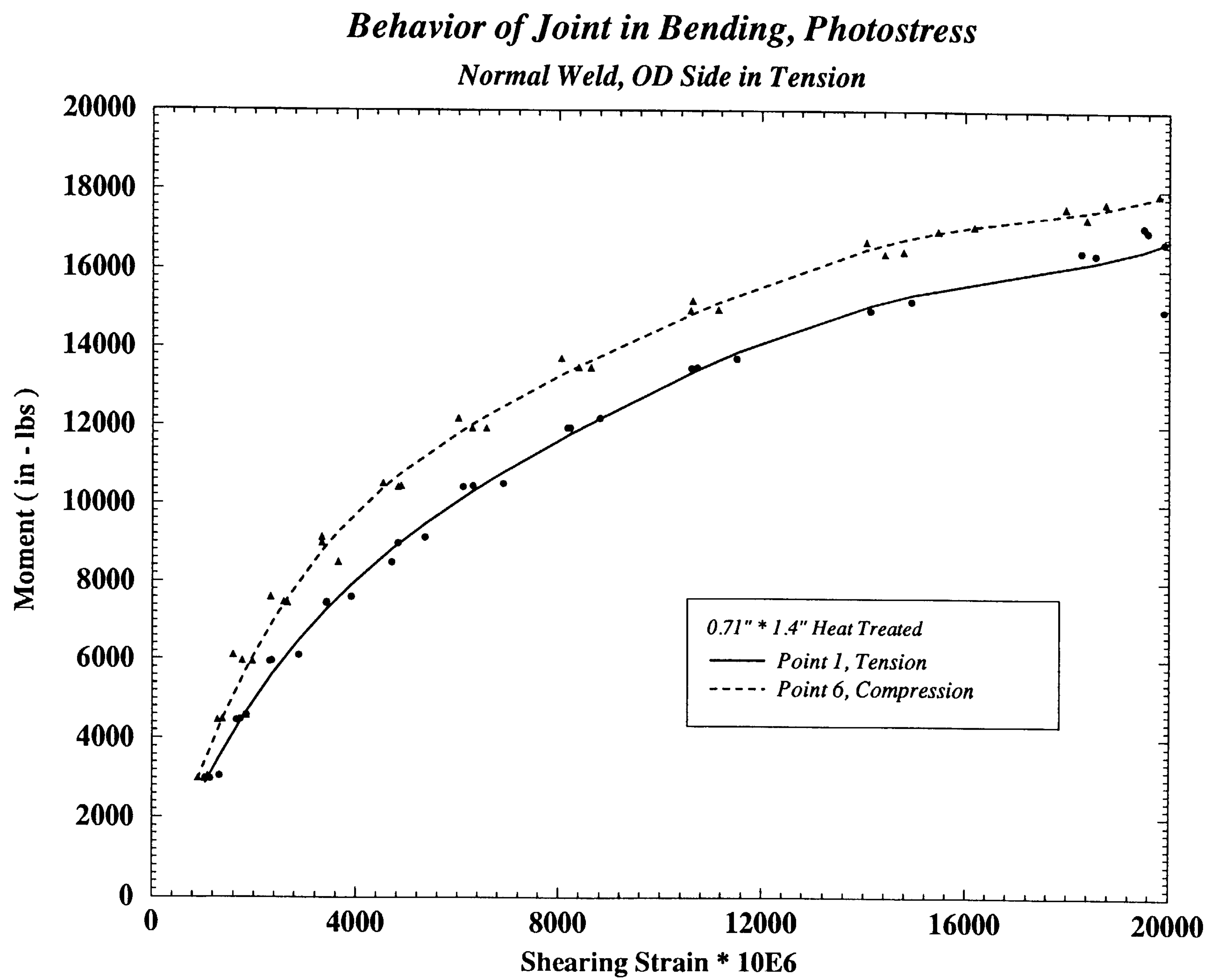

Figure C3. Comparison, OD Side Tension, Points 1 and 6

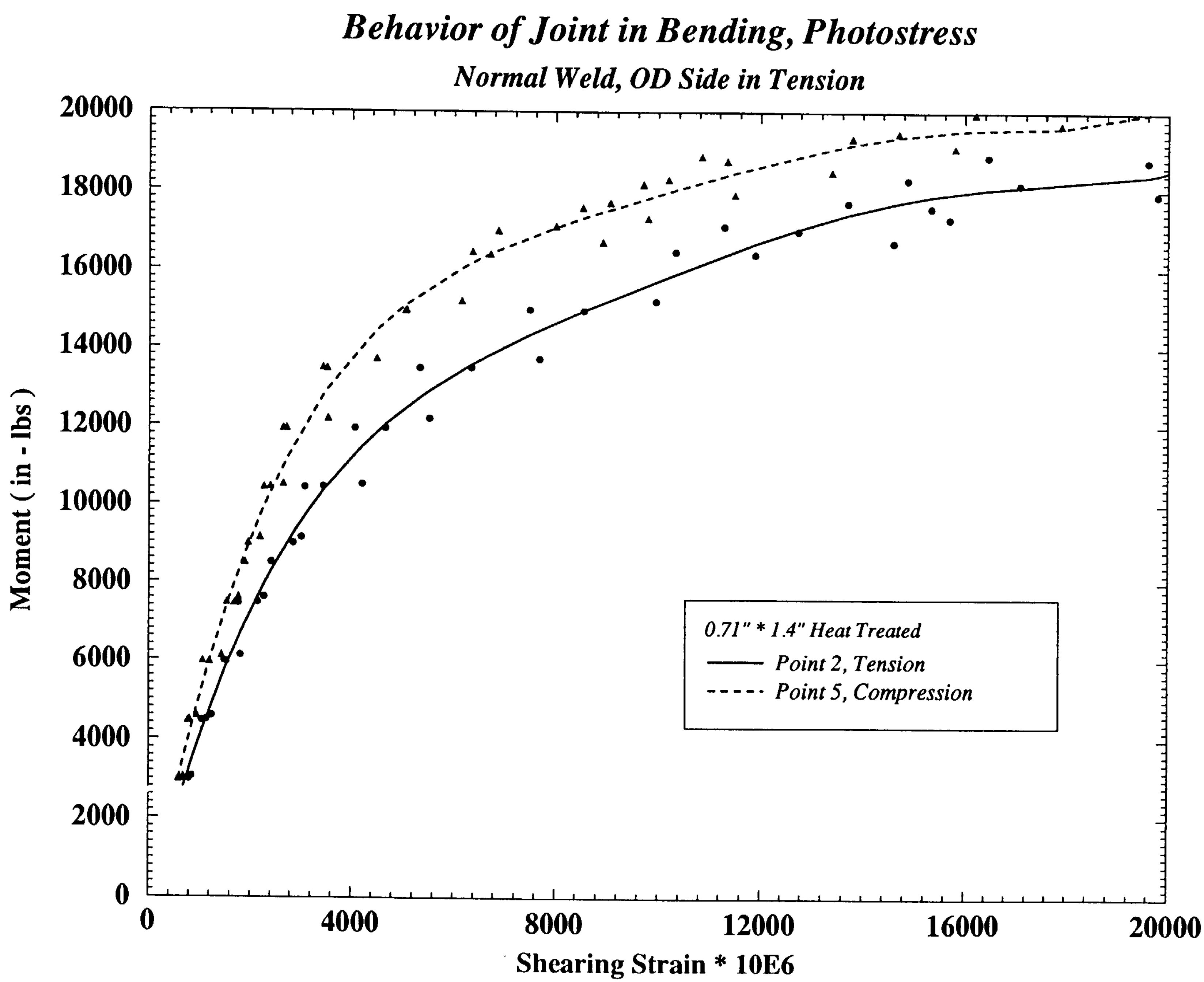

Figure C4. Comparison, OD Side Tension, Points 2 and 5

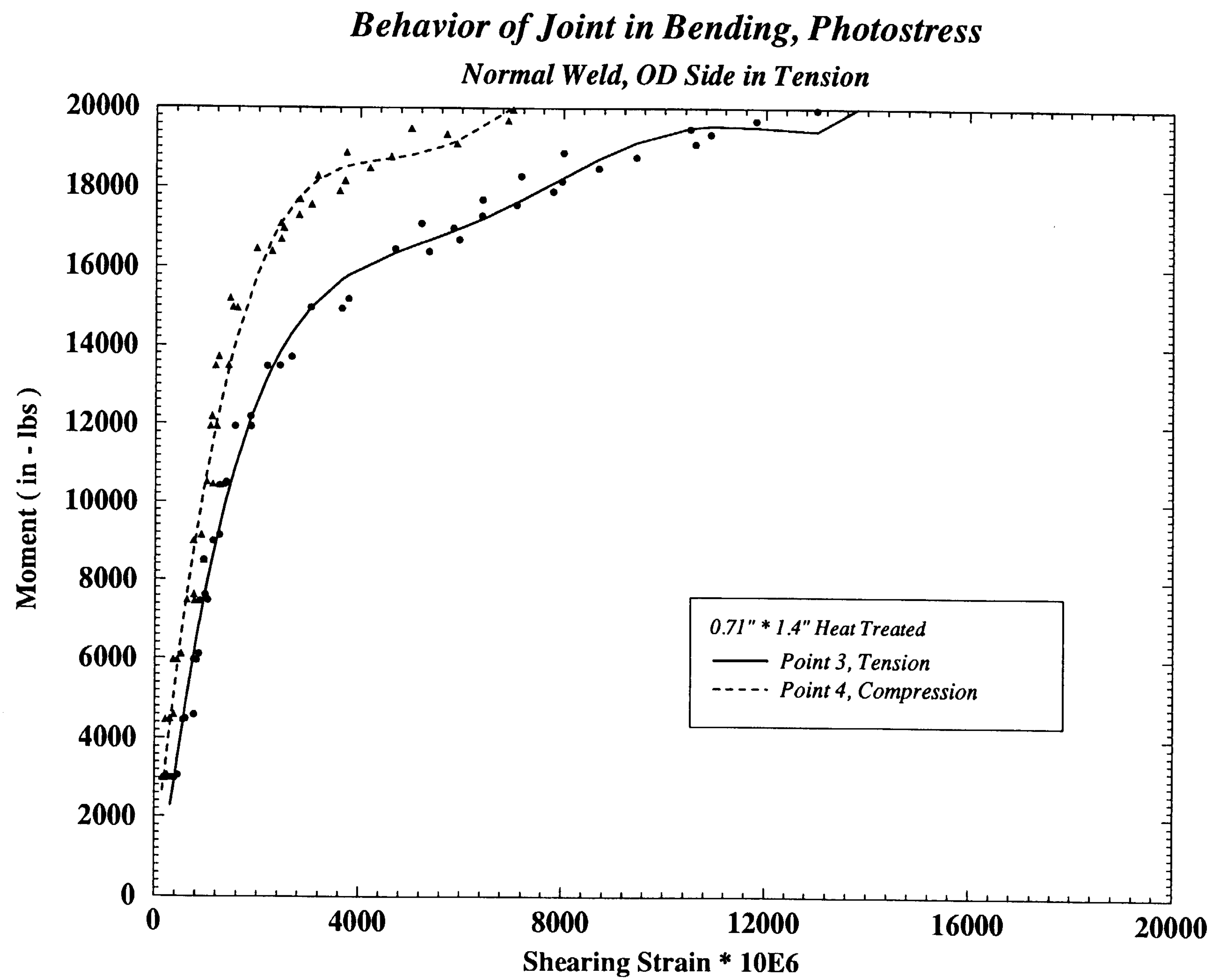

Figure C5. Comparison, OD Side Tension, Points 3 and 4

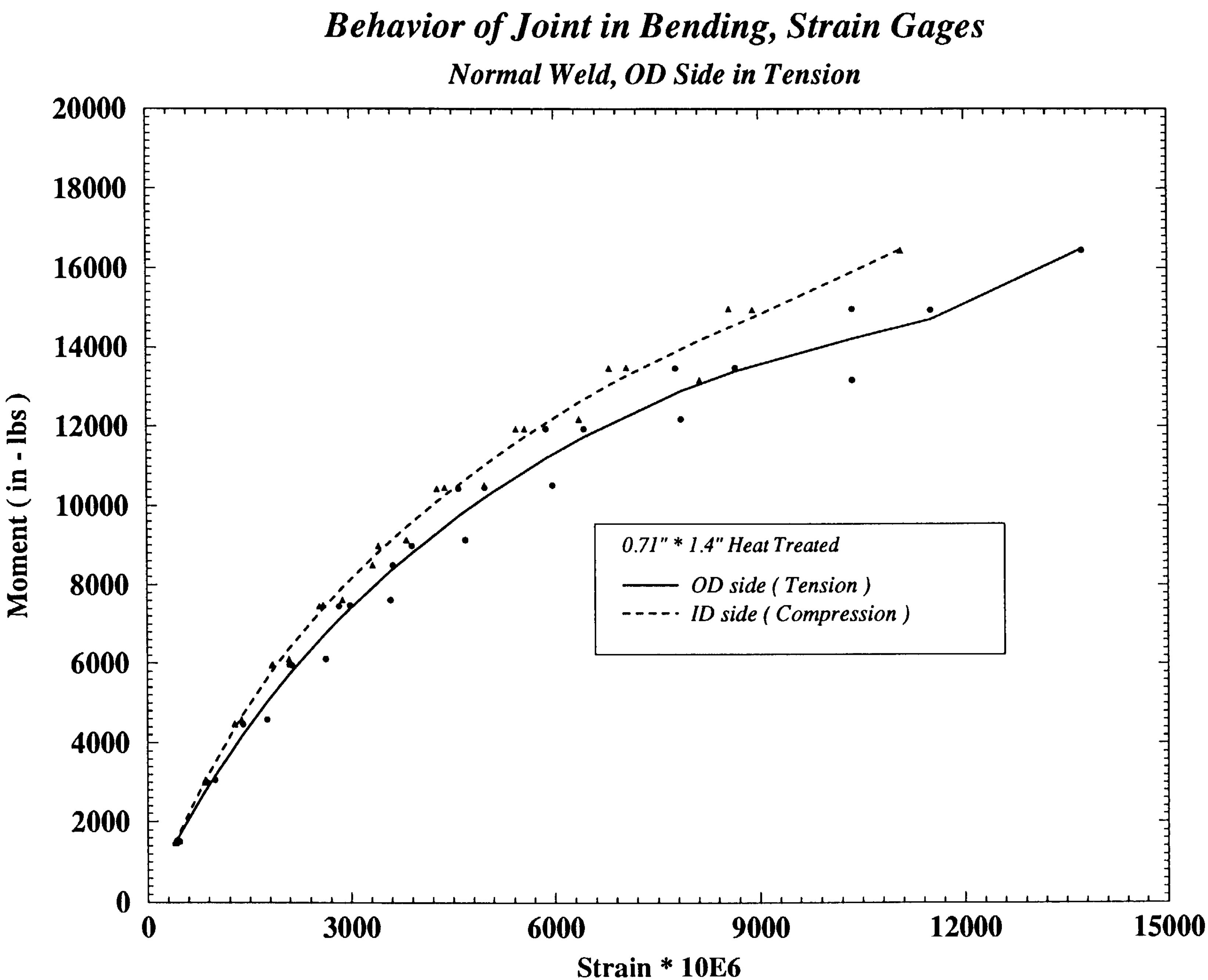

Figure C6. Material Behavior, OD Side Tension, OD and ID Points

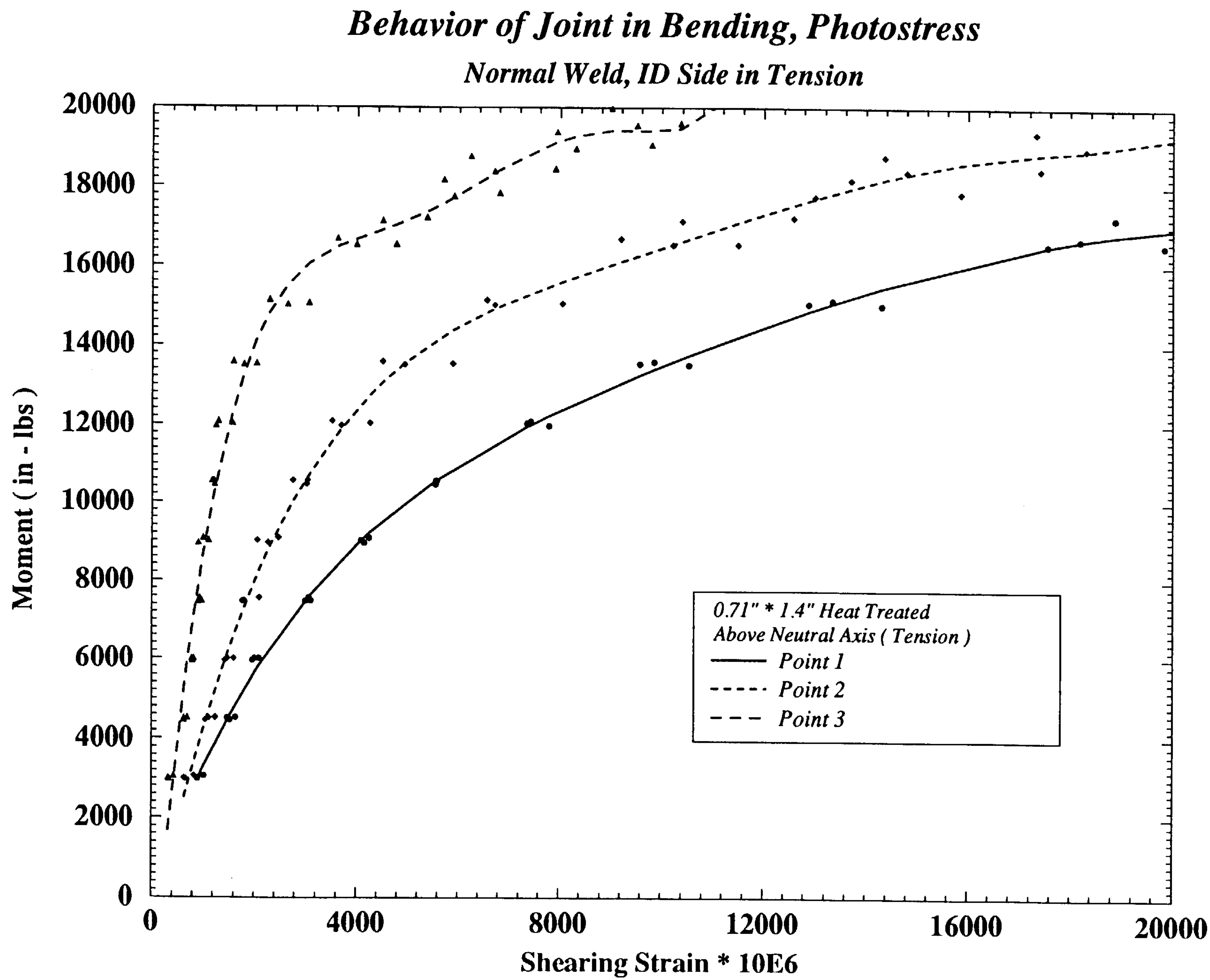

Figure C7. Material Behavior, ID Side Tension, Above NA

C-3

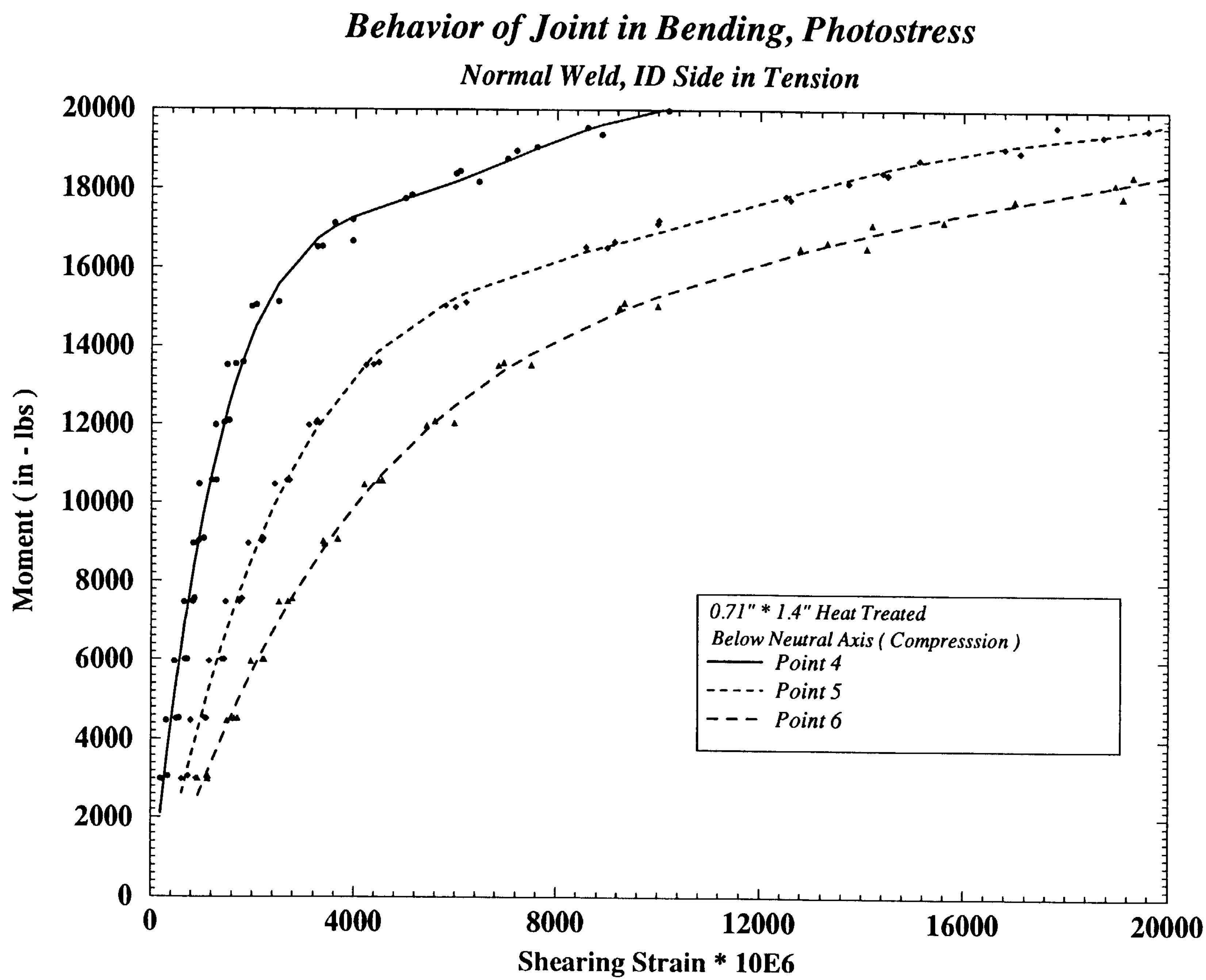

Figure C8. Material Behavior, ID Side Tension, Below NA

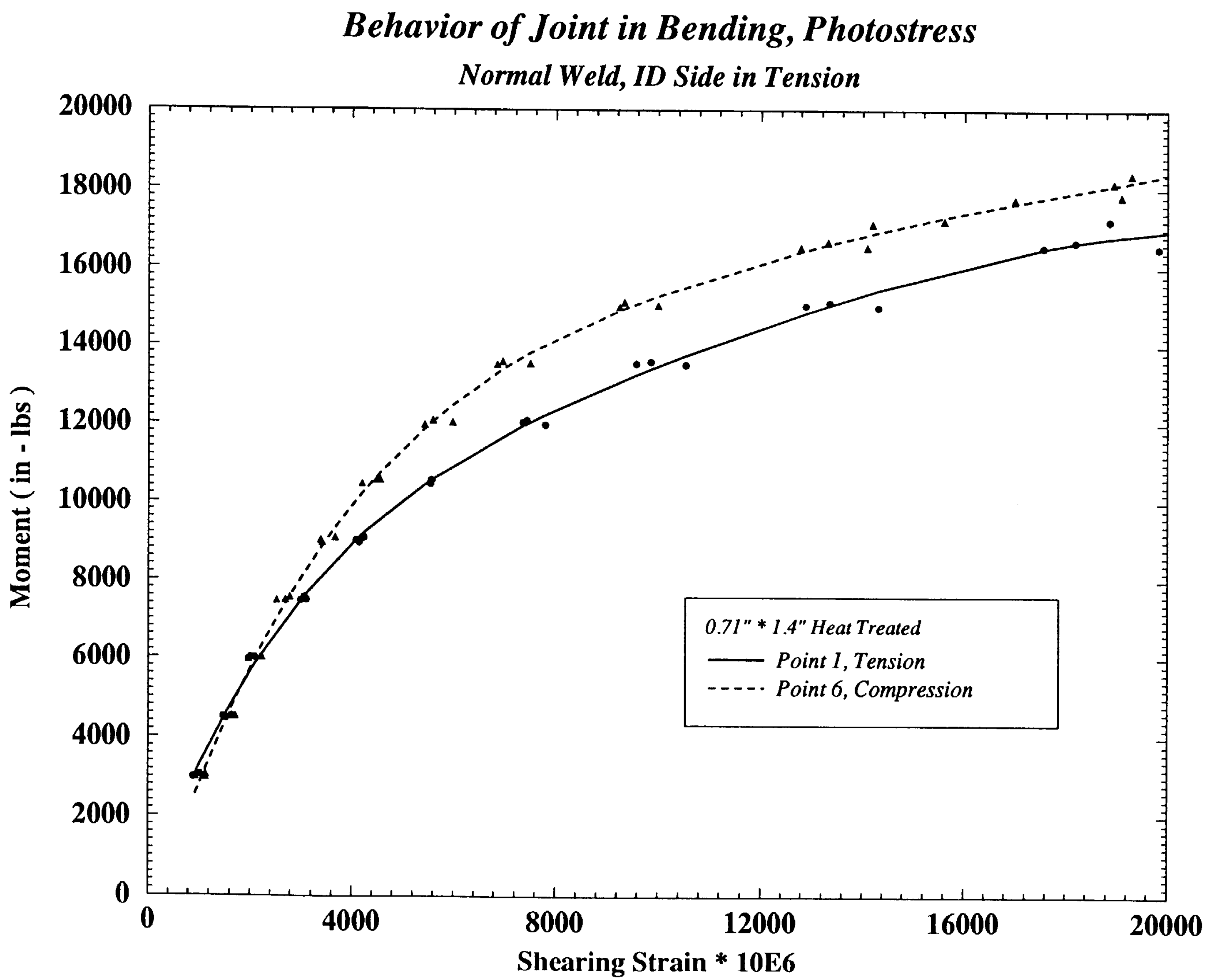

Figure C9. Comparison, ID Side Tension, Points 1 and 6

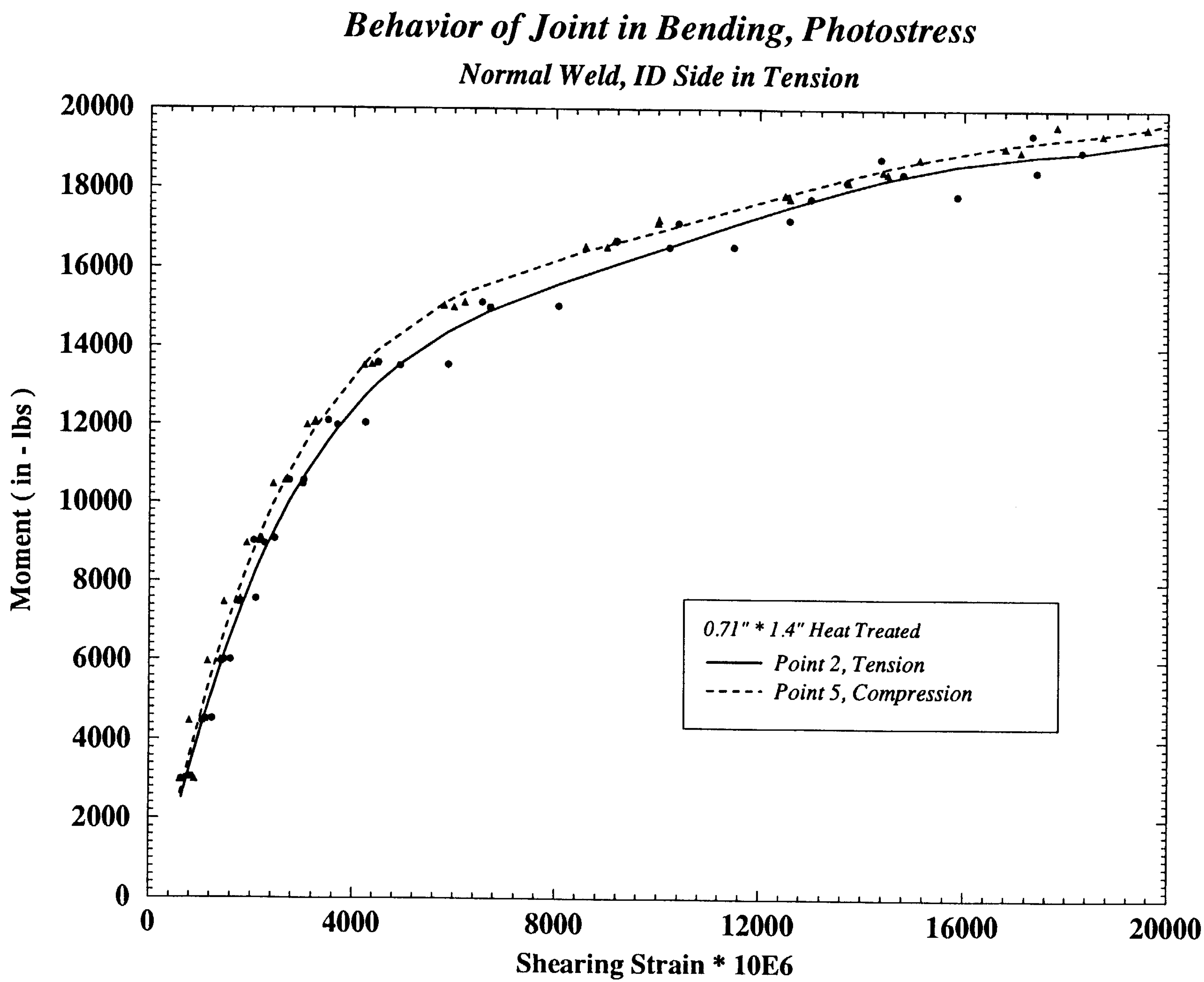

Figure C10. Comparison, ID Side Tension, Points 2 and 5

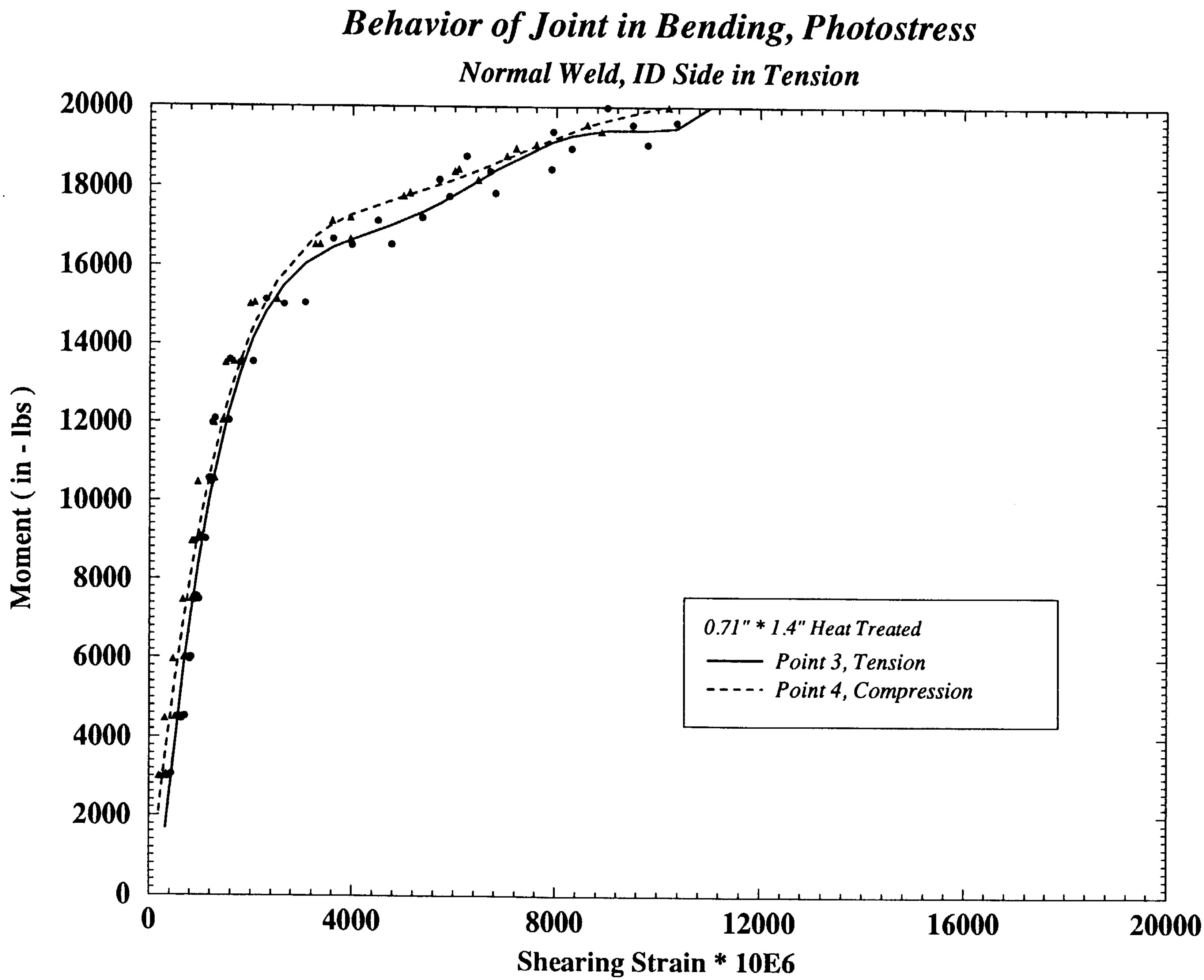

Figure C11. Comparison, ID Side Tension, Points 3 and 4

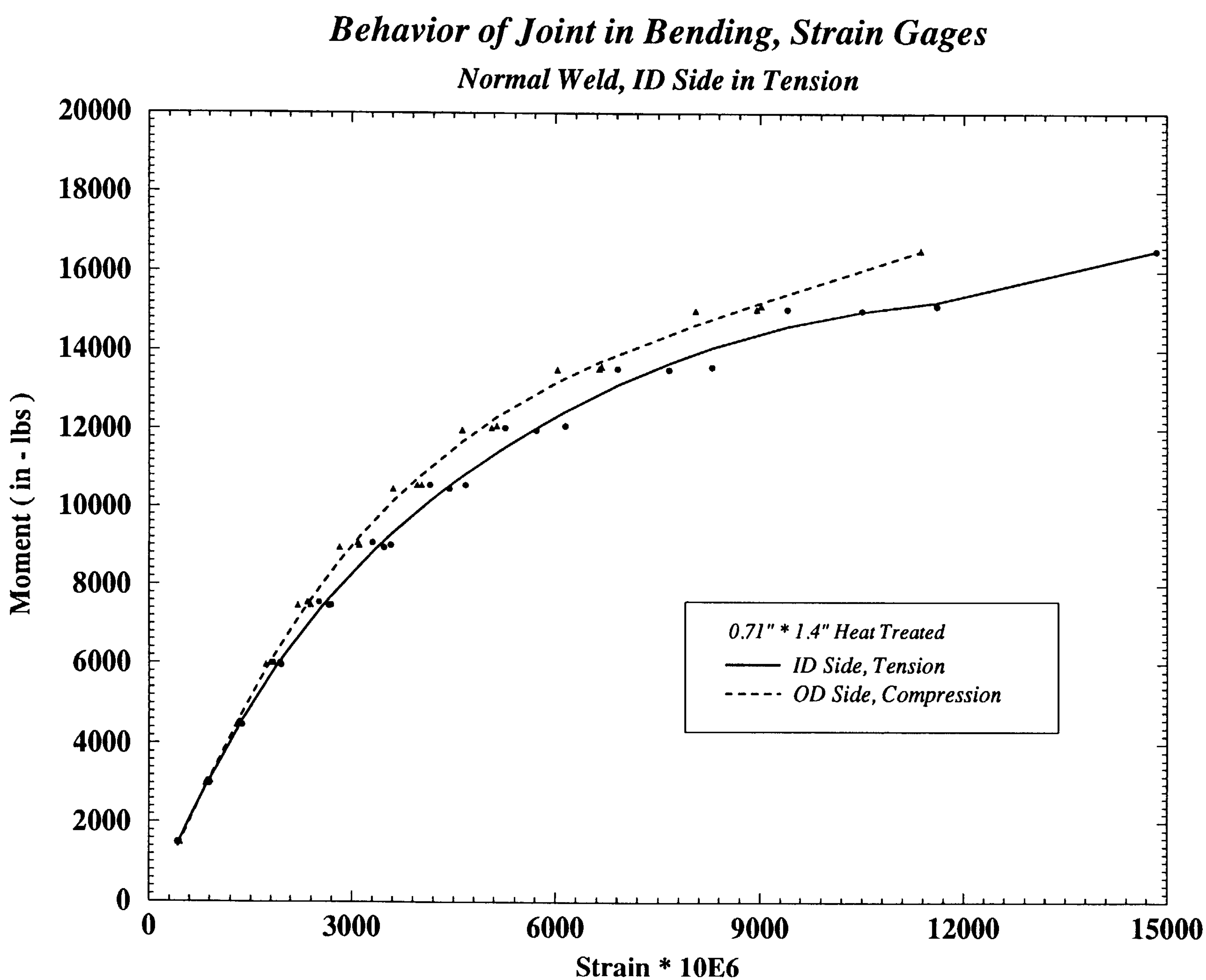

Figure C12. Material Behavior, ID Side Tension, OD and ID Points

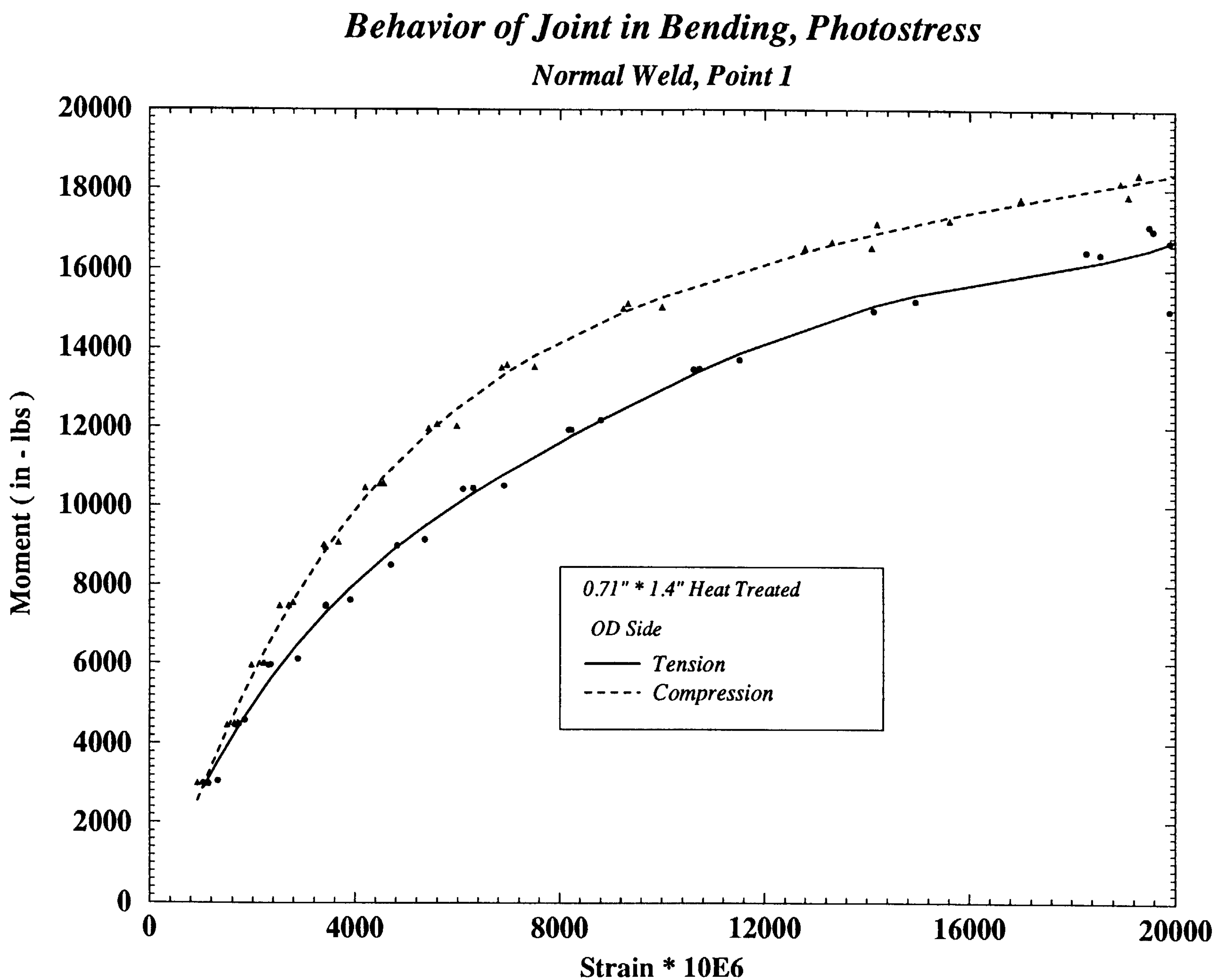

Figure C13. Behavior, OD Side, Point 1, Tension and Compression

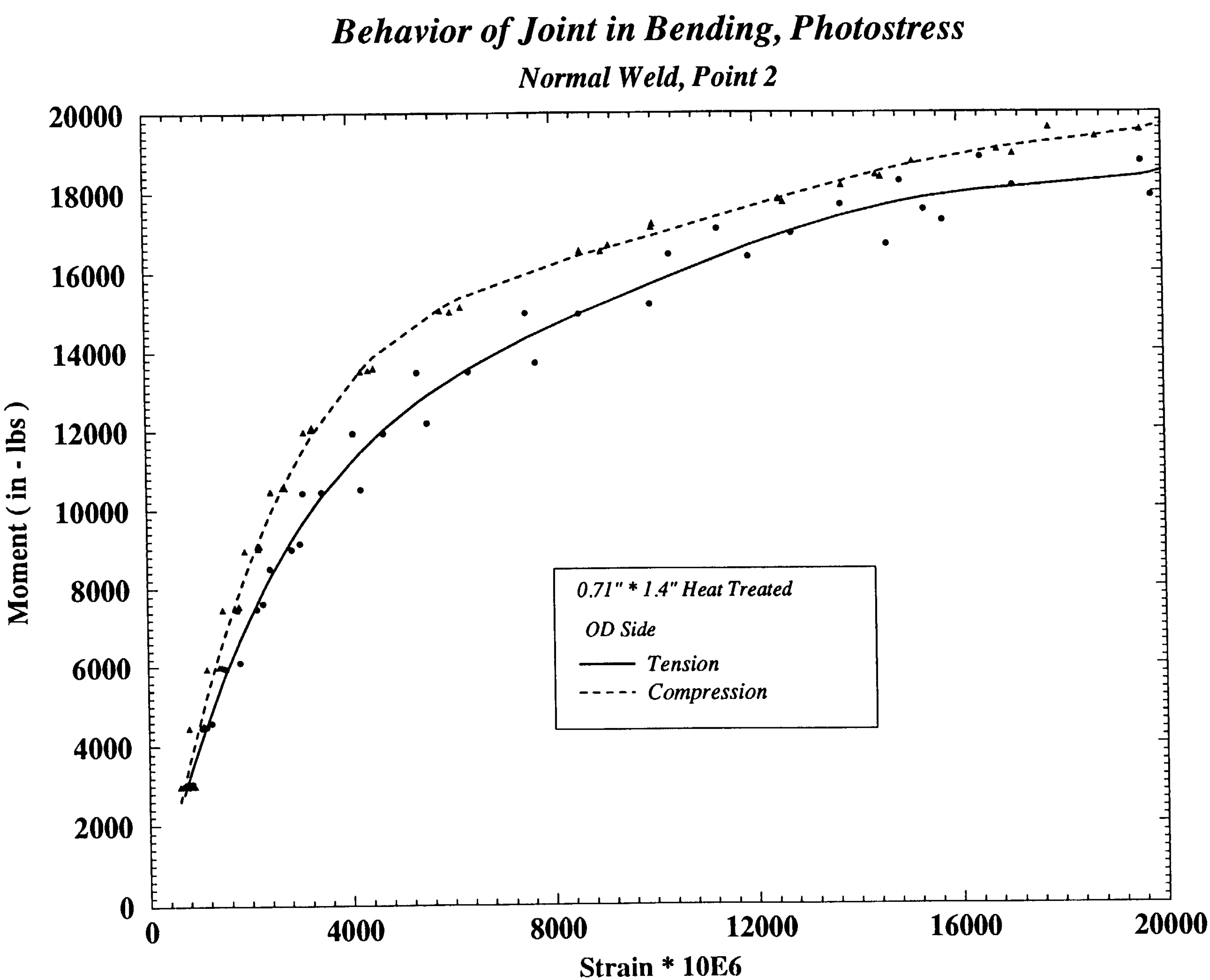

Figure C14. Behavior, OD Side, Point 2, Tension and Compression

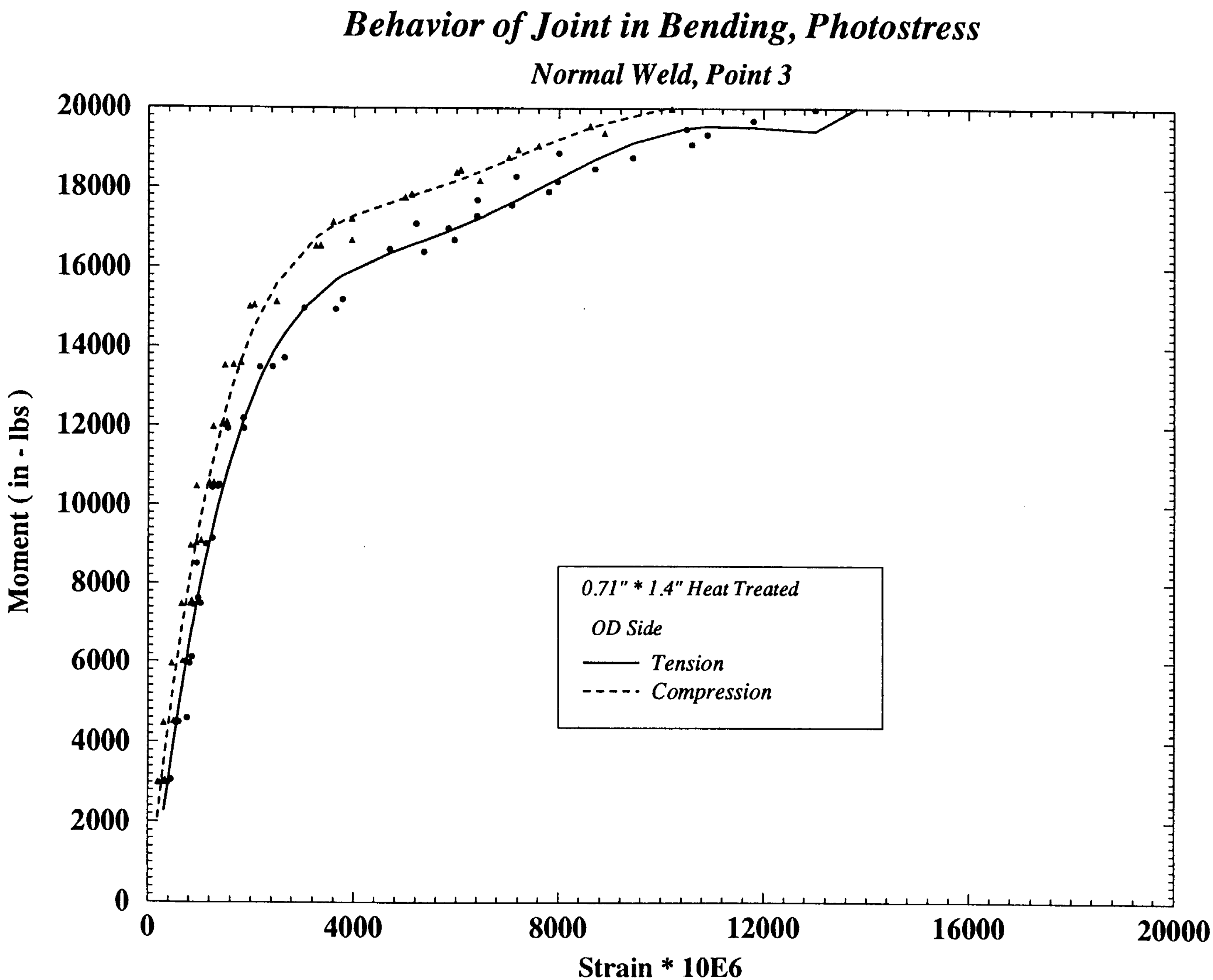

Figure C15. Behavior, OD Side, Point 3, Tension and Compression

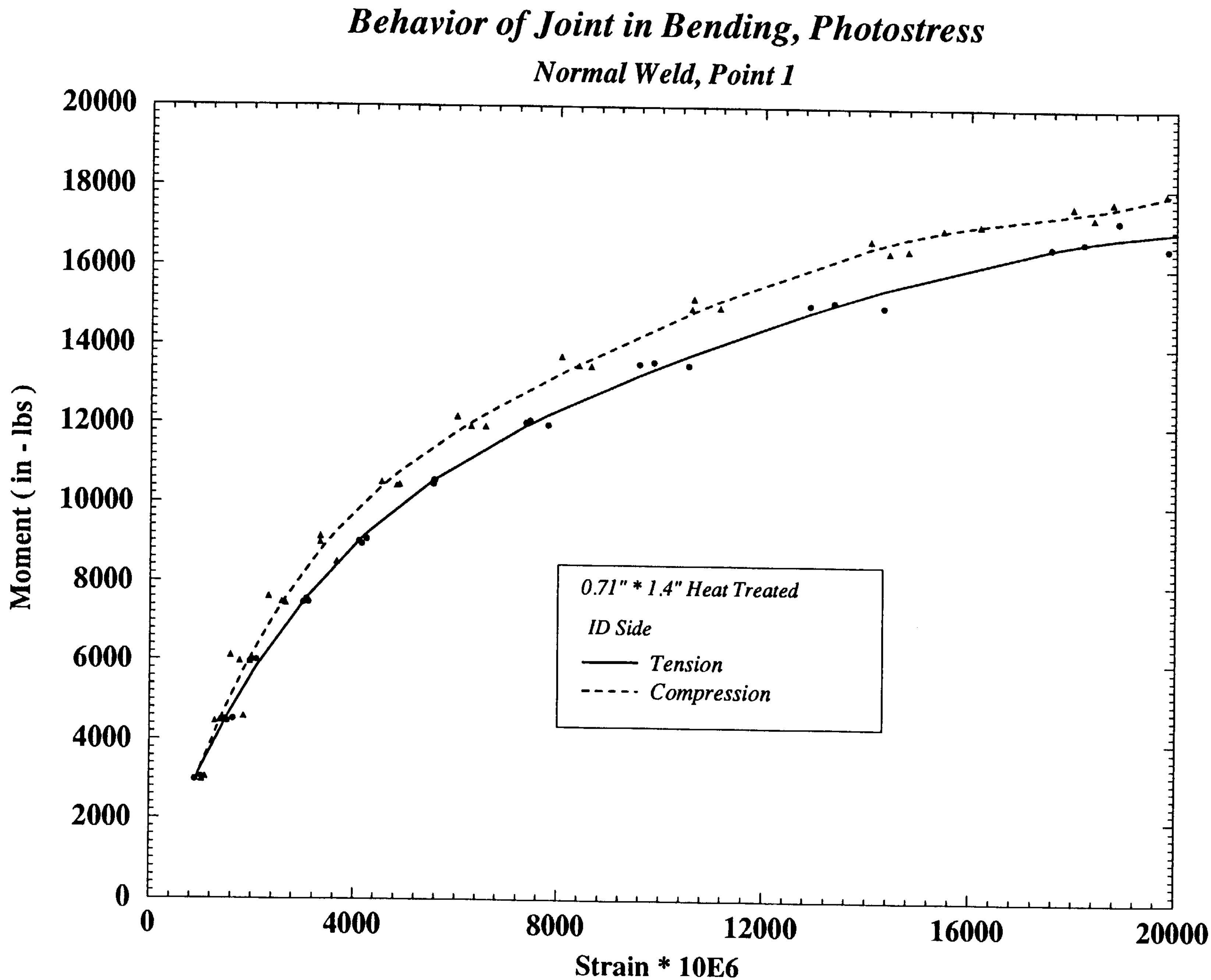

Figure C16. Behavior, ID Side, Point 1, Tension and Compression

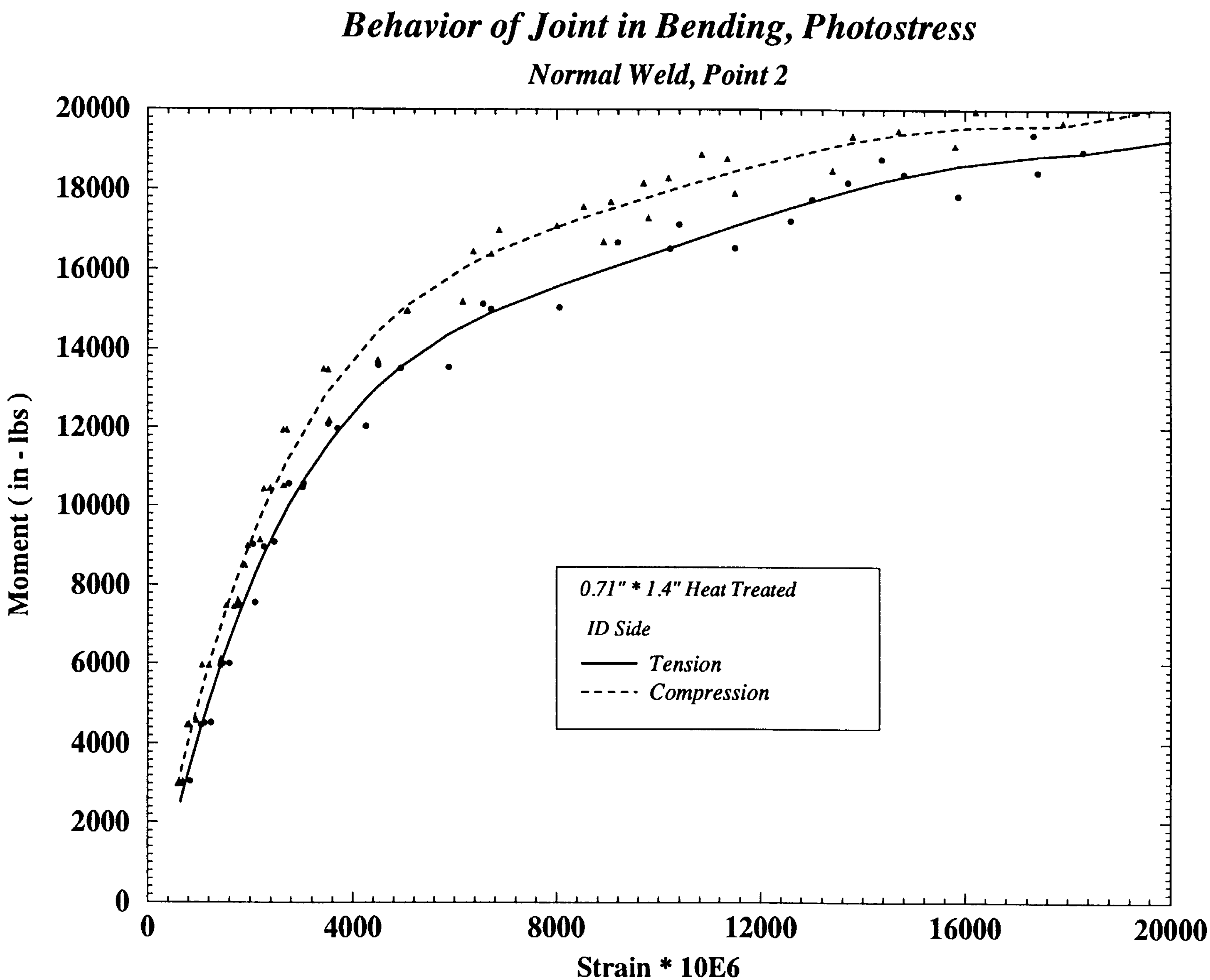

Figure C17. Behavior, ID Side, Point 2, Tension and Compression

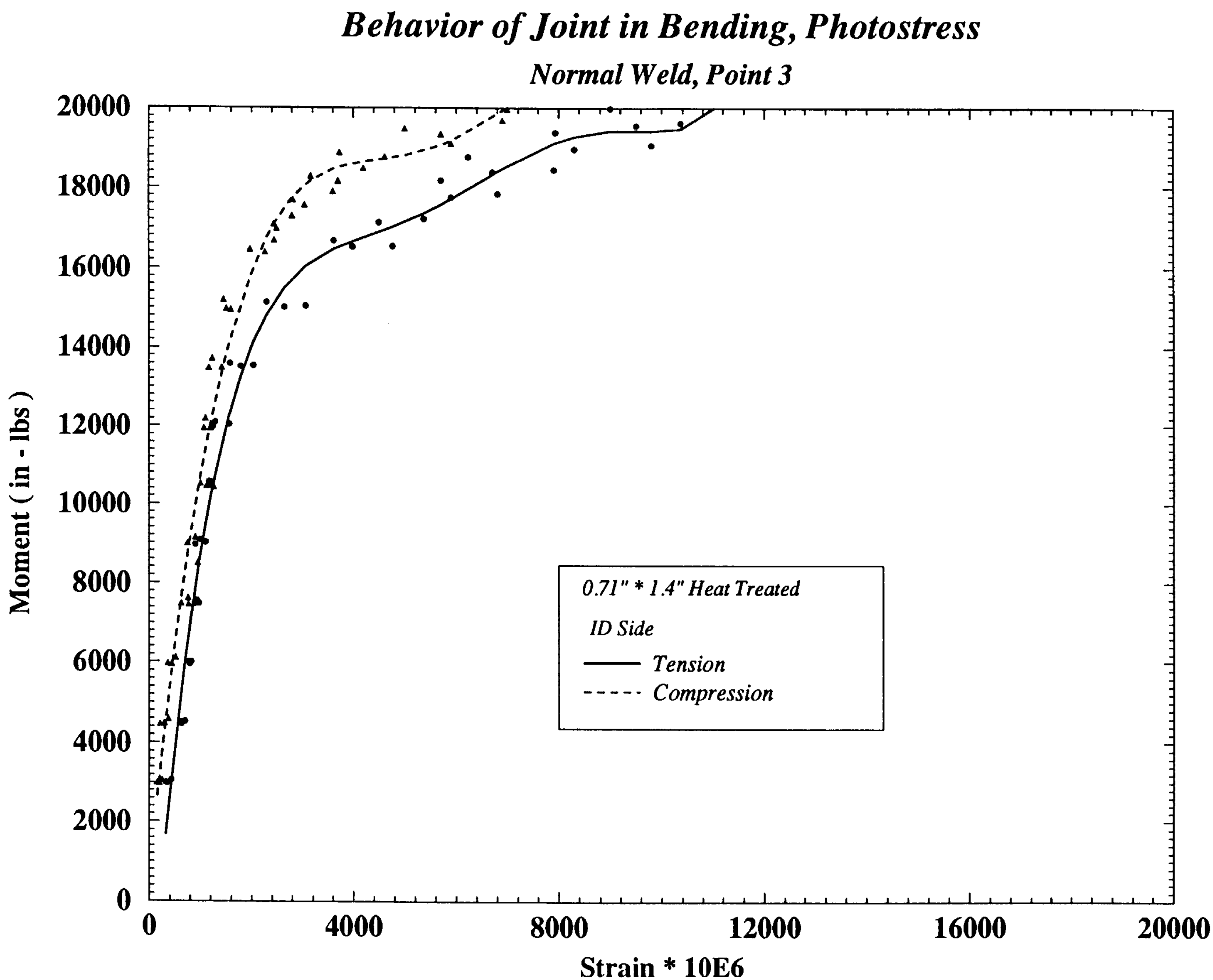

Figure C18. Behavior, ID Side, Point 3, Tension and Compression

APPENDIX D

Task 4

Tensile Tests

0.50" x 1.0" Material

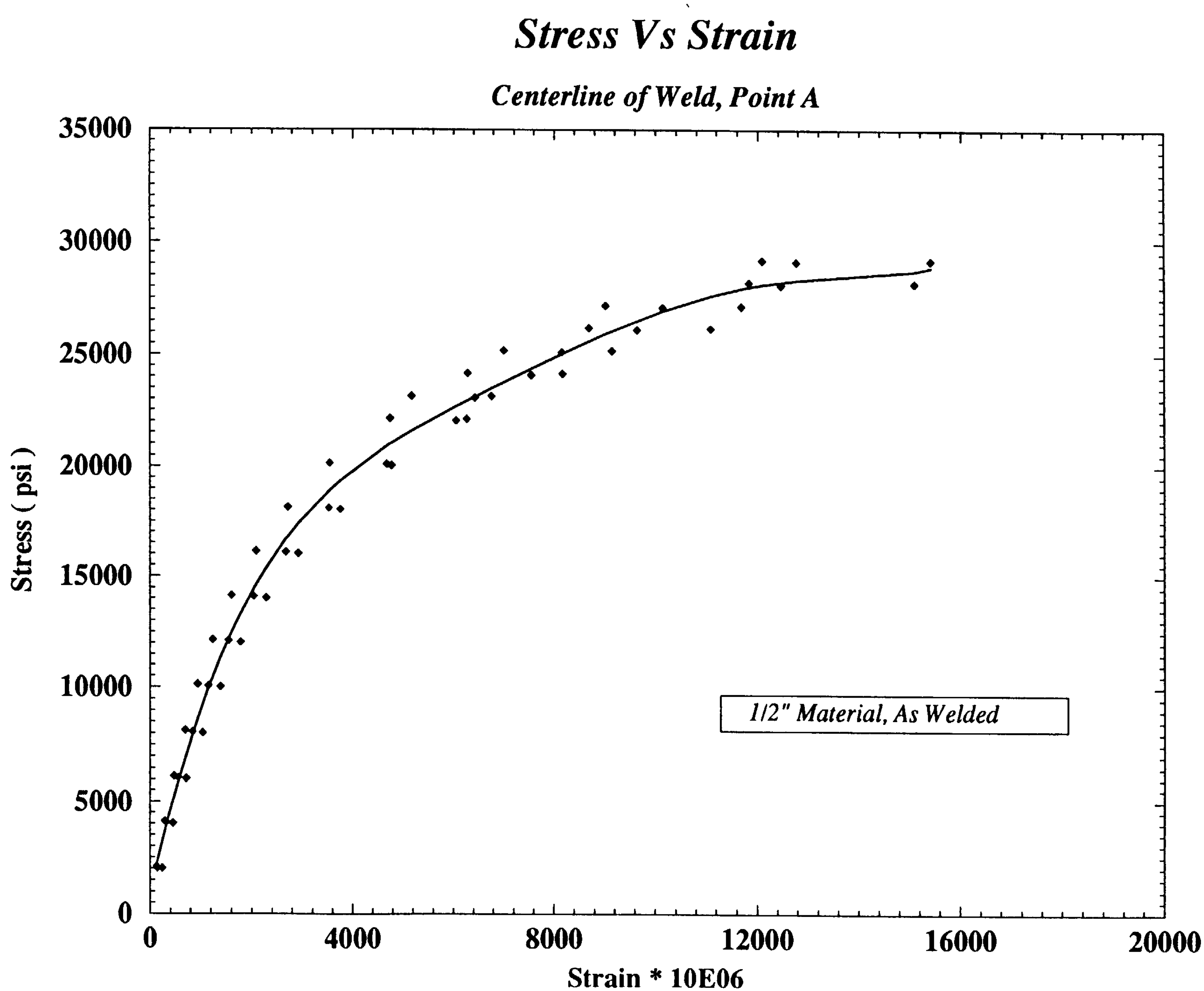

Figure D1. Material Behavior, Point A

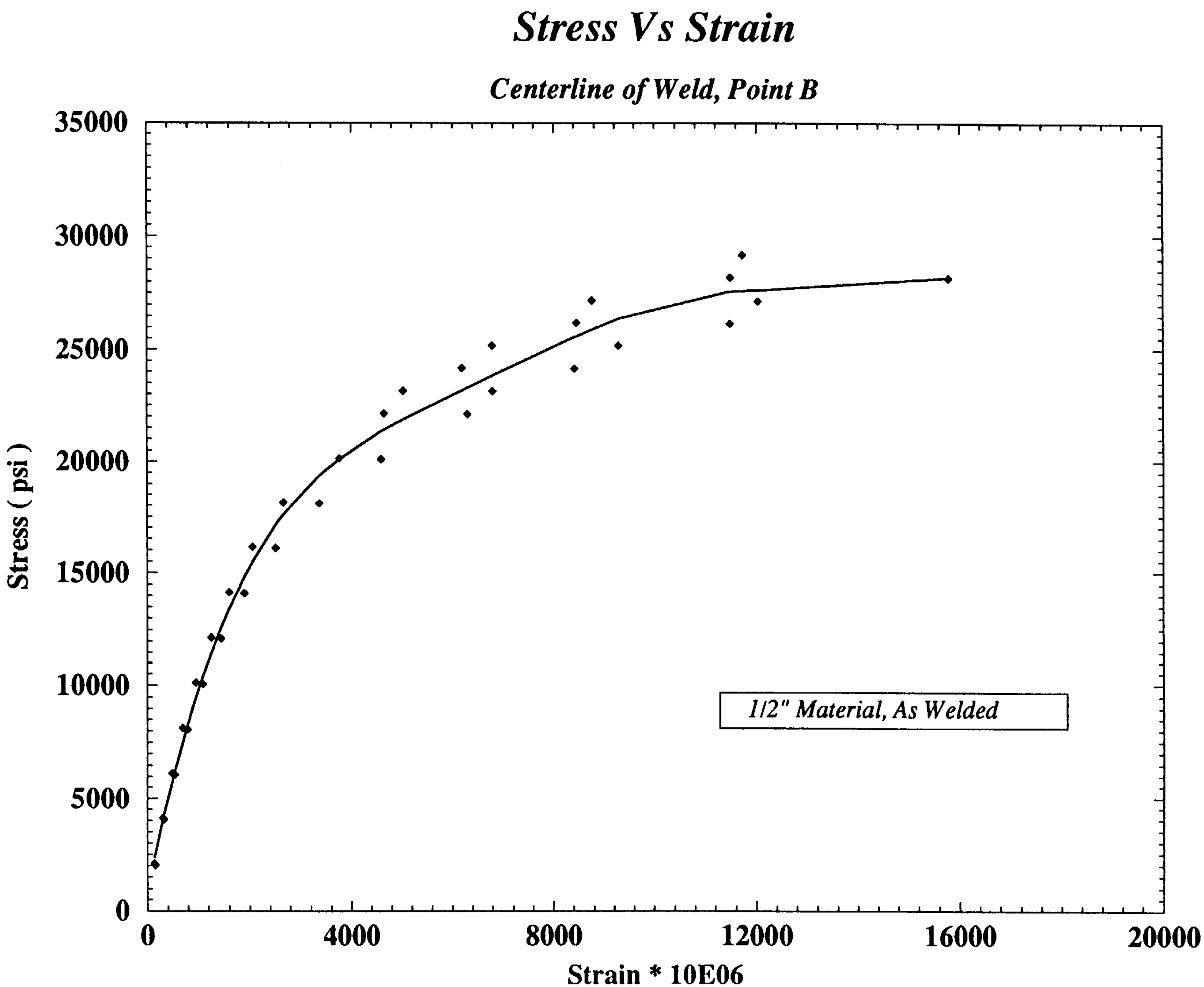

Figure D2. Material Behavior, Point B

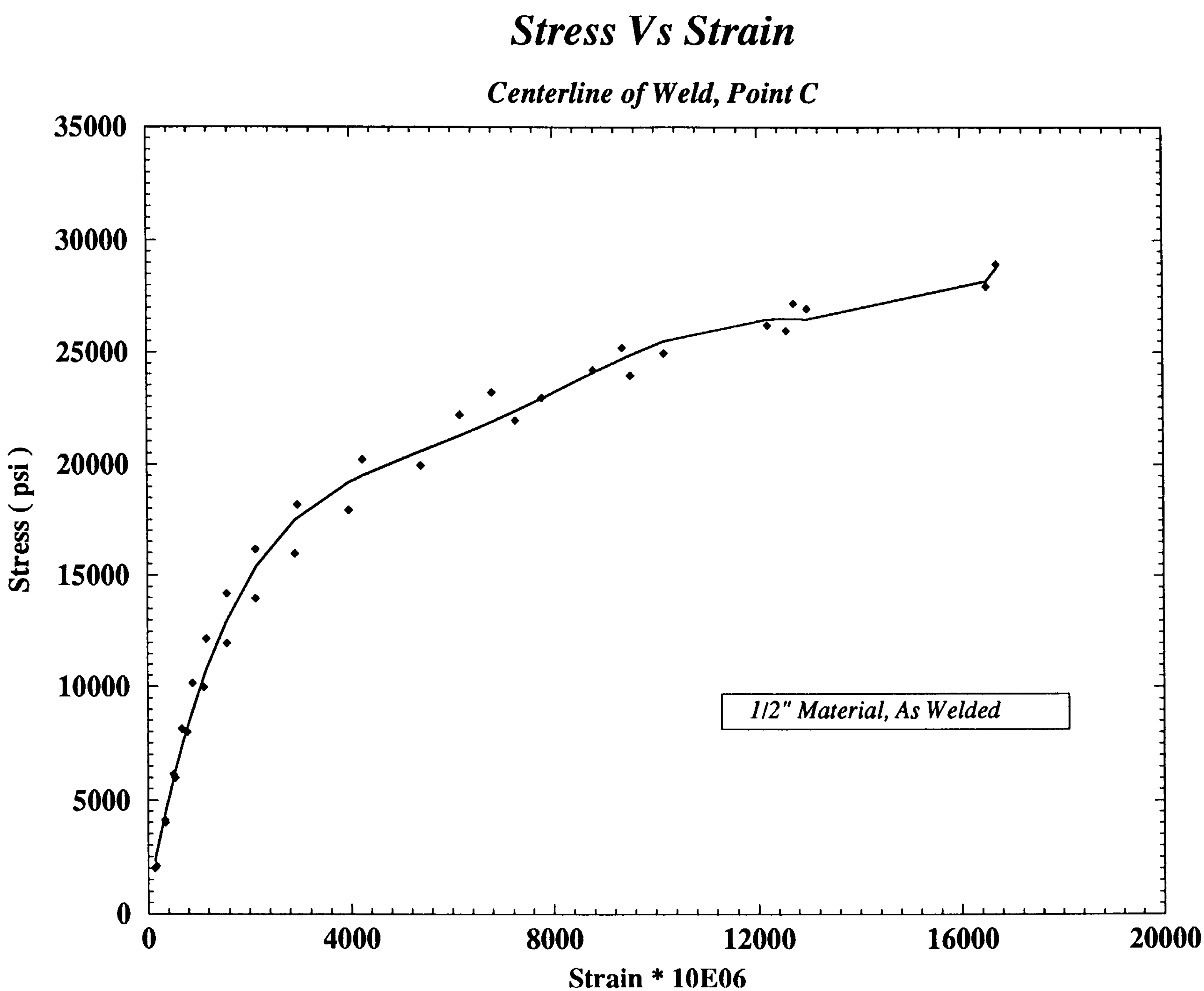

Figure D3. Material Behavior, Point C

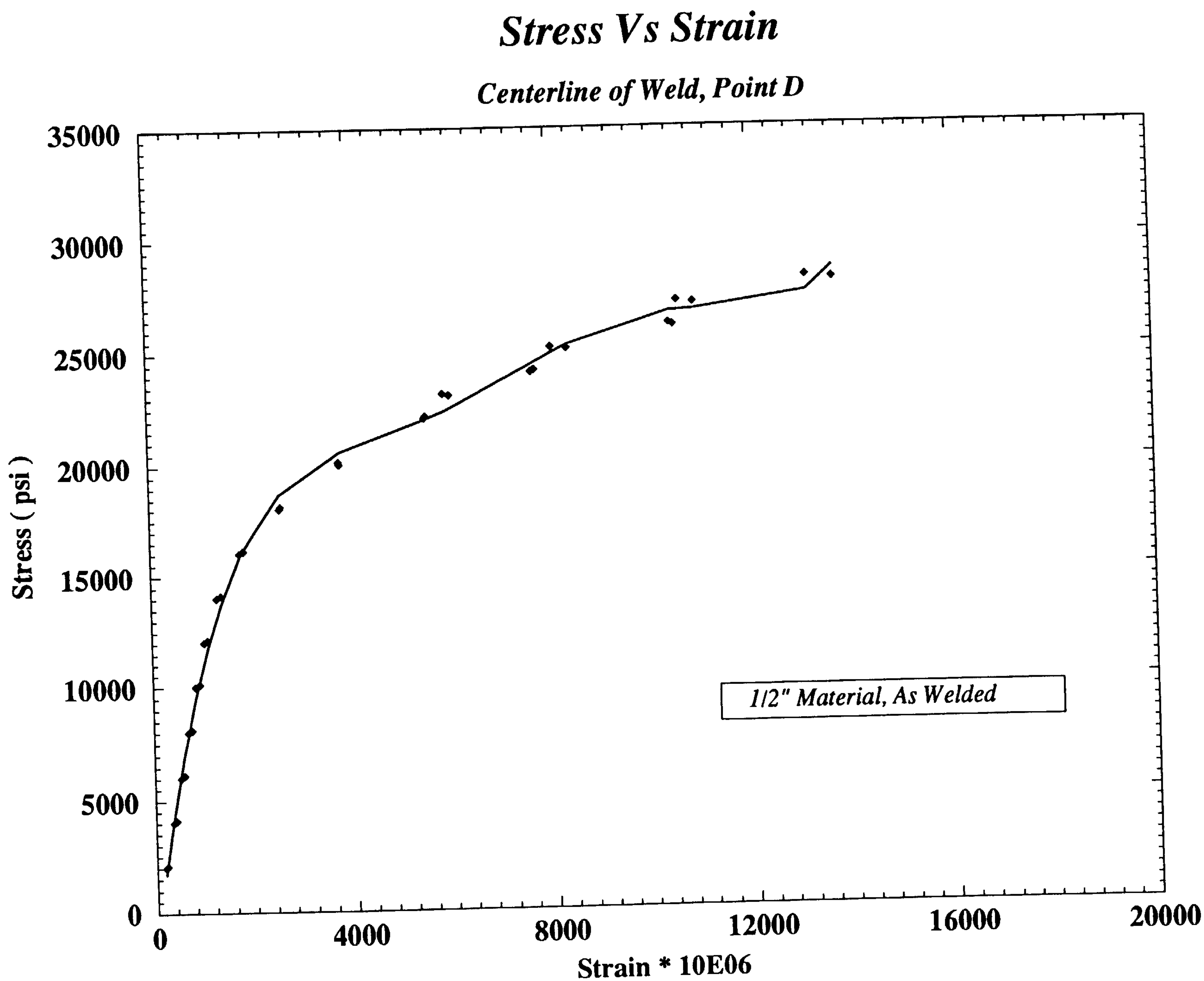

Figure D4. Material Behavior, Point D

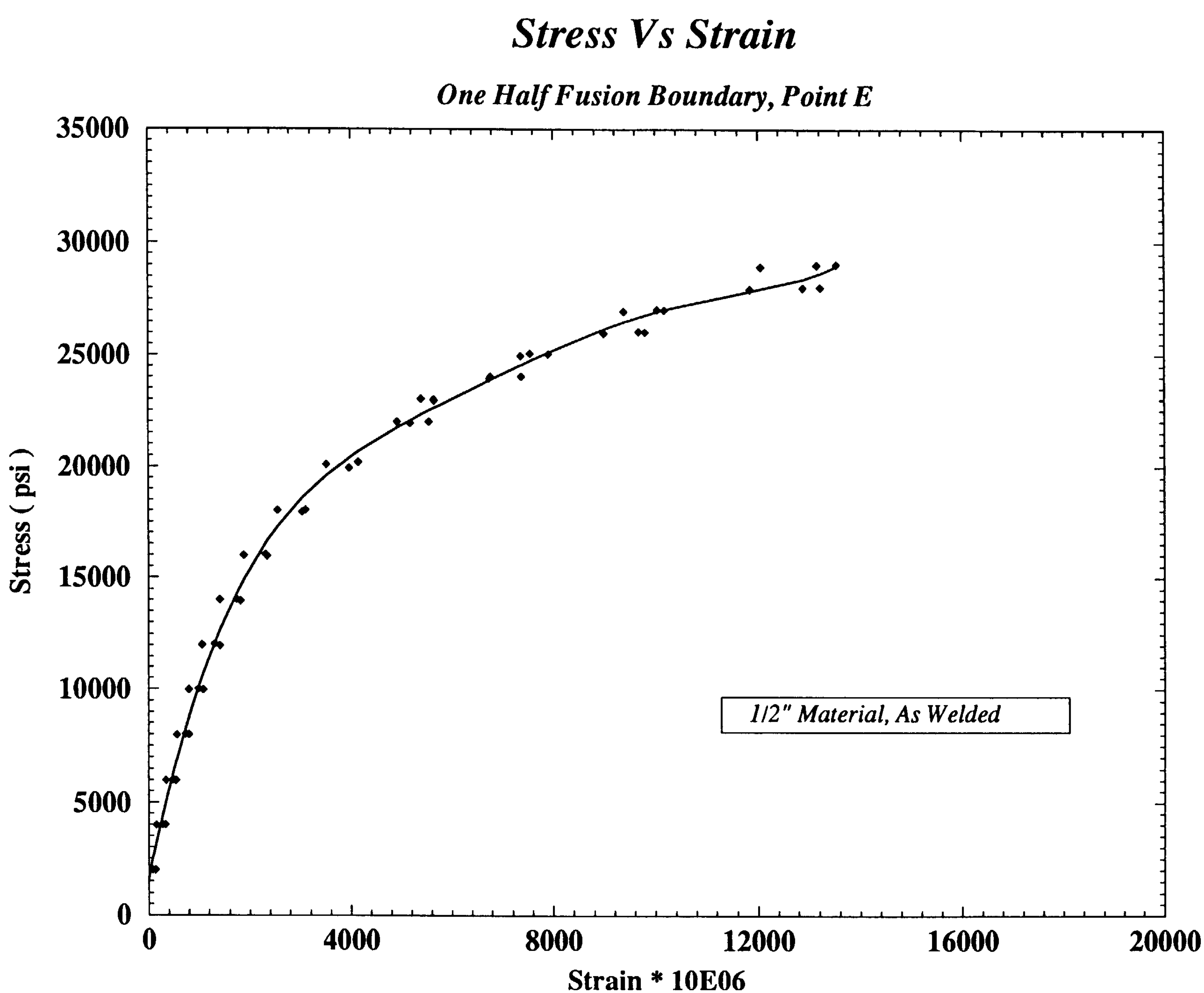

Figure D5. Material Behavior, Point E

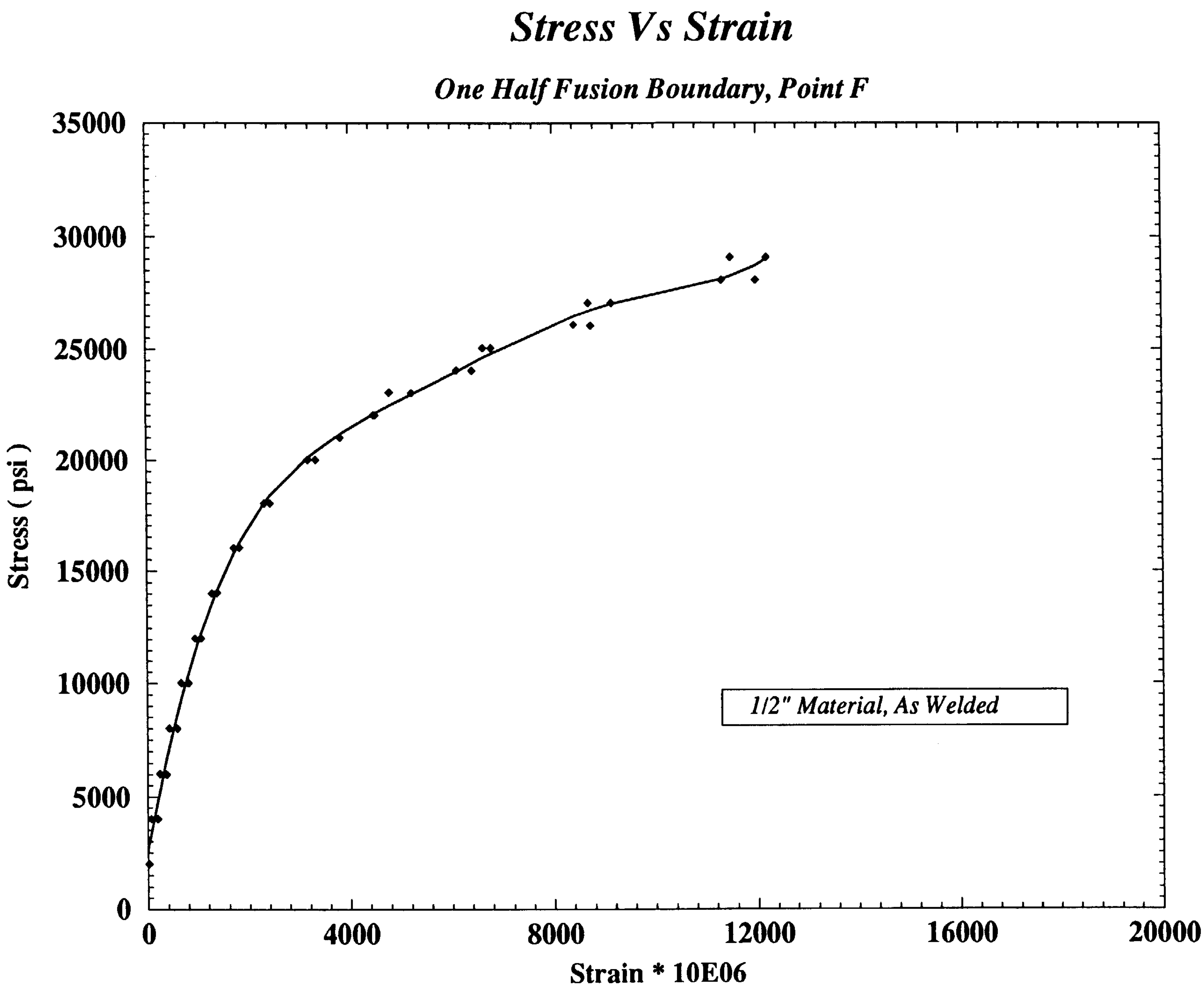

Figure D6. Material Behavior, Point F

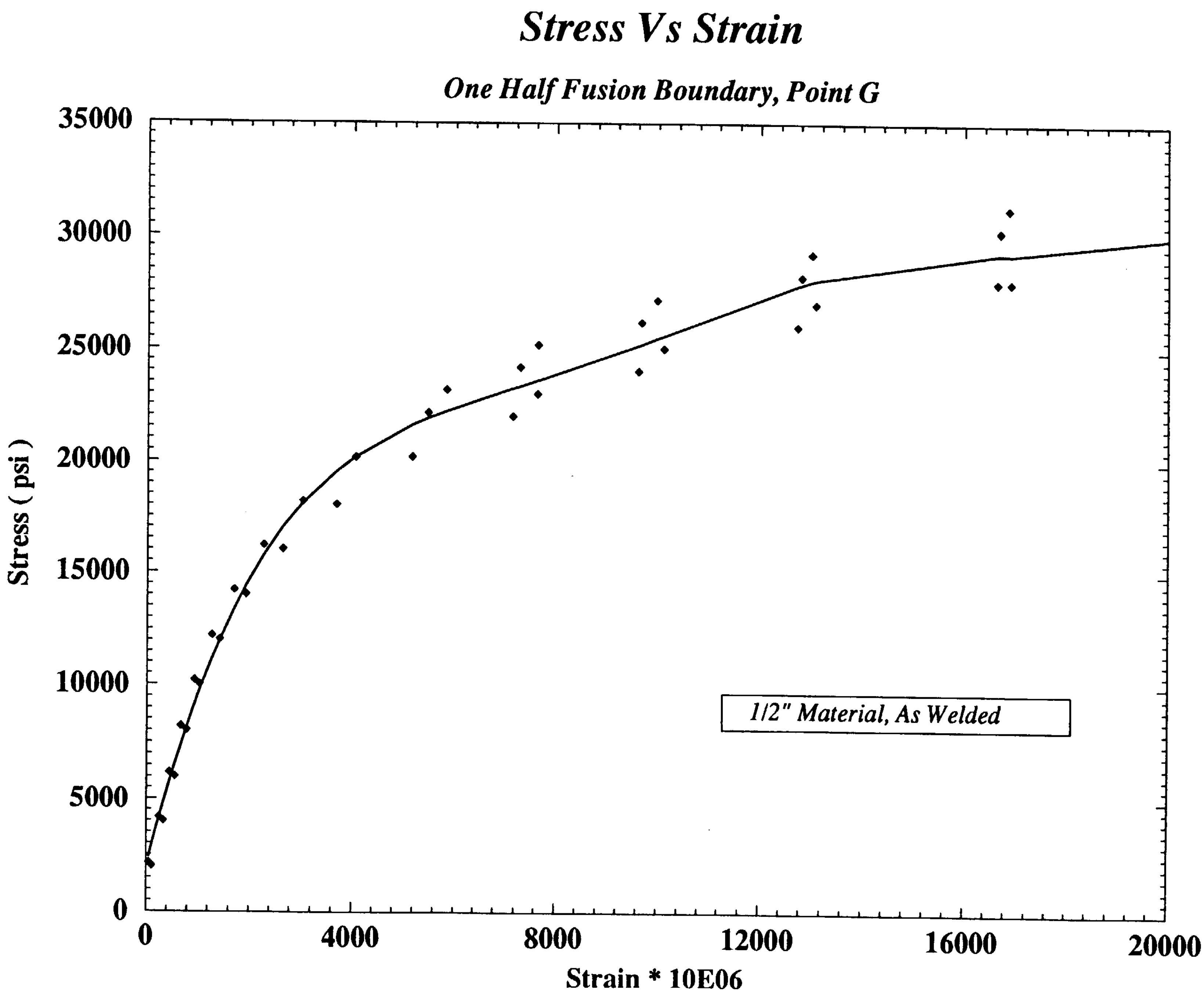

Figure D7. Material Behavior, Point G

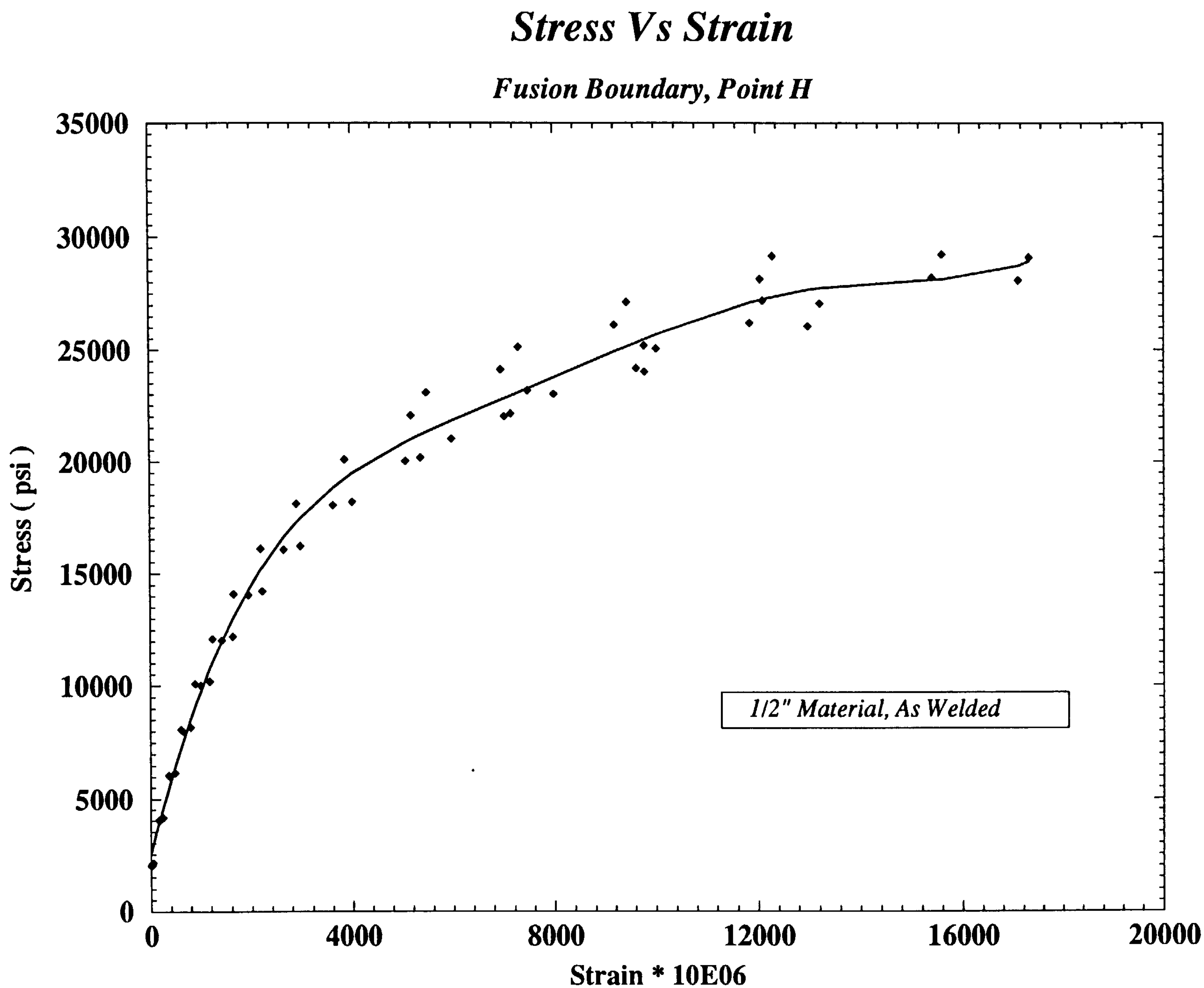

Figure D8. Material Behavior, Point H

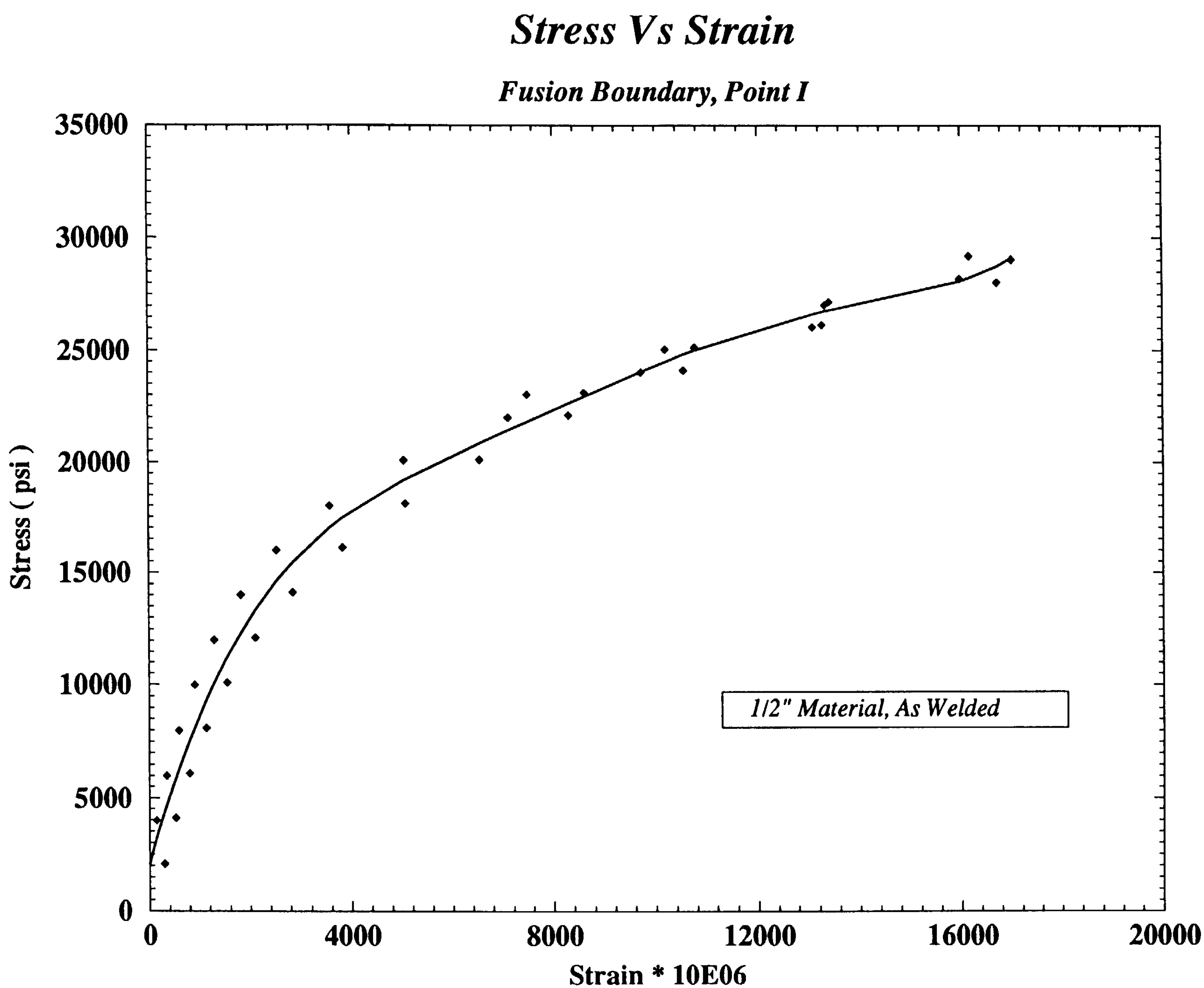

Figure D9. Material Behavior, Point I

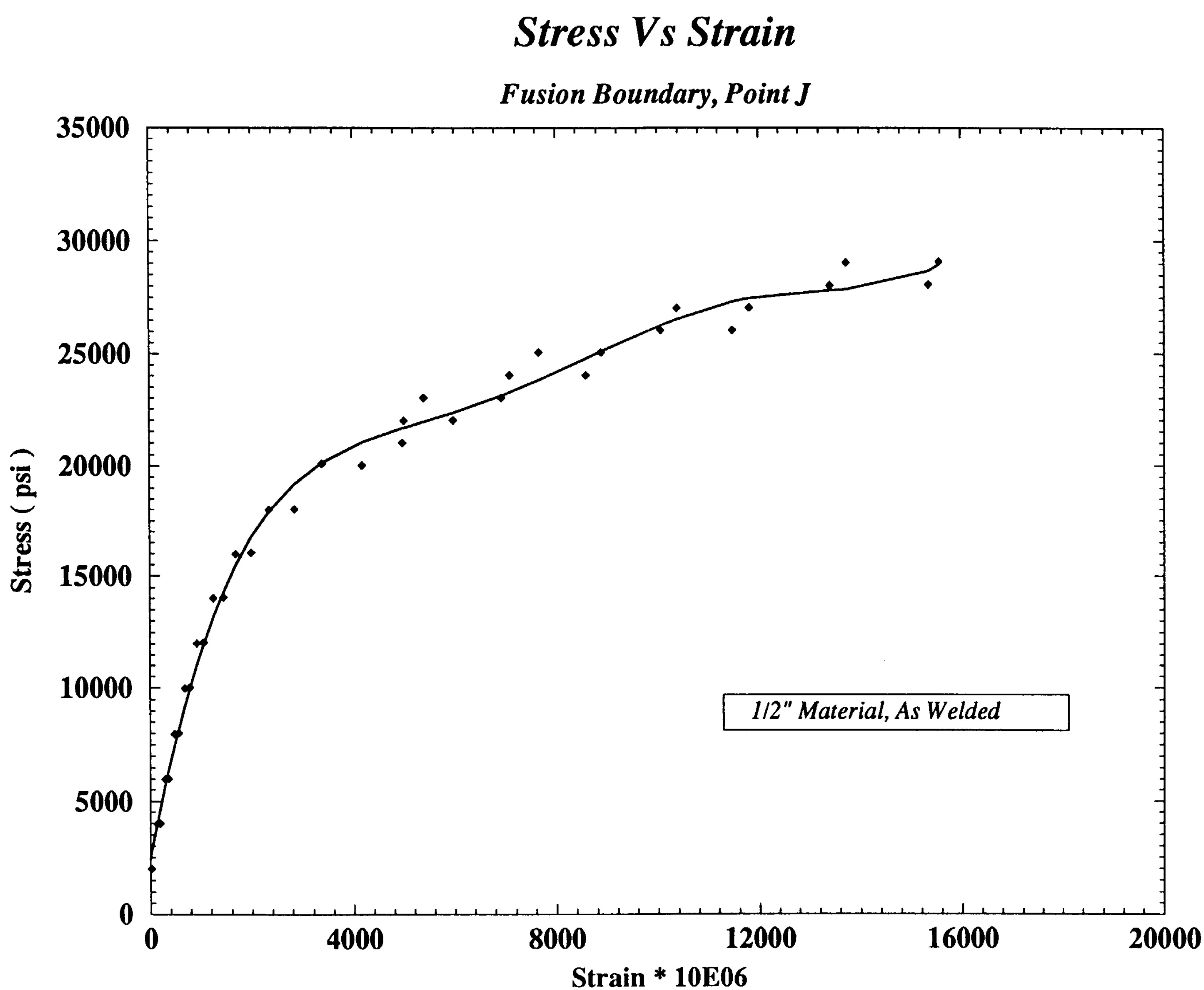

Figure D10. Material Behavior, Point J

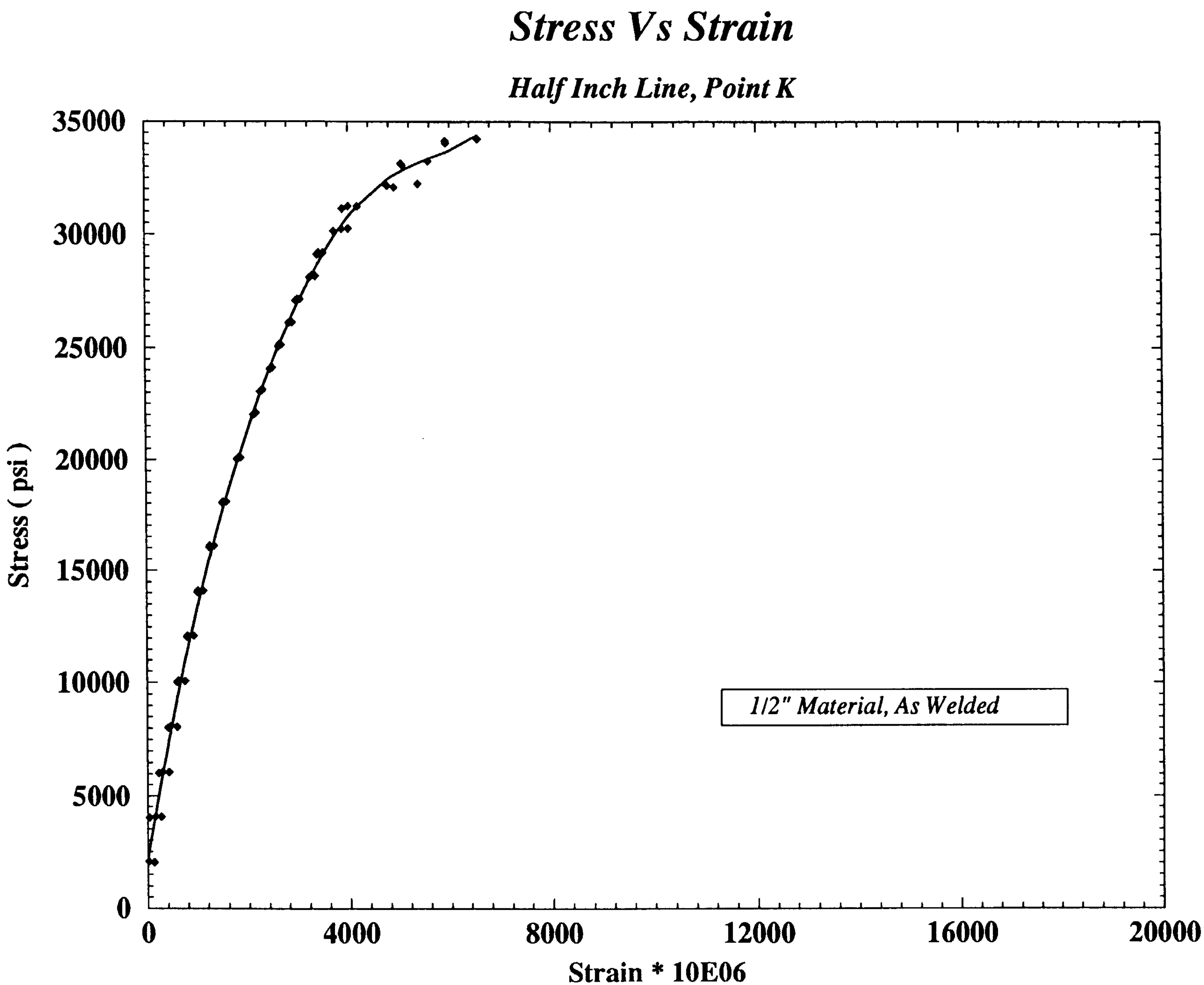

Figure D11. Material Behavior, Point K

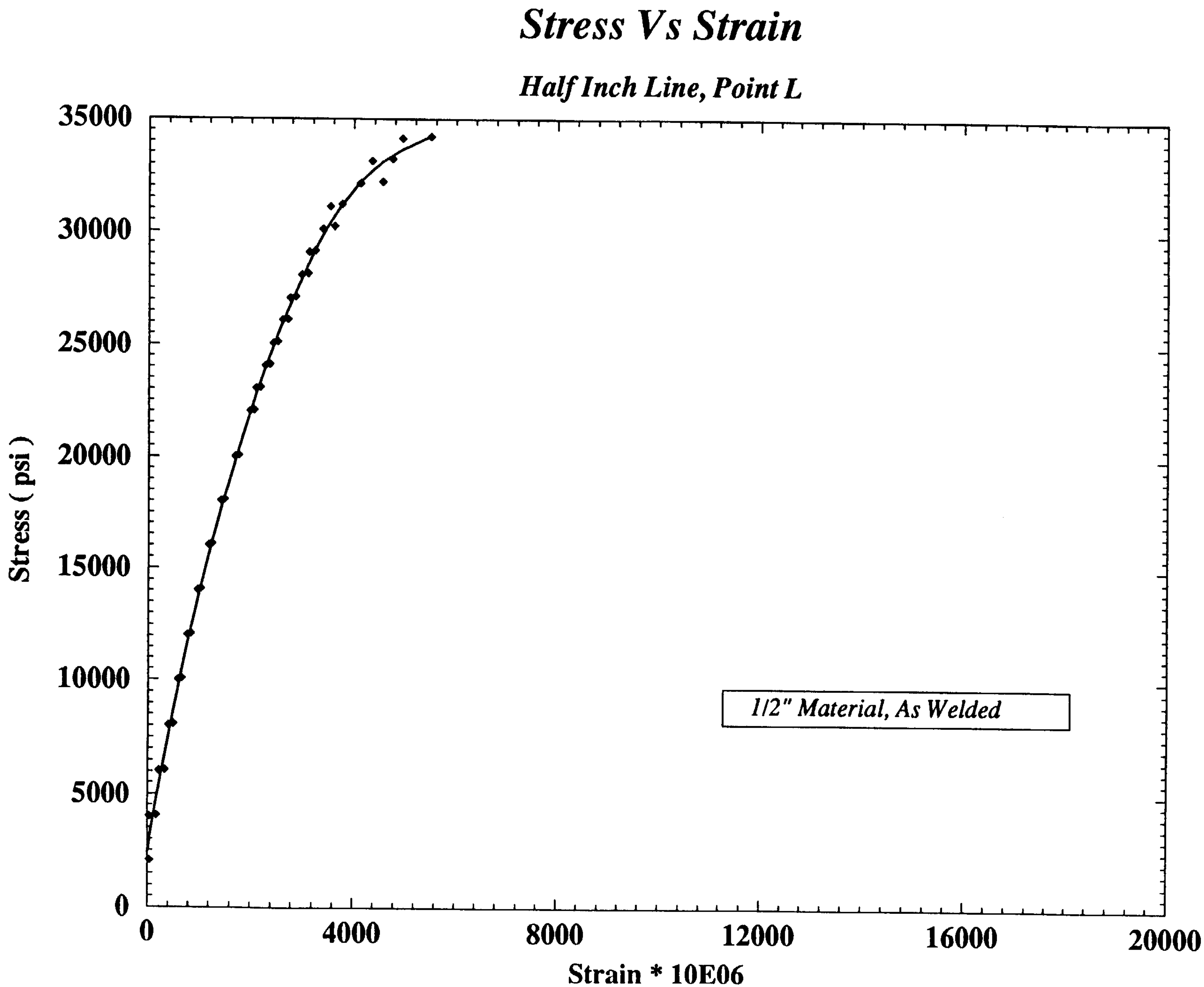

Figure D12. Material Behavior, Point L

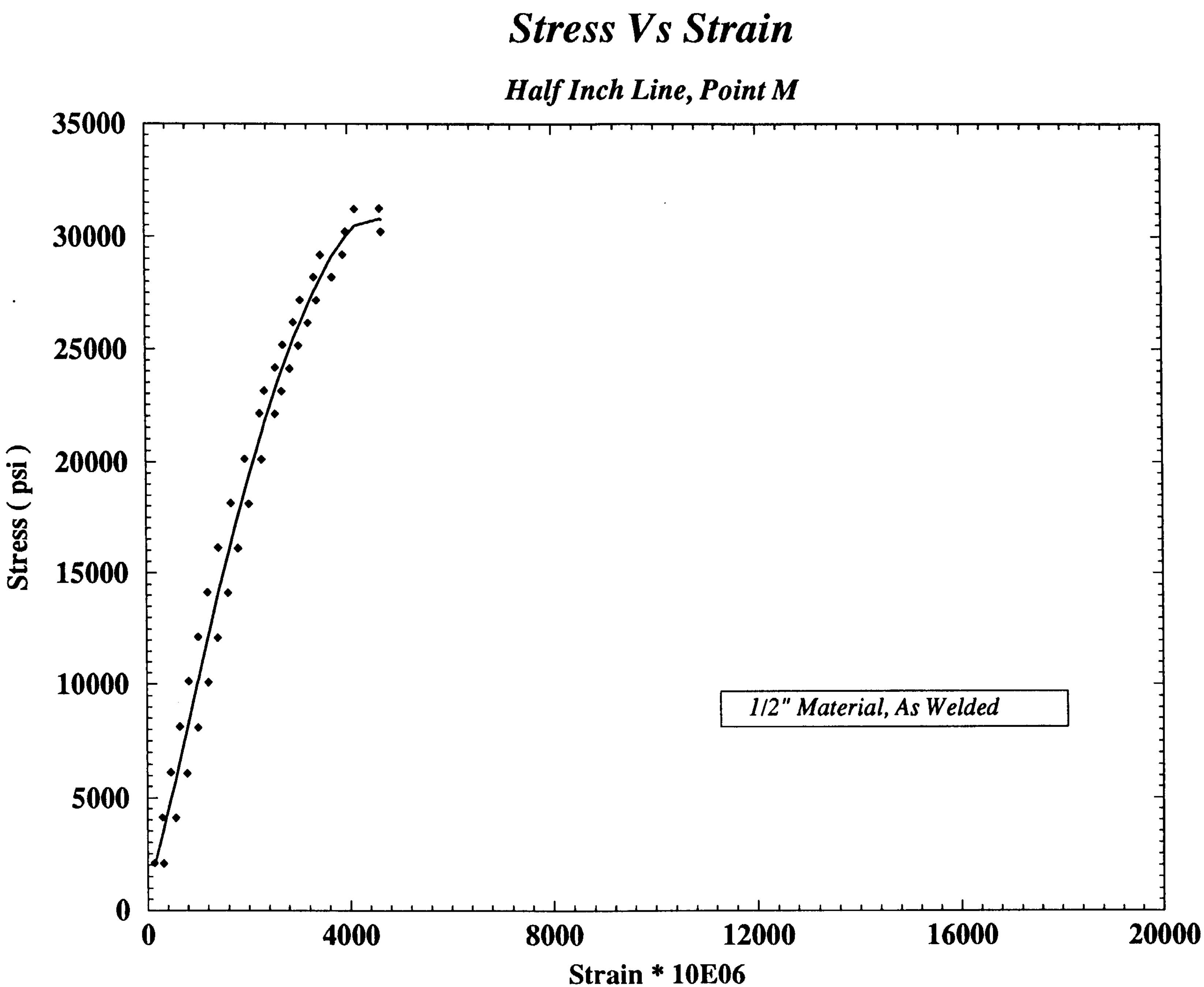

Figure D13. Material Behavior, Point M

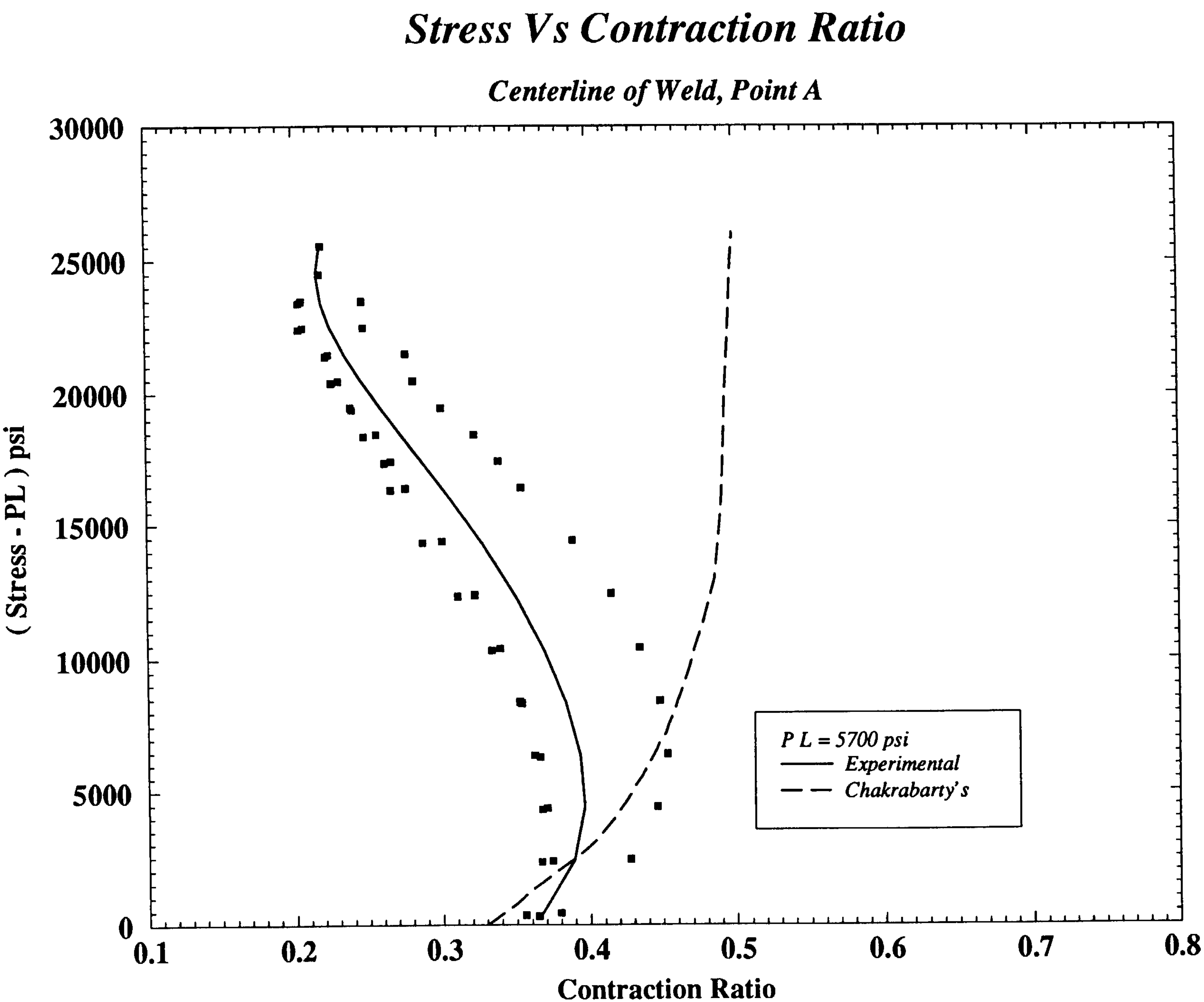

Figure D14. In-Plane Contraction Ratios, Point A

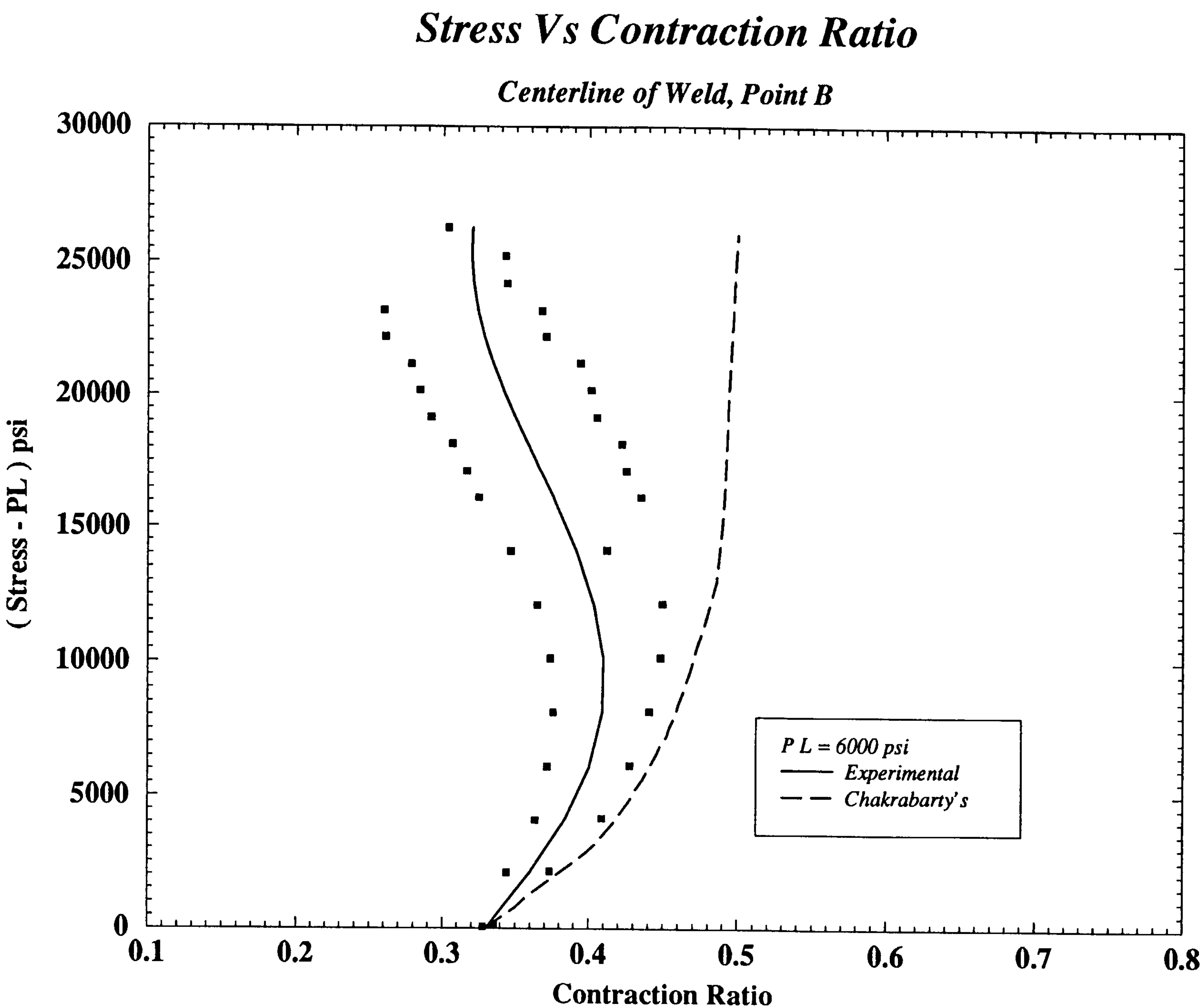

Figure D15. In-Plane Contraction Ratios, Point B

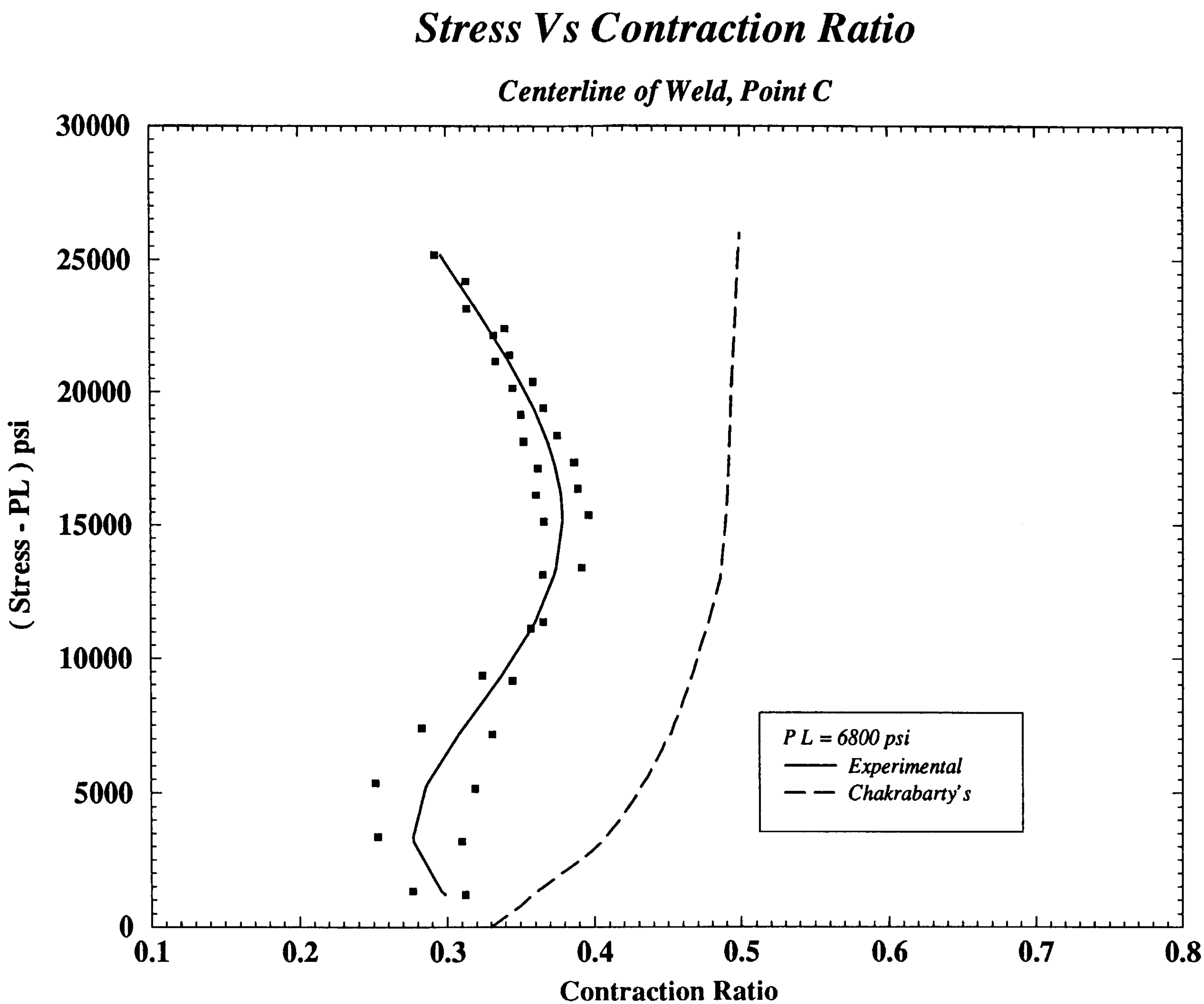

Figure D16. In-Plane Contraction Ratios, Point C

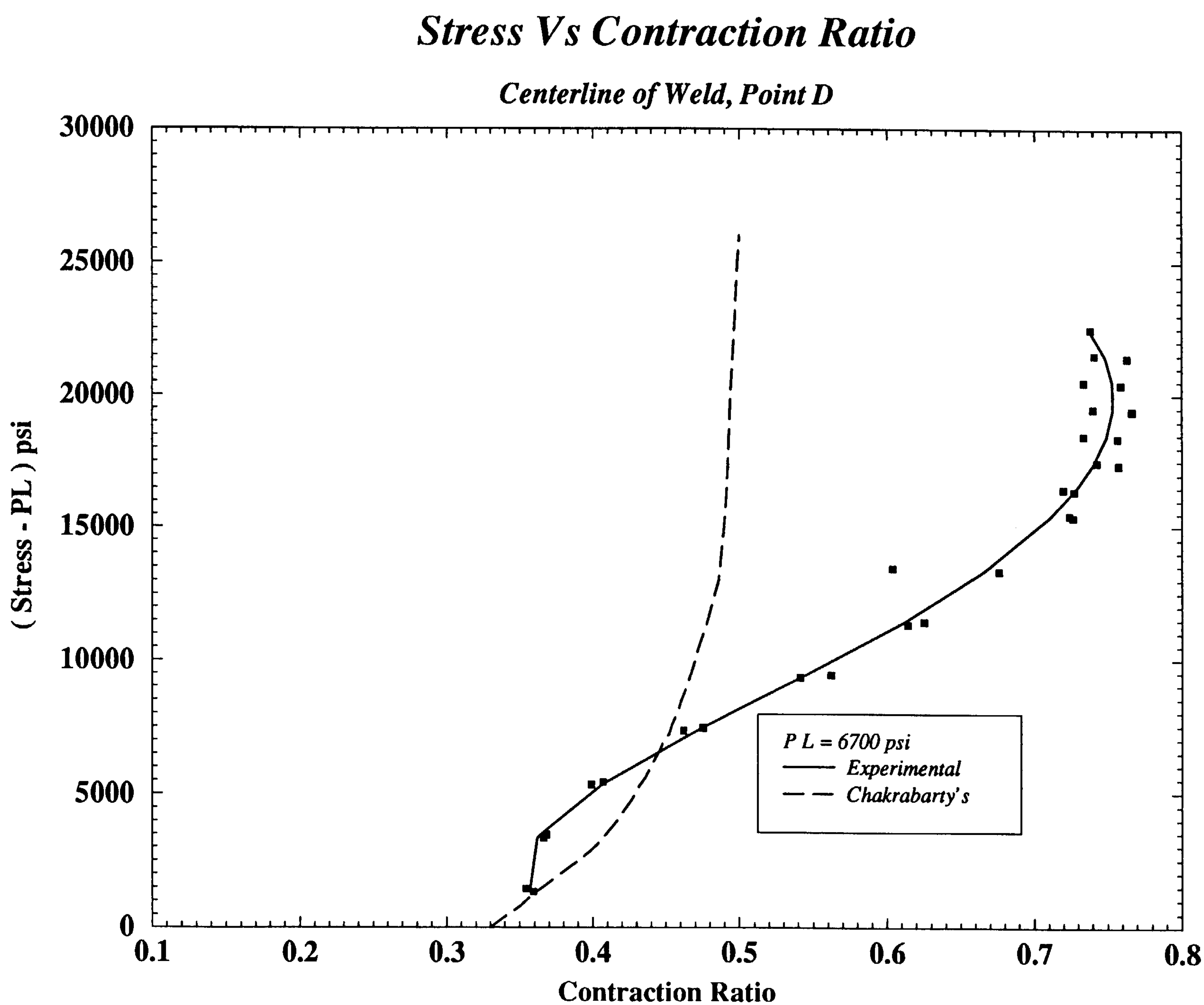

Figure D17. In-Plane Contraction Ratios, Point D

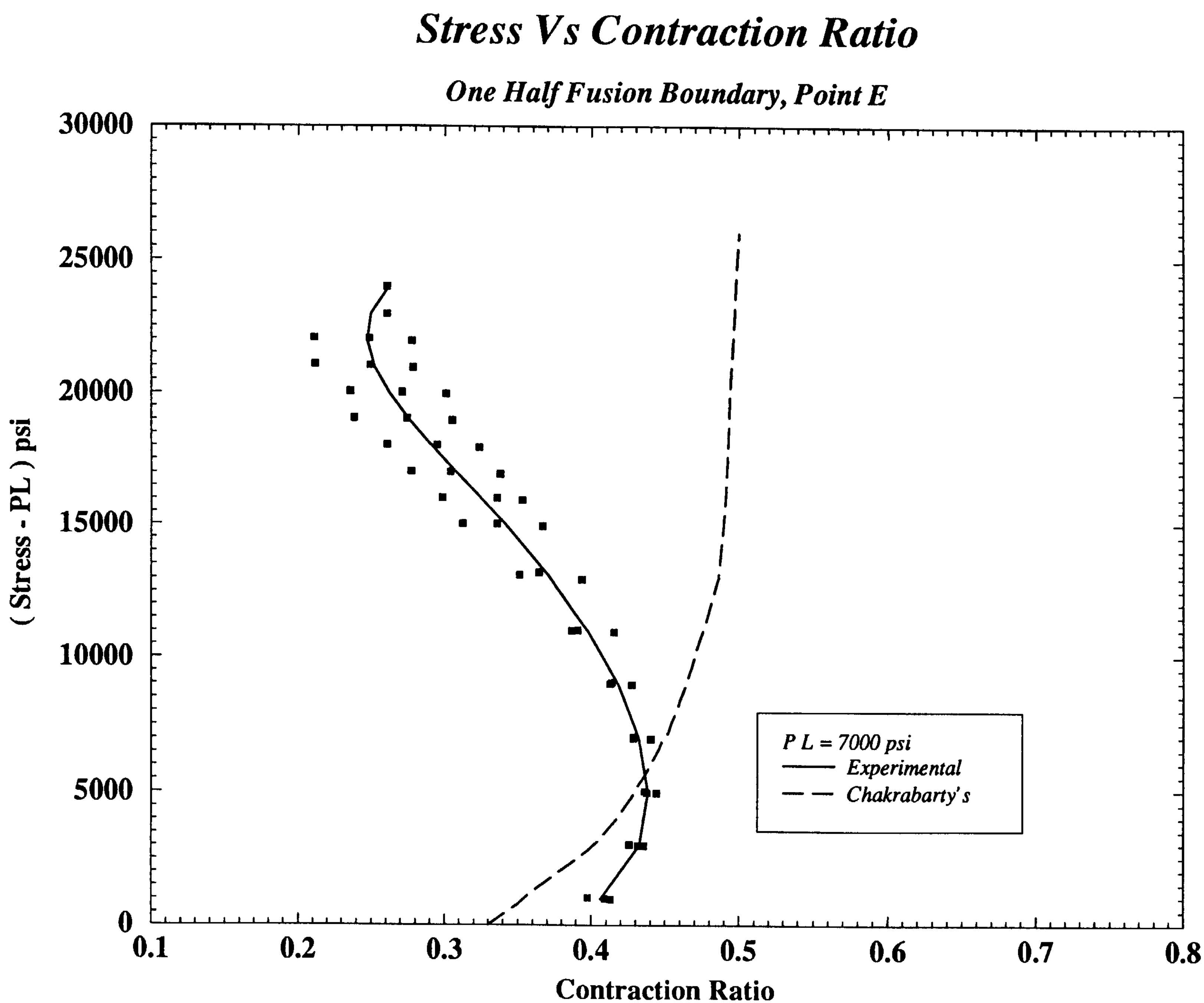

Figure D18. In-Plane Contraction Ratios, Point E

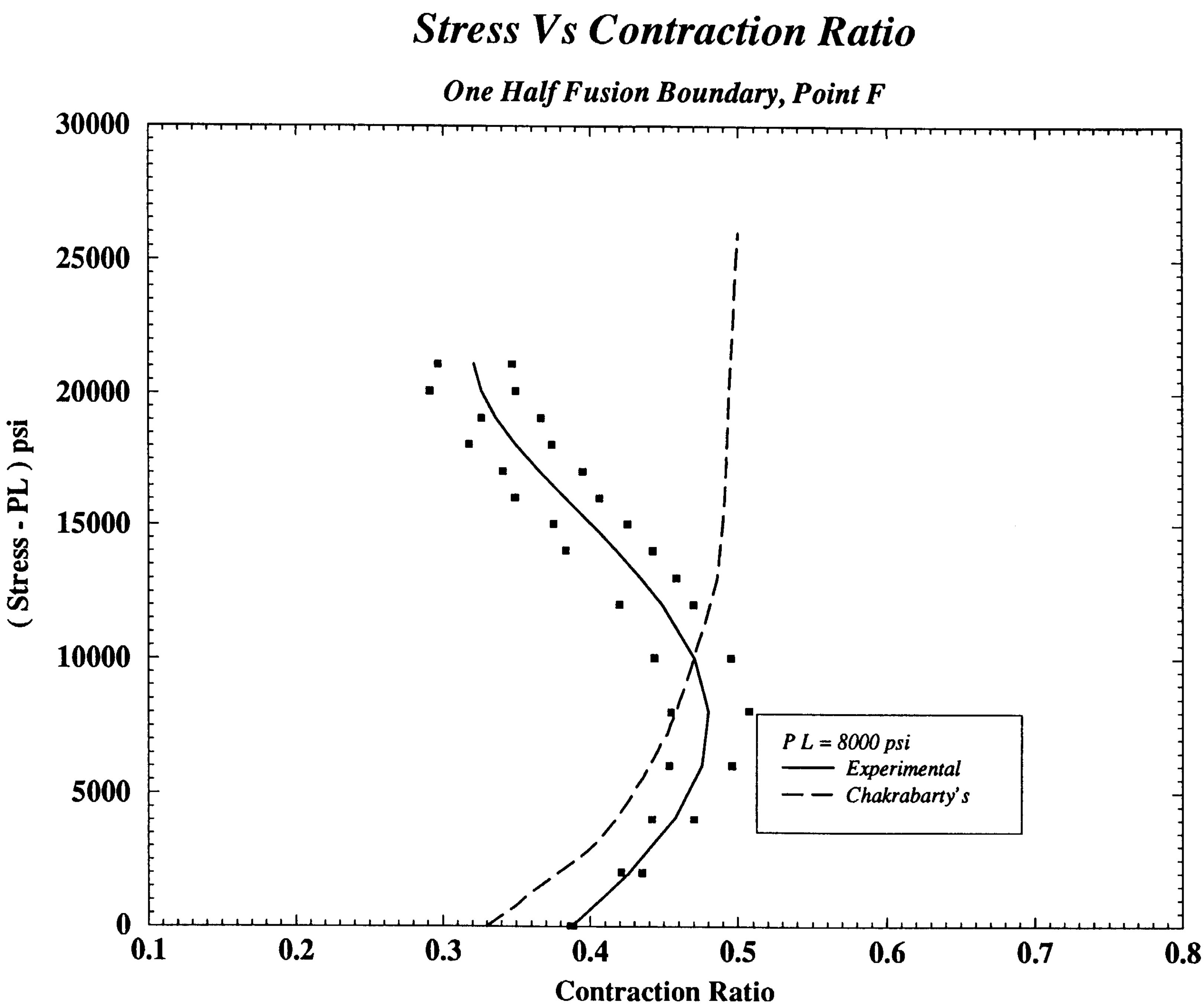

Figure D19. In-Plane Contraction Ratios, Point F

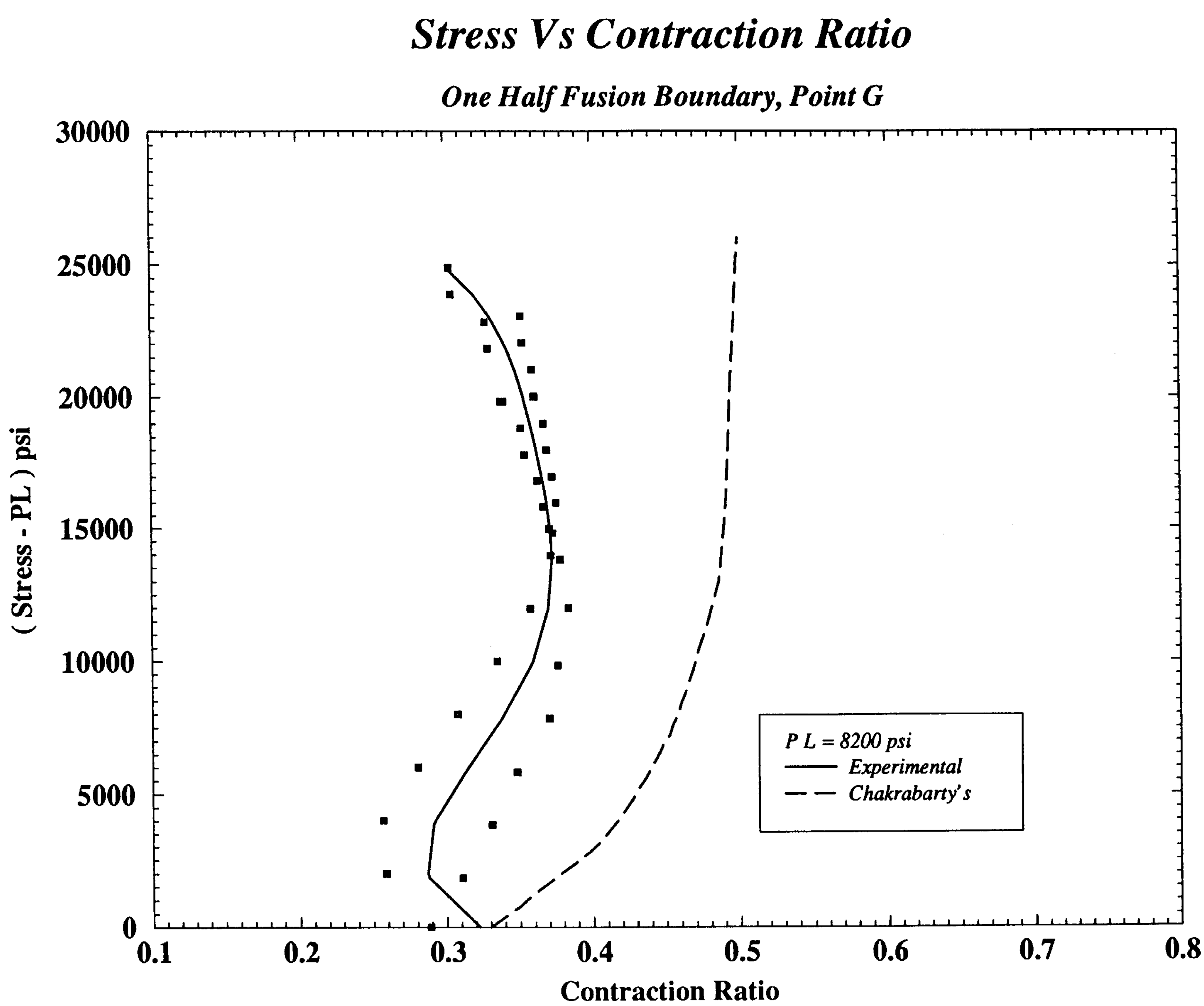

Figure D20. In-Plane Contraction Ratios, Point G

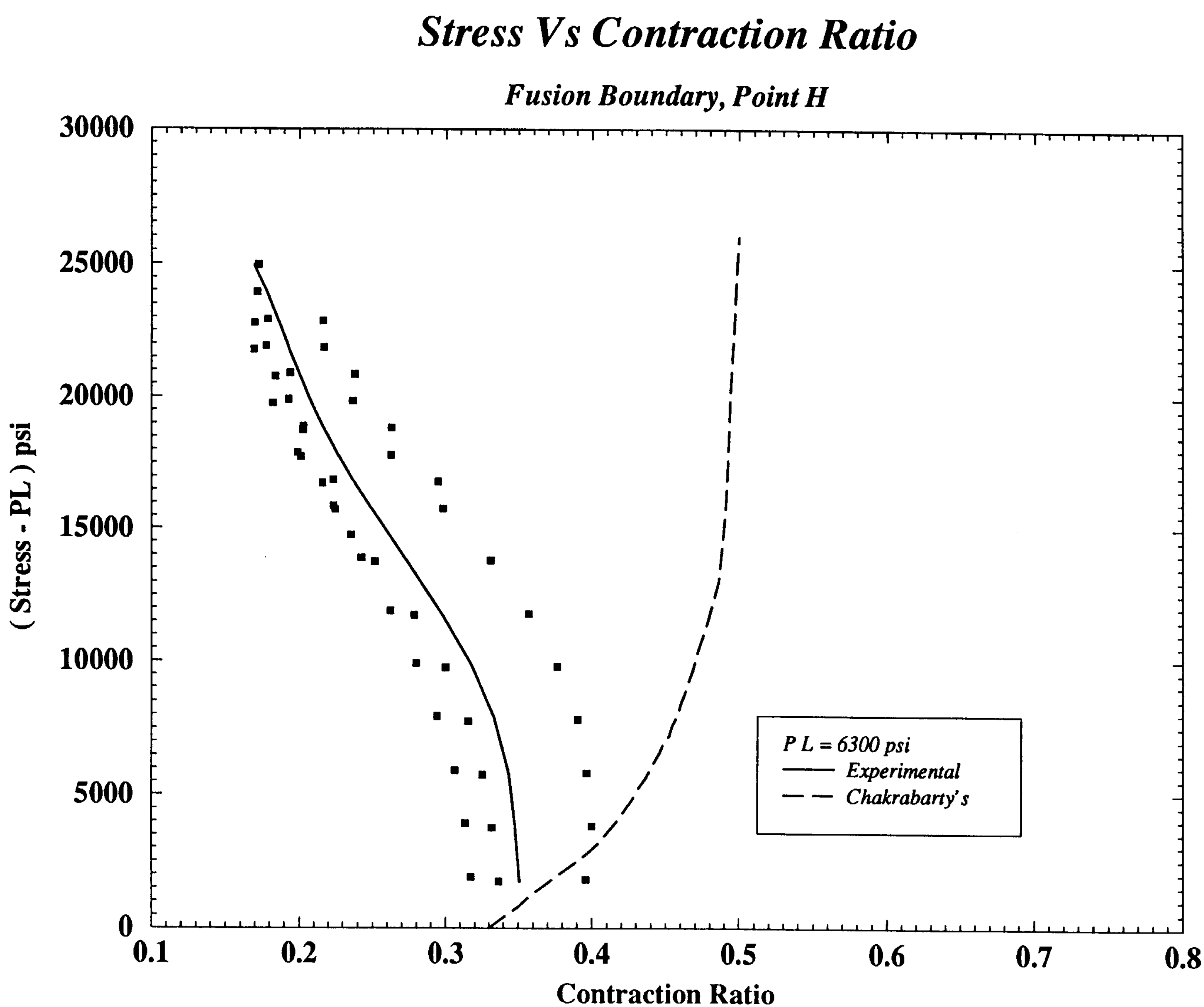

Figure D21. In-Plane Contraction Ratios, Point H

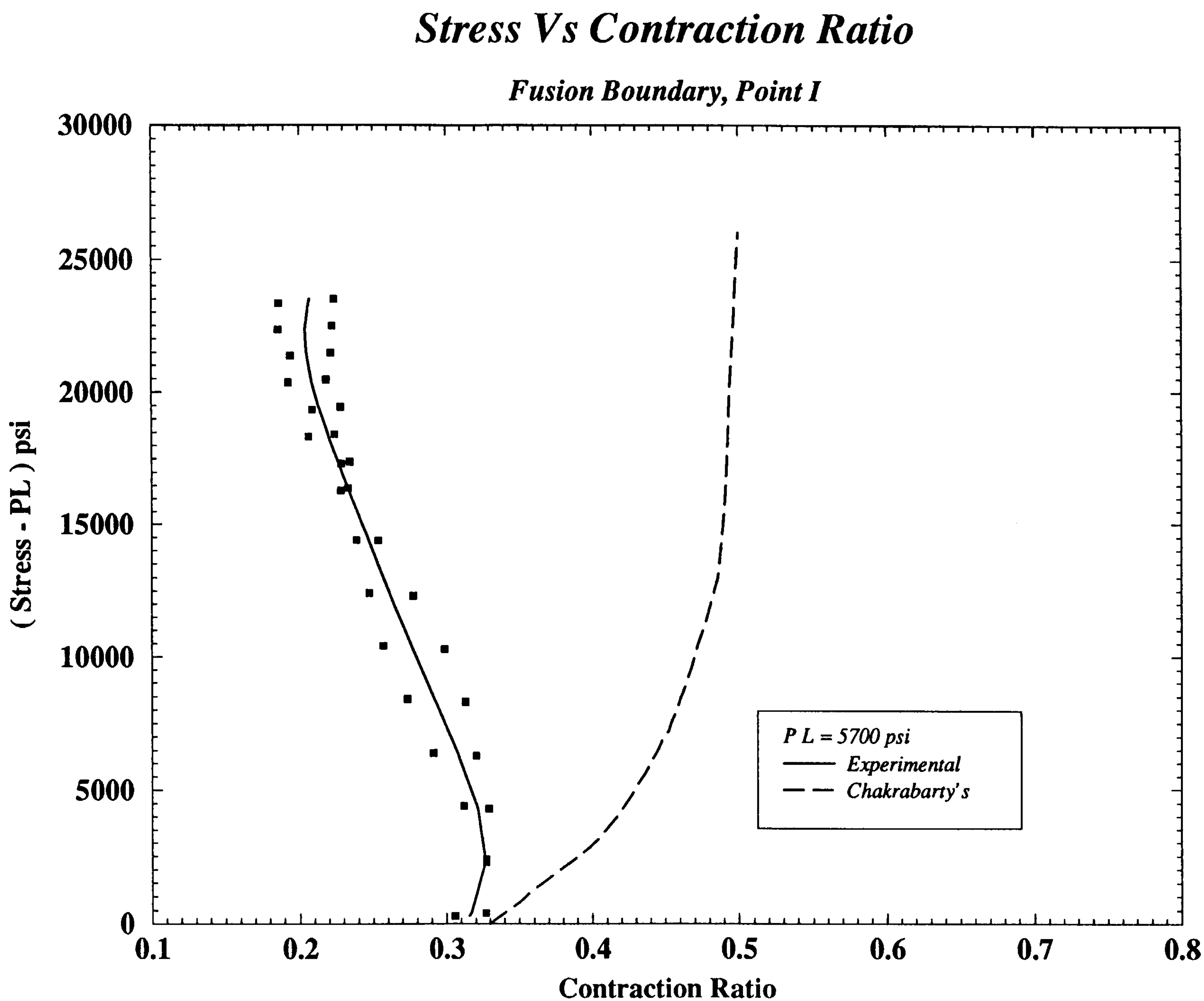

Figure D22. In-Plane Contraction Ratios, Point I

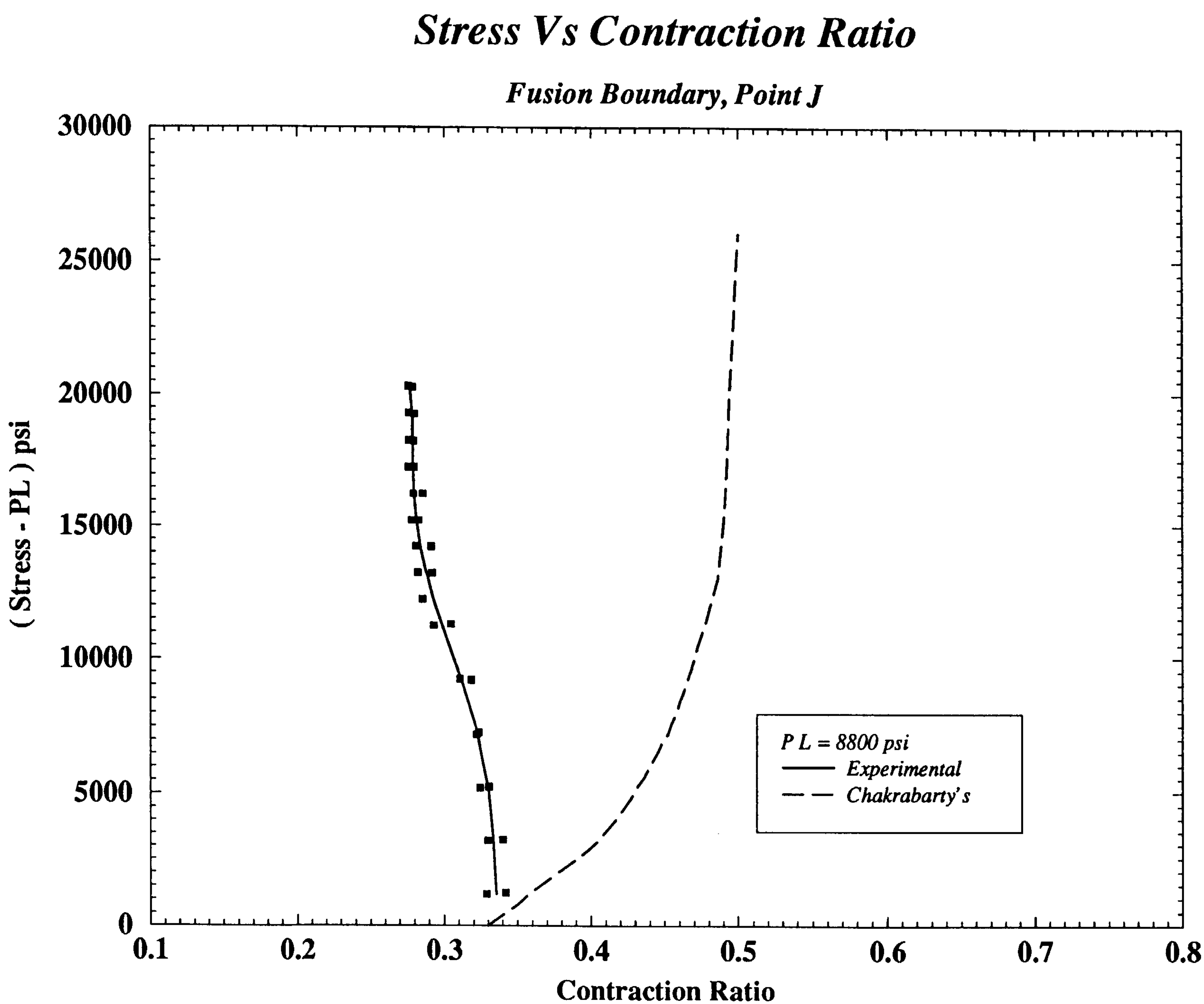

Figure D23. In-Plane Contraction Ratios, Point J

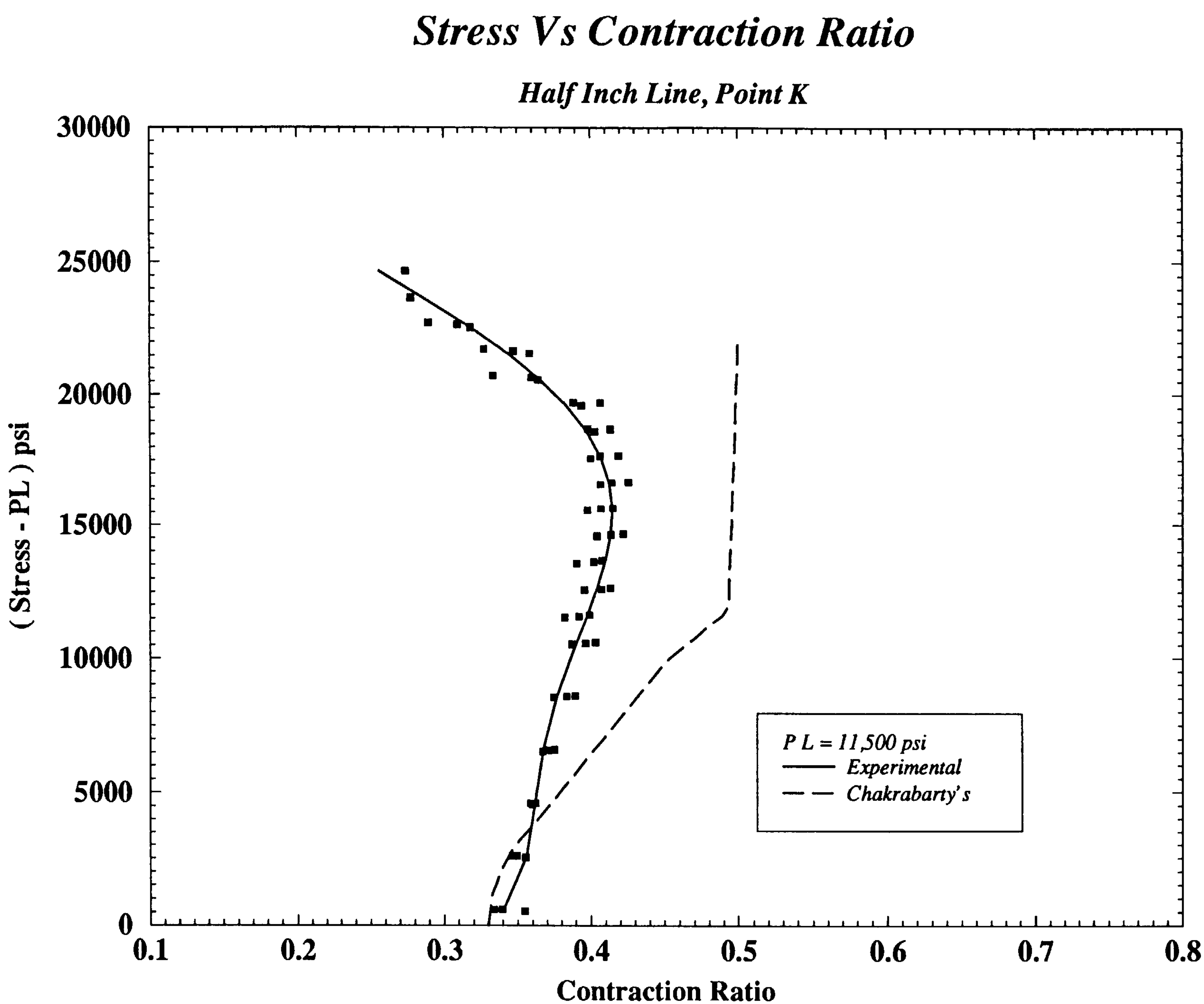

Figure D24. In-Plane Contraction Ratios, Point K

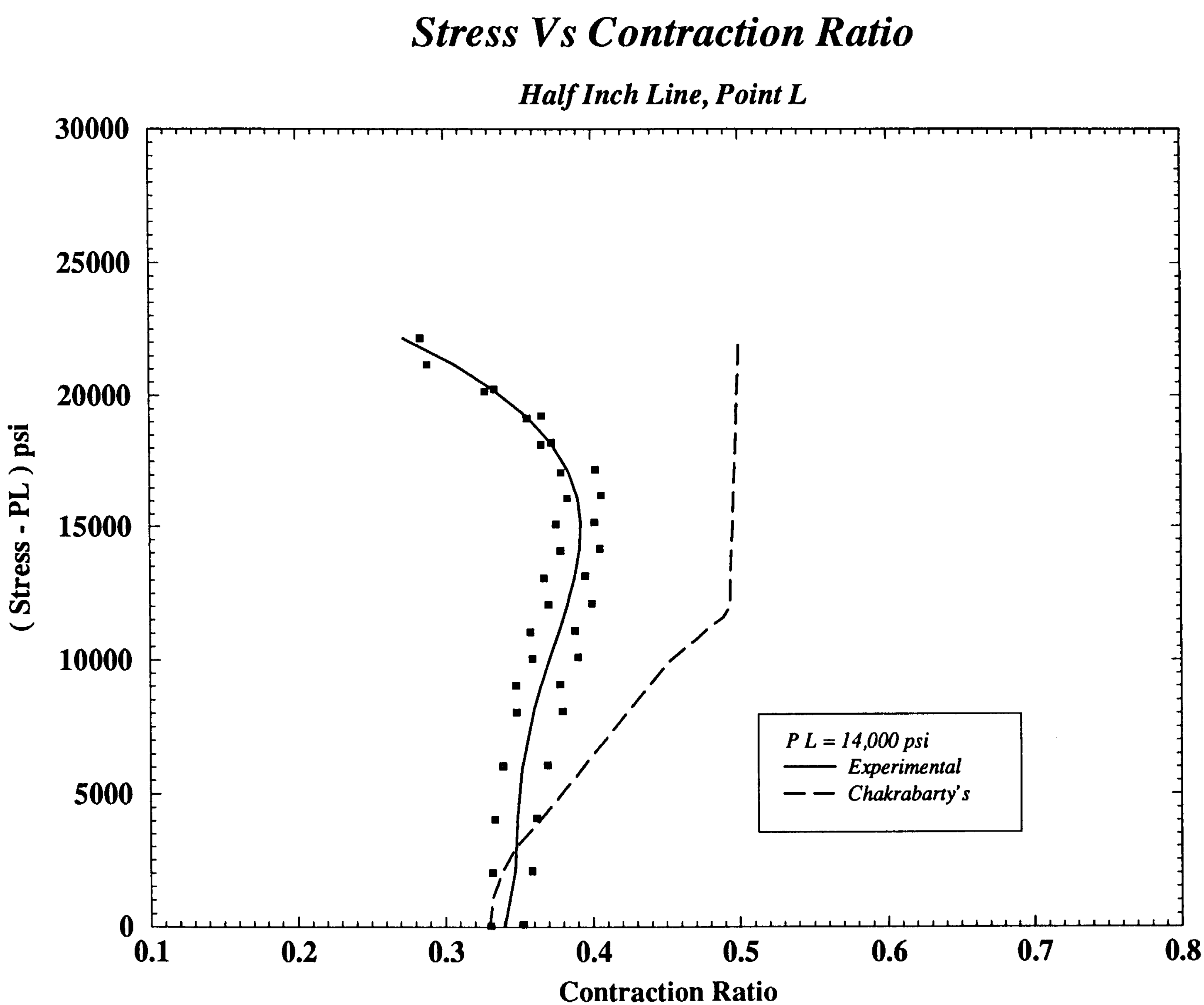

Figure D25. In-Plane Contraction Ratios, Point L

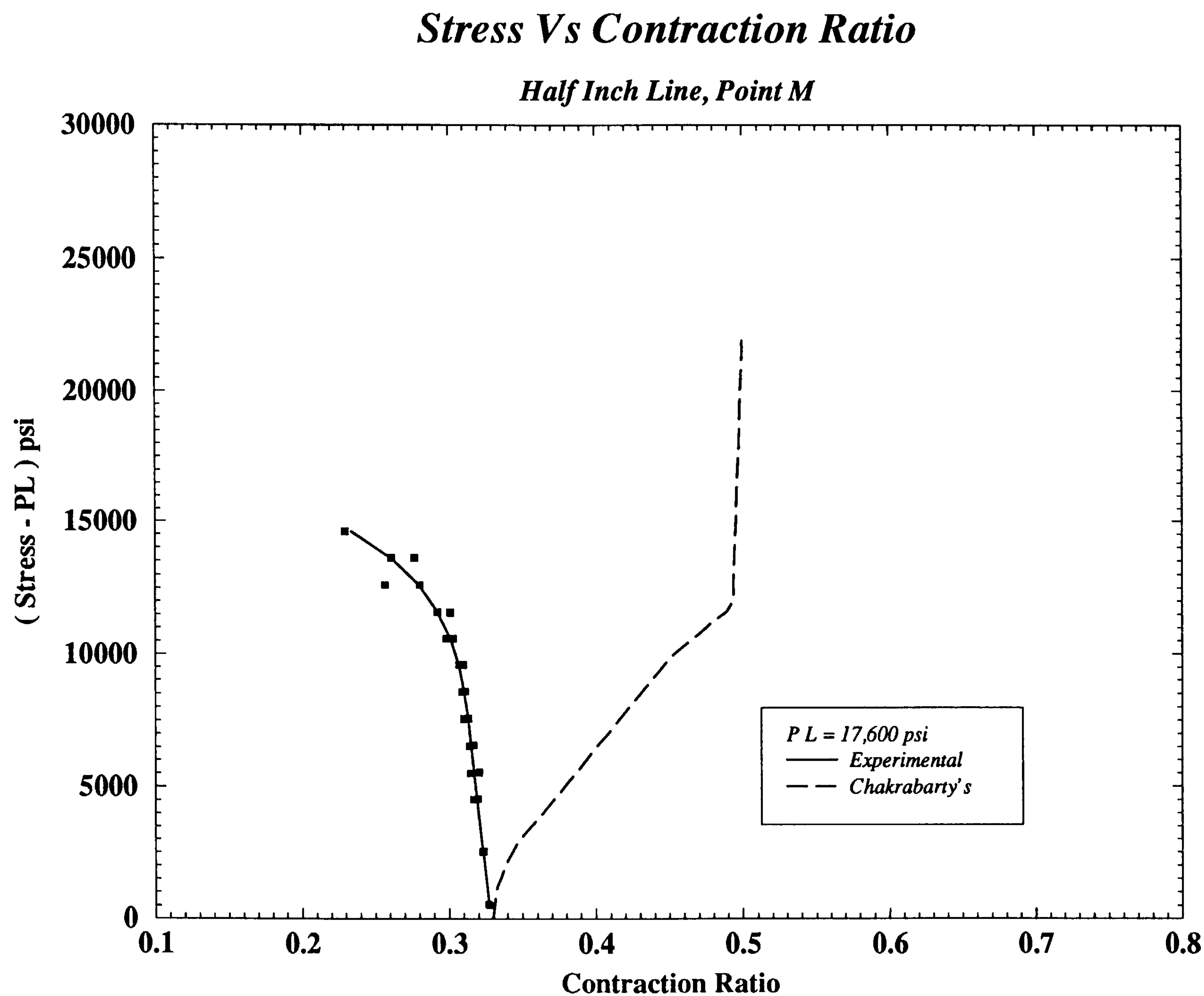

Figure D26. In-Plane Contraction Ratios, Point M

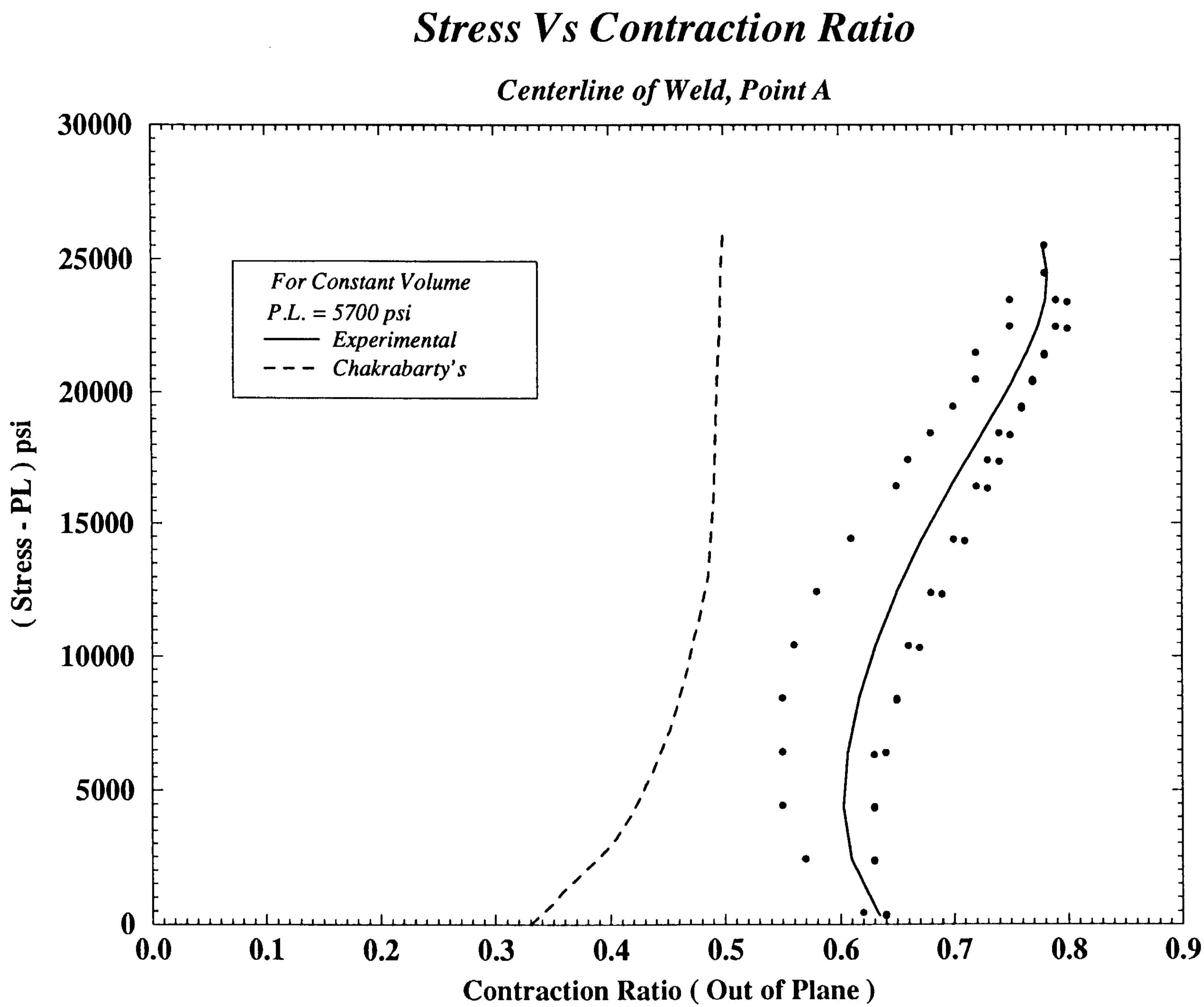

Figure D27. Out-of-Plane Contraction Ratios, Point A

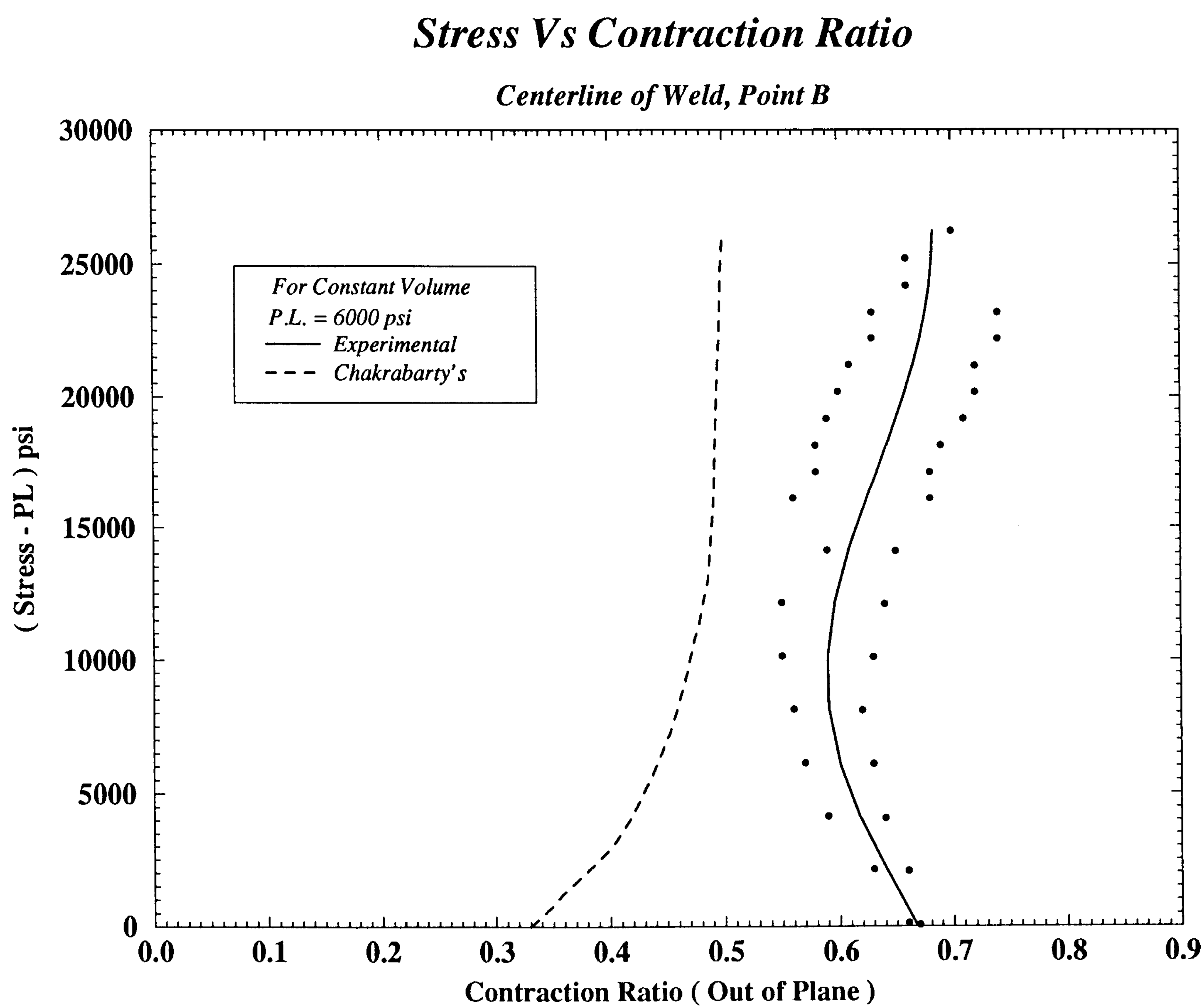

Figure D28. Out-of-Plane Contraction Ratios, Point B

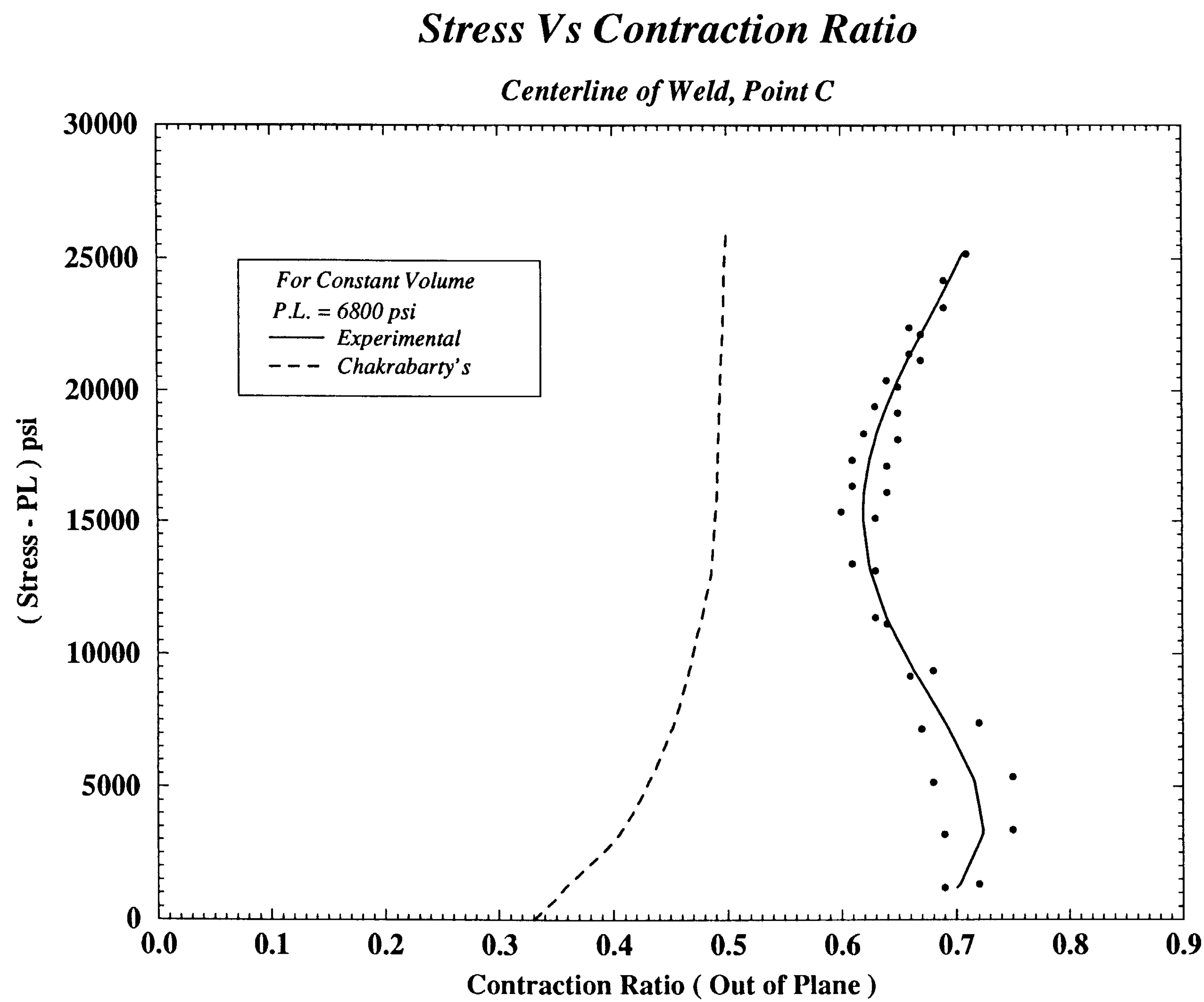

Figure D29. Out-of-Plane Contraction Ratios, Point C

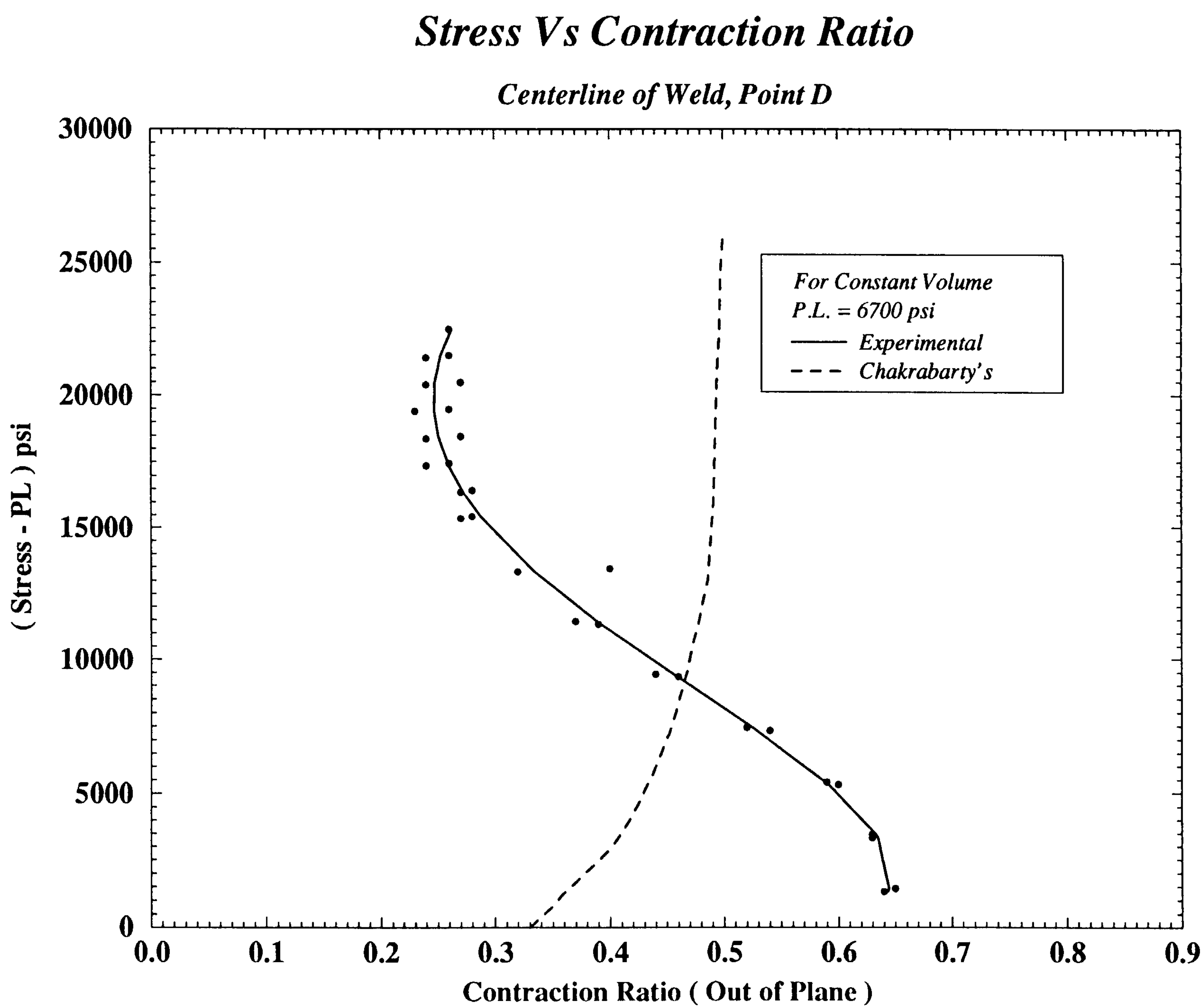

Figure D30. Out-of-Plane Contraction Ratios, Point D

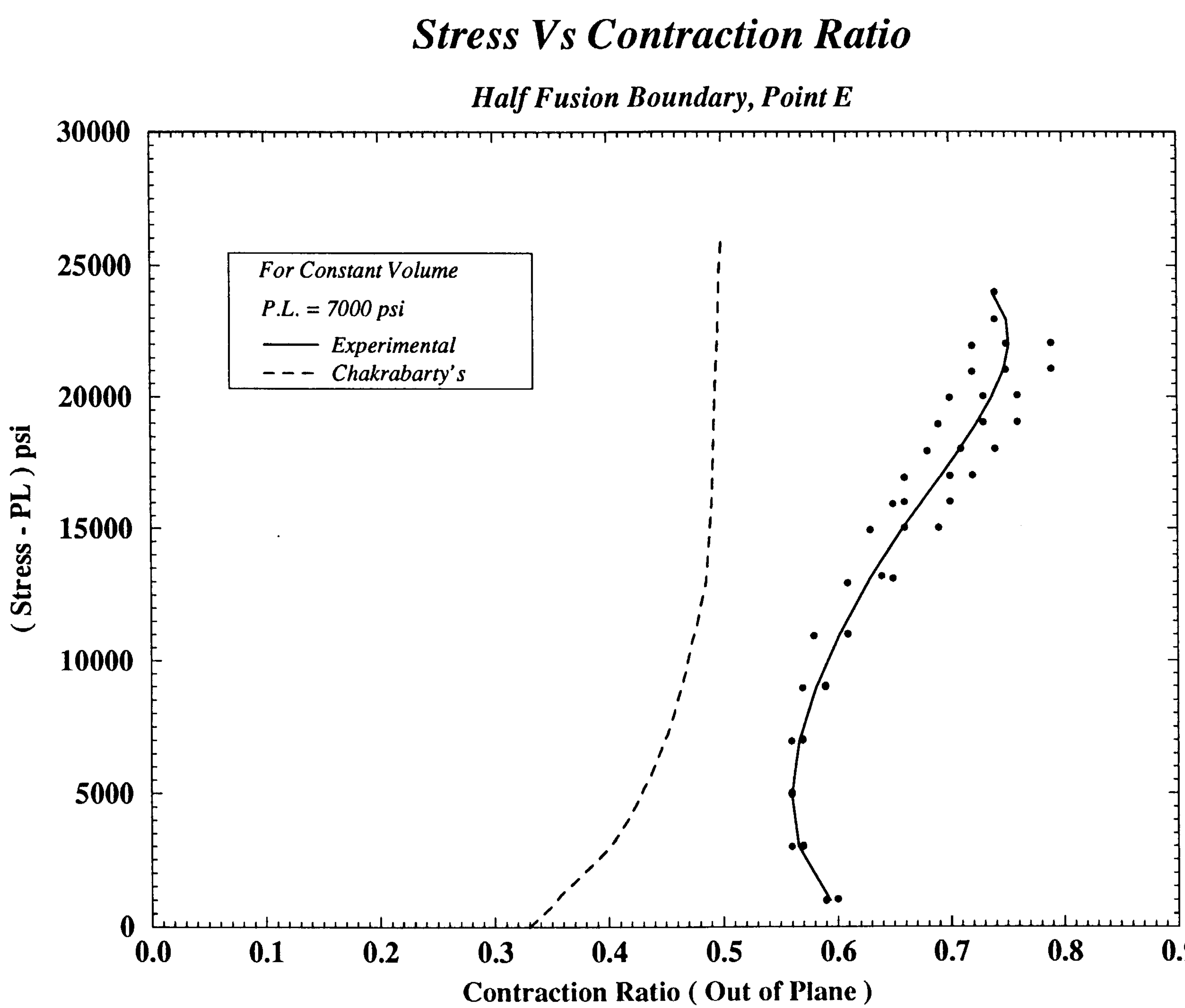

Figure D31. Out-of-Plane Contraction Ratios, Point E

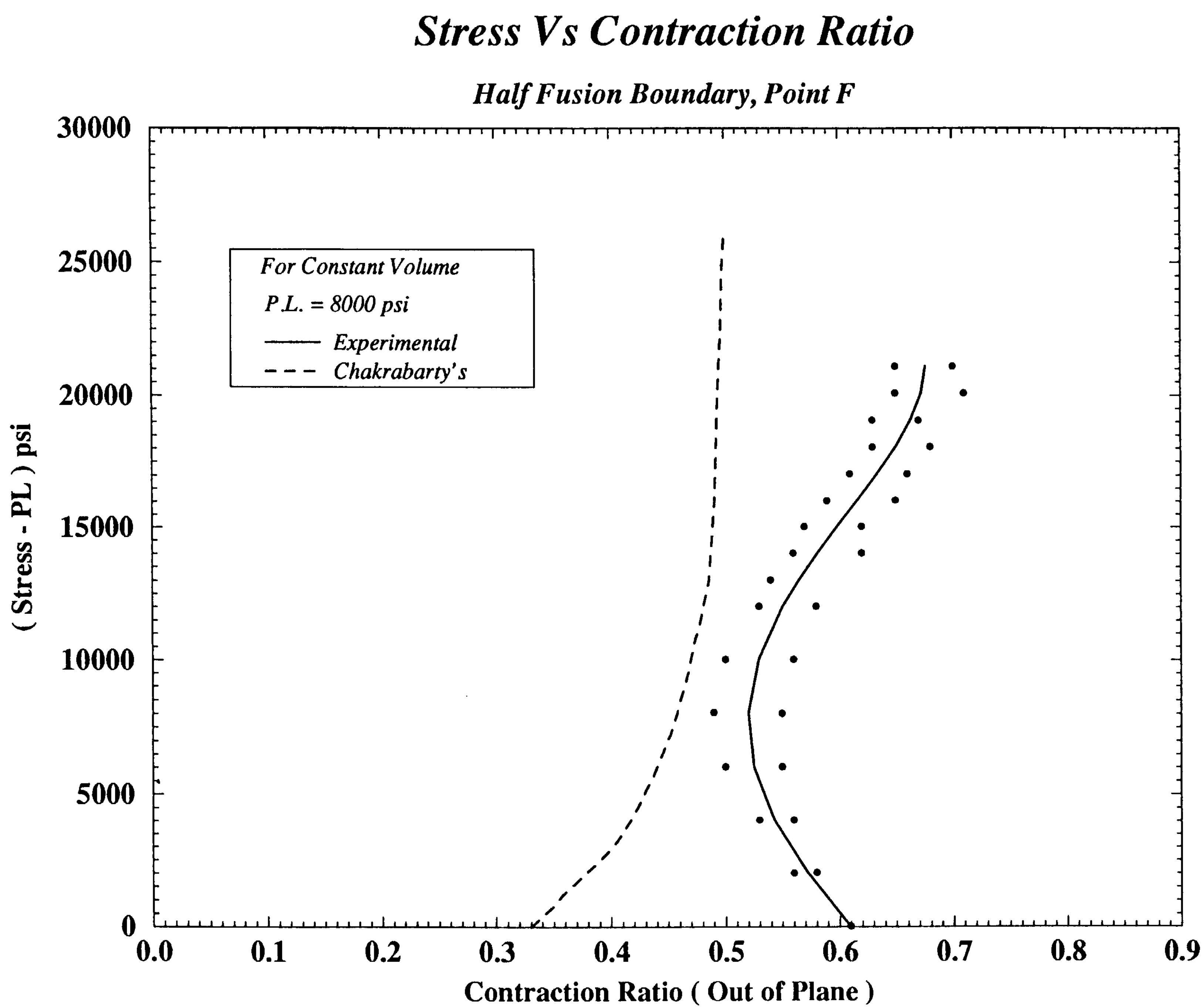

Figure D32. Out-of-Plane Contraction Ratios, Point F

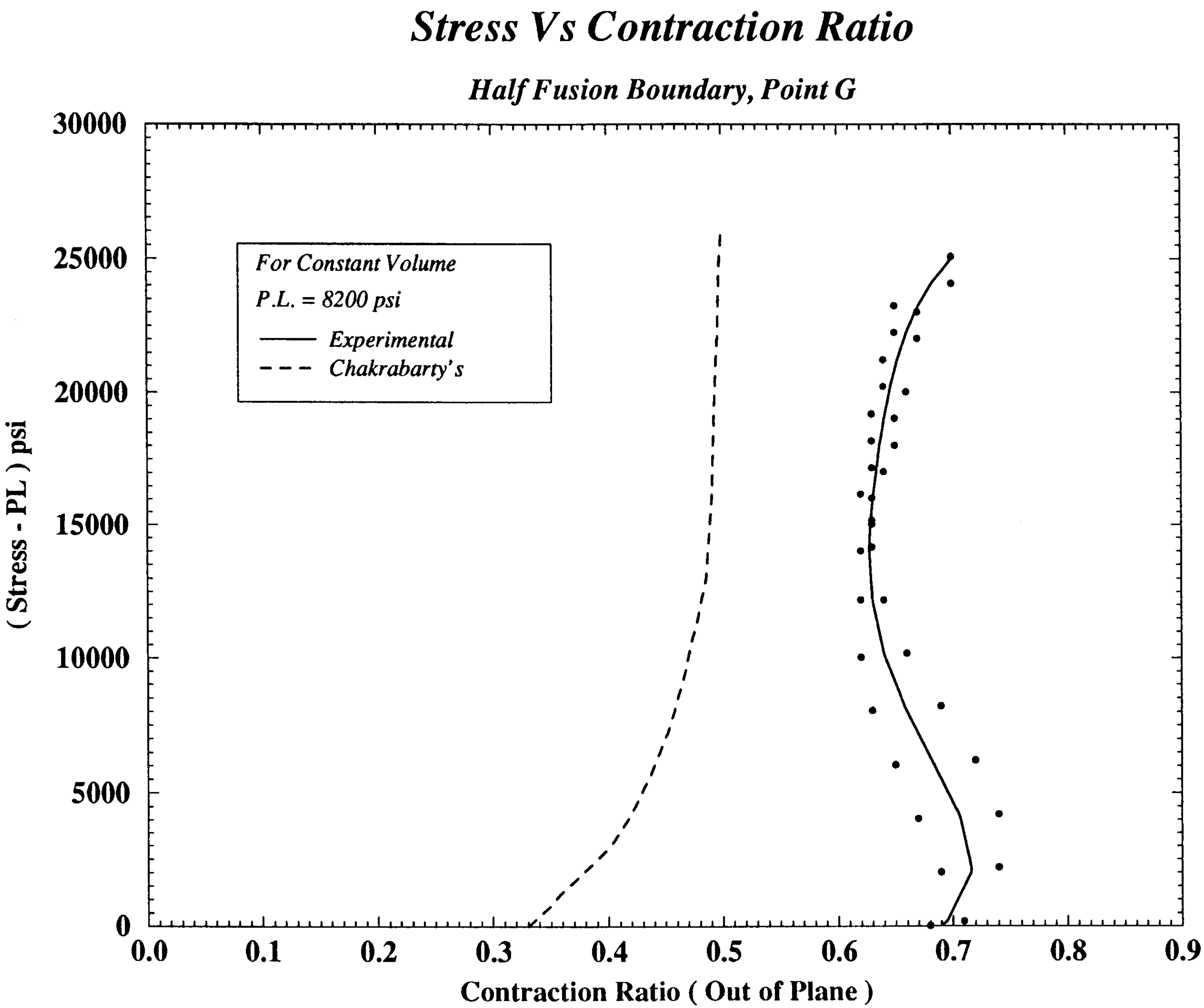

Figure D33. Out-of-Plane Contraction Ratios, Point G

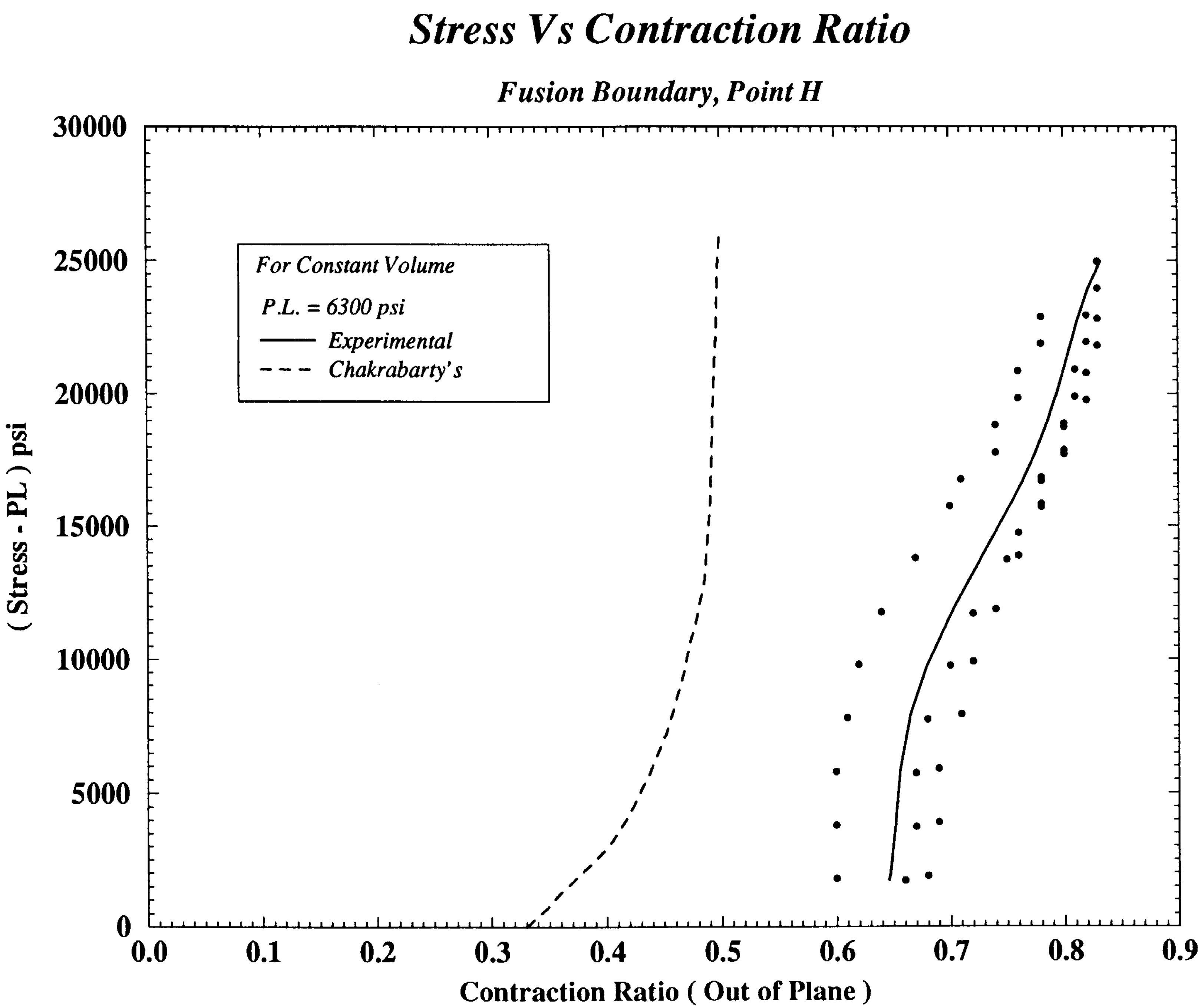

Figure D34. Out-of-Plane Contraction Ratios, Point H

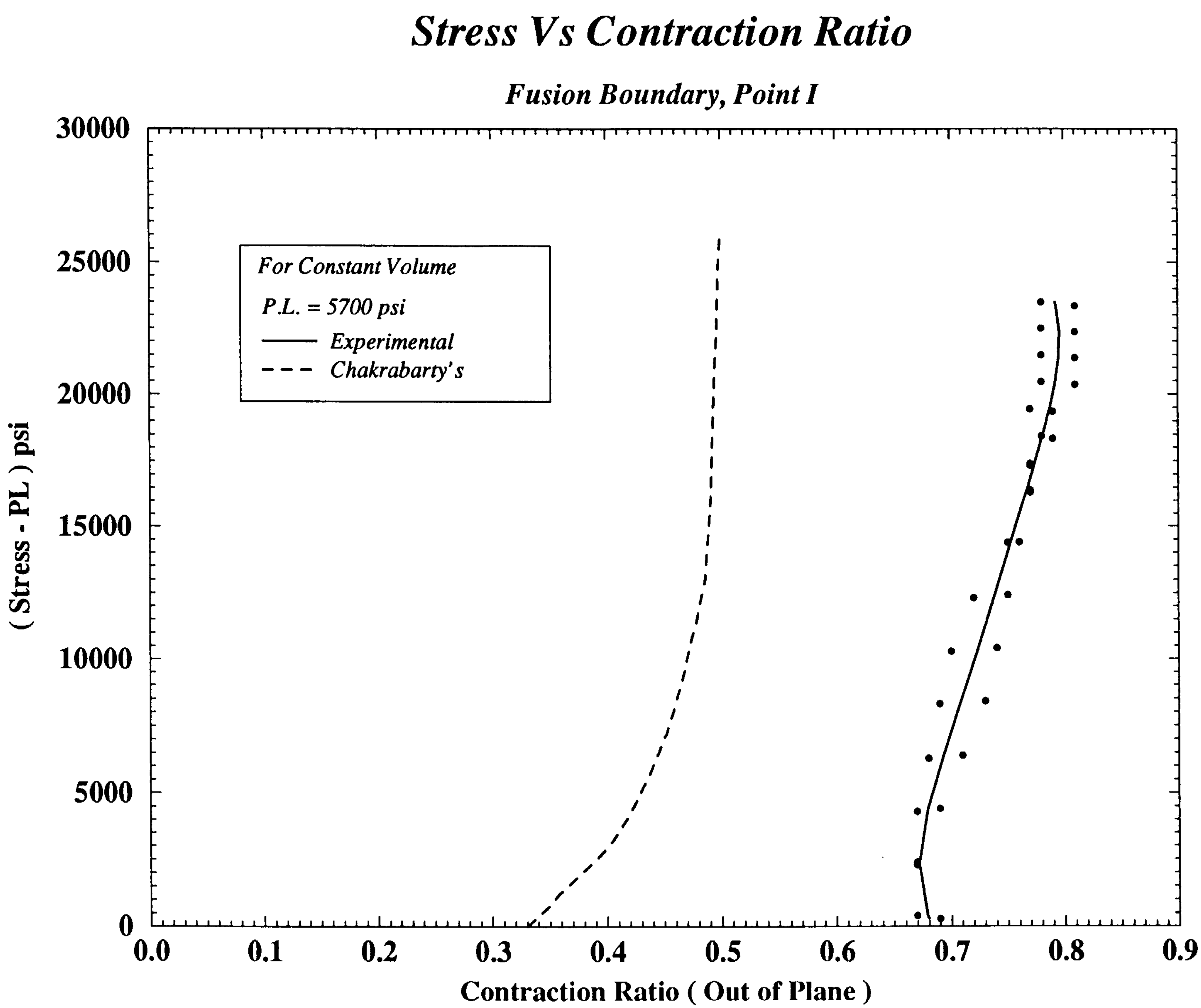

Figure D35. Out-of-Plane Contraction Ratios, Point I

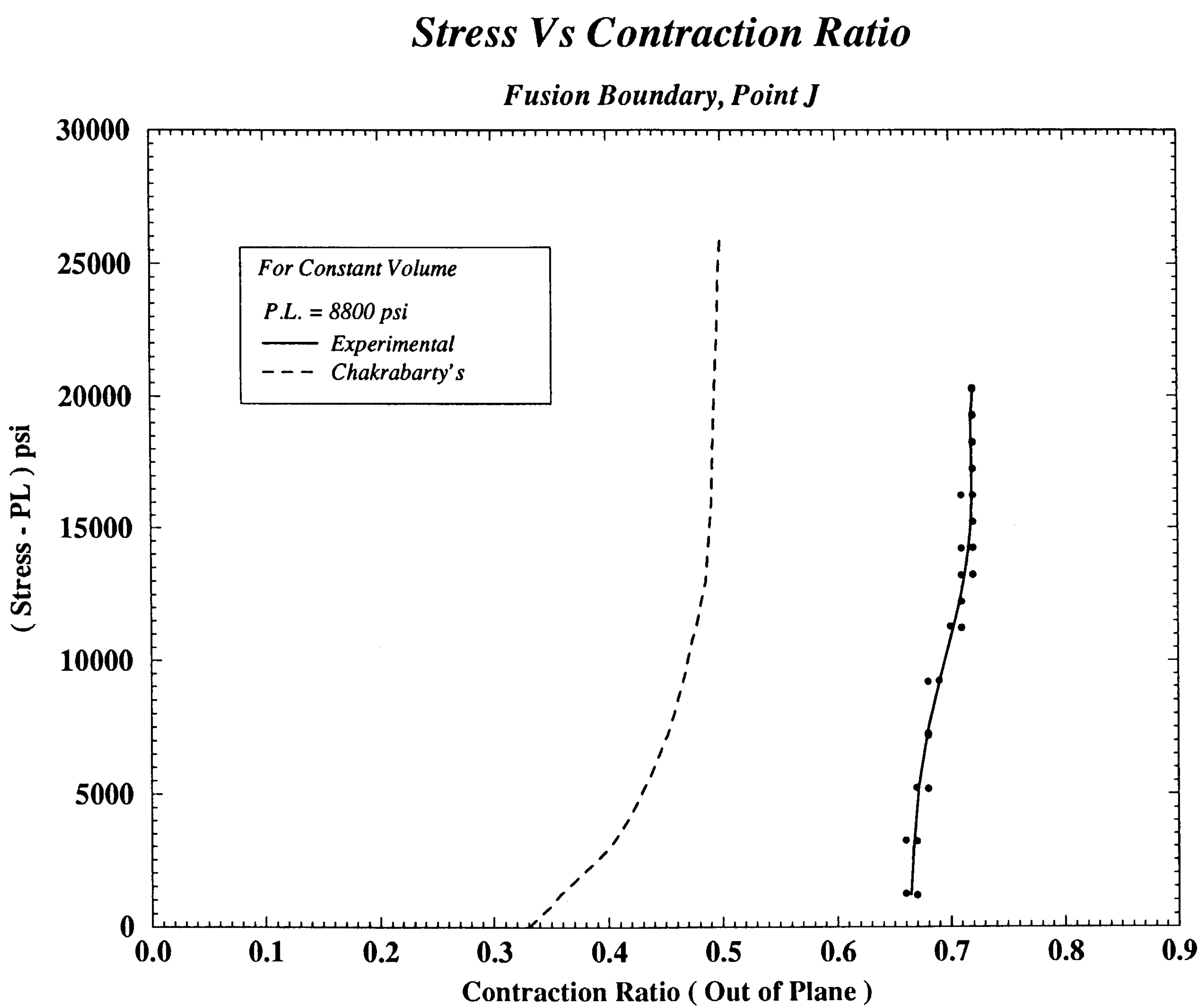

Figure D36. Out-of-Plane Contraction Ratios, Point J

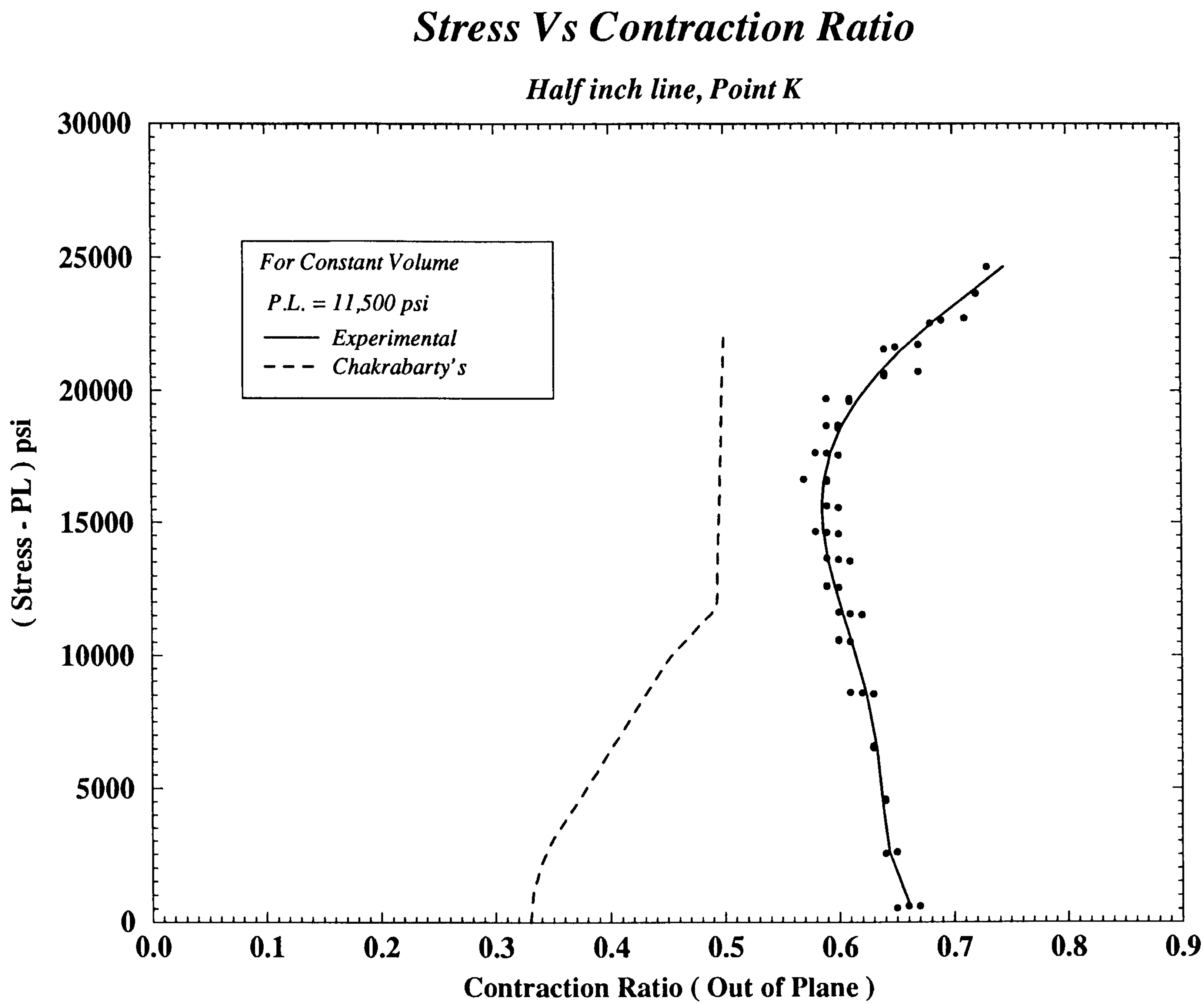

Figure D37. Out-of-Plane Contraction Ratios, Point K

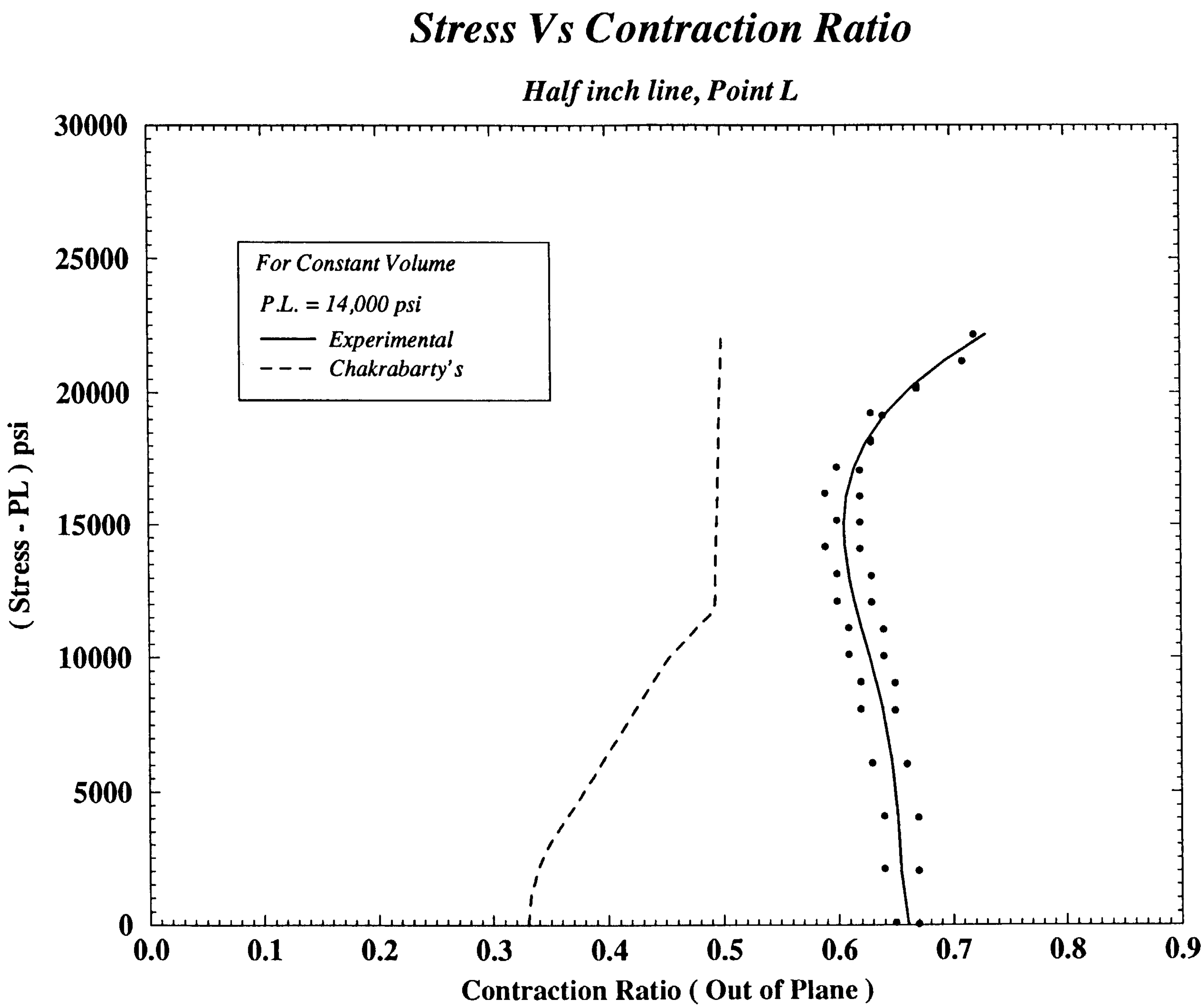

Figure D38. Out-of-Plane Contraction Ratios, Point L

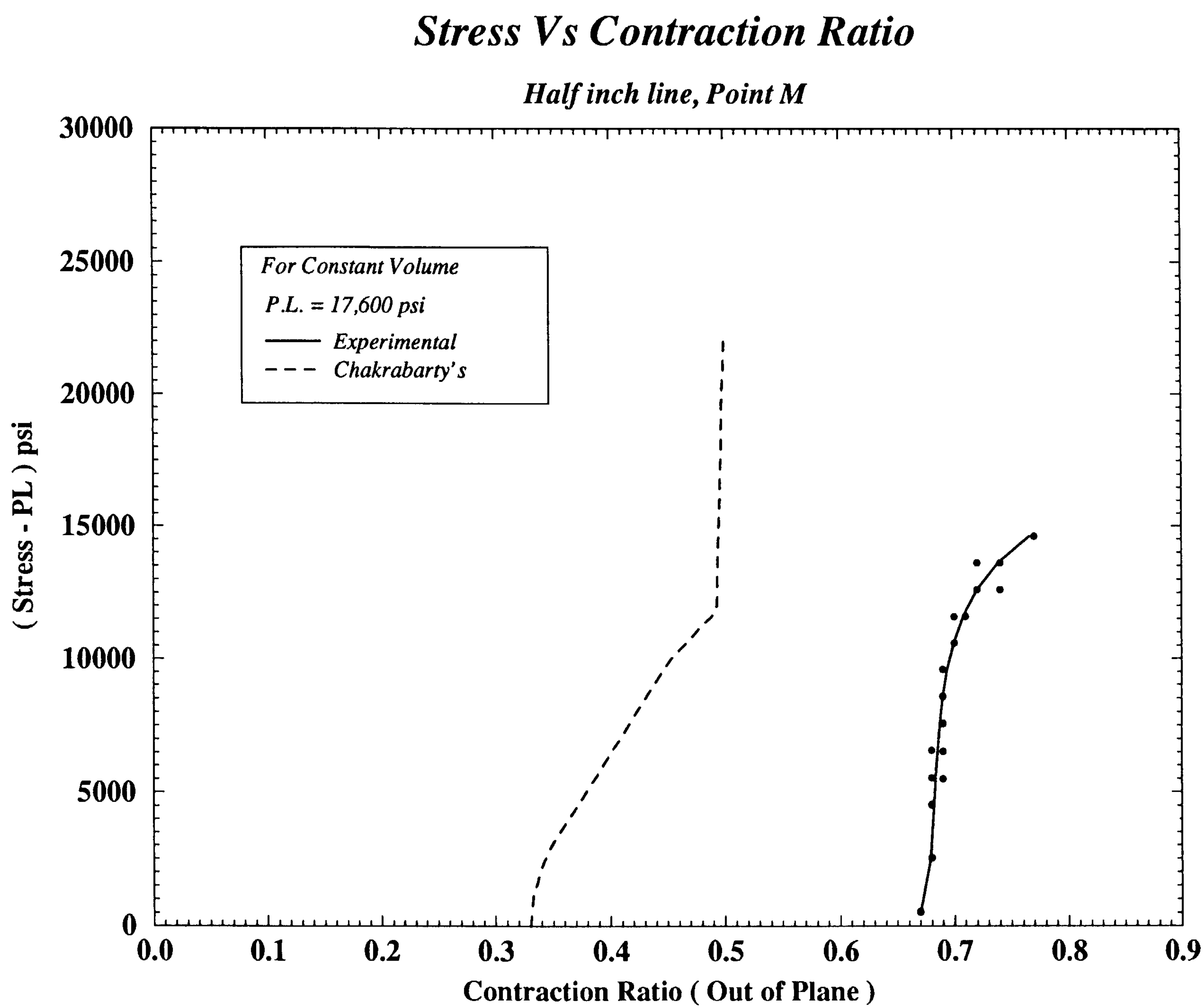

Figure D39. Out-of-Plane Contraction Ratios, Point M

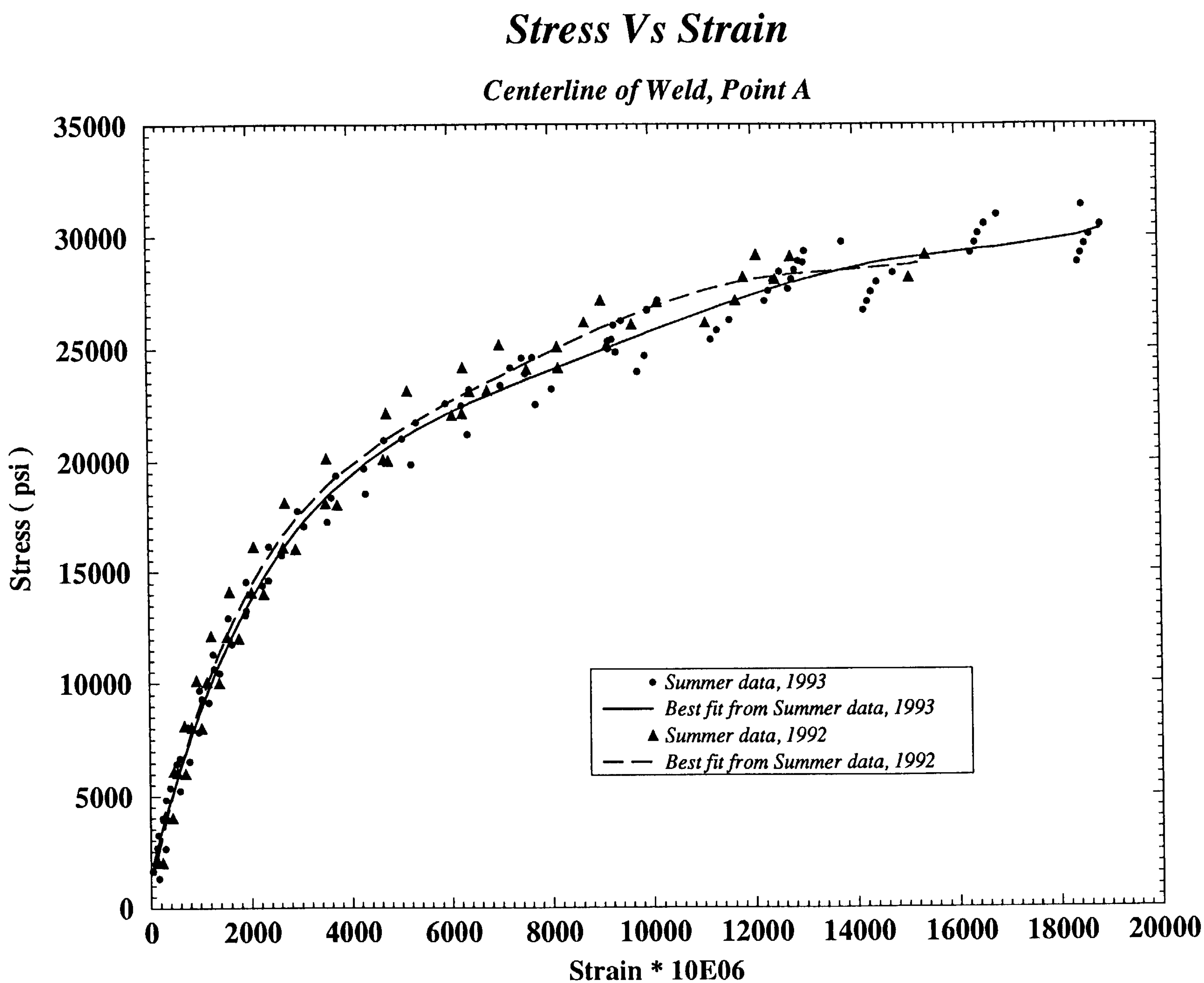

Figure D40. Data for Point A, 1992 and 1993